

STUDY OF REACTOR CONSTITUTIVE MODEL AND ANALYSIS OF NUCLEAR REACTOR KINETICS BY FRACTIONAL CALCULUS APPROACH

Ashrita Patra



**DEPARTMENT OF MATHEMATICS
NATIONAL INSTITUTE OF TECHNOLOGY
ROURKELA- 769008, INDIA**

STUDY OF REACTOR CONSTITUTIVE MODEL AND ANALYSIS OF NUCLEAR REACTOR KINETICS BY FRACTIONAL CALCULUS APPROACH

**A THESIS SUBMITTED TO THE
NATIONAL INSTITUTE OF TECHNOLOGY, ROURKELA
IN PARTIAL FULFILMENT OF THE REQUIREMENTS
FOR THE DEGREE OF**

DOCTOR OF PHILOSOPHY

IN

MATHEMATICS

BY

Ashrita Patra

**UNDER THE SUPERVISION OF
Prof. Santanu Saha Ray**



**DEPARTMENT OF MATHEMATICS
NATIONAL INSTITUTE OF TECHNOLOGY
ROURKELA- 769008, ODISHA, INDIA
JULY – 2014**

**DEDICATED TO MY
TEACHER
&
PARENTS**

Declaration

I hereby declare that the thesis entitled “**Study of Reactor Constitutive Model and Analysis of Nuclear Reactor Kinetics by Fractional Calculus Approach**” which is being submitted by me to National Institute of Technology for the award of degree of **Doctor of Philosophy (Mathematics)** is original and authentic work conducted by me in the Department of Mathematics, National Institute of Technology, Rourkela under the supervision of **Prof. Santanu Saha Ray**, Department of Mathematics, National Institute of Technology, Rourkela. No part or full form of this thesis work has been submitted elsewhere for a similar or any other degree.

Date:

Ashrita Patra



DEPARTMENT OF MATHEMATICS
NATIONAL INSTITUTE OF TECHNOLOGY
ROURKELA- 769008, ODISHA, INDIA

CERTIFICATE

This is to certify that the thesis entitled “**Study of Reactor Constitutive Model and Analysis of Nuclear Reactor Kinetics by Fractional Calculus Approach**” submitted by **Ashrita Patra** to the National Institute of Technology, Rourkela for the award of the degree of **Doctor of Philosophy (Mathematics)** is a record of bonafide research work carried out by her under my supervision and guidance. In my opinion, the the work has reached the standard fulfilling the requirements and regulations for the degree. To the best of my knowledge, the work incorporated in this thesis has not been submitted in part or full to any other University or Institute for the award of any degree or diploma.

Signature of Supervisor

Prof. S. Saha Ray
Associate Professor
Department of Mathematics
National Institute of Technology
Rourkela-769008

Acknowledgements

The time that, I have spent at National Institute of Technology, Rourkela given me a source of most precious experience in my life. I take the opportunity to acknowledge all those who directly or indirectly helped me throughout this difficult journey.

Foremost, I would like to express my deepest sense of gratitude to **Dr. S. Saha Ray** for his guidance, lively discussion, constant encouragement, expert advice, constructive and honest criticism. I am greatly indebted to him for his invaluable and sustained supervision in the preparation of this thesis. He is an excellent mentor and very supportive throughout the work. I feel extremely fortunate to have had an excellent supervision from him during the past years.

This work was financially supported by BARC, Trombay, Mumbai, Department of Atomic Energy, and Government of India under Grant No. 2007/37/35f/BRNS/3180 in which I have been appointed as Junior Research Fellow (JRF). I am gratefully thankful to BRNS officials specially **Mr. B. B. Biswas**, **Mr. Santanu Das** and others. I am extremely thankful to **Council of Scientific and Industrial Research (CSIR)** for selecting me as a Senior Research Fellow (SRF) which helps me to complete my Ph.D. work.

I also must acknowledge **Dr. S. K. Sarangi**, Director, National institute of Technology, Rourkela for providing me a platform to carry out this research.

I also would like to express my gratitude to the rest of my doctoral scrutiny committee members: **Dr. G. K. Panda**, **Dr. S. K. Rath**, **Dr. P. Sarkar** and **Dr. S. Chakraverty** for their invaluable, insightful comments and suggestions that improved the quality of this work.

I am extremely thankful to all the supporting and technical staff of the Department of Mathematics for their kind help and moral support. I am really thankful to all my fellow research colleagues specially **Prakash Kumar Sahu**. My sincere thanks to everyone who has provided me new ideas and useful criticism, I am truly indebted.

I extended my heart-felt thanks to my beloved parents **Mr. Labanya Patra** and **Mrs. Pankajini Patra** and I am greatly indebted to them for bearing the inconvenience during my thesis work. I owe a deep sense of indebtedness to my in-laws parents **Mr. Sauri Charan Harichandan** and **Mrs. Sandhyarani Harichandan** for their affection, wholehearted, untiring and immeasurable support at every stage of my post marriage life. Finally, I would also like to acknowledge the contribution of my lovely husband **Mr. Ranjan Kumar Harichandan** who has supported to me in each step for proceed to my Ph.D. work and without him it never possible to me for doing a great job. I sincerely give special and loving thanks to him for his moral support, encouragement, timely help and cooperation during this study.

Ashrita Patra
Dt:

CONTENTS

| TITLE | PAGE NUMBER |
|---------------|-------------|
| ABSTRACT | i |
| PRELIMINARIES | iv |
| INTRODUCTION | xxv |

CHAPTER 1

Part-A

ANALYTICAL METHODS AND NUMERICAL TECHNIQUES FOR SOLVING NEUTRON DIFFUSION AND KINETIC MODELS

| | | |
|-----|---|----|
| 1.1 | Homotopy Analysis Method (HAM) | 1 |
| 1.2 | Adomian Decomposition Method (ADM) | 4 |
| 1.3 | Modified Decomposition Method (MDM) | 6 |
| 1.4 | Variational Iteration Method (VIM) | 8 |
| 1.5 | Explicit Finite Difference Method (EFDM) | 9 |
| 1.6 | Differential Transform Method (DTM) | 11 |
| 1.7 | Multi-step Differential Transform Method (MDTM) | 14 |
| 1.8 | Fractional Differential Transform Method (FDTM) | 16 |

Part-B

NUMERICAL METHODS FOR SOLVING STOCHASTIC POINT KINETIC EQUATION

| | | |
|------|--------------------------------|----|
| 1.9 | Wiener Process | 16 |
| 1.10 | Euler Maruyama Method | 18 |
| 1.11 | Order 1.5 Strong Taylor Method | 19 |

CHAPTER 2

NEUTRON DIFFUSION EQUATION MODEL IN DYNAMICAL SYSTEMS

| | | |
|------------------|---|----|
| 2.1 | Introduction | 21 |
| 2.2 | Outline of the present study | 22 |
| 2.3 | Application of VIM to obtain the analytical solution of Neutron Diffusion Equation (NDE) | 23 |
| 2.4 | Application of MDM to obtain the analytical solution of NDE | 27 |
| 2.5 | Numerical results and discussions for NDE | 31 |
| 2.6 | One-Group NDE in Cylindrical and Hemispherical Reactors | 33 |
| 2.6.1 | Application of HAM to Cylindrical Reactor | 34 |
| 2.6.2 | Numerical Results for Cylindrical Reactor | 40 |
| 2.6.3 | Calculation for Critical Radius of Cylinder | 41 |
| 2.6.4 | Solution for Bare Hemisphere using ADM | 44 |
| 2.6.5 | Numerical Results for Hemispherical Reactor | 49 |
| 2.6.6 | Radiation Boundary Condition | 50 |
| 2.7 | Conclusion | 55 |
| CHAPTER 3 | FRACTIONAL ORDER NEUTRON POINT KINETIC MODEL | |
| 3.1 | Introduction | 57 |
| 3.2 | Brief Description for Fractional Calculus | 57 |
| 3.2.1 | Riemann-Liouville integral and derivative operator | 59 |
| 3.2.2 | Caputo Fractional Derivative | 60 |
| 3.2.3 | Grunwald- Letnikov definition of fractional derivatives | 61 |
| 3.2.4 | Lemma | 62 |
| 3.3 | Fractional Neutron Point Kinetic Equation and its Derivation | 63 |
| 3.4 | Application of Explicit Finite Difference Scheme for Fractional Neutron Point Kinetic Equation | 69 |

| | | |
|------------------|--|-----|
| 3.5 | Analysis for Stability of Numerical Computation | 70 |
| 3.6 | Numerical Experiments with change of reactivity | 72 |
| 3.7 | Conclusion | 77 |
| CHAPTER 4 | NUMERICAL SOLUTION FOR DETERMINISTIC CLASSICAL AND FRACTIONAL ORDER NEUTRON POINT KINETIC MODEL | |
| 4.1 | Introduction | 78 |
| 4.2 | Application of MDTM to classical Neutron Point Kinetic Equation(NPK) | 78 |
| 4.3 | Numerical Results and Discussions using variable reactivity functions for Classical order NPK model | 82 |
| 4.3.1 | Results obtained for Step-Reactivity | 83 |
| 4.3.2 | Results obtained for Ramp-Reactivity | 86 |
| 4.3.3 | Results obtained for Sinusoidal-Reactivity | 87 |
| 4.4 | Mathematical Model for Fractional Order Neutron Point Kinetic Model | 88 |
| 4.5 | Fractional Differential Transform Method | 89 |
| 4.6 | Application of MDTM to Fractional Order Neutron Point Kinetic Equation (FNPKE) | 91 |
| 4.7 | Numerical Results and Discussions for FNPKE | 93 |
| 4.7.1 | Results obtained for Step-Reactivity | 93 |
| 4.7.2 | Results obtained for Ramp-Reactivity | 100 |
| 4.7.3 | Results obtained for Sinusoidal-Reactivity | 102 |
| 4.8 | Conclusion | 105 |
| CHAPTER 5 | CLASSICAL AND FRACTIONAL ORDER STOCHASTIC NEUTRON POINT KINETIC MODEL | |
| 5.1 | Introduction | 106 |
| 5.2 | Classical order Stochastic Neutron Point Kinetic Model | 108 |
| 5.3 | Numerical solution of classical Stochastic Neutron | |

| | | |
|------------------|---|-----|
| | Point Kinetic Equation | 113 |
| 5.3.1 | Euler–Maruyama method for the solution of stochastic point-kinetic model | 113 |
| 5.3.2 | Strong Taylor of order 1.5 method for the solution of stochastic point-kinetic model | 114 |
| 5.4 | Numerical Results and Discussions for classical Stochastic Neutron Point Kinetic Equation | 116 |
| 5.5 | Application of Explicit Finite Difference Method for solving Fractional order Stochastic Neutron Point Kinetic Model | 123 |
| 5.6 | Numerical Results and Discussions for Fractional Stochastic Neutron Point Kinetic Equation | 125 |
| 5.7 | Analysis for Stability of Fractional Stochastic Neutron Point Kinetic Equation | 133 |
| 5.8 | Conclusion | 134 |
| CHAPTER 6 | SOLUTION FOR NONLINEAR CLASSICAL AND FRACTIONAL ORDER NEUTRON POINT KINETIC MODEL WITH NEWTONIAN TEMPERATURE FEEDBACK REACTIVITY | |
| 6.1 | Introduction | 135 |
| 6.2 | Classical order Nonlinear Neutron Point Kinetic Model | 137 |
| 6.3 | Numerical solution of Nonlinear Neutron Point Kinetic Equation in presence of reactivity function | 138 |
| 6.4 | Numerical Results and Discussions for classical order Nonlinear Neutron Point Kinetic Equation | 139 |
| 6.4.1 | Step-Reactivity Insertions | 139 |
| 6.4.2 | Ramp Reactivity Insertions | 140 |
| 6.4.3 | Temperature-Feedback Reactivity Insertions | 140 |
| 6.5 | Mathematical Model for Nonlinear Fractional Neutron Point Kinetics Equation | 146 |
| 6.6 | Application of Explicit Finite Difference Method for solving Fractional order Nonlinear Neutron Point Kinetic Model | 148 |
| 6.6 | Numerical Results and Discussions for Fractional Nonlinear Neutron Point Kinetic Equation with temperature feedback reactivity function | 149 |
| 6.7 | Computational Error Analysis for Fractional order Nonlinear | |

| | | |
|------------------|---|-----|
| | Neutron Point Kinetic Equation | 156 |
| 6.8 | Conclusion | 157 |
| CHAPTER 7 | NUMERICAL SIMULATION USING HAAR WAVELET METHOD FOR NEUTRON POINT KINETICS EQUATION INVOLVING IMPOSED REACTIVITY FUNCTION | |
| 7.1 | Introduction | 159 |
| 7.2 | Haar Wavelets | 162 |
| 7.3 | Function Approximation and Operational Matrix of the general order Integration | 163 |
| 7.4 | Application of Haar wavelet Operational Method for solving Neutron Point Kinetics Equation | 165 |
| 7.5 | Numerical Results and Discussions | 167 |
| 7.5.1 | Step reactivity Insertion | 167 |
| 7.5.2 | Ramp reactivity Insertion | 169 |
| 7.5.2.1 | Positive ramp reactivity | 169 |
| 7.5.2.2 | Negative ramp reactivity | 170 |
| 7.5.3 | Zig-Zag reactivity Insertion | 171 |
| 7.5.4 | Sinusoidal reactivity Insertion | 172 |
| 7.5.5 | Pulse reactivity Insertion | 176 |
| 7.6 | Convergence Analysis and Error estimation | 177 |
| 7.7 | Conclusion | 180 |
| CHAPTER 8 | NUMERICAL SOLUTION USING TWO-DIMENSIONAL HAAR WAVELET METHOD FOR STATIONARY NEUTRON TRANSPORT EQUATION IN HOMOGENEOUS ISOTROPIC MEDIUM | |
| 8.1 | Introduction | 182 |
| 8.2 | Formulation of Neutron Transport Equation model | 183 |
| 8.3 | Mathematical model of the stationary neutron transport equation in a homogeneous isotropic medium | 186 |
| 8.4 | Application of two-dimensional Haar wavelet collocation method to solve stationary neutron transport equation | 188 |
| 8.5 | Numerical results and discussions for stationary integer-order neutron transport equation | 190 |

| | | |
|--|--|-----|
| 8.6 | Mathematical Model for fractional order Stationary Neutron Transport Equation | 196 |
| 8.7 | Application of Two-dimensional Haar Wavelet Collocation Method to fractional order Stationary Neutron transport equation | 199 |
| 8.8 | Numerical Results and Discussions for fractional order neutron transport equation | 201 |
| 8.9 | Convergence Analysis of two-dimensional Haar wavelet method | 212 |
| 8.10 | Conclusion | 217 |
| BIBLIOGRAPHY | | 218 |
| LIST OF PUBLICATIONS/ACCEPTED/COMMUNICATED PAPERS | | 230 |

Abstract

The diffusion theory model of neutron transport plays a crucial role in reactor theory since it is simple enough to allow scientific insight, and it is sufficiently realistic to study many important design problems. The neutrons are here characterized by a single energy or speed, and the model allows preliminary design estimates. The mathematical methods used to analyze such a model are the same as those applied in more sophisticated methods such as multi-group diffusion theory, and transport theory. The neutron diffusion and point kinetic equations are most vital models of nuclear engineering which are included to countless studies and applications under neutron dynamics. By the help of neutron diffusion concept, we understand the complex behavior of average neutron motion. The simplest group diffusion problems involve only, one group of neutrons, which for simplicity, are assumed to be all thermal neutrons. A more accurate procedure, particularly for thermal reactors, is to split the neutrons into two groups; in which case thermal neutrons are included in one group called the thermal or slow group and all the other are included in fast group. The neutrons within each group are lumped together and their diffusion, scattering, absorption and other interactions are described in terms of suitably average diffusion coefficients and cross-sections, which are collectively known as group constants.

We have applied Variational Iteration Method and Modified Decomposition Method to obtain the analytical approximate solution of the Neutron Diffusion Equation with fixed source. The analytical methods like Homotopy Analysis Method and Adomian Decomposition Method have been used to obtain the analytical approximate solutions of neutron diffusion equation for both finite cylinders and bare hemisphere. In addition to these, the boundary conditions like zero flux as well as extrapolated boundary conditions are investigated. The explicit solution for critical radius and flux distributions are also calculated. The solution obtained in explicit form which is suitable for computer programming and other purposes such as analysis of flux distribution in a square critical reactor. The Homotopy Analysis Method is a very powerful and efficient technique which yields analytical solutions. With the help of this method we can solve many functional equations such as ordinary, partial differential equations, integral equations and so many other equations. It does not require enough memory space in computer, free from rounding off errors and discretization of space variables. By using the excellence of these methods, we obtained the solutions which have been shown graphically.

The fractional differential equations appear more and more frequently in different research areas of applied science and engineering applications. The fractional neutron point kinetic equations have been solved by using Explicit Finite Difference Method which is very efficient and convenient numerical technique. The numerical solution for this fractional model is not only investigated but also presented by graphically.

Fractional kinetic equations have been proved particularly useful in the context of anomalous slow diffusion. Fractional Neutron Point Kinetic Model has been analyzed for the dynamic behavior of the neutron motion in which the relaxation time associated with a variation in the neutron flux involves a fractional order acting as exponent of the relaxation time, to obtain the best operation of a nuclear reactor dynamics. Results for neutron dynamic behavior for subcritical reactivity, supercritical reactivity and critical reactivity and also for different values of fractional order are analyzed and compared with the classical neutron point kinetic equations.

In dynamical system of nuclear reactor, the point-kinetic equations are the coupled linear differential equations for neutron density and delayed neutron precursor concentrations. The point kinetic equations are most essential model in the field of nuclear engineering. By the help of neutron diffusion concept we understand the complex behaviour of average neutron motion which is diffused at very low or high neutron density. The modeling of these equations intimates the time-dependent behavior of a nuclear reactor. The standard deterministic point kinetic model have been the subject of countless studies and applications to understand the neutron dynamics and its effects, such as developed of different methods for their solution. The reactivity function and neutron source term are the parametric quantity of this vital system. The dynamical process explained by the point-kinetic equations is stochastic in nature. The neutron density and delayed neutron precursor concentrations differ randomly with respect to time. At the levels of high power, the random behavior is imperceptible. But at low power levels, such as at the beginning, random fluctuation in the neutron density and neutron precursor concentrations can be crucial. We have applied the numerical methods like Euler Maruyama and Strong order 1.5 Taylor which are used as a powerful solver for stochastic neutron point kinetic equation. The main advantages of Euler-Maruyama method and Strong order 1.5 Taylor method are they do not require piecewise constant approximation (PCA) over a partition for reactivity function and source functions.

Differential Transform method has been applied to compute the numerical solution for classical neutron point kinetic equations in nuclear reactor. Differential transform method (DTM) is an iterative procedure for obtaining analytic Taylor series solutions of differential equations. The new algorithm multi-step

differential transform method (MDTM) is also applied here for solving classical neutron point kinetic equation. The multi-step DTM is treated as an algorithm in a sequence of intervals for finding simple and an accurate solution. Moreover, numerical examples with variable step reactivities, ramp reactivity and sinusoidal reactivity are used to illustrate the preciseness and effectiveness of the proposed method.

Fractional stochastic neutron point kinetic equation is also solved using the Explicit Finite Difference Scheme. The numerical solution of Fractional Stochastic Neutron Point Kinetic Equation has been obtained very efficiently and elegantly. Fractional Stochastic Neutron Point Kinetic Model has been analyzed for the dynamic behavior of the neutron. The Explicit Finite Difference method is investigated over the experimental data, with given initial conditions and step reactivity. The computational results designate that this numerical approximation method is straightforward, effective and easy for solving fractional stochastic point kinetic equations. Numerical results showing the behavior of neutron density and precursor concentration have been presented graphically for different values of fractional order. Foremost the random behavior of neutron density and neutron precursor concentrations has been analyzed in fractional order. The random behaviors of neutron density and neutron precursor concentrations have not been analyzed before in fractional order. The results of the numerical approximations for the solution of neutron population density and sum of precursors population for different arbitrary values of α are computed numerically. In nuclear reactors, the continuous indication of the neutron density and its rate of change are important for the safe startup and operation of reactors.

The Haar wavelet operational method (HWOM) is proposed to obtain the numerical approximate solution of neutron point kinetic equation appeared in nuclear reactor with time-dependent and independent reactivity function. Using HWOM, stiff point kinetics equations have been analyzed elegantly with step, ramp, zig-zag, sinusoidal and pulse reactivity insertions. On finding the solution for a stationary neutron transport equation in a homogeneous isotropic medium, we also used Haar wavelet Collocation Method. Recently Haar wavelet method has gained the reputation of being a very easy and effective tool for many practical applications in applied science and technology. To demonstrate about the efficiency of the method, some test problems have been discussed.

Keywords: Neutron Diffusion Equation; Fractional Point Kinetic Equation; Stochastic neutron point kinetic equation; Stationary Neutron Transport Equation; Sinusoidal Reactivity; Pulse Reactivity; Temperature feedback Reactivity; Wiener Process; Neutron population density; Caputo fractional derivative; Grunwald-Letnikov fractional derivative; Haar Wavelets; Homotopy Analysis Method; Variational Iteration Method; Adomian Decomposition Method; Fractional Differential Transform; Multi-step Differential Transform Method

PRELIMINARIES

Elements of Nuclear Reactor Theory

- **Nuclear Reactor Theory and Reactor Analysis**

In “Elements of Nuclear Reactor Theory”, we study an overview of nuclear reactors and how nuclear energy is extracted from reactors. Here, nuclear energy means the energy released in nuclear fission. This occurs because of the absorption of neutrons by fissile material. Neutrons are released by nuclear fission, and since the number of neutrons released is sufficiently greater than 1, a chain reaction of nuclear fission can be established. This allows, in turn, for energy to be extracted from the process. The amount of extracted energy can be adjusted by controlling the number of neutrons. The higher the power density is raised, the greater the economic efficiency of the reactor. The energy is extracted usually as heat via the coolant circulating in the reactor core. Finding the most efficient way to extract the energy is a critical issue. The higher the coolant output temperature is raised, the greater the energy conversion efficiency of the reactor. Ultimately, considerations of material temperature limits and other constraints make a uniform power density level which means careful control of the neutron distribution. If there is an accident in a reactor system, the power output will run out of control. This situation is almost the same as an increase in the number of neutrons. Thus, the theory of nuclear reactors can be considered the study of the behavior of neutrons in a nuclear reactor.

Here, “nuclear reactor theory” and “reactor analysis”, are used to mean nearly the same thing. The terms “reactor physics” is also sometimes used. This field addresses the neutron transport

including changes of neutron characteristics. Basically, Nuclear Reactor is a device in which controlled nuclear fission chain reactions can be maintained. These nuclei fission into lighter nuclei (fission products) accompanied by the release of energy ($\cong 200$ MeV per event) plus several additional neutrons. Again these fission neutrons can then be utilized to induce still further fission reactions. The study of how to design the reactor so that there is a balance between the production of neutrons in fission reactions and the loss of neutrons due to capture or leakage is known as nuclear reactor theory or nuclear reactor physics or neutronics.

- **Discovery of the Neutron, Nuclear Fission and Invention of the Nuclear Reactor**

Technology generally progresses gradually by the accumulation of basic knowledge and technological developments. In contrast, nuclear engineering was born with the unexpected discovery of neutrons and nuclear fission, leading to a sudden development of the technology. The neutron was discovered by Chadwick in 1932. This particle had previously been observed by Irene and Frederic Joliot-Curie. However, they interpreted the particle as being a high energy γ -ray. The discovery of neutrons clarified the basic structure of the atomic nucleus (often referred to as simply the “nucleus”), which consists of protons and neutrons. Since the nucleus is very small, it is necessary to bring reacting nuclei close to each other in order to cause a nuclear reaction. Since the nucleus has a positive charge, a very large amount of energy is required to bring the nuclei close enough so that a reaction can take place. However, the neutron has no electric charge; thus, it can easily be brought close to a nucleus.

Nuclear fission was discovered by Hahn, Stresemann, and Meitner in 1939. Fission should have taken place in Fermi’s experiments. The fact that Fermi did not notice this reaction indicates that

nuclear fission is an unpredictable phenomenon. In 1942, Fermi created a critical pile after learning about nuclear fission and achieved a chain reaction of nuclear fission. The output power of the reaction was close to nil; however, this can be considered the first nuclear reactor made by a human being. However, it is not the case that a nuclear reactor can be built simply by causing fissions by bombarding nuclei with neutrons. The following conditions have to be satisfied for nuclear fission reactions

- Exoergic reaction
- Sustainable as a chain reaction
- Controllable

The first nuclear reactor was built by Fermi under a plutonium production project for atomic bombs. In a nuclear reactor, radioactive material is rapidly formed. Therefore, nuclear reactors have the following unique and difficult issues, which did not have to be considered for other power generators.

- Safety
- Waste
- Nuclear proliferation

Its products were the atomic bombs using enriched uranium and plutonium. One of the reasons for this war was to secure energy sources. After the war, the energy problem remained a big issue. Thus, large-scale development of nuclear engineering was started in preparation for the exhaustion of fossil fuels. Light-water reactors, which were put into practical use in nuclear submarines, were established in many countries. These reactors are not a solution to the energy problem, since they can utilize less than 1% of natural uranium. Fast reactors, on the other hand, can use almost 100% of natural uranium. Nuclear Reactor are made of with

- Fuel: Any fissionable material
- Fuel element: The smallest sealed unit of fuel
- Reactor Core: Total array of fuel, moderator and control elements
- Moderator: Material of low mass number which is inserted into the reactor to slow down or moderate neutrons via scattering collisions.

Ex.- Light water, heavy water, graphite and beryllium

- Coolant: A fluid which circulates through the reactor removing fission heat

Ex.- Coolant used as liquid: Water and Sodium

Coolant used as gaseous state: He_2^4 and CO_2

- Control Elements: Absorbing material inserted into the reactor to control core multiplication. Commonly absorbing materials include boron, cadmium, gadolinium and hafnium.

Nuclear engineering is an excellent technology by which tremendous amounts of energy is generated from a small amount of fuel. In addition to power generation, numerous applications are expected in the future. As well as being used in energy generation, neutrons are expected to be widely used as a medium in nuclear reactions.

• **Constitution of Atomic Nucleus**

In the constitution of matter an atom from elementary fundamental particles are made of protons, neutrons, and electrons. Among these, the proton and neutron have approximately the same mass. However, the mass of the electron is only 0.05% that of these two particles. The proton has a positive charge and its absolute value is the same as the electric charge of one electron (the elementary electric charge). The proton and neutron are called nucleons and they constitute a

nucleus. An atom is constituted of a nucleus and electrons that circle the nucleus due to Coulomb attraction. Species of atoms and nuclei are called elements and nuclides, respectively. An element is determined by its proton number (the number of protons). The proton number is generally called the atomic number and is denoted by Z . A nuclide is determined by both the proton number and the neutron number (the number of neutrons denoted by N). The sum of the proton number and neutron number, namely, the nucleon number, is called the mass number and is denoted by A ($A=Z+N$). Obviously, a nuclide can also be determined by the atomic number and mass number.

In order to identify a nuclide, A and Z are usually added on the left side of the atomic symbol as superscript and subscript, respectively. For example, there are two representative nuclides for uranium, described as U_{92}^{235} and U_{92}^{238} . The chemical properties of an atom are determined by the atomic number. These nuclides are called isotopic elements or isotopes. If the mass numbers are the same and the atomic numbers are different, they are called isobars. If the neutron numbers are the same, they are called isotones.

- **Nuclear Reaction**

In chemical reactions, electrons are shared, lost or gained, in order to form new compounds. In these processes, the nuclei just sit there and watch the show, passively sitting by and never changing their identities. In nuclear reactions, the roles of the subatomic particles are reversed. The electrons do not participate in the reactions, instead they stay in their orbitals while the protons and neutrons undergo changes. Nuclear reactions are accompanied by energy changes that are a million times greater than those in chemical reactions. Energy changes that are so great that changes in mass are detectable. Also, nuclear reaction yields and rates are not affected

by the same factors (e.g. pressure, temperature, and catalysts) that influence chemical reactions. When nuclei are unstable, they are termed radioactive. The spontaneous change in the nucleus of an unstable atom that results in the emission of radiation is called radioactivity and this process of change is often referred to as the *decay* of atoms.

- Atoms of one element typically are converted into atoms of another element.
- Protons, neutrons, and other particles are involved; orbital electrons rarely take part.
- Reactions are accompanied by relatively large changes in energy and measurable changes in mass.
- Reactions rates are affected by number of nuclei, but not by temperature, catalyst, or normally, the compound in which an element occurs.

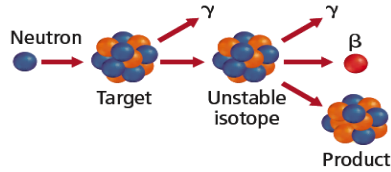
Two types of Nuclear Reactions are there as follows:

- **Fission** : The splitting of nuclei
- **Fusion** : The joining of nuclei (they fuse together)

Both reactions involve extremely large amounts of energy

Nuclear fission is the splitting of one heavy nucleus into two or smaller nuclei, as well as some sub-atomic particles and energy. A heavy nucleus is usually unstable, due to many positive protons pushing apart.

When fission occurs energy is produced, more neutrons are given off and neutrons are used to make nuclei unstable. It is much easier to crash a neutral neutron than a positive proton into a nucleus to release energy.



- **Delayed Neutrons**

A very few neutrons (less than 1%) appear with an appreciable time delay from the subsequent decay of radioactive fission products called delayed neutrons. These are more vital for the effective control of the fission chain reaction.

- **Prompt Neutrons**

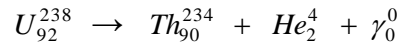
Some of the fission neutrons appear essentially and instantaneously (within 10^{-14} sec.) of the fission event called prompt neutrons.

- **Decay of Nucleus**

The decay of a nucleus is briefly explained in this section. Typical decays are α -decay, β -decay, and γ -decay, which emit α -rays, β -rays, and γ -rays, respectively. An α -ray is a nucleus of He^4 , a β -ray is an electron, and a γ -ray is a high-energy photon. In β -decay, a positron may be emitted, which is called β^+ -decay. As a competitive process for γ -decay, internal conversion occurs when an orbital electron is ejected, rather than a γ -ray being emitted. By α -decay, Z and N both decrease by 2. When a positively charged particle is emitted from a nucleus, the particle should normally have to overcome the potential of the Coulomb repulsive force, since the nucleus also has a positive charge. Spontaneous fission is another important decay for heavy nuclei. In this case, a Coulomb repulsive force even stronger than for α -decay applies, and the masses of the emitted particles are large, therefore the parent nucleus must have a sufficiently

high energy. Since the neutron has no Coulomb barrier, a neutron can easily jump out of a nucleus if energy permits. Although it is not appropriate to call this decay, it is important in relation to the later-described delayed neutron, which accompanies nuclear fission.

Gamma Emission: Gamma emission involves the radiation of high energy or gamma (γ) photons being emitted from an excited nucleus. Those electrons cannot stay in the higher level indefinitely, the atom releases the energy absorbed, the electron falls, and the energy is released as a photon which is of a specific energy – usually in the *UV* or visible region, but also the IR. A nucleus that is excited will need to release that energy also, and it does so by releasing a photon in the gamma region. The gamma photon is of much higher energy (shorter wavelength) than a *UV* or visible photon. For example, when uranium-238 undergoes alpha decay, a gamma ray is also emitted.



The time rate of change of the number of original nuclei present at that time

$$-\frac{dN}{dt} = \lambda N(t)$$

where λ = Radioactive decay constant (sec^{-1})

Here $N(t) = N_0 e^{-\lambda t}$ where N_0 = nuclei initially present. Radioactive half-life period is

$$N(T_{1/2}) = \frac{N_0}{2} = N_0 e^{-\lambda(T_{1/2})} \text{ with } T_{1/2} = \frac{\ln 2}{\lambda} = \frac{0.693}{\lambda}.$$

The fission products whose beta-decay yields a daughter nucleus which subsequently decays via delayed neutron emission as a delayed neutron precursor. There are six group for delayed

neutron precursor characterized into six classes approximately half-lives of 55sec., 22sec., 6sec., 2sec., 0.5sec., 0.2sec.

- **Cross Section**

The probability of a neutron interacting with a nucleus for a particular reaction is dependent upon not only the kind of nucleus involved, but also the energy of the neutron. Accordingly, the absorption of a thermal neutron in most materials is much more probable than the absorption of a fast neutron. Also, the probability of interaction will vary depending upon the type of reaction involved. The probability of a particular reaction occurring between a neutron and a nucleus is called the microscopic cross section (σ) of the nucleus for the particular reaction. This cross section will vary with the energy of the neutron. The microscopic cross section may also be regarded as the effective area the nucleus presents to the neutron for the particular reaction. The larger the effective area results the greater the probability for reaction.

Because the microscopic cross section is an area, it is expressed in units of area, or square centimeters. A square centimeter is tremendously large in comparison to the effective area of a nucleus, and it has been suggested that a physicist once referred to the measure of a square centimeter as being "as big as a barn" when applied to nuclear processes. The name has persisted and microscopic cross sections are expressed in terms of barns. The relationship between barns and cm^2 is shown below.

$$1 \text{ barn} = 10^{-24} \text{ cm}^2$$

Whether a neutron will interact with a certain volume of material depends not only on the microscopic cross section of the individual nuclei but also on the number of nuclei within that volume. Therefore, it is necessary to define another kind of cross section known as the

macroscopic cross section (Σ). The macroscopic cross section is the probability of a given reaction occurring per unit travel of the neutron. Σ is related to the microscopic cross section (σ) by the relationship shown below.

$$\Sigma = N\sigma$$

where Σ = macroscopic cross section (cm^{-1})

N = atom density of material (atoms/ cm^3)

σ = microscopic cross-section (cm^2)

The difference between the microscopic and macroscopic cross sections is the microscopic cross section (σ) represents the effective target area that a single nucleus presents to a bombarding particle. The units are given in barns or cm^2 . The macroscopic cross section (Σ) represents the effective target area that is presented by all of the nuclei contained in 1 cm^3 of the material. The units are given as $1/\text{cm}$ or cm^{-1} .

A neutron interacts with an atom of the material it enters in two basic ways. It will either interact through a scattering interaction or through an absorption reaction. The probability of a neutron being absorbed by a particular atom is the microscopic cross section for absorption, σ_a . The probability of a neutron scattering off of a particular nucleus is the microscopic cross-section for scattering, σ_s . The sum of the microscopic cross section for absorption and the microscopic cross section for scattering is the total microscopic cross section, σ_t presented as

$$\sigma_t = \sigma_a + \sigma_s .$$

- **Mean Free Path**

If a neutron has a certain probability of undergoing a particular interaction in one centimetre of travel, then the inverse of this value describes how far the neutron will travel (in the average case) before undergoing an interaction. This average distance travelled by a neutron before interaction is known as the mean free path for that interaction and is represented by the symbol (λ). The relationship between the mean free path (λ) and the macroscopic cross section (Σ) is

$$\lambda = \frac{1}{\Sigma}.$$

- **Diffusion Coefficient**

From diffusion theory, the diffusion coefficient is expressed in terms of macroscopic scattering cross section as

$$D = \frac{1}{3\Sigma_s}$$

where Σ_s is the macroscopic scattering cross section. In a weakly absorbing medium where macroscopic absorption cross-section is much less than macroscopic scattering cross section i.e.

$$\Sigma_a \ll \Sigma_s, D \text{ becomes } D = \frac{1}{3\Sigma_{tr}} = \frac{\lambda_{tr}}{3}$$

where λ_{tr} is the transport mean free path (cm).

- **Neutron Flux**

To consider the number of neutrons existing in one cubic centimeter at any one instant and the total distance they travel each second while in that cubic centimeter. The number of neutrons

existing in a cm^3 of material at any instant is called neutron density and is represented by the symbol n with units of neutrons/ cm^3 . The total distance these neutrons can travel each second will be determined by their velocity. A good way of defining neutron flux (ϕ) is to consider it to be the total path length covered by all neutrons in one cubic centimetre during one second. Mathematically,

$$\phi = n v$$

where ϕ = Neutron flux (neutrons/ cm^2 -sec)

n = Neutron density (neutrons/ cm^3)

v = Neutron velocity (cm/sec)

- **Fick's law and Neutron Diffusion Equation**

The process in which the concentration of a solute in one region is greater than in another of a solution, so the solute diffuses from the region of higher concentration to the region of lower concentration is called diffusion.

Fick's law states that the current density vector is proportional to the negative gradient of the flux. Thus Fick's law for neutron diffusion is given by

$$J = -D \nabla \phi$$

where J is the neutron current density that is the net amount of neutrons that pass per unit time through a unit area, D is the diffusion coefficient, ϕ is the neutron flux and ∇ is the del or gradient operator.

The use of this law in reactor theory leads to the diffusion approximation. Diffusion theory is based on Fick's Law and the Equation of Continuity equation. To derive the neutron diffusion equation we adopt the following assumptions:

1. We use a one-speed or one-group approximation where the neutrons can be characterized by a single average kinetic energy.
2. We characterize the neutron distribution in the reactor by the particle density $n(t)$ which is the number of neutrons per unit volume at a position \vec{r} at time t . Its relationship to the flux is

$$\phi(\vec{r}, t) = v n(t)$$

We consider an arbitrary volume V and write the balance equation or equation of continuity

$$\left[\begin{array}{l} \text{time rate of} \\ \text{the number of} \\ \text{neutrons in } V \end{array} \right] = \left[\begin{array}{l} \text{production} \\ \text{rate in } V \end{array} \right] - \left[\begin{array}{l} \text{absorption} \\ \text{in } V \end{array} \right] - \left[\begin{array}{l} \text{net leakage from} \\ \text{the surface of } V \end{array} \right]$$

The first term is expressed mathematically as

$$\frac{d}{dt} \left[\int_V n(\vec{r}, t) dV \right] = \frac{d}{dt} \left[\int_V \frac{1}{v} \phi(\vec{r}, t) dV \right] = \frac{1}{v} \frac{d}{dt} \left[\int_V \phi(\vec{r}, t) dV \right]$$

The production rate can be written as

$$\int_V S(\vec{r}, t) dV$$

The absorption term is

$$\int_V \Sigma_a(\vec{r}) \phi(\vec{r}, t) dV$$

and the leakage term is

$$\int_V \nabla \cdot J(\vec{r}, t) dV$$

where we converted the surface integral to a volume integral by use of Gauss' Theorem or the divergence theorem.

Substituting for the different terms in the balance equation we get

$$\frac{1}{\nu} \frac{d}{dt} \left[\int_V \phi(\vec{r}, t) dV \right] = \int_V S(\vec{r}, t) dV - \int_V \sum_a(\vec{r}) \phi(\vec{r}, t) dV - \int_V \nabla \cdot J(\vec{r}, t) dV$$

or we can obtain

$$\int_V \left(\frac{1}{\nu} \frac{\partial \phi(\vec{r}, t)}{\partial t} - S + \sum_a \phi + \nabla \cdot J(\vec{r}, t) \right) dV = 0$$

Since the volume V is arbitrary we can write

$$\frac{1}{\nu} \frac{\partial \phi(\vec{r}, t)}{\partial t} = -\nabla \cdot J(\vec{r}, t) - \sum_a \phi + S$$

We now use the relationship between J and ϕ (Fick's law) to write the diffusion equation

$$\frac{1}{\nu} \frac{\partial \phi(\vec{r}, t)}{\partial t} = \nabla \cdot [D(\vec{r}) \nabla \phi(\vec{r}, t)] - \sum_a(\vec{r}) \phi(\vec{r}, t) + S(\vec{r}, t)$$

This equation is the basis of much of the development in reactor theory using diffusion theory.

- **Reproduction Factor**

Most of the neutrons absorbed in the fuel cause fission, but some do not. The reproduction factor (η) is defined as the ratio of the number of fast neutrons produced by thermal fission to the number of thermal neutrons absorbed in the fuel. The reproduction factor is shown below.

$$\eta = \frac{\text{number of fast neutrons produced by thermal fission}}{\text{number of thermal neutrons absorbed in the fuel}}$$

The reproduction factor can also be stated as a ratio of rates as

$$\eta = \frac{\text{rate of production of fast neutrons by thermal fission}}{\text{rate of absorption of thermal neutrons by the fuel}} .$$

- **Effective Multiplication Factor**

The infinite multiplication factor can fully represent only a reactor that is infinitely large, because it assumes that no neutrons leak out of the reactor. To completely describe the neutron life cycle in a real, finite reactor, it is necessary to account for neutrons that leak out. The multiplication factor that takes leakage into account is the effective multiplication factor (k_{eff}), which is defined as the ratio of the neutrons produced by fission in one generation to the number of neutrons lost through absorption and leakage in the preceding generation. The effective multiplication factor may be expressed mathematically as

$$k_{eff} = \frac{\text{neutron production from fission in one generation}}{\text{neutron absorption and neutron leakage in preceeding generation}}$$

The condition where the neutron chain reaction is self-sustaining and the neutron population is neither increasing nor decreasing is referred to as the critical condition and can be expressed by the simple equation $k_{eff} = 1$. If the neutron production is greater than the absorption and leakage, the reactor is called supercritical. In a supercritical reactor, $k_{eff} > 1$, and the neutron flux increases each generation. If, on the other hand, the neutron production is less than the absorption and leakage, the reactor is called subcritical. In a subcritical reactor, $k_{eff} < 1$, this means that the flux decreases in each generation.

- **Buckling**

The buckling is a measure of extent to which the flux curves or “buckles.” In a nuclear reactor, criticality is achieved when the rate of neutron leakage. Geometric buckling is a measure of neutron leakage, while material buckling is a measure of neutron production minus absorption. Thus, in the simplest case of a bare, homogeneous, steady state reactor, the geometric and material buckling must be equal.

The diffusion equation is usually written as

$$\frac{\partial \phi(\vec{r}, t)}{\partial t} = \nabla \cdot [D(\phi, \vec{r}) \nabla \phi(\vec{r}, t)]$$

where $\phi(\vec{r}, t)$ is the density of the diffusing material at location \vec{r} and time t and $D(\phi, \vec{r})$ is the collective diffusion coefficient for density ϕ at location \vec{r} ; and ∇ represents the vector differential operator del. If the diffusion coefficient depends on the density then the equation is nonlinear, otherwise it is linear.

If flux is not a function of time, then the buckling terms can be derived from the diffusion equation

$$-D\nabla^2\phi + \Sigma_a\phi = \frac{1}{k}\nu\Sigma_f\phi$$

where k is the criticality eigen value, ν is the number of neutrons emitted per fission, Σ_f is the macroscopic fission cross-section and D is the diffusion coefficient.

Rearranging the terms, the diffusion equation becomes:

$$-\frac{\nabla^2\phi}{\phi} = \frac{\frac{k_\infty}{k} - 1}{L^2} = B_g^2$$

where the diffusion length $L \equiv \sqrt{\frac{D}{\Sigma_a}}$ and $k_\infty = \frac{\nu\Sigma_f}{\Sigma_a}$

We also can write

$$B_g^2 = \frac{\frac{k_\infty}{k} - 1}{L^2} = \frac{\frac{1}{k} \nu\Sigma_f - \Sigma_a}{D}$$

By diffusion theory, $k = k_{eff} = \frac{\nu\Sigma_f}{\Sigma_a + DB_g^2}$ or $k = \frac{\frac{\nu\Sigma_f}{\Sigma_a}}{1 + L^2 B_g^2}$

Assuming the reactor is in a critical state ($k = 1$), then geometric buckling is $B_g^2 = \frac{\nu\Sigma_f - \Sigma_a}{D}$.

By equating the geometric and material buckling, one can determine the critical dimensions of a one region nuclear reactor.

- One-group diffusion model- All the neutrons of the reaction characterized by a single kinetic energy of range from 10^{-3} to 10^7 eV.
- Multi-group Diffusion Model: Sophisticated model of the neutron density behaviour based on breaking up the range of neutron energies into intervals or “groups” and then describing the diffusion of neutrons in each of these groups separately, accounting for the transfer of neutrons between groups caused by scattering called multi-group diffusion model.

- **Reactivity**

Reactivity is a measure of the departure of a reactor from criticality. The reactivity is related to the value of k_{eff} . Reactivity is a useful concept to predict how the neutron population of a reactor will change over time.

$$\rho = \frac{k_{eff} - 1}{k_{eff}}$$

ρ may be positive, zero, or negative, depending upon the value of k_{eff} . The larger the absolute value of reactivity in the reactor core, the further the reactor is from criticality. It may be convenient to think of reactivity as a measure of a reactor's departure from criticality. Such processes whereby the reactor operating conditions will affect the criticality of the core are known as feedback reactivity. In reactivities, step, ramp, zig-zag, sinusoidal, pulse and temperature feedback reactivity are used to solve neutron kinetic problems in nuclear reactor dynamics.

- **Mean generation time**

The mean generation time, Λ , is the average time from a neutron emission to a capture that results in fission. The mean generation time is different from the prompt neutron lifetime because the mean generation time only includes neutron absorptions that lead to fission reactions (not other absorption reactions). The two times are related by the following formula:

$$\Lambda = \frac{l}{k_{eff}}$$

Here, k_{eff} is the effective neutron multiplication factor.

- **Nuclear Reactor Dynamics**

The study of the time-dependence of the related process involved in determining the core multiplication as a function of power level of the reactor is known as nuclear reactor dynamics.

- **Point Reactor Kinetic Model**

The one-group diffusion model we have been using to study reactor criticality is also capable of describing qualitatively the time behavior of a nuclear reactor, provided the effects of delayed neutrons. The model does not really treat the reactor as a point but rather merely assumes that the flux shape does not change with time.

Delayed neutrons are extremely important for reactor time behavior. For thermal reactors and for fast reactors, prompt neutron lifetimes are 10^{-4} sec and 10^{-7} sec respectively. The reactor period predicted by this model is too small for effective control of reactor.

The influence of the delayed neutron on the reactor, the effective lifetime of such neutrons given by their prompt lifetime + additional delay time λ_i^{-1} characterizing the β -decay of their precursor is considerably longer than prompt $l \approx 10^{-6}$ sec - 10^{-4} sec. Hence delayed neutrons substantially increase the time constant of a reactor so that effective control is possible. The neutron point kinetic model defined as

$$\frac{dn(t)}{dt} = \left(\frac{k(1-\beta)-1}{l} \right) n(t) + \sum_i \lambda_i c_i$$

$$\frac{dc_i}{dt} = \beta_i \left(\frac{k}{l} \right) n(t) - \lambda_i c_i.$$

where $\lambda_i \equiv$ Decay constant of the i^{th} - precursor group, $\beta_i \equiv$ fraction of all fission neutrons emitted per fission that appear from the i^{th} - precursor group, $\beta = \sum_i \beta_i \equiv$ Total fraction of fission neutrons which are delayed.

Nuclear energy is the only available source able to fulfil current and future energetic demands of mankind without polluting the Earth any further. Preceding its useful utilization, such as generation of electricity, materials irradiation or for medical purposes, its extraction within a nuclear reactor must occur. Design of nuclear reactors and analysis of their various operational modes is therefore a complicated task that encompasses several areas of science and engineering. At its start, however, determination of neutronic conditions within the reactor core plays a crucial role and received a substantial attention in the field of reactor physics in past decades. Main objective of such neutronic analyses is to describe and predict the states of the reactor under various circumstances and to find its optimal configuration, in which it is capable of long-term self-sustained operation with only a minimal human intervention.

In neutron diffusion theory, equations that govern the dynamics of space-time and the neutron population are called kinetics equations. The kinetics equations are dividing into point kinetics equations and space kinetics equations. In this work, we will emphasize the point kinetic model, more specifically, variations in the neutron density for small time scales, or equivalently changes in criticality due to changes of nuclear parameter in small time intervals. The point kinetic equations describe only the behaviour of the neutron density with time, assuming total separability of time from spatial degrees of freedom but with an a priori known spatial shape of the density. The point kinetic model plays still a significant role in reactor physics and is used to estimate the power response of the reactor, allowing for control and intervention in the power

plant operation that may also be helpful to avoid the occurrence of incidents or accidents. The new aspect is a fractional kinetics model, which reproduces the classical model and thus allows capturing effects that differ from the usually employed hypothesis of Fick. The fractional point kinetics model presented here is derived thoroughly and solved numerically, which hopefully will mark the beginning of an extensive research for future validation and applications of this kind of approach in nuclear reactor theory. The diffusion theory model of neutron transport has played a crucial role in reactor theory since it is simple enough to allow scientific insight, and it is sufficiently realistic to study many important design problems. The neutron transport equation models the transport of neutral particles in a scattering, fission, and absorption events with no self-interactions. Hence, the Point Kinetics Model is widely used in reactor dynamics because of the apparent simplicity of the resulting equations.

INTRODUCTION

In **Chapter 1**, some analytical and numerical methods have been introduced to solve nuclear reactor kinetic problems. The analytical methods like Homotopy analysis method, Adomian decomposition method, Variational iteration method and Modified decomposition method have been used to obtain the approximate solution of neutron kinetic equations in the closed form of infinite convergent series in nuclear reactor dynamics. These analytical methods are providing us more convergent series solution in real physical problems. The numerical methods like Explicit finite difference method, Differential transform method, Multi-step differential transform method, Fractional differential transform method have been discussed to find the numerical solutions for neutron kinetic problems. These numerical techniques have several advantages including easy programming on a computer and the convenience with which they handle complex problems.

In **Chapter 2**, One-group neutron diffusion equation has introduced. Variational Iteration Method (VIM) and Modified Decomposition method (MDM) have been applied to solve the analytical approximate solution of the Neutron Diffusion Equation with fixed source. The main properties of these methods lie in its flexibility and ability to solve linear as well as nonlinear equations accurately and conveniently. The explicit solution of the Neutron Diffusion equation has been presented in the closed form by an infinite series and then the numerical solution has been represented graphically. We have also obtained the solution for neutron diffusion equation in bare hemispherical and cylindrical reactors with considering zero-flux boundary condition and

extrapolated boundary condition. The solution for flux distribution with radiation boundary condition has also discussed. The comparison results for different angular flux have been shown. The critical radiuses for both symmetrical reactors have been obtained using these boundary conditions.

In **Chapter 3**, the explicit finite difference method is applied to solve the fractional neutron point kinetic equation with the Grunwald- Letnikov (GL) definition. Fractional Neutron Point Kinetic Model has been analyzed for the dynamic behavior of the neutron motion in which the relaxation time associated with a variation in the neutron flux involves a fractional order acting as exponent of the relaxation time, to obtain the best operation of a nuclear reactor dynamics. Results for neutron dynamic behavior for subcritical reactivity, supercritical reactivity and critical reactivity and also for different values of fractional order have been presented and compared with the classical neutron point kinetic (NPK) equation.

In **Chapter 4**, the multi-step differential transform method is applied to solve the classical and fractional order neutron point kinetic equation with the Caputo definition. The Differential Transform technique is one of the semi numerical analytical solution for solving a wide variety of differential equations and normally gets the solution in a series form. The multi-step DTM is treated as an algorithm in a sequence of intervals for finding simple and an accurate solution. Here, integer order and fractional neutron point kinetic equation have been solved using the new algorithm known as multi-step differential transform method (MDTM). Moreover, numerical examples with variable step reactivities, ramp reactivity and sinusoidal reactivity are used to illustrate the preciseness and effectiveness of the proposed method.

In **Chapter 5**, the numerical methods are applied to calculate the solution for stochastic neutron point-kinetic equations with sinusoidal reactivity in dynamical system of nuclear reactor. The resulting system of differential equations is solved for each time step-size. Using experimental data, the methods are investigated over initial conditions and with sinusoidal and pulse reactivity function. The computational results designate that these numerical approximation methods are straightforward, effective and easy for solving stochastic point-kinetic equations. We have also used explicit finite difference method, a numerical procedure which is efficiently calculating the solution for fractional stochastic neutron point kinetic equation (FSNPK) in the dynamical system of nuclear reactor with the Grunwald–Letnikov (GL) definition. Fractional stochastic neutron point kinetic model has been analysed for the dynamic behaviour of the neutron. The method is investigated over the experimental data, with given initial conditions and step reactivity. The computational results designate that this numerical approximation method is straightforward, effective and easy for solving fractional stochastic point kinetic equations. Numerical results for showing the behavior of neutron density and precursor concentration have been presented graphically for different values of fractional order.

In **Chapter 6**, we have used a numerical procedure which is efficient for calculating the solution for nonlinear neutron point kinetic equation in the field of nuclear reactor dynamics. The explicit finite difference method is applied to solve both integer or classical order and fractional order nonlinear neutron point kinetic equation with Newtonian temperature feedback reactivity. Nonlinear Neutron Point Kinetic Model has been analyzed in the presence of temperature feedback reactivity. The numerical solution obtained by explicit finite difference scheme is an

approximate solution which is based upon neutron density, precursor concentrations of multi-group delayed neutron and the reactivity function. The method is investigated over three sets of reactivity: step, ramp and temperature feedback reactivities like Newtonian temperature feedback reactivity. The computational results designate that this numerical approximation method is straightforward and effective for solving nonlinear point kinetic equations. Numerical results citing the behavior of neutron density and results of this method with different types of reactivity have been presented graphically. The comparisons of results with other referred methods have also been discussed.

In **Chapter 7**, the Haar wavelet operational method (HWOM) is proposed to obtain the numerical approximate solution of neutron point kinetic equation appeared in nuclear reactor with time-dependent and independent reactivity function. The numerical solution of point kinetics equation with a group of delayed neutrons is useful in predicting neutron density variation during the operation of a nuclear reactor. The continuous indication of the neutron density and its rate of change are important for the safe startup and operation of reactors. The present method has been applied to solve stiff point kinetics equations elegantly with step, ramp, zig-zag, sinusoidal and pulse reactivity insertions. This numerical method has turned out as an accurate computational technique for many applications. The accuracy of the obtained solutions are quite high even if the number of collocation points is small. By increasing the number of collocation points, the error of the approximation solution rapidly decreases. It manifests that the results obtained by the HWOM are in good agreement with other available results even for large time range and it is certainly simpler than other methods in open literature.

In **Chapter 8**, we have solved classical order and fractional order stationary neutron transport equation using two-dimensional Haar wavelet Collocation Method (HWCM) in a homogeneous and isotropic medium. Haar wavelet collocation method is efficient and powerful in solving wide class of linear and nonlinear differential equations. The proposed method is mathematically very simple, easy and fast. This chapter intends to provide the great utility of Haar wavelets to nuclear science problem. This chapter has also emphasized on the application of two-dimensional Haar wavelets for the numerical approximate solution of fractional order stationary neutron transport equation in homogeneous isotropic medium. To demonstrate about the efficiency and applicability of the method, two test problems have been discussed.

CHAPTER 1

It is the intent of this chapter to provide a brief description of the analytical and numerical methods to obtain the solution of neutron point kinetic models in the nuclear dynamical system. The basic ideas of linear and non-linear analytical methods have been introduced to solve the kinetic equation in the field of nuclear reactor dynamics using Homotopy Analysis Method (HAM), Variational Iteration Method (VIM), Adomian Decomposition Method (ADM) etc. The numerical techniques like Differential Transform Method (DTM), Multi-step Differential Transform Method (MDTM), and Explicit Finite Difference Method etc. have been also applied to obtain the numerical approximation solution for neutron point kinetic equation in nuclear reactor dynamical system.

1.1 *Homotopy Analysis Method (HAM)*

Nonlinear equations are difficult to solve, especially anal differential equations, partial differential equations, differential-integral equations, differential-difference equations, and coupled equations. Unlike perturbation methods, the HAM is independent of small/large physical parameters, and provides us a simple way to ensure the convergence of solution series. The method was first devised by Shijun Liao in 1992 then more and more researchers have successfully applied this method to various nonlinear problems in science and engineering.

We consider the following differential equation

$$N[u(x,t)]=0, \tag{1.1}$$

where N is the nonlinear operator, x and t are the independent variables and $u(x,t)$ is an unknown function. For simplicity, we ignore all boundary or initial conditions which are treated in the same way. By means of generalizing Homotopy Analysis Method [1, 2], we first construct the zeroth order deformation equation

$$(1-q)L[\phi(x,t;q)-u_0(x,t)]=qhH(x,t)N[\phi(x,t;q)] \quad (1.2)$$

where $q \in [0,1]$ is the embedding parameter, $h \neq 0$ is an auxiliary parameter, L is an auxiliary linear operator, $\phi(x,t;q)$ is an unknown function, $u_0(x,t)$ is an initial guess of $u(x,t)$ and $H(x,t)$ is a non-zero auxiliary function.

For $q=0$ and $q=1$, the zeroth order deformation equation given by eq. (1.2) leads to

$$\phi(x,t;0)=u_0(x,t) \quad \text{and} \quad \phi(x,t;1)=u(x,t) \quad (1.3)$$

when the value of q increases from 0 to 1, the solution $\phi(x,t;q)$ varies from the initial guess $u_0(x,t)$ to the solution $u(x,t)$. Expanding $\phi(x,t;q)$ in Taylor's series with respect to q , we have,

$$\phi(x,t;q)=u_0(x,t)+\sum_{m=1}^{\infty}u_m(x,t)q^m \quad (1.4)$$

where

$$u_m(x,t)=\frac{1}{m!}\left.\frac{\partial^m \phi(x,t;q)}{\partial q^m}\right|_{q=0}. \quad (1.5)$$

The convergence of the series (1.4) is depending upon the auxiliary parameter h . If it is convergent at $q=1$, we get

$$u(x, t) = u_0(x, t) + \sum_{m=1}^{\infty} u_m(x, t) \quad (1.6)$$

which must be one of the solutions of the original differential equation. Now we define the vector

$$\vec{u}_m(x, t) = \{u_0(x, t), u_1(x, t), u_2(x, t), \dots, u_m(x, t)\}. \quad (1.7)$$

Differentiating the zeroth order deformation eq. (1.2) for m times with respect to q then dividing them by $m!$ and finally setting $q=0$, we obtain the following m^{th} order deformation equation

$$L[u_m(x, t) - \chi_m u_{m-1}(x, t)] = hH(x, t)\mathfrak{R}_m(\vec{u}_{m-1}(x, t)) \quad (1.8)$$

where
$$\mathfrak{R}_m(\vec{u}_{m-1}) = \frac{1}{(m-1)!} \left. \frac{\partial^{m-1} N[\phi(x, t; q)]}{\partial q^{m-1}} \right|_{q=0} \quad (1.9)$$

and
$$\chi_m = \begin{cases} 0, & m \leq 1 \\ 1, & m > 1 \end{cases} \quad (1.10)$$

Now, the solution for m^{th} order deformation eq. (1.8) by applying L^{-1} on both sides, we get

$$u_m(x, t) = \chi_m u_{m-1}(x, t) + L^{-1}[hH(x, t)\mathfrak{R}_m(u_{m-1}(x, t))] \quad (1.11)$$

In this way, it is easy to obtain u_m for $m \geq 1$, at M^{th} order, we have

$$u(x, t) = \sum_{m=0}^M u_m(x, t) \quad (1.12)$$

when $M \rightarrow +\infty$, we obtain an accurate approximation of the original eq.(1.1).

It provides a simple way to ensure the convergence of the solution, freedom to choose the basis functions of the desired solution, and flexibility in determining the linear operator of the homotopy.

1.2 *Adomian Decomposition Method (ADM)*

The Adomian Decomposition method (ADM) is a semi-analytical method for solving ordinary and partial nonlinear differential equations. The method was developed from the 1970's to the 1990's by George Adomian. The main aim of this method has been superseded by more general theory of the Homotopy Analysis method. The vital aspect of the method is employment of the "Adomian Polynomials" which allow for solution convergence of the nonlinear portion of the equation, without simply linearizing the system. This algorithm provides the solution in a rapidly convergent series.

Let us consider the general form of a differential equation [3]

$$\mathcal{F} y = g \quad (1.13)$$

where \mathcal{F} is the non-linear differential operator with linear and non-linear terms. The differential operator is decomposed as

$$\mathcal{F} \equiv L + R \quad (1.14)$$

where L is easily invertible linear operator and R is the remainder of the linear operator. For our convenience L is taken as the highest order derivative then the eq. (1.13)

$$\text{can be written as} \quad Ly + Ry + Ny = g \quad (1.15)$$

where Ny corresponds to the non-linear term. Solving Ly from (1.15), we have

$$Ly = g - Ry - Ny \quad (1.16)$$

Because L is invertible, then L^{-1} is to be the integral operator

$$L^{-1}(Ly) = L^{-1}(g) - L^{-1}(Ry) - L^{-1}(Ny) \quad (1.17)$$

If L is a second order operator, then L^{-1} is a two-fold integral operator

$$L^{-1} \equiv \int_0^t \int_0^t (\cdot) dt dt \text{ and } L^{-1}(Ly) = y(t) - y(0) - ty'(0)$$

$$\text{Then eq. (1.17) for } y \text{ yields, } y = y(0) + ty'(0) + L^{-1}(g) - L^{-1}(Ry) - L^{-1}(Ny) \quad (1.18)$$

Let us consider the unknown function $y(t)$ in the infinite series as

$$y(t) = \sum_{n=0}^{\infty} y_n \quad (1.19)$$

The non-linear term $N(y)$ will be decomposed by the infinite series of Adomian polynomials A_n ($n \geq 0$) [3, 4] as

$$Ny = \sum_{n=0}^{\infty} A_n \quad (1.20)$$

$$\text{where } A_n \text{'s are obtained by } A_n = \frac{1}{n!} \left[\frac{d^n}{d\lambda^n} N \left(\sum_{i=0}^{\infty} y_i \lambda^i \right) \right]_{\lambda=0} \quad (1.21)$$

Now, substituting (1.19) and (1.20) into (1.18), we obtain

$$\sum_{n=0}^{\infty} y_n = y(0) + ty'(0) + L^{-1}(g) - L^{-1} \left[R \left(\sum_{n=0}^{\infty} y_n \right) \right] - L^{-1} \left[\left(\sum_{n=0}^{\infty} A_n \right) \right] \quad (1.22)$$

Consequently we can obtain,

$$\begin{aligned} y_0 &= y(0) + ty'(0) + L^{-1}(g) \\ y_1 &= -L^{-1}R(y_0) - L^{-1}(A_0) \\ y_2 &= -L^{-1}R(y_1) - L^{-1}(A_1) \\ &\dots\dots\dots \\ y_{n+1} &= -L^{-1}R(y_n) - L^{-1}(A_n) \end{aligned} \quad (1.23)$$

and so on.

Based on the Adomian Decomposition method, we shall consider the solution $y(t)$ as

$$y \cong \sum_{k=0}^{n-1} y_k = \varphi_n \quad \text{with} \quad \lim_{n \rightarrow \infty} \varphi_n = y(t)$$

We can apply this method to many real physical problems, and the obtained results are of high degree of accuracy. In most of the problems, the practical solution φ_n , the n -term approximation, is convergent and accurate even for small value of n .

1.3 *Modified Decomposition Method (MDM)*

A powerful modification of the Adomian decomposition methods (ADM) [3, 4] has been proposed by notable researcher Wazwaz [5]. A large amount of literature developed concerning Adomian Decomposition method, and the related modification to investigate various scientific models.

We consider the general differential equation

$$Lu + Ru + Nu = g(t) \quad (1.24)$$

where L is the operator of the highest-order derivative with respect to t and R is the remainder of the linear operator. The nonlinear term is represented by Nu .

Thus we obtain

$$Lu = g(t) - Ru - Nu \quad (1.25)$$

Since L is easily invertible linear operator, the inverse L^{-1} is assumed to be an integral operator given by

$$L_t^{-1} = \int_0^t (\cdot) dt \quad (1.26)$$

Operating the integral operator L^{-1} on both sides of eq. (1.25) we get

$$u = \varphi + L^{-1}g(t) - L^{-1}Ru - L^{-1}Nu \quad (1.27)$$

where φ is the solution of homogeneous equation

$$Lu=0 \quad (1.28)$$

and the integration constants involved in $f = \varphi + L^{-1}g(t)$ are to be determined by the initial or boundary conditions of the corresponding problem.

The Adomian Decomposition Method assumes that the unknown function $u(x, t)$ can be expressed by an infinite series of the form

$$u(x, t) = \sum_{n=0}^{\infty} u_n(x, t) \quad (1.29)$$

and the nonlinear operator Nu can be decomposed by an infinite series of polynomials given by

$$N(u) = \sum_{n=0}^{\infty} A_n \quad (1.30)$$

where A_n are the Adomian polynomials given by

$$A_n = \frac{1}{n!} \frac{d^n}{d\lambda^n} \left[N \left(\sum_{i=0}^{\infty} \lambda^i u_i \right) \right]_{\lambda=0}, \quad n = 0, 1, 2, \dots \quad (1.31)$$

According to the modified decomposition method [5], the recursive scheme is given by

$$u_0(x, t) = f_1$$

$$u_1(x, t) = f_2 - L^{-1}Ru_0(x, t) - L^{-1}A_0 \quad (1.32)$$

$$u_{n+1}(x, t) = -L^{-1}Ru_n(x, t) - L^{-1}A_n, \quad n \geq 1$$

where the solution of the homogeneous eq. (1.28) is given by

$$f = f_1 + f_2 \quad (1.33)$$

If the zeroth component u_0 is defined then the remaining components u_n , $n \geq 1$ can be determined completely such that each term is determined in term of the previous term and

the series solution is thus entirely determined. Finally, we approximate the solution $u(x, t)$ by the truncated series.

$$\phi_N(x, t) = \sum_{n=0}^{N-1} u_n(x, t) \quad \text{and} \quad \lim_{N \rightarrow \infty} \phi_N(x, t) = u(x, t) \quad (1.34)$$

The method provides the solution in the form of a rapidly convergent series that may lead to the exact solution in the case of linear differential equations and to an efficient numerical solution with high accuracy for nonlinear differential equations. The convergence of the decomposition series has been investigated by several notable researchers [6, 7]. The method can significantly reduce the volume of computational work. In comparisons with the standard Adomian method, the modified algorithm gives better performance in many cases. The MDM accelerates the convergence of the series solution rapidly if compared with the standard Adomian decomposition method.

1.4 Variational Iteration Method (VIM)

Variational Iteration Method (VIM) has been favorably applied to various kinds of nonlinear problems. The main property of the method is in its flexibility and ability to solve nonlinear equations accurately and conveniently. Major applications to nonlinear diffusion equation, nonlinear fractional differential equations, nonlinear oscillations and nonlinear problems arising in various engineering applications are surveyed. The Variational Iteration Method was proposed by Ji-Huan He [8, 9] which successfully applied to autonomous ordinary and partial differential equations and other fields. The main advantages of this method are the correction functions can be constructed easily by the general Lagrange multipliers, which can be optimally determined by the variational theory. The application of restricted variations in correction functional makes it much easier to determine the multiplier. The initial approximation can be freely selected with

possible unknown constants which can be identified via various methods. The approximations obtained by this method are valid for not only for small parameter, but also for very large parameter.

To illustrate the basic concept of variation iteration method [8-11] we consider the following general nonlinear ordinary differential equation given by

$$Lu(t) + Nu(t) = g(t) \quad (1.35)$$

where L is a linear operator, N is a nonlinear operator and $g(t)$ is a known analytical function. According to He's variational iteration method; we can construct the correction functional as follows

$$u_{n+1}(t) = u_n(t) + \int_0^t \lambda (Lu_n(\xi) + N\tilde{u}_n(\xi) - g(\xi)) d\xi \quad (1.36)$$

where u_0 is an initial approximation with possible unknowns, λ is a general Lagrange multiplier and \tilde{u}_n is considered as a restricted variation, i.e., $\delta\tilde{u}_n = 0$. The Lagrange multiplier λ can be determined from the stationary condition of the correction functional $\delta u_{n+1} = 0$.

Being different from the other non-linear analytical methods, such as perturbation methods, this method does not depend on small or large parameters, such that it can find wide application in non-linear problems without linearization, discretization or small perturbations.

1.5 *Explicit Finite Difference Method (EFDM)*

Finite difference methods are approximate in the sense that derivatives at a point are approximated by difference quotients over a small interval [12].

Let us consider the heat conduction equation

$$\frac{\partial u}{\partial t} = \frac{\partial^2 u}{\partial x^2} \quad (1.37)$$

Using finite difference approximation method, eq. (1.37) can be discretized into

$$\frac{u_{i,j+1} - u_{i,j}}{k} = \frac{u_{i+1,j} - 2u_{i,j} + u_{i-1,j}}{h^2} \quad (1.38)$$

where

$$x_i = ih \quad (i = 0, 1, 2, \dots),$$

and

$$t_j = jk \quad (j = 0, 1, 2, \dots).$$

Then eq. (1.38) can be written as

$$u_{i,j+1} = ru_{i-1,j} + (1-2r)u_{i,j} + ru_{i+1,j} \quad (1.39)$$

$$\text{where } r = \frac{\Delta t}{\Delta x^2} = \frac{k}{h^2},$$

and eq. (1.39) gives an explicit formula for the unknown “temperature” $u_{i,j+1}$ at the $(i, j+1)^{\text{th}}$ mesh point in terms of known “temperatures” along the j^{th} time-row.

Similarly, next we consider fractional diffusion equation [13]

$$\frac{\partial}{\partial t} u(x, t) = K_{\gamma 0} D_t^{1-\gamma} \frac{\partial^2}{\partial x^2} u(x, t) \quad (1.40)$$

where ${}_0 D_t^{1-\gamma}$ is the fractional derivative defined through the Riemann-Liouville operator.

For any function $f(t)$ can be expressed in the form of a power series. The fractional

derivative of order $1-\gamma$ at any point inside the convergence region of the power series can be written using Grunwald-Letnikov fractional derivative in the form of

$${}_0D_t^{1-\gamma} f(t) = \lim_{h \rightarrow 0} \frac{1}{h^{1-\gamma}} \sum_{k=0}^{[t/h]} w_k^{(1-\gamma)} f(t-kh), \quad (1.41)$$

where $[t/h]$ means the integer part of t/h . The Grunwald-Letnikov definition is simply a generalization of the ordinary discretization formulas for integer order derivatives.

Using explicit difference scheme, eq. (1.40) can be discretized into

$$u_j^{m+1} = u_j^m + S_\gamma \sum_{k=0}^m w_k^{(1-\gamma)} [u_{j-1}^{(m-k)} - 2u_j^{(m-k)} + u_{j+1}^{(m-k)}] \quad (1.42)$$

where $x_j = j\Delta x$ for $(j=0,1,2,\dots)$, $t_m = m\Delta t$ for $(m=0,1,2,\dots)$ and $u(x_j, t_m) \equiv u_j^{(m)}$ stands for the numerical estimate of the exact value of $u(x, t)$ at the point (x_j, t_m) . Here, $S_\gamma = K_\gamma \Delta t / [h^{1-\gamma} (\Delta x)^2]$. In this scheme, u_j^{m+1} , for every given position j , is given explicitly in terms of all the previous states u_j^n , $n=0,1,\dots,m$.

1.6 Differential Transform Method (DTM)

Many problems in science and engineering fields can be described by the ordinary and partial differential equations. A variety of numerical and analytical methods have been developed to obtain accurate approximate and analytic solutions for the problems in the literature.

The classical Taylor series method is one of the earliest analytic techniques to many problems but it requires a lot of symbolic calculation for the derivatives of functions and for the higher order derivatives. The updated version of the Taylor series is called differential Transform method. The concept of differential transform method was first

proposed by Zhou in 1986[14]. The DTM is very effective and powerful solver for solving various kinds of differential equations. The main advantage of this method is that it can be applied directly to linear and nonlinear differential equations without requiring linearization, discretization or perturbation.

The differential transform of $f(t)$ can be defined as follows

$$F(k) = \frac{1}{k!} \left[\frac{d^k f(t)}{dt^k} \right]_{t=t_0} \quad (1.43)$$

Here $F(k)$ is the transformed function of $f(t)$. The inverse differential transform of $F(k)$ is defined by

$$f(t) = \sum_{k=0}^{\infty} F(k)(t-t_0)^k \quad (1.44)$$

From eqs. (1.43) and (1.44), we get

$$f(t) = \sum_{k=0}^{\infty} \frac{(t-t_0)^k}{k!} \left[\frac{d^k f(t)}{dt^k} \right]_{t=t_0} . \quad (1.45)$$

It implies that the concept of differential transform is derived from Taylor series expansion, but the method never evaluates the derivatives symbolically.

In particular, case when $t_0 = 0$, which is referred to Maclaurin series of $f(t)$ and it can be

expressed as $f(t) = \sum_{k=0}^{\infty} t^k F(k) \equiv DT^{-1} F(k)$

where DT^{-1} stands for inverse differential transform.

The function $f(t)$ can be expressed by a finite series defined as follows

$$f(t) = \sum_{k=0}^N F(k)(t-t_0)^k \quad (1.46)$$

Here N is the finite sum of terms of the truncated series solution. The DTM is an important tool for solving different class of nonlinear problems.

Table-1: The fundamental operations of differential transformation

| Properties | Time function | Transformed function |
|------------|-----------------------------------|--|
| 1 | $f(t) = \alpha u(t) + \beta v(t)$ | $F(k) = \alpha U(k) + \beta V(k)$ |
| 2 | $f(t) = u(t)v(t)$ | $F(k) = \sum_{l=0}^k U(l)V(k-l)$ |
| 3 | $f(t) = \frac{du(t)}{dt}$ | $F(k) = (k+1)U(k+1)$ |
| 4 | $f(t) = \frac{d^m u(t)}{dt^m}$ | $F(k) = \frac{(k+m)!}{k!} U(k+m)$ |
| 5 | $f(t) = t^m$ | $F(k) = \frac{1}{k!} \left. \frac{d^k(f(t))}{dt^k} \right _{t=0} = \delta(k-m) = \begin{cases} 1, & k=m \\ 0, & k \neq m \end{cases}$ $F(k) = \frac{1}{k!} \left. \frac{d^k(f(t))}{dt^k} \right _{t=t_i} = \frac{m(m-1)\cdots(m-k+1)t_i^{m-k}}{k!}$ |
| 6 | $f(t) = \sin(\omega t + \alpha)$ | $F(k) = \frac{1}{k!} \left. \frac{d^k(f(t))}{dt^k} \right _{t=0} = \frac{\omega^k}{k!} \sin\left(\frac{k\pi}{2} + \alpha\right)$ $F(k) = \frac{1}{k!} \left. \frac{d^k(f(t))}{dt^k} \right _{t=t_i} = \frac{\omega^k}{k!} \sin\left(\frac{k\pi}{2} + \omega t_i + \alpha\right)$ |

If the system considered has a solution in terms of the series expansion of known functions then using this powerful method, we can obtain the exact solution. DTM is an effective and reliable tool for the solution of system of ordinary differential equations. The method gives rapidly convergent series solution. The accuracy of the obtained

solution can be improved by taking more terms in the solution. In many cases, the series solution obtained with DTM can be written in exact closed form. This method reduces the computational difficulties of the other traditional methods and all the calculations can be done easily and efficiently.

1.7 *Multi-step differential transform method (MDTM)*

DTM is always used to provide the approximate solutions for a class of nonlinear problems in terms of convergent series with easily computable components. But also it has few drawbacks that the series solution converges in a very small region and it has slow convergent rate in the wider regions. To overcome this problem, we represent in this section the multi-step differential transform method. For describing this, let us consider the following nonlinear initial value problem,

$$f(t, u, u', \dots, u^{(p)}) = 0, \quad u^{(p)} \text{ is } p^{\text{th}} \text{ derivative of } u. \quad (1.47)$$

subject to the initial conditions $u^{(k)}(0) = c_k$, for $k = 0, 1, \dots, p-1$

We find the solution over the interval $[0, T]$. The approximate solution of the initial value problem can be expressed by the finite series

$$u(t) = \sum_{m=0}^M a_m t^m, \quad t \in [0, T] \quad (1.48)$$

Assume that the interval $[0, T]$ is divided into N subintervals $[t_{n-1}, t_n]$, $n = 1, 2, \dots, N$ of equal step size $h = T/N$ by using the node point $t_n = nh$. The main idea of multi-step DTM is to apply first the DTM to eq.(1.47) over the interval $[0, t_1]$, we obtain the following approximate solutions [15].

$$u_1(t) = \sum_{m=0}^{M_1} a_{1m} t^m, \quad t \in [0, t_1] \quad (1.49)$$

using the initial conditions $u_1^{(k)}(0) = c_k$. For $n \geq 2$ and at each subinterval $[t_{n-1}, t_n]$ we use the initial conditions $u_n^{(k)}(t_{n-1}) = u_{n-1}^{(k)}(t_{n-1})$ and apply the DTM to eq.(1.47) over the interval $[t_{n-1}, t_n]$, where t_0 in Eq.(1.43) is replaced by t_{n-1} . This process is repeated and generates a series of approximate solutions $u_n(t)$, $n = 1, 2, \dots, N$. Now

$$u_n(t) = \sum_{m=0}^{M_1} a_{nm} (t - t_{n-1})^m, \quad t \in [t_n, t_{n+1}] \quad (1.50)$$

where $M = M_1 \cdot N$. Hence, the multi-step DTM assumes the following solution

$$u(t) = \begin{cases} u_1(t), & t \in [0, t_1] \\ u_2(t), & t \in [t_1, t_2] \\ \vdots \\ u_N(t), & t \in [t_{N-1}, t_N] \end{cases} \quad (1.51)$$

The multi-step DTM [15-18] is a simple for computational techniques for all values of h . It can be easily shown that if the step size $h = T$, then multi-step DTM reduces to classical DTM. The main advantage of this new algorithm is that the obtained series solution converges for wide time regions.

These analytical methods and numerical techniques are the most vital solver for ordinary as well as partial differential equations, linear and nonlinear problems and fractional differential equations appearing in the field of science and engineering. The numerical methods are iterative process by using which we can obtain the solution more accurately and also accuracy can be further improved when the step size of each subinterval becomes smaller. The approximate solutions obtained by the analytical methods are presented by a truncated form of infinite series.

1.8 Fractional Differential Transform Method (FDTM)

The differential transform method (DTM) was first applied in the engineering domain by Zhou [14]. This method is a numerical method based on the Taylor series expansion which constructs an analytical solution in form of a polynomial. The traditional higher order Taylor series method requires symbolic computation. The Taylor series method is computationally taken long time for large orders. The DTM is an iterative procedure for obtaining analytic Taylor series solution of ordinary or partial differential equations. In this section we define the fractional differential transform method (FDTM) that is based on generalized Taylor series formula as

$$F_{\alpha}(k) = \frac{1}{\Gamma(\alpha k + 1)} \left[(D_{x_0}^{\alpha})^k f(x) \right]_{x=x_0}, \quad (1.52)$$

where $(D_{x_0}^{\alpha})^k = D_{x_0}^{\alpha} . D_{x_0}^{\alpha} \dots D_{x_0}^{\alpha}$, k -times, and the differential inverse transform of $F_{\alpha}(k)$ is defined as follows

$$f(x) = \sum_{k=0}^{\infty} F_{\alpha}(k) (x - x_0)^{\alpha k}. \quad (1.53)$$

If we substitute eq. (1.52) into eq. (1.53), we obtain

$$\sum_{k=0}^{\infty} F_{\alpha}(k) (x - x_0)^{\alpha k} = \sum_{k=0}^{\infty} \frac{(x - x_0)^{\alpha k}}{\Gamma(\alpha k + 1)} \left[(D_{x_0}^{\alpha})^k f(x) \right]_{x=x_0} = f(x)$$

Hence, eq. (1.53) is the inverse fractional differential transform of eq. (1.52).

In case of $\alpha = 1$, then the fractional differential transform in eq. (1.52) reduces to the classical differential transform.

1.9 Wiener Process or Brownian motion Process

A standard Wiener process (often called Brownian motion) on the interval $[0, T]$ is a continuous time stochastic process $W(t)$ that depends continuously on $t \in [0, T]$ and satisfies the following properties [19-21]

- (i) $W(0) = 0$ (with probability 1).
- (ii) For $0 \leq s \leq t \leq T$ the increment $W(t) - W(s)$ is normally distributed with mean $E(W(t)) = 0$, variance $E(W(t) - W(s))^2 = |t - s|$ and covariance $E(W(t)W(s)) = \min(t, s)$; equivalently $W(t) - W(s) \sim \sqrt{t - s}N(0, 1)$ where $N(0, 1)$ denotes a normal distribution with zero mean and unit variance.
- (iii) For $0 \leq s < t < u < v \leq T$, the increments $W(t) - W(s)$ and $W(v) - W(u)$ are independent. For computational purpose, it is useful to consider discretized Brownian motion, where $W(t)$ is specified at discrete t values. We thus set $\Delta t = T/N$ for some positive integer N and let $W_i = W(t_i)$ with $t_i = i\Delta t$. We discretize the Wiener process with time-step Δt as $W_i = W_{i-1} + dW_i$, $i = 1, 2, \dots, N$, where each $dW_i \sim \sqrt{\Delta t}N(0, 1)$.

Stochastic Differential Equation (SDE) models play a prominent role in a range of application areas, including biology, chemistry, epidemiology, mechanics, microelectronics, economics and finance.

An Itô -process (or stochastic integral) $X = \{X_t, t \geq 0\}$ has the form [19-21]

$$X_t = X_0 + \int_0^t a(X_s)ds + \int_0^t b(X_s)dW_s, \text{ for } t \geq 0 \quad (1.54)$$

It consists of an initial value $X_0 = x_0$, which may be random, a slowly varying continuous component called the drift and rapid varying continuous random component called the diffusion. The second integral in eq. (1.54) is an Itô stochastic integral with respect to the Wiener process $W = \{W_t, t \geq 0\}$. The integral equation in eq. (1.54) is often written in the differential form

$$dX_t = a(X_t)dt + b(X_t)dW_t, \quad (1.55)$$

then eq. (1.55) is called Stochastic Differential Equation (or Itô Stochastic Differential Equation). Here we describe Euler-Maruyama Method and the order 1.5 Strong Taylor methods to simulate a stochastic point kinetic equation.

1.10 Euler-Maruyama Method

The Euler-Maruyama approximation is the simplest time discrete approximations of an Itô process. Let $\{Y_\tau\}$ be an Itô process on $\tau \in [t_0, T]$ satisfying the stochastic differential equation (SDE)

$$\begin{cases} dY_\tau = a(\tau, Y_\tau)d\tau + b(\tau, Y_\tau)dW_\tau \\ Y_{t_0} = Y_0 \end{cases} \quad (1.56)$$

$$\text{For a given time-discretization } t_0 = \tau_0 < \tau_1 < \dots < \tau_n = T, \quad (1.57)$$

an Euler approximation is a continuous time stochastic process $\{X(\tau), t_0 \leq \tau \leq T\}$ satisfying the iterative scheme [20, 21]

$$X_{n+1} = X_n + a(\tau_n, X_n)\Delta\tau_{n+1} + b(\tau_n, X_n)\Delta W_{n+1} \quad (1.58)$$

for $n = 0, 1, 2, \dots, N-1$

with initial value

$$X_0 = X(\tau_0)$$

where $X_n = X(\tau_n)$, $\Delta\tau_{n+1} = \tau_{n+1} - \tau_n$ and $\Delta W_{n+1} = W(\tau_{n+1}) - W(\tau_n)$. Here, each random number ΔW_n is computed as $\Delta W_n = \eta_n \sqrt{\Delta\tau_n}$ where η_n is chosen from standard normal distribution $N(0,1)$.

We have considered the equidistant discretized times

$$\tau_n = \tau_0 + n\Delta \text{ with } \Delta = \Delta_n = \frac{(T - \tau_0)}{N} \text{ for some integer } N \text{ large enough so that } \Delta \in (0,1).$$

1.11 *The order 1.5 strong Taylor Method*

Here we consider Taylor approximation having strong order $\alpha = 1.5$. The order 1.5 strong Taylor scheme can be obtained by adding more terms from Itô -Taylor expansion to the Milstein scheme [20, 21]. The order 1.5 strong Itô -Taylor scheme is

$$\begin{aligned} Y_{n+1} = & Y_n + a\Delta_n + b\Delta W_n + \frac{1}{2}bb_x(\Delta W_n^2 - \Delta_n) + a_xb\Delta Z_n + \frac{1}{2}(aa_x + \frac{1}{2}b^2a_{xx})\Delta_n^2 \\ & + (ab_x + \frac{1}{2}b^2b_{xx})(\Delta W_n\Delta_n - \Delta Z_n) + \frac{1}{2}b(bb_{xx} + b_x^2)(\frac{1}{3}\Delta W_n^2 - \Delta_n)\Delta W_n \end{aligned} \quad (1.59)$$

for $n = 0, 1, 2, \dots, N-1$

with initial value

$$Y_0 = Y(\tau_0) \text{ and } \Delta_n = \Delta\tau_n$$

Here, partial derivatives are denoted by subscripts and the random variable ΔZ_n is normally distributed with mean $E(\Delta Z_n) = 0$ and variance $E(\Delta Z_n^2) = \frac{1}{3}\Delta\tau_n^3$ and correlated

with ΔW_n by covariance

$$E(\Delta Z_n \Delta W_n) = \frac{1}{2} \Delta \tau_n^2.$$

We can generate ΔZ_n as

$$\Delta Z_n = \frac{1}{2} \Delta \tau_n (\Delta W_n + \Delta V_n / \sqrt{3}) \tag{1.60}$$

where ΔV_n is chosen independently from $\sqrt{\Delta \tau_n} N(0,1)$. Here the approximation, $Y_n = Y(\tau_n)$ is the continuous time stochastic process $\{Y(\tau), t_0 \leq \tau \leq T\}$, the time step-size $\Delta \tau_n = \tau_n - \tau_{n-1}$ and $\Delta W_n = W(\tau_n) - W(\tau_{n-1})$.

CHAPTER 2

2.1 *Introduction*

The nuclear reactor forms the heart of a Nuclear Power Plant (NPP). Fundamental to a nuclear reactor are the subjects of nuclear physics and reactor physics which deal with the basic aspects of the physics design of nuclear reactors. This knowledge is essential for understanding the reactor behavior during, both normal operation as well as abnormal conditions. Nuclear engineering is an excellent technology by which tremendous amounts of energy is generated from a small amount of fuel. In addition to power generation, numerous applications are expected in the future. As well as being used in energy generation, neutrons are expected to be widely used as a medium in nuclear reactions. Here, nuclear energy means the energy released in nuclear fission. This occurs because of the absorption of neutrons by fissile material. Neutrons are released by nuclear fission, and since the number of neutrons released is sufficiently greater than 1, a chain reaction of nuclear fission can be established. This allows, in turn, for energy to be extracted from the process. The amount of extracted energy can be adjusted by controlling the number of neutrons. The higher the power density is raised, the greater the economic efficiency of the reactor. Ultimately, this means careful control of the neutron distribution. If there is an accident in a reactor system, the power output will run out of control. This situation is almost the same as an increase in the number of neutrons. Thus, the theory of nuclear reactors can be considered the study of the behavior of neutrons in a nuclear reactor. The study for design the nuclear reactors so that there is a balance between the production of neutron in fission reactions and the loss of neutrons due to capture or leakage. The study of such process is known as nuclear reactor theory or nuclear reactor physics [22-24].

In nuclear physics, for purpose of optimizing the performance and regulating the safety of a nuclear reactor, it is important that the nuclear reactor run at a level of critical. To describe the state of criticality, we must understand the nature of nuclear power. Nuclear power is based upon a process called fission, a process in which a neutron approaches a fissile isotope, and its very proximity, as the neutron slows near atom, causes it to split into two or more pieces, generating fission products and generating even more neutrons called prompt and delayed neutrons. These neutrons collide with hydrogen in the water surrounding the fuel pins, depositing their energy and increasing the temperature of the water causing it to boil. The heat of the water or rather the stream is then used to power turbines and generate power.

Therefore, the neutron diffusion equations (NDE) as well as neutron point kinetic equations (NPK) have been analyzed to study the population of neutron density in the system and precursor density or the population of fission products that results in delayed neutrons.

2.2 Outline of the present study

In this chapter, we have applied the effective analytical and numerical methods which discussed in Chapter 1 to obtain the solution for Neutron Diffusion Equation (NDE). The neutrons are here characterized by a single energy or speed, and the model allows preliminary design estimates.

Now, we consider the time independent fixed source one group neutron diffusion equation [22] for a homogeneous region where geometry with the vacuum boundary conditions are valid and is given by

$$\nabla^2 \phi(\vec{r}) - \kappa^2 \phi(\vec{r}) = -\frac{S(\vec{r})}{D}, \vec{r} \in V, \phi(\vec{r}) = 0, \vec{r} \in S \quad (2.1)$$

where $\phi(\vec{r})$ is the neutron flux, $S(\vec{r})$ is the neutron source, Σ_a is the absorption cross section and the diffusion constant D is given by inverse diffusion length $\kappa^2 = \Sigma_a / D$.

We consider the neutron diffusion equation (NDE)¹ with the fixed source for a two dimensional system with a square geometry, it is symmetric with respect to both x and y -axes. In this scenario, neutron diffusion equation together with the boundary conditions given by eq. (2.1) reduces to

$$\frac{\partial^2 \phi(x, y)}{\partial x^2} + \frac{\partial^2 \phi(x, y)}{\partial y^2} - \kappa^2 \phi(x, y) = -\frac{S}{D} \quad (2.2)$$

$$\left. \frac{\partial \phi(x, y)}{\partial x} \right|_{x=0} = 0, \quad \phi(x, y)|_{x=a} = 0 \quad (2.3a)$$

$$\left. \frac{\partial \phi(x, y)}{\partial y} \right|_{y=0} = 0, \quad \phi(x, y)|_{y=a} = 0 \quad (2.3b)$$

2.3 Application of VIM to obtain the analytical solution of NDE

The variational iteration method (VIM) is a powerful method to investigate approximate solutions. It is based on the incorporation of a general Lagrange multiplier in the construction of correction functional for the equation. In addition, no linearization and perturbation is required by the method. The VIM method, which is also known as modified

¹ S. Saha Ray and A. Patra, 2011, "Application of Modified decomposition method and Variational Iteration Method for the solution of the one group neutron diffusion equation with fixed source", **Int. Journal of Nuclear Energy Science and Technology** (Inderscience), Vol. 6, No. 4, 310-320.

general Lagrange's multiplier method [8, 25], has been shown to solve effectively, easily and accurately a large class of nonlinear models of real physical problems.

In this section to solve the Neutron Diffusion Equation eq. (2.1) we apply the VIM method. To illustrate the basic concept of variation iteration method [8, 9] we consider the following general nonlinear ordinary differential equation given by

$$Lu(t) + Nu(t) = g(t)$$

where L is a linear operator, N is a nonlinear operator and $g(t)$ is a known analytical function. According to He's variational iteration method; we can construct the correction functional as follows

$$u_{n+1}(t) = u_n(t) + \int_0^t \lambda (Lu_n(\xi) + N\tilde{u}_n(\xi) - g(\xi)) d\xi$$

where u_0 is an initial approximation with possible unknowns, λ is a general Lagrange multiplier and \tilde{u}_n is considered as a restricted variation, i.e., $\delta\tilde{u}_n = 0$. The Lagrange multiplier λ can be determined from the stationary condition of the correction functional $\delta u_{n+1} = 0$.

Now, for solving neutron diffusion eq. (2.1) we construct a correction functional as follows

$$\phi_{n+1}(x, y) = \phi_n(x, y) + \int_0^x \lambda(x') \left[\frac{\partial^2 \phi_n(x', y)}{\partial x'^2} + \frac{\partial^2 \tilde{\phi}_n(x', y)}{\partial y^2} - \kappa^2 \tilde{\phi}_n(x', y) + \frac{S}{D} \right] dx' \quad (2.4)$$

where λ is a general Lagrange multiplier [26] which can be identified optimally via variational theory, $\phi(x, 0)$ is an initial approximation with possible unknowns, and $\tilde{\phi}_n(x', y)$ is considered as the restricted variation i.e. $\delta\tilde{\phi}_n = 0$.

Making the above correction functional stationary and to find the optimal value of λ , we have

$$\delta\phi_{n+1}(x, y) = \delta\phi_n(x, y) + \delta \int_0^x \lambda(x') \left[\frac{\partial^2 \phi_n(x', y)}{\partial x'^2} + \frac{\partial^2 \tilde{\phi}_n(x', y)}{\partial y^2} - \kappa^2 \tilde{\phi}_n(x', y) + \frac{S}{D} \right] dx' = 0 \quad (2.5)$$

which yields the following stationary conditions

$$\ddot{\lambda}(x') = 0 \quad (2.6)$$

$$\lambda(x') \Big|_{x'=x} = 0 \quad (2.7)$$

$$1 - \dot{\lambda}(x') \Big|_{x'=x} = 0 \quad (2.8)$$

Eq. (2.6) is called Lagrange-Euler equation and eqs. (2.7), (2.8) are Natural Boundary conditions.

The Lagrange multiplier can, therefore, be identified as

$$\lambda(x') = x' - x \quad (2.9)$$

Considering the boundary conditions in eq. (2.3), we assume an initial approximation in the form of infinite Cosine series

$$\phi_0(x, y) = \sum_{i=0}^{\infty} b_i \cos(\beta_i y) \quad (2.10)$$

Now, the eq. (2.10) satisfying the boundary condition at $y=a$ yields that

$$\beta_n = \frac{(2n+1)\pi}{2a}, \quad n = 0, 1, 2, \dots \quad (2.11)$$

For convenience, we consider the known force term in the same basis set with eq. (2.10),
i.e.

$$\frac{S}{D} = \sum_{i=0}^{\infty} b_i \cos(\beta_i y) \quad (2.12)$$

where the orthogonality property of the Fourier basis yields that

$$b_i = \frac{(-1)^i 2S}{aD\beta_i} \quad (2.13)$$

Using the eq. (2.9) and the initial approximation eq. (2.10), the first approximation is

$$\begin{aligned} \phi_1(x, y) &= \phi_0(x, y) + \int_0^x (x' - x) \left[\frac{\partial^2 \phi_0(x', y)}{\partial x'^2} + \frac{\partial^2 \phi_0(x', y)}{\partial y^2} - \kappa^2 \phi_0(x', y) + \frac{S}{D} \right] dx' \\ &= \sum_{i=0}^{\infty} b_i \cos(\beta_i y) + \int_0^x (x' - x) \left[\frac{\partial^2 \phi_0(x', y)}{\partial x'^2} + \frac{\partial^2 \phi_0(x', y)}{\partial y^2} - \kappa^2 \phi_0(x', y) + \sum_{i=0}^{\infty} b_i \cos(\beta_i y) \right] dx' \\ &= \sum_{i=0}^{\infty} b_i \cos(\beta_i y) \left[1 + \left(\alpha_i^2 - 1 \right) \frac{x^2}{2!} \right] \quad \text{where } \alpha_i^2 = \beta_i^2 + \kappa^2 \end{aligned} \quad (2.14)$$

The second approximation is

$$\begin{aligned} \phi_2(x, y) &= \phi_1(x, y) + \int_0^x (x' - x) \left[\frac{\partial^2 \phi_1(x', y)}{\partial x'^2} + \frac{\partial^2 \phi_1(x', y)}{\partial y^2} - \kappa^2 \phi_1(x', y) + \frac{S}{D} \right] dx' \\ &= \sum_{i=0}^{\infty} b_i \cos(\beta_i y) \left[1 + \left(\alpha_i^2 - 1 \right) \frac{x^2}{2!} \right] \\ &\quad + \int_0^x (x' - x) \left[\frac{\partial^2 \phi_1(x', y)}{\partial x'^2} + \frac{\partial^2 \phi_1(x', y)}{\partial y^2} - \kappa^2 \phi_1(x', y) + \sum_{i=0}^{\infty} b_i \cos(\beta_i y) \right] dx' \\ &= \sum_{i=0}^{\infty} b_i \cos(\beta_i y) \left[1 + \left(\alpha_i^2 - 1 \right) \frac{x^2}{2!} + \frac{\alpha_i^4 x^4}{4!} - \frac{\alpha_i^2 x^4}{4!} \right] \end{aligned} \quad (2.15)$$

The third approximation is

$$\begin{aligned}
\phi_3(x, y) &= \phi_2(x, y) + \int_0^x (x' - x) \left[\frac{\partial^2 \phi_2(x', y)}{\partial x'^2} + \frac{\partial^2 \phi_2(x', y)}{\partial y^2} - \kappa^2 \phi_2(x', y) + \frac{S}{D} \right] dx' \\
&= \sum_{i=0}^{\infty} b_i \cos(\beta_i y) \left[1 + \left(\alpha_i^2 - 1 \right) \frac{x^2}{2!} + \frac{\alpha_i^4 x^4}{4!} - \frac{\alpha_i^2 x^4}{4!} \right] \\
&\quad + \int_0^x (x' - x) \left[\frac{\partial^2 \phi_2(x', y)}{\partial x'^2} + \frac{\partial^2 \phi_2(x', y)}{\partial y^2} - \kappa^2 \phi_2(x', y) + \sum_{i=0}^{\infty} b_i \cos(\beta_i y) \right] dx' \\
&= \sum_{i=0}^{\infty} b_i \cos(\beta_i y) \left[1 + \left(\alpha_i^2 - 1 \right) \frac{x^2}{2!} + \frac{\alpha_i^4 x^4}{4!} - \frac{\alpha_i^2 x^4}{4!} + \frac{\alpha_i^6 x^6}{6!} - \frac{\alpha_i^4 x^6}{6!} \right] \tag{2.16}
\end{aligned}$$

and in the similar manner, the rest of the approximations of the iteration results can be obtained. Here VIM has been successfully applied to find the approximate solution to the one-group neutron diffusion equation.

2.4 Application of MDM to obtain the analytical solution of NDE

In this section, we use the modified decomposition method (MDM) to obtain the approximate solution of one-group neutron diffusion equation (2.1). Large classes of linear and nonlinear differential equations, both ordinary as well as partial, can be solved by MDM. A reliable modification of Adomian decomposition method has been done by Wazwaz [5]. The decomposition method provides an effective procedure for analytical solution of a wide and general class of dynamical systems representing real physical problems [27-29]. This method efficiently works for initial-value or boundary-value problems and for linear or nonlinear, ordinary or partial differential equations. Moreover, we have the advantage of a single global method MDM for solving ordinary or partial differential equations as well as many types of other equations.

We rewrite the eq. (2.2) in the following operator form

$$L_x \phi(x, y) = -\frac{S}{D} - L_y \{\phi(x, y)\} + \kappa^2 \phi(x, y) \quad (2.17)$$

$$\text{where } L_x \equiv \frac{\partial^2}{\partial x^2}, L_y \equiv \frac{\partial^2}{\partial y^2}$$

Now we applying the two-fold integration inverse operator L_x^{-1} to eq. (2.17), we obtain

$$L_x^{-1} L_x \phi(x, y) = -L_x^{-1} \left[\frac{S}{D} \right] - L_x^{-1} [L_y \{\phi(x, y)\} + L_x^{-1} (\kappa^2 \phi(x, y))] \quad (2.18)$$

$$\phi(x, y) = f(x, y) - L_x^{-1} \left[\frac{S}{D} \right] - L_x^{-1} [L_y \{\phi(x, y)\} + L_x^{-1} (\kappa^2 \phi(x, y))] \quad (2.19)$$

where $f(x, y)$ is the solution of $L_x \phi(x, y) = 0$. From MDM methodology [5], we assume the infinite series solution for $\phi(x, y)$ as

$$\phi(x, y) = \sum_{n=0}^{\infty} \phi_n(x, y)$$

From the recursive scheme eq. (1.32) of MDM, we obtain

$$\phi_0(x, y) = f \quad (2.20)$$

$$\phi_1(x, y) = -L_x^{-1} \left[\frac{S}{D} \right] - L_x^{-1} [L_y \{\phi_0(x, y)\} + L_x^{-1} (\kappa^2 \phi_0(x, y))] \quad (2.21)$$

$$\phi_2(x, y) = -L_x^{-1} [L_y \{\phi_1(x, y)\} + L_x^{-1} (\kappa^2 \phi_1(x, y))] \quad (2.22)$$

In general $\phi_{n+1}(x, y) = -L_x^{-1} [L_y \{\phi_n(x, y)\} + L_x^{-1} (\kappa^2 \phi_n(x, y))]$, for all $n \geq 1$

Considering the boundary conditions, we assume an initial approximation in the form of Fourier cosine series

$$\phi_0(x, y) = \sum_{i=0}^{\infty} b_i \cos(\beta_i y) \quad (2.23)$$

Now eq. (2.23) satisfying the boundary conditions at $y = a$ yields that

$$\beta_n = \frac{(2n+1)\pi}{2a}, \quad n = 0, 1, 2, \dots \quad (2.24)$$

For convenience, we consider the known force term in the same basis set with eq. (2.23),

i.e.

$$\frac{S}{D} = \sum_{i=0}^{\infty} b_i \cos(\beta_i y) \quad (2.25)$$

where the orthogonality property of Fourier basis yields that

$$s_i = \frac{(-1)^i 2S}{aD\beta_i} \quad (2.26)$$

$$\begin{aligned} \phi_1(x, y) &= -L_x^{-1} \left[\frac{S}{D} \right] - L_x^{-1} (L_y \{ \phi_0(x, y) \}) + L_x^{-1} (\kappa^2 \phi_0(x, y)) \\ &= -L_x^{-1} \left[\sum_{i=0}^{\infty} s_i \cos(\beta_i y) \right] - L_x^{-1} L_y \left\{ \sum_{i=0}^{\infty} b_i \cos(\beta_i y) \right\} + L_x^{-1} (\kappa^2 \sum_{i=0}^{\infty} b_i \cos(\beta_i y)) \\ &= \sum_{i=0}^{\infty} b_i \cos(\beta_i y) \left[\frac{\alpha_i^2 x^2}{2!} \right] - \sum_{i=0}^{\infty} s_i \cos(\beta_i y) \frac{x^2}{2!} \quad , \text{ where } \alpha_i^2 = \beta_i^2 + \kappa^2 \end{aligned}$$

$$\begin{aligned} \phi_2(x, y) &= -L_x^{-1} (L_y \{ \phi_1(x, y) \}) + L_x^{-1} (\kappa^2 \phi_1(x, y)) \\ &= -L_x^{-1} L_y \left\{ \sum_{i=0}^{\infty} b_i \cos(\beta_i y) \left[\frac{\alpha_i^2 x^2}{2!} \right] - \sum_{i=0}^{\infty} s_i \cos(\beta_i y) \frac{x^2}{2!} \right\} \\ &\quad + \kappa^2 L_x^{-1} \left(\sum_{i=0}^{\infty} b_i \cos(\beta_i y) \left[\frac{\alpha_i^2 x^2}{2!} \right] - \sum_{i=0}^{\infty} s_i \cos(\beta_i y) \frac{x^2}{2!} \right) \end{aligned}$$

$$= \sum_{i=0}^{\infty} b_i \cos(\beta_i y) \left[\frac{\alpha_i^4 x^4}{4!} \right] - \sum_{i=0}^{\infty} s_i \cos(\beta_i y) \frac{\alpha_i^2 x^4}{4!} \quad (2.27)$$

and so on.

In this manner, we can completely determine all the remaining components of the infinite series. Therefore, the solution of the neutron diffusion equation is given by

$$\begin{aligned} \phi(x, y) &= \sum_{i=0}^{\infty} \phi_i(x, y) \\ &= \sum_{i=0}^{\infty} b_i \cos(\beta_i y) \cosh(\alpha_i x) + \sum_{i=0}^{\infty} \frac{s_i}{\alpha_i^2} \cos(\beta_i y) [1 - \cosh(\alpha_i x)] \end{aligned} \quad (2.28)$$

Now, applying the boundary condition at $x = a$, we obtain

$$b_i \cosh(\alpha_i a) + \frac{s_i}{\alpha_i^2} (1 - \cosh(\alpha_i a)) = 0, \quad i = 0, 1, 2, \dots \quad (2.29)$$

This implies that

$$b_i = \frac{(-1)^i 2S}{aD\beta_i \alpha_i^2} \left(\frac{\cosh(\alpha_i a) - 1}{\cosh(\alpha_i a)} \right), \quad i = 0, 1, 2, \dots \quad (2.30)$$

Consequently, we obtain

$$1 - \alpha_i^2 = \frac{1}{\cosh(\alpha_i a)}, \quad i = 0, 1, 2, \dots \quad (2.31)$$

By substituting s_i value given by eq. (2.26) together with eq. (2.31) in (2.28) yields

$$\phi(x, y) = \frac{2S}{aD} \sum_{i=0}^{\infty} \frac{(-1)^i}{\beta_i \alpha_i^2} \cos(\beta_i y) \left[1 - \frac{\cosh(\alpha_i x)}{\cosh(\alpha_i a)} \right] \quad (2.32)$$

which is the exact solution [30]. In practical computation, we shall take 3-term approximation to $\phi(x, y)$ viz. $\Phi(x, y) = \phi_0 + \phi_1 + \phi_2$

$$= \sum_{i=0}^{\infty} b_i \cos(\beta_i y) \left[1 + (\alpha_i^2 - 1) \frac{x^2}{2!} + \frac{\alpha_i^4 x^4}{4!} - \frac{\alpha_i^2 x^4}{4!} \right] \quad (2.33)$$

The modified decomposition method accelerates the convergence of the series solution rapidly, dramatically reduces the size of work, and provides the exact solution by using few number of iteration only. In view of the present analysis, the modified decomposition method can be employed for the solution of neutron diffusion equation with fixed source [31].

2.5 Numerical Results and Discussions for neutron diffusion equation

In this present analysis, we consider a square reactor core with edge length $2a = 50$ cm and apply VIM and MDM to obtain the numerical solution for one quadrant of the system which is sufficient owing to the symmetricity regarding the vacuum conditions at the left and upper boundaries together with the reflector conditions at the right and lower boundaries as expressed in eq. (2.2).

In this numerical discussion, we assume the constant parameters of the reactor as presented in Table 1.

Table-1: Constants of the reactor

| Constants | a (cm) | D (cm) | Σ_a (cm ⁻¹) | S |
|-----------|----------|----------|--------------------------------|-----|
| Value | 25 | 1.77764 | 1 | 1 |

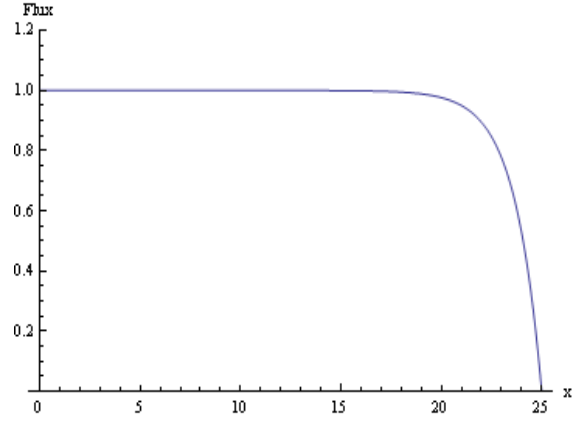


Fig. 1. Neutron Flux for $y = 0$

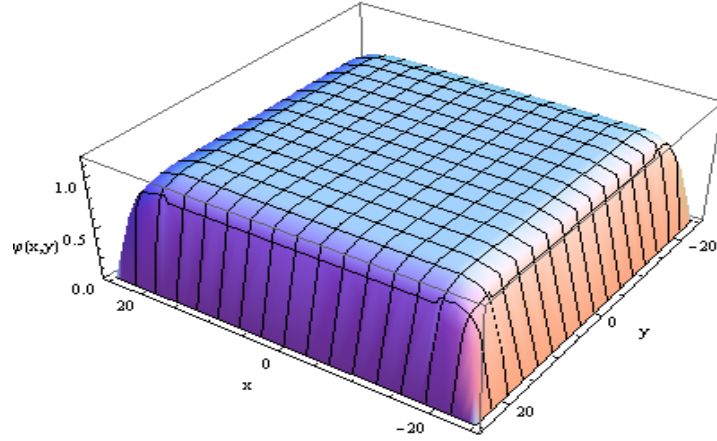
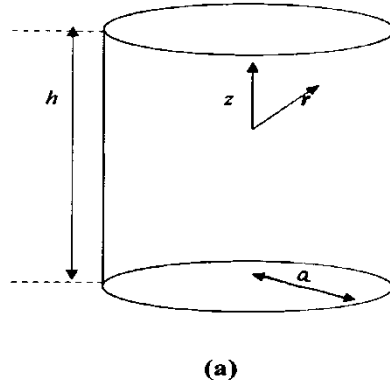


Fig. 2. Neutron Flux Distribution

We present the numerically computed result obtained by VIM and MDM in Fig. 1 for $y = 0$ and the Neutron Flux distribution $\phi(x, y)$ in Fig. 2 respectively. The computational results indicate that the two analytical methods like VIM and MDM, compared to the widely used analytic method of separation of variables, yields efficient and relatively straightforward expressions for the solution of neutron diffusion equation.

2.6 One-Group Neutron Diffusion Equation in Cylindrical and Hemispherical Reactors

In the present section, the nonlinear analytical Homotopy Analysis method (HAM) and Adomian decomposition method (ADM) have been implemented as means to solve one group neutron diffusion equation [22, 32] in hemispherical and cylindrical reactors². This work provides the application of HAM and ADM to compute the critical radius and flux distribution of time-independent neutron diffusion equation for both symmetrical bodies. The different boundary conditions are utilized like zero flux at boundary as well as the zero flux at extrapolated boundary. The process of flux distribution takes place in two symmetrical reactors (see Figure 3). Figure 3(a) represents finite cylinder having height h and radius a , Figure 3(b) represents hemispherical geometry of radius a where the flux in this reactor is the function of both r and θ .



² S. Saha Ray and A. Patra, 2011, Application of Homotopy Analysis Method and Adomian Decomposition Method for the Solution of Neutron Diffusion Equation in the Hemisphere and Cylindrical Reactors, **Journal of Nuclear Engineering and Technology** (STM), Vol. 1, Issue 1-3, pp. 1-14.

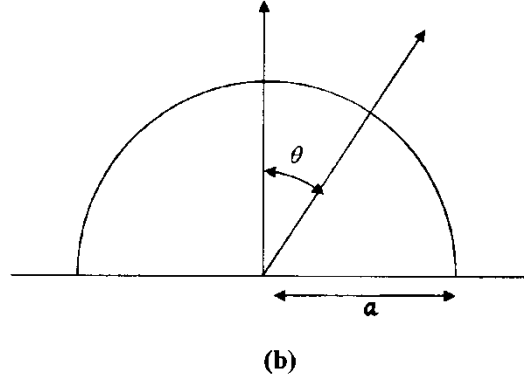


Fig. 3. Flux Distribution of Symmetrical Reactors through (a) Cylindrical Reactor; (b) Hemisphere geometry.

2.6.1 Application of HAM to Cylindrical Reactor

The homotopy analysis method (HAM) is used to formulate a new analytic solution of the neutron diffusion equation for cylindrical reactor. The method [1, 33, 34] has been proved useful for problems involving algebraic, linear/non-linear and ordinary/partial differential equations. Being an analytic recursive method, it provides a series sum solution. It has the advantage of offering a certain freedom for the choice of its arguments such as the initial guess, the auxiliary linear operator and the convergence control parameter, and it allows us to effectively control the rate and region of convergence of the series solution.

To illustrate HAM, we consider the following differential equation

$$N[u(x, t)] = 0, \quad (2.34)$$

where N is the nonlinear operator, x and t are the independent variables and $u(x, t)$ is an unknown function. For simplicity, we ignore all boundary or initial conditions which are treated in the same way. By means of generalizing Homotopy Analysis Method [1, 33, 34], we first construct the zeroth order deformation equation

$$(1 - q)L[\phi(x, t; q) - u_0(x, t)] = qhH(x, t)N[\phi(x, t; q)] \quad (2.35)$$

where $q \in [0,1]$ is the embedding parameter, $h \neq 0$ is an auxiliary parameter, L is an auxiliary linear operator, $\phi(x,t;q)$ is an unknown function, $u_0(x,t)$ is an initial guess of $u(x,t)$ and $H(x,t)$ is a non-zero auxiliary function.

For $q = 0$ and $q = 1$, the zeroth order deformation equation given by (2.35) leads to

$$\phi(x,t;0) = u_0(x,t) \quad \text{and} \quad \phi(x,t;1) = u(x,t) \quad (2.36)$$

when the value of q increases from 0 to 1, the solution $\phi(x,t;q)$ varies from the initial guess $u_0(x,t)$ to the solution $u(x,t)$. Expanding $\phi(x,t;q)$ in Taylor's series with respect to q we have

$$\phi(x,t;q) = u_0(x,t) + \sum_{m=1}^{\infty} u_m(x,t) q^m \quad (2.37)$$

where

$$u_m(x,t) = \frac{1}{m!} \left. \frac{\partial^m \phi(x,t;q)}{\partial q^m} \right|_{q=0}. \quad (2.38)$$

The convergence of the series (2.37) is depending upon the auxiliary parameter h . If it is convergent at $q = 1$, we get

$$u(x,t) = u_0(x,t) + \sum_{m=1}^{\infty} u_m(x,t) \quad (2.39)$$

which must be one of the solutions of the original differential equation. Now we define the vector

$$\vec{u}_m(x,t) = \{u_0(x,t), u_1(x,t), u_2(x,t), \dots, u_m(x,t)\}. \quad (2.40)$$

Differentiating the zeroth order deformation eq. (2.35) for m times with respect to q then dividing them by $m!$ and finally setting $q=0$, we obtain the following m^{th} order deformation equation

$$L[u_m(x,t) - \chi_m u_{m-1}(x,t)] = hH(x,t)\mathfrak{R}_m(\bar{u}_{m-1}(x,t)) \quad (2.41)$$

where
$$\mathfrak{R}_m(\bar{u}_{m-1}) = \frac{1}{(m-1)!} \left. \frac{\partial^{m-1} N[\phi(x,t;q)]}{\partial q^{m-1}} \right|_{q=0} \quad (2.42)$$

and
$$\chi_m = \begin{cases} 0, & m \leq 1 \\ 1, & m > 1 \end{cases} \quad (2.43)$$

Now, the solution for m^{th} order deformation eq. (2.41) by applying L^{-1} on both sides, we get

$$u_m(x,t) = \chi_m u_{m-1}(x,t) + L^{-1}[hH(x,t)\mathfrak{R}_m(u_{m-1}(x,t))] \quad (2.44)$$

In this way, it is easy to obtain u_m for $m \geq 1$, at M^{th} order, we have

$$u(x,t) = \sum_{m=0}^M u_m(x,t) \quad (2.45)$$

when $M \rightarrow +\infty$, we obtain an accurate approximation of the original eq.(2.34).

In the present analysis, we calculate the critical radius and flux distribution in a finite cylinder having height h and radius a as shown in Figure 3(a).

The time-independent diffusion equation in the nuclear reactor dynamics is given by

$$\nabla^2 \phi(r,z) + B^2 \phi(r,z) = 0 \quad (2.46)$$

where the buckling of reactors B^2 is given by

$$B^2 = \frac{\nu \Sigma_f - \Sigma_a}{D} \quad (2.47)$$

where $\nu \equiv$ Average number of neutrons emitted per fission

$\Sigma_f \equiv$ Macroscopic fission cross section

$\Sigma_a \equiv$ Macroscopic absorption cross section

$D \equiv$ Diffusion coefficient

Using Laplacian in cylindrical coordinates, we obtain

$$\frac{1}{r} \frac{d}{dr} \left(r \frac{d\phi(r, z)}{dr} \right) + \frac{d^2 \phi(r, z)}{dz^2} + B^2 \phi(r, z) = 0 \quad (2.48)$$

Then for applying separation of variable method, let us consider

$$\phi(r, z) = R(r)Z(z) \quad (2.49)$$

Consequently, the two separated differential equations are as follows

$$\frac{1}{rR} \frac{d}{dr} \left(r \frac{dR}{dr} \right) + B^2 = \alpha^2 \quad (2.50)$$

$$\frac{1}{Z} \frac{d^2 Z}{dz^2} = -\alpha^2 \quad (2.51)$$

where $\alpha^2 (>0)$ is the separation constant.

For solving the radial part of the finite cylinder, we can write Eq. (2.50) as

$$\frac{1}{r} \frac{d}{dr} \left(r \frac{dR}{dr} \right) + \beta_\alpha^2 R = 0 \quad (2.52)$$

where

$$\beta_\alpha^2 + \alpha^2 = B^2 \quad (2.53)$$

Replacing R with ϕ and considering

$$x = \beta_\alpha r, \quad (2.54)$$

we obtain

$$x^2 \phi''(x) + x \phi'(x) + x^2 \phi(x) = 0$$

$$\text{This implies } \phi''(x) + \frac{1}{x} \phi'(x) + \phi(x) = 0 \quad (2.55)$$

Now, we will apply HAM in Eq. (2.55) by taking an initial approximation

$$\phi_0(x) = C \quad (2.56)$$

where C is a constant.

The n th order deformation for Eq. (2.55) is obtained as

$$L[\phi_n(x) - \chi_n \phi_{n-1}(x)] = h H(x) \mathfrak{R}_n(\vec{\phi}_{n-1}(x)) \quad (2.57)$$

$$\text{where } \mathfrak{R}_n(\vec{\phi}_{n-1}) = \frac{1}{(n-1)!} \left. \frac{\partial^{n-1} N(\phi(x; q))}{\partial q^{n-1}} \right|_{q=0} \quad (2.58)$$

$$N(\phi(x; q)) = \phi''(x; q) + \left(\frac{1}{x} \right) \phi'(x; q) + \phi(x; q) \text{ and } \phi(x; q) = \phi_0(x) + \sum_{m=1}^{\infty} \phi_m(x) q^m,$$

$$\phi_m(x) = \frac{1}{m!} \left. \frac{\partial^m \phi(x; q)}{\partial q^m} \right|_{q=0}$$

Now, the solution of the first deformation of Eq. (2.55) by considering $h = -1$ and $H(x, t) = 1$ is given by

$$\phi_1(x) = -L^{-1}[\phi_0''(x) + \frac{1}{x}\phi_0'(x) + \phi_0(x)], \quad \text{where } \chi_1 = 0$$

Without loss of generality, we define the differential operator

$$L \equiv \frac{1}{x} \frac{d}{dx} \left(x \frac{d}{dx} \right) \quad (2.59)$$

Here, we choose the inverse of the differential operator $L^{-1} \equiv \int_0^x \frac{dx}{x} \int_0^x x(\cdot) dx$

Therefore, we obtain the 1st deformation equation as

$$\begin{aligned} \phi_1(x) &= - \int_0^x \frac{dx}{x} \int_0^x x(\phi_0(x)) dx \\ &= \frac{-Cx^2}{4} \end{aligned} \quad (2.60)$$

Similarly, the solution for second deformation equation is

$$\begin{aligned} \phi_2(x) &= \phi_1(x) - L^{-1}[\phi_1''(x) + \frac{1}{x}\phi_1'(x) + \phi_1(x)], \quad \text{where } \chi_2 = 1 \\ &= \frac{-Cx^2}{4} - \int_0^x \frac{dx}{x} \int_0^x x \left(\phi_1''(x) + \frac{1}{x}\phi_1'(x) + \phi_1(x) \right) dx \\ &= \frac{Cx^4}{64} \end{aligned} \quad (2.61)$$

The solution for third deformation equation is

$$\begin{aligned} \phi_3(x) &= \phi_2(x) - L^{-1} \left(\phi_2''(x) + \frac{1}{x}\phi_2'(x) + \phi_2(x) \right) \\ &= \frac{Cx^4}{64} - \int_0^x \frac{dx}{x} \int_0^x x \left(\phi_2''(x) + \frac{1}{x}\phi_2'(x) + \phi_2(x) \right) dx \end{aligned}$$

$$= \frac{-Cx^6}{64 \times 6 \times 6} \quad (2.62)$$

Hence, we finally obtain the solution for the radial part of finite cylinder as

$$\phi(x) = \sum_{k=0}^{\infty} C \frac{(-1)^k}{4^k k! k!} (x)^{2k} \quad (2.63)$$

The eq. (2.63) can be written as

$$R_{\alpha}(\beta_{\alpha} r) = \sum_{k=0}^{\infty} C \frac{(-1)^k}{4^k k! k!} (\beta_{\alpha} r)^{2k}, \text{ where } x = \beta_{\alpha} r \text{ and } \phi = R_{\alpha} \quad (2.64)$$

Similarly, the solution for axial part which is given in eq. (2.51) obtained as

$$Z_{\alpha}(z) = \cos(\alpha z) \quad (2.65)$$

Thus, the final solution of the time-independent diffusion eq. (2.46)

$$\phi(r, z) = \sum_{n=0}^{\infty} A_n R_n(\beta_{\alpha} r) Z_{\alpha}(z) \quad (2.66)$$

The numerical results are provided for one-speed fast neutrons in ^{235}U . The results reveal that the homotopy analysis method provides an accurate alternative to the Legendre function based solutions for the cylindrical reactor geometry [35]. This also holds when HAM is applied for the fixed source neutron diffusion equations for which case the HAM produces the result in a rather straightforward manner compared to that of the separation of variables approach which is yield through tedious algebraic manipulations of complicated mathematical expressions.

2.6.2 Numerical Results for Cylindrical Reactor

For providing the numerical results, 1 MeV neutrons diffusing in pure ^{235}U are considered.

The following data will be used [36, 37].

$$\nu = 2.42, \quad \sigma_f = 1.336b, \quad \sigma_s = 5.959b, \quad \sigma_c = 0.153b,$$

$$N_c = 0.0478 \times 10^{24} \text{ atoms cm}^{-3}$$

The diffusion coefficient $D = \frac{1}{3N_c \sigma_{total}}$ is equal to 0.9363 cm where $\sigma_{total} = \sigma_f + \sigma_s + \sigma_c$

Here, the absorption coefficient $\sigma_a = \sigma_f + \sigma_c$ and corresponding macroscopic absorption cross section is $\Sigma_a = N_c \sigma_a$. Similarly, the macroscopic fission cross section is $\Sigma_f = N_c \sigma_f$.

In order to calculate the solution for the flux distribution, the above data will be used.

2.6.3 Calculation for Critical Radius of Cylinder

We consider the ZF boundary conditions (or flux is zero at the boundary i.e. the advective and diffusive fluxes must exactly balance) for obtaining the critical radius for finite cylinder. According to ZF boundary conditions, for the flux to vanish on the top and bottom surfaces of the cylinder, i.e.,

$$\phi\left(r, \pm \frac{h_c}{2}\right) = 0 \quad (2.67)$$

Now, we apply the boundary conditions on the axial part

$$Z_\alpha\left(\pm \frac{h_c}{2}\right) = 0 \quad (2.68)$$

$$\text{or we can write, } \cos\left(\pm \alpha \frac{h_c}{2}\right) = 0 \quad (2.69)$$

Moreover, the eq. (2.69) yields

$$\alpha \frac{h_c}{2} = n \frac{\pi}{2}, \quad \text{where } n = 1, 2, 3, \dots$$

(2.70)

Then, the corresponding Eigen values are

$$\alpha = \frac{m\pi}{h_c}, \quad m = 1, 2, 3, \dots \quad (2.71)$$

For the first zero of the solution of the axial part, i.e., $m = 1$, we can write

$$Z(z) = \cos\left(\frac{\pi}{h_c} z\right) \quad (2.72)$$

Next, we apply the boundary condition on the radial part

$$R_\alpha(\beta_\alpha a_c) = 0 \quad (2.73)$$

From Eq. (2.64), by calculating the first zero, we obtained $\beta_\alpha a_c = 2.40483$.

Using the values of α and β_α , the critical radius depends upon critical heights (Table 2). Then

buckling B^2 for reactor from eq. (2.53), is

$$B^2 = \left(\frac{2.40483}{a_c}\right)^2 + \left(\frac{\pi}{h_c}\right)^2 \quad (2.74)$$

Table 2: Critical Radii for Corresponding Critical Heights.

| h_c | a_c at ZF | a_c at EBC |
|-------|-------------|--------------|
| 15 | 11.3144 | 9.44178 |
| 20 | 9.4788 | 7.6062 |
| 25 | 8.88551 | 7.01291 |
| 30 | 8.60656 | 6.73396 |

| | | |
|----|---------|---------|
| 35 | 8.45055 | 6.57795 |
| 40 | 8.35371 | 6.48111 |
| 45 | 8.28922 | 6.41662 |
| 50 | 8.24399 | 6.37139 |
| 55 | 8.21100 | 6.3384 |
| 60 | 8.18617 | 6.31357 |

The flux distribution in the finite cylinder is given by

$$\phi(r, z) = C \left(\sum_{p=0}^{\infty} \frac{(-1)^p}{4^p p! p!} \left(\frac{2.40483}{a_c} r \right)^{2p} \right) \cos \left(\frac{\pi z}{h_c} \right) \quad (2.75)$$

where C is known as normalization constant. The maximized flux occurs at the center of the cylinder ($r = 0, z = 0$) and flux decreases when it is going towards any surface. Finally, the flux is zero at $r = a_{c,ZF}$ and $z = \frac{H_c}{2}$. Table 2 cites calculated critical radii of a finite cylinder for a set of chosen critical height values. The smallest critical height $h_c = 15$ cm and corresponding critical radius is $a_c = 11.3144$ and $a_c = 9.44178$ at EBC. The flux distributions for a finite cylinder are shown in Figure 4.

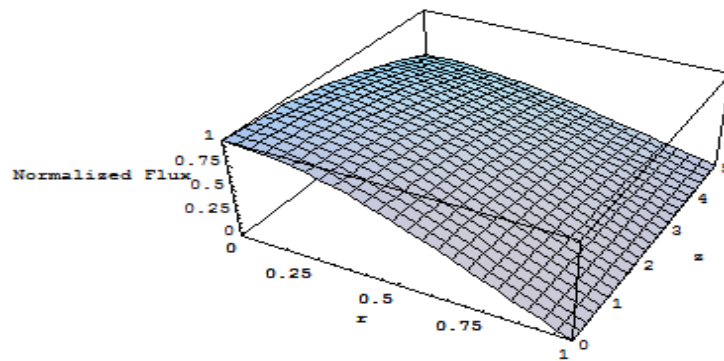


Fig. 4. Flux Distribution of a Finite Circular Cylinder

2.6.4 *Solution for Bare Hemisphere using ADM*

The adomian decomposition method (ADM) is applied to formulate a new analytic solution of the neutron diffusion equation for a hemisphere. Different boundary conditions are investigated; including zero flux on boundary, zero flux on extrapolated boundary, and radiation boundary condition. Numerical results are provided for one-speed fast neutrons in U^{235} . A comparison with Bessel function based solutions demonstrates that the method ADM can exactly reproduce the results more easily and efficiently. Let us consider the hemisphere as shown in Figure 3(b).

The time-independent diffusion equation is

$$D\nabla^2\phi(r, \theta) + (\nu\Sigma_f - \Sigma_a)\phi(r, \theta) = 0 \quad (2.76)$$

Considering the Laplacian in spherical coordinates and using $\mu = \cos\theta$, Eq. (2.76) reduces to

$$\frac{\partial^2\phi(r, \mu)}{\partial r^2} + \frac{2}{r}\frac{\partial\phi(r, \mu)}{\partial r} + \frac{1}{r^2}\frac{\partial}{\partial\mu}[(1-\mu^2)\frac{\partial\phi(r, \mu)}{\partial\mu}] + B^2\phi(r, \mu) = 0 \quad (2.77)$$

where the buckling of reactors B^2 is given by

$$B^2 = \frac{\nu\Sigma_f - \Sigma_a}{D} \quad (2.78)$$

Now, by applying the separation of variables method, let us consider $\phi(r, \mu) = R(r)\Phi(\mu)$.

Consequently, we get the differential equations as follows

$$\frac{r^2}{R(r)}\frac{d^2R(r)}{dr^2} + \frac{2r}{R(r)}\frac{dR(r)}{dr} + B^2r^2 = n(n+1) \quad (2.79)$$

$$\frac{1}{\Phi(\mu)} \frac{d}{d\mu} [(1-\mu^2) \frac{d\Phi(\mu)}{d\mu}] = n(n+1) \quad (2.80)$$

For solving the radial part we apply ADM [3, 38]. To illustrate ADM, let us consider the general form of a differential equation

$$\mathcal{F}y = g \quad (2.81)$$

where \mathcal{F} is the non-linear differential operator with linear and non-linear terms. The differential operator is decomposed as

$$\mathcal{F} \equiv L + R \quad (2.82)$$

where L is easily invertible linear operator and R is the remainder of the linear operator. For our convenience L is taken as the highest order derivative then the eq. (2.81) can be written as

$$Ly + Ry + Ny = g \quad (2.83)$$

where Ny corresponds to the non-linear term. Solving Ly from (2.83), we have

$$Ly = g - Ry - Ny \quad (2.84)$$

Because L is invertible, then L^{-1} is to be the integral operator

$$L^{-1}(Ly) = L^{-1}(g) - L^{-1}(Ry) - L^{-1}(Ny) \quad (2.85)$$

If L is a second order operator, then L^{-1} is a two-fold integral operator

$$L^{-1} \equiv \int_0^t \int_0^t (\cdot) dt dt \text{ and } L^{-1}(Ly) = y(t) - y(0) - ty'(0)$$

Then eq. (2.85) for y yields,

$$y = y(0) + ty'(0) + L^{-1}(g) - L^{-1}(Ry) - L^{-1}(Ny) \quad (2.86)$$

Let us consider the unknown function $y(t)$ in the infinite series as

$$y(t) = \sum_{n=0}^{\infty} y_n \cdot \quad (2.87)$$

The non-linear term $N(y)$ will be decomposed by the infinite series of Adomian polynomials

$$A_n \quad (n \geq 0)$$

$$Ny = \sum_{n=0}^{\infty} A_n \quad (2.88)$$

$$\text{where } A_n \text{'s are obtained by } A_n = \frac{1}{n!} \left[\frac{d^n}{d\lambda^n} N \left(\sum_{i=0}^{\infty} y_i \lambda^i \right) \right]_{\lambda=0} \quad (2.89)$$

Now, substituting (2.87) and (2.88) into (2.86), we obtained

$$\sum_{n=0}^{\infty} y_n = y(0) + ty'(0) + L^{-1}(g) - L^{-1} \left[R \left(\sum_{n=0}^{\infty} y_n \right) \right] - L^{-1} \left[\left(\sum_{n=0}^{\infty} A_n \right) \right] \quad (2.90)$$

Consequently we can obtain,

$$y_0 = y(0) + ty'(0) + L^{-1}(g)$$

$$y_1 = -L^{-1}R(y_0) - L^{-1}(A_0)$$

$$y_2 = -L^{-1}R(y_1) - L^{-1}(A_1)$$

.....

$$y_{n+1} = -L^{-1}R(y_n) - L^{-1}(A_n) \quad (2.91)$$

and so on.

Based on the Adomian Decomposition method, we shall consider the solution $y(t)$ as

$$y \cong \sum_{k=0}^{n-1} y_k = \varphi_n \quad \text{with} \quad \lim_{n \rightarrow \infty} \varphi_n = y(t)$$

We can apply this method to many real physical problems, and the obtained results are of high degree of accuracy. In most of the problems, the practical solution φ_n the n -term approximation is convergent and accurate even for small value of n .

Here, we first consider $x = Br$ and rewrite the Eq. (2.79) as

$$x^2 \frac{d^2 R(x)}{dx^2} + 2x \frac{dR(x)}{dx} + (x^2 - n(n+1))R(x) = 0 \quad (2.92)$$

$$\frac{d^2 R(x)}{dx^2} + \frac{2}{x} \frac{dR(x)}{dx} - \frac{n(n+1)}{x^2} R(x) = -R(x) \quad (2.93)$$

We compare eq. (2.93) with a general second order differential equation

$$f''(x) + a(x)f'(x) + b(x)f(x) = h(x) \quad (2.94)$$

Let $\varphi(x) \neq 0$ be a solution for the corresponding homogeneous differential equation of eq. (2.94).

By applying the method of variation of parameters, we obtain the general solution of eq. (2.94) as

$$f(x) = C_1 \varphi(x) + C_2 \varphi(x) \int \frac{dx}{E(x)\varphi^2(x)} + \varphi(x) \int \frac{1}{E(x)\varphi^2(x)} \left(\int E(x)\varphi(x)h(x)dx \right) dx \quad (2.95)$$

where $E(x) = e^{\int a(x)dx}$, C_1 and C_2 are constants.

In the above form L^{-1} is defined as an indefinite integral; for any other problem also we have to transform it into a definite integral according with the solution for our problem.

We consider the Bessel equation in the form

$$f''(x) + \frac{1}{x} f'(x) - \frac{\nu^2}{x^2} f(x) = -f(x) \quad (2.96)$$

The solution for the homogeneous part is $\varphi(x) = x^{\pm \nu}$ and considering $C_1 = 2^{-\nu} / \Gamma(\nu + 1)$, $C_2 = 0$, we obtain the solution of eq. (2.96) according to eq. (2.95) in the form of integral equation which is given by

$$f(x) = \frac{\left(\frac{x}{2}\right)^\nu}{\Gamma(\nu + 1)} - x^\nu \int_0^x \left(x^{-1-2\nu} \int_0^x x^{1+\nu} f(x) dx \right) dx \quad (2.97)$$

The initial approximation which is the solution of homogeneous part of eq. (2.96) is

$$f_0(x) = \frac{\left(\frac{x}{2}\right)^\nu}{\Gamma(\nu+1)} \quad (2.98)$$

From above we get next approximation as

$$\begin{aligned} f_1(x) &= -x^\nu \int_0^x \left(x^{-1-2\nu} \int_0^x x^{1+\nu} f_0(x) dx \right) dx \\ &= -\frac{\left(\frac{x}{2}\right)^{\nu+2}}{\Gamma(\nu+2)} \end{aligned}$$

Continuing in this manner, we can find the solution in the series form given by

$$f(x) = \sum_{k=0}^{\infty} (-1)^k \frac{\left(\frac{x}{2}\right)^{\nu+2k}}{k! \Gamma(\nu+k+1)} \quad (2.99)$$

For this bare hemisphere, we consider $\phi(x) = x^n$ is a solution for corresponding homogeneous equation (2.92).

By applying the method of variation of parameters and with the help of integral Eq. (2.95), we obtain the general solution for Eq. (2.93) as

$$R(x) = Cx^n - x^n \int_0^x \frac{1}{x^2 x^{2n}} \left(\int_0^x x^2 x^n R(x) dx \right) dx \quad (2.100)$$

where $E(x) = e^{\int \frac{2}{x} dx} = x^2$ and $C_1 = C$ is a constant and $C_2 = 0$.

The initial approximation is $R_0(x) = Cx^n$ (2.101)

Next, the first iterative value is

$$\begin{aligned}
R_1(x) &= -x^n \int_0^x \frac{1}{x^{2n+2}} \left(\int_0^x x^{n+2} R_0(x) dx \right) dx = -Cx^n \int_0^x \frac{1}{x^{2n+2}} \left(\int_0^x x^{n+2} x^n(x) dx \right) dx \\
&= \frac{-Cx^{n+2}}{(4n+6)}
\end{aligned} \tag{2.102}$$

The second iterative value is

$$\begin{aligned}
R_2(x) &= -x^n \int_0^x \frac{1}{x^{2n+2}} \left(\int_0^x x^{n+2} R_1(x) dx \right) dx \\
&= \frac{Cx^n}{4n+6} \int_0^x \frac{1}{x^{2n+2}} \left(\int_0^x \frac{x^{2n+5}}{(2n+5)} dx \right) dx \\
&= \frac{Cx^{n+4}}{(4n+6)(8n+20)}
\end{aligned} \tag{2.103}$$

In general, the solution for the differential equation (2.92) is

$$R_n(Br) = \sum_{k=0}^{\infty} C_n \frac{(-1)^k \Gamma(2n+2) \Gamma(n+k+1)}{\Gamma(n+1) \Gamma(k+1) \Gamma(2n+2k+1)} (Br)^{n+2k} \tag{2.104}$$

while the solution for angular part, viz., eq. (2.80) is just the Legendre polynomials

$$\Phi_n(\mu) = P_n(\mu) = \sum_{k=0}^n \frac{1}{2^k k!} \frac{d^k}{d\mu^k} (\mu^2 - 1)^k \tag{2.105}$$

The final solution of Eq. (2.77) is therefore

$$\phi(r, \mu) = \sum_{n=0}^{\infty} C_n R_n(Br) P_n(\mu) \tag{2.106}$$

2.6.5 Numerical Results for Hemispherical Symmetry

In order to provide numerical results, we adopt the same data as taken in Section 2.6.2.

According to ZF boundary condition, for the flux to vanish on the angular part (on the flat

surface) $\mu = 0$, the properties from Legendre's polynomial implies that the even amplitudes must be equal to zero.

On the other hand, applying the ZF boundary condition on the radial part

$$R_n(Br) = 0$$

The first zero calculated using Eq. (2.104) is $Ba_c = 4.4934$

This reduces the summation in Eq. (2.106) to the simple form

$$\phi(r, \mu) = C_1 R_1(Br) P_1(\mu) = \sum_{k=0}^{\infty} C_1 \frac{(-1)^k (6)(k+1)}{\Gamma(2k+4)} (Br)^{1+2k} \mu. \quad (2.107)$$

Hence, we obtain, for hemisphere the critical radius is $a_{c,ZF} = 15.085 \text{ cm}$. Since the flux is assumed to converge to zero at $a_c + 2D$ using the EBC, then $a_{c,EBC} = 13.185 \text{ cm}$.

2.6.6 Radiation Boundary Condition

After applying the two simple boundary conditions like ZF and EBC, the system yields inaccurate results. Now, we will apply radiation boundary condition (RBC), which gave more accurate results for the critical radius. We consider the two hemispheres of radius a separated by distance $2b$ from their flat surfaces. The condition can be written in the form as [39, 40]

$$n \cdot \nabla \phi = g(r) \phi \quad (2.108)$$

where $g(r)$ varies over surface, the condition on the curved surface is

$$\left. \frac{\partial \phi(r, \mu)}{\partial r} \right|_{r=a} = -g_1 \phi(a, \mu) \quad (2.109)$$

For the flat surface where $\theta = \frac{\pi}{2}$, the condition becomes

$$\left. \frac{1}{r} \frac{\partial \phi(r, \mu)}{\partial \mu} \right|_{\mu=0} = g_2 \phi(r, 0) \quad (2.110)$$

By Marshak's P1 boundary condition [39]

$$g_1 = \frac{1}{2D} \quad (2.111)$$

$$g_2 = \frac{g(b/a)}{2D} \quad (2.112)$$

where $g(x)$ is given by [36, 37]

$$g(x) = \frac{1 - 2 \int_0^1 d\mu \mu \exp \left(-f(x) \left(\frac{\sqrt{1-\mu^2}}{\mu} \right) \right)}{1 + 3 \int_0^1 d\mu \mu^2 \exp \left(-f(x) \left(\frac{\sqrt{1-\mu^2}}{\mu} \right) \right)}, \quad (2.113)$$

$$\text{with} \quad f(x) = \frac{x}{1+x} \left(\frac{2}{\pi} + \sqrt{2x} \right) \quad (2.114)$$

For a sphere $b = 0$ and hence $x = 0$, causing g and g_2 to vanish but in hemisphere, b and x go to infinity where g becomes unity (Table 3).

In order to solve, $\phi(r, \mu)$ we apply RBC on the flat surface

$$\frac{1}{r} \sum A_n R_n(Br) P'_n(0) = g_2 \sum A_n R_n(Br) P_n(0) \quad (2.115)$$

By properties of Legendre polynomials,

$$P'_n(0) = 0, \quad n \text{ is even}$$

$$P_n(0) = 0, \quad n \text{ is odd}$$

$$P_{2n}(0) = \frac{(-1)^n \Gamma(n+1/2)}{\sqrt{\pi} n!}, \quad n=0,1,2,\dots$$

$$P'_{2n+1}(0) = \frac{2(-1)^n \Gamma(n+3/2)}{\sqrt{\pi} n!}, \quad n=0,1,2,\dots$$

Eq. (2.115) reduces to

$$\frac{1}{r} \sum A_{2n+1} R_{2n+1}(Br) \frac{2(-1)^n \Gamma(n+3/2)}{\sqrt{\pi} n!} = g_2 \sum A_{2n} R_{2n}(Br) \frac{(-1)^n \Gamma(n+1/2)}{\sqrt{\pi} n!} \quad (2.116)$$

Using the recurrence relation

$$\begin{aligned} \sum_{n=0}^{\infty} R_{2n} \frac{(-1)^n \Gamma(n+1/2)}{\sqrt{\pi} n!} (2B(n+1/2)A_{2n+1} - g_2 A_{2n}) + \\ \sum_{n=0}^{\infty} A_{2n-1} (2nB) \frac{R_{2n}}{(4n+1)(4n-1)} \frac{(-1)^n \Gamma(n+1/2)}{\sqrt{\pi} n!} = 0 \end{aligned} \quad (2.117)$$

A_n , the amplitudes are related by

$$B(2n+1)A_{2n+1} - \frac{2nB}{(4n+1)(4n-1)} A_{2n-1} = g_2 A_{2n} \quad (2.118)$$

The odd order amplitudes can be written in terms of even one by

$$A_{2n+1} = \sum_{k=0}^n \gamma_{nk} A_{2k} \quad (2.119)$$

$$\text{where } \gamma_{nk} = \frac{(2n)!!(2k-1)!!(4k+1)!!}{(2k)!!(2n+1)!!(4n+1)!!} \quad (2.120)$$

Similarly, by applying RBC on curved surface

$$\sum_{n=0}^{\infty} A_n R'_n(Ba) P_n(\mu) = -g_1 \sum_{n=0}^{\infty} A_n R_n(Ba) P_n(\mu) \quad (2.121)$$

or

$$\sum_{n=0}^{\infty} A_n f_n P_n(\mu) = 0 \quad (2.122)$$

$$\text{where } f_n = \left(\frac{n}{a} + g_1 \right) R_n(Ba) - \frac{B}{(2n+3)} R_{2n+1}(Ba) \quad (2.123)$$

To make computational implementation, we introduce the shifted Legendre polynomial

$$P_n^*(\mu) = P_n(2\mu - 1) \quad (2.124)$$

which form a complete orthogonal set over $0 < \mu < 1$, while classical Legendre polynomial

$P_n(\mu)$ forms an orthogonal set over $-1 < \mu < 1$

$$P_n(\mu) = \sum_{k=0}^n \beta_{nk} P_k^*(\mu) \quad (2.125)$$

$$\text{where } \beta_{nk} = (2k+1) \int_0^1 d\mu P_n(\mu) P_k^*(\mu) \quad (2.126)$$

Hence, Eq. (2.122) becomes

$$\sum_{n=0}^{\infty} A_n f_n \sum_{k=0}^n \beta_{nk} P_k^*(\mu) = 0 \quad (2.127)$$

By interchanging order of summation, $\beta_{nk} = 0$ for $n < k$, we obtain

$$\sum_{k=0}^{\infty} \left(\sum_{n=0}^{\infty} \beta_{nk} f_n A_n \right) P_k^*(\mu) = 0 \quad (2.128)$$

$$\text{which concludes, } \sum_{n=0}^{\infty} \beta_{nk} f_n A_n = 0, \quad k = 0, 1, 2, \dots \quad (2.129)$$

Now we separate the even and odd amplitudes and with use of eq. (2.119),

$$\sum_{k=0}^{\infty} \hat{H}_{nk} A_{2n} = 0, \quad k = 0, 1, 2, \dots \quad (2.130)$$

$$\text{where } \hat{H}_{nk} = \beta_{2n,k} f_{2n} + \sum_{l=n}^{\infty} \beta_{2l+1,k} f_{2l+1} \gamma_{ln} \quad (2.131)$$

In order to get the numerical results by the cut-off value N , the infinite sum becomes

$$\sum_{n=0}^N \hat{H}_{nk} A_{2n} = 0, \quad k = 0, 1, 2, \dots, N \quad (2.132)$$

$$\text{where } \hat{H}_{nk} = \beta_{2n,k} f_{2n} + \sum_{l=n}^N \beta_{2l+1,k} f_{2l+1} \gamma_{ln} \quad (2.133)$$

Therefore, the series in the general solution contained $2N + 2$ terms

$$\phi(r, \mu) = \sum_{n=0}^{2N+1} A_n R_n(Br) P_n(\mu) \quad (2.134)$$

In order to calculate the amplitudes A_{2n} by Eq. (2.132), we obtained

$$\sum_{n=1}^N \hat{H}_{nk} A_{2n} = -\hat{H}_{0k} A_0 \quad (2.135)$$

$$\text{where } A_1 = 1 \text{ and } A_0 = 1/\gamma_{00} \quad (2.136)$$

The calculated flux is normalized to the volume averaged flux $\bar{\phi}$

$$\bar{\phi} = \frac{3}{a^3} \int_0^a dr r^2 \int_0^1 d\mu \phi(r, \mu) \quad (2.137)$$

where $a = 11.80396$ cm and using $N = 22$, the value of volume averaged flux is 0.633771.

Table 3: Critical Radius for Hemisphere in Two Different Boundary Conditions

| BC | ADM | Bessel Williams (2004) | Cassell and Khasawneh, Dababneh and Odibat HPM (2009) |
|----|-----|---------------------------|--|
|----|-----|---------------------------|--|

| | | | |
|-----|--------|----------|--------|
| ZF | 15.085 | 15.06 | 15.085 |
| EBC | 13.185 | 13.19 | 13.185 |
| RBC | 11.804 | 11.80397 | 11.804 |

The numerical solution for flux distribution of a hemisphere at different angles is shown graphically in Figure 5.

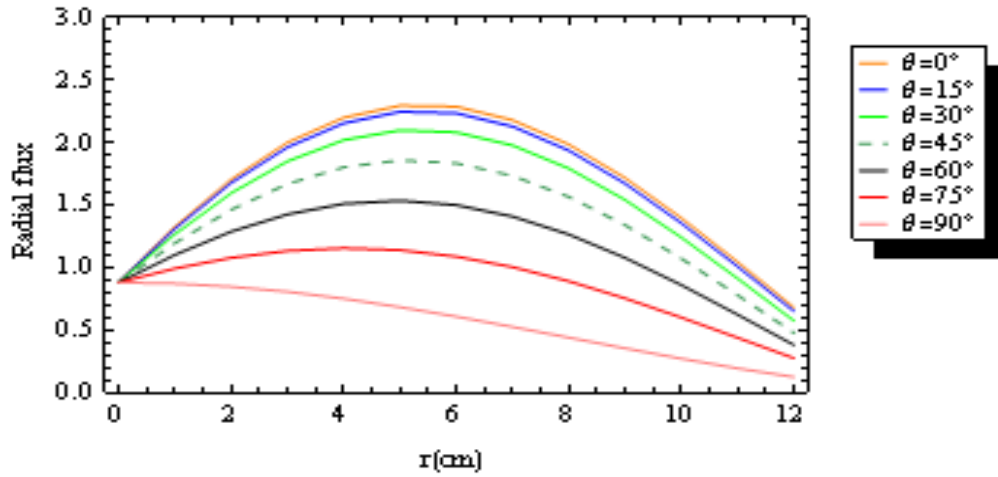


Fig. 5. Flux distribution across a Bare Hemisphere along different angles.

Using HAM and ADM, we successfully obtain the approximate solution of neutron flux for one-group diffusion equation [35] in the closed form of infinite convergent series in two symmetrical bodies.

2.7 Conclusion

In this Chapter, Variational Iteration Method and Modified Decomposition Method have been successfully applied to find the analytical approximate as well as numerical solutions of the Neutron Diffusion equation with fixed source. The decomposition method is straightforward, without restrictive assumptions and the components of the series solution can be easily computed using any mathematical symbolic package. The neutron diffusion equations in

symmetrical bodies like cylindrical reactor and hemisphere have been solved using Homotopy Analysis Method and Adomian Decomposition Method. The analytical approximate as well as numerical solutions of critical radius and flux distribution for bare hemisphere and cylindrical reactor have been also obtained very easily and accurately. The homotopy analysis method is a very powerful and efficient technique which yields analytical solutions for one-group neutron diffusion equation. The decomposition method is easy to compute any kind of equation by providing more convergent series in real physical problems, which can be solved with the help of any mathematical package. Moreover, it neither requires any type of discretization for variables nor does it affect computational round off errors. The computational size of fast convergence for series solution will be reduced. We can solve many functional equations such as ordinary, partial differential equations, integral equations and so many other equations using these analytical methods. It does not require enough memory space in computer, is free from rounding off errors and discretization of space variables. By using the excellence of these methods, we can obtain the solutions for diffusion and kinetic equations in the dynamic system of nuclear reactor.

CHAPTER 3

3.1 *Introduction*

In this chapter, the brief description for fractional calculus and the numerical solution for fraction neutron point kinetic equation are discussed. The efficient and accurate numerical computation for fractional neutron point kinetic equation (FNPKE) with different values of reactivity is introduced. Fractional Neutron Point Kinetic Model has been analyzed for the dynamic behavior of the neutron motion in which the relaxation time associated with a variation in the neutron flux involves a fractional order acting as exponent of the relaxation time, to obtain the best operation of a nuclear reactor dynamics. Results for neutron dynamic behavior for subcritical reactivity, supercritical reactivity and critical reactivity and also for different values of fractional order have been presented and compared with the classical neutron point kinetic (CNPKE).

3.2 *Brief Description for Fractional Calculus*

Fractional Calculus is three centuries old as the conventional calculus, but not very popular amongst science and or engineering community. The traditional integral and derivative are, to say the least, a staple for the technology professional, essential as a means of understanding and working with natural and artificial systems. Fractional Calculus is a branch of calculus that generalizes the derivative of a function to non-integer order. The beauty of this subject is that fractional derivatives are not a local property. The fractional differential equations appear more and more frequently in different research areas and engineering applications. In recent years, considerable

interest in fractional differential equations has been stimulated due to their numerous applications in the areas of physics and engineering. Many important phenomena in electromagnetics, acoustics, viscoelasticity, electrochemistry, control theory, neutron point kinetic model, anomalous diffusion, Brownian motion, signal and image processing, fluid dynamics and material science are well described by differential equations of fractional order.

Fractional calculus is a field of applied mathematics that deals with derivatives and integrals of arbitrary orders. It is also known as generalized integral and differential calculus of arbitrary order (Kilbas et al. [41] and Sabatier et al. [42]). Fractional calculus was described by Gorenflo and Mainardi [43] as the field of mathematical analysis which deals with investigation and applications of integrals and derivatives of arbitrary order. And many great mathematician (pure and applied) such as Abel, Caputo, Euler, Fourier, Grünwald, Hadamard, Hardy, Heaviside, Holmgren, Laplace, Leibniz, Letnikov, Liouville, Riemann, Riesz and Weyl made major contributions to the theory of fractional calculus. The history of fractional calculus was started at the end of the 17th century and the birth of fractional calculus was due to a letter exchange. At that time scientific journals did not exist and Scientist were exchange their information through letters. The first conference on fractional calculus and its applications was organized in June 1974 by Ross and held at university of new Haven.

In recent years, fractional calculus has become the focus of interest for many researchers in different disciplines of applied science and engineering because of the fact that a realistic modelling of a physical phenomenon can be successfully achieved by using fractional calculus. The fractional calculus has gained considerable importance during the past decades mainly due to its applications in diverse fields of science and engineering.

For the purpose of this paper the Caputo's definition of fractional derivative will be used, taking the advantage of Caputo's approach that the initial conditions for fractional differential equations [44] with Caputo's derivatives take on the traditional form as for integer-order differential equations. For that reason we need a reliable and efficient technique for the solution of fractional differential equations.

3.2.1 Definition - Riemann-Liouville integral and derivative operator

The concept of non-integer order of integration can be traced by the philosopher and creator of modern calculus G. W. Leibniz made some remarks on the meaning and possibility of fractional derivative of order $\frac{1}{2}$ in the late 17th century. However a rigorous investigation was first carried out by Liouville in a series of papers from 1832-1837, where he defined first fractional integral. Later investigations and further developments by many others led to the construction of the integral-based Riemann-Liouville fractional integral operator, which has been a valuable cornerstone in fractional calculus ever since. Prior to Liouville and Riemann, Euler took the first step in the study of fractional integration when he studied the simple case of fractional integrals of monomials of arbitrary real order in the heuristic fashion of time; it has been said to have lead him to construct the Gamma function for fractional powers of the factorial. An early attempt by Liouville was later purified by the Swedish mathematician Holmgren [45], who in 1865 made important contributions to the growing study of fractional calculus. But it was Riemann [46] who reconstructed it to fit Abel's integral equation, and thus made it vastly more useful. Today there exist many different forms of fractional integral operators, ranging from divided-difference types to infinite-sum types, but the Riemann-Liouville operator is still the most frequently used when fractional integration is performed.

The most frequently encountered definition of an integral of fractional order is the Riemann-Liouville integral [44], in which the fractional integral of order α (>0) is defined as

$$J^\alpha f(t) = \frac{1}{\Gamma(\alpha)} \int_0^t (t-\tau)^{\alpha-1} f(\tau) d\tau, \quad t > 0, \quad \alpha \in \mathbb{R}^+ \quad (3.1)$$

where \mathbb{R}^+ is the set of positive real numbers .

The gamma function Γ is defined by

$$\Gamma(n) = \int_0^\infty e^{-t} t^{n-1} dt \text{ and for real number } n, \Gamma(n) = 1.2...(n-1).$$

The Riemann-Liouville fractional derivative is defined by

$$D^\alpha f(t) = D^m J^{m-\alpha} f(t) = \frac{d^m}{dt^m} \left[\frac{1}{\Gamma(m-\alpha)} \int_0^t \frac{f(\tau)}{(t-\tau)^{\alpha-m+1}} d\tau \right], \quad m-1 < \alpha < m, \quad m \in \mathbb{N} \quad (3.2)$$

Left- Riemann-Liouville fractional derivative can be defined by

$${}_a D_t^\alpha f(t) = \frac{1}{\Gamma(n-\alpha)} \left(\frac{d}{dt} \right)^n \int_a^t (t-\tau)^{n-\alpha-1} f(\tau) d\tau \quad (3.3)$$

Right- Riemann-Liouville fractional derivative can be defined by

$${}_t D_b^\alpha f(t) = \frac{1}{\Gamma(n-\alpha)} \left(-\frac{d}{dt} \right)^n \int_t^b (\tau-t)^{n-\alpha-1} f(\tau) d\tau \quad (3.4)$$

Fractional Riemann-Liouville derivatives have various interesting properties. For example the fractional derivative of a constant is not zero, namely

$${}_a D_t^\alpha C = \frac{C(t-a)^{-\alpha}}{\Gamma(1-\alpha)} \text{ where } 0 < \alpha < 1, \quad \alpha \in \mathbb{R}^+ \quad (3.5)$$

3.2.2 Definition-Caputo Fractional Derivative

There is another option for computing fractional derivatives; the Caputo fractional derivative. It was introduced by M. Caputo in his paper in the year 1967. In contrast to the Riemann Liouville fractional derivative, when solving differential equations using

Caputo's definition [43, 44], it is not necessary to define the fractional order initial conditions. Caputo's definition is illustrated as follows

$$D_t^\alpha f(t) = J^{m-\alpha} D^m f(t) = \begin{cases} \frac{1}{\Gamma(m-\alpha)} \int_0^t (t-\tau)^{(m-\alpha-1)} \frac{d^m f(\tau)}{d\tau^m} d\tau, & \text{if } m-1 < \alpha < m, m \in \mathbb{N} \\ \frac{d^m f(t)}{dt^m}, & \text{if } \alpha = m, m \in \mathbb{N} \end{cases} \quad (3.6)$$

where the parameter α is the order of the derivative and is allowed to be real or even complex.

For the Caputo's derivative, we have

$$D^\alpha C = 0, \quad (C \text{ is a constant}) \quad (3.8)$$

$$D^\alpha t^\beta = \begin{cases} 0, & \beta \leq \alpha - 1 \\ \frac{\Gamma(\beta+1)t^{\beta-\alpha}}{\Gamma(\beta-\alpha+1)}, & \beta > \alpha - 1 \end{cases} \quad (3.9)$$

Similar to integer order differentiation Caputo's derivative is linear.

$$D^\alpha (\gamma f(t) + \delta g(t)) = \gamma D^\alpha f(t) + \delta D^\alpha g(t) \quad (3.10)$$

where γ and δ are constants, and satisfies so called Leibnitz's rule

$$D^\alpha (g(t)f(t)) = \sum_{k=0}^{\infty} \binom{\alpha}{k} g^{(k)}(t) D^{\alpha-k} f(t), \quad (3.11)$$

if $f(\tau)$ is continuous in $[0, t]$ and $g(\tau)$ has continuous derivatives sufficient number of times in $[0, t]$.

3.2.3 Grünwald- Letnikov definition of fractional derivatives

In mathematics, the Grünwald-Letnikov fractional order derivative is a basic extension of the derivative in fractional calculus that allows one to take the derivative a non-integer number of times. It was introduced by Anton Karl Grünwald (1838–1920) from Prague, in 1867, and by Aleksey Vasilievich Letnikov (1837-1888) in Moscow in 1868. Grünwald-Letnikov (GL) fractional derivative [41- 44] is defined by

$${}_a D_t^p f(t) = \lim_{\substack{h \rightarrow 0 \\ nh = t-a}} h^{-p} \sum_{r=0}^n \omega_r^p f(t - rh) \quad (3.12)$$

$$\text{where} \quad \omega_r^p = (-1)^r \binom{p}{r}$$

$$\omega_0^p = 1 \quad \text{and} \quad \omega_r^p = \left(1 - \frac{p+1}{r}\right) \omega_{r-1}^p, \quad r = 1, 2, \dots$$

3.2.4 Lemma

If $m-1 < \alpha < m, m \in \mathbb{N}$, then

$$D^\alpha J^\alpha f(t) = f(t) \quad (3.13)$$

and

$$J^\alpha D^\alpha f(t) = f(t) - \sum_{k=0}^{m-1} \frac{t^k}{k!} f^{(k)}(0+), \quad t > 0 \quad (3.14)$$

In the field of nuclear engineering, the neutron diffusion and point kinetic equations are most vital models; they have been included to countless studies and applications under neutron dynamics and its effects. By the help of neutron diffusion concept we understand the complex behaviour of average neutron motion. From many reactor studies, we get the

idea that neutron motion is a diffusion process. It is also assumed that the neutrons are in average motion diffused at very low or high neutron density. The concept of neutron transport as a diffusion process has only limited validation due to that neutron stream at relatively large distances between interactions. The process of neutron diffusion takes place in a very highly heterogeneous hierarchical configuration. Here, we propose a numerical scheme for the solution of fractional diffusion model as a constitutive equation of neutron current density. Fractional point kinetic equation has proved particularly useful in the context of anomalous slow diffusion.

3.3 *Fractional Neutron Point Kinetic Equation and its Derivation*

The diffusion theory model of neutron transport has played a crucial role in reactor theory since it is simple enough to allow scientific insight, and it is sufficiently realistic to study many important design problems. The mathematical methods used to analyze such a model are the same as those applied in more sophisticated methods such as multi-group neutron transport theory. The neutron flux (ψ) and current (J) in the diffusion theory model are related in a simple way under certain conditions. This relationship between ψ and J is identical in form to a law used in the study of diffusion phenomena in liquids and gases: Fick's law. The use of this law in reactor theory leads to the diffusion approximation, which is a result of a number of simplifying assumptions. On the other hand, higher-order neutron transport codes have always been deployed in nuclear engineering for mostly time-independent problems out-of-core shielding calculations.

Fractional point neutron kinetics (FPNK) model³ is based on the diffusion theory using all known theoretical arguments. The scope of the FPNK is to describe the neutron transient behavior in a highly heterogeneous configuration in nuclear reactors, in presence of strong neutron absorbers in the fuel, control rods and chemical shim in the coolant. In summary, there are many interesting problems to consider from the point of view of the fractional differential equations (FDEs), the challenge is the modeling and simulation of the new generation of nuclear reactors, as well as advanced molten salt reactor [47], where the old paradigms can no longer be valid.

The fractional model retains the main dynamic characteristics of the neutron motion. The physical interpretation of the fractional order is related with non-Fickian effects from the neutron diffusion equation point of view.

To derive the fractional neutron point kinetic (NPK) equation [48-50] for point reactor, we consider with a source term given by

$$\frac{\tau^\kappa}{\nu} \frac{\partial^{\kappa+1} \phi}{\partial t^{\kappa+1}} + \tau^\kappa \sum_a \frac{\partial^\kappa \phi}{\partial t^\kappa} + \frac{1}{\nu} \frac{\partial \phi}{\partial t} = S - \sum_a \phi + D \nabla^2 \phi + \tau^\kappa \frac{\partial^\kappa S}{\partial t^\kappa} \quad (3.15)$$

The one-group source term S is given by [23]

$$S = (1 - \beta) k_\infty \sum_a \phi + \sum_{i=1}^m \lambda_i \hat{C}_i \quad (3.16)$$

where $\phi \equiv$ Neutron flux

$S \equiv$ Source term

$\nu \equiv$ Average no. of neutrons emitted per fission

$D \equiv$ Diffusion coefficient

³ S. Saha Ray and A. **Patra**, 2012, An Explicit Finite Difference Scheme for numerical solution of fractional neutron point kinetic equation, **Annals of Nuclear Energy** (Elsevier), Vol. 41, pp. 61-66.

$\Sigma_a \equiv$ Macroscopic Absorption cross section

$k_\infty \equiv$ Effective multiplication factor

$\phi = \phi(r, t)$, $S = S(r, t)$ and $\hat{C}_i = \hat{C}_i(r, t)$ are all functions of position and time.

By substituting eq. (3.16) in eq. (3.15), we obtain,

$$\begin{aligned} \frac{\tau^\kappa}{\nu} \frac{\partial^{\kappa+1} \phi}{\partial t^{\kappa+1}} + \tau^\kappa [\Sigma_a + (1 - \beta) k_\infty \Sigma_a] \frac{\partial^\kappa \phi}{\partial t^\kappa} + \frac{1}{\nu} \frac{\partial \phi}{\partial t} = \\ [(1 - \beta) k_\infty \Sigma_a - \Sigma_a] \phi + D \nabla^2 \phi + \sum_{i=1}^m \lambda_i \hat{C}_i + \tau^\kappa \sum_{i=1}^m \left(\lambda_i \frac{\partial^\kappa \hat{C}_i}{\partial t^\kappa} \right) \end{aligned} \quad (3.17)$$

According to Glasstone and Sesonske (1981), $\nabla^2 \phi$ is replaced by $-B_g^2 \phi$, where B_g^2 is geometric buckling. Then eq. (3.17) can be written as

$$\begin{aligned} \frac{\tau^\kappa}{\nu} \frac{\partial^{\kappa+1} \phi}{\partial t^{\kappa+1}} + \tau^\kappa [\Sigma_a + (1 - \beta) k_\infty \Sigma_a] \frac{\partial^\kappa \phi}{\partial t^\kappa} + \frac{1}{\nu} \frac{\partial \phi}{\partial t} = \\ [(1 - \beta) k_\infty \Sigma_a - \Sigma_a - D B_g^2] \phi + \sum_{i=1}^m \lambda_i \hat{C}_i + \tau^\kappa \sum_{i=1}^m \left(\lambda_i \frac{\partial^\kappa \hat{C}_i}{\partial t^\kappa} \right) \end{aligned} \quad (3.18)$$

Now by using $\phi = \nu n(t)$, eq. (3.18) leads to

$$\begin{aligned} \tau^\kappa \frac{d^{\kappa+1} n(t)}{dt^{\kappa+1}} + \tau^\kappa [\Sigma_a + (1 - \beta) k_\infty \Sigma_a] \nu \frac{d^\kappa n(t)}{dt^\kappa} + \frac{dn(t)}{dt} = \\ [(1 - \beta) k_\infty \Sigma_a - \Sigma_a - D B_g^2] \nu n(t) + \sum_{i=1}^m \lambda_i \hat{C}_i + \tau^\kappa \sum_{i=1}^m \left(\lambda_i \frac{\partial^\kappa \hat{C}_i}{\partial t^\kappa} \right) \end{aligned} \quad (3.19)$$

In order to solve the fractional point kinetic equation, we consider the following definition for nuclear parameters [23, 51]

$$L^2 = \frac{D}{\Sigma_a} \equiv \text{Diffusion area}$$

$$l = \frac{1}{\nu \Sigma_a (1 + L^2 B_g^2)} \equiv \text{Prompt neutron lifetime}$$

$$\Lambda = \frac{1}{k_{\infty} \nu \Sigma_a} \equiv \text{Neutron generation time}$$

$$k_{eff} = \frac{k_{\infty}}{1 + L^2 B_g^2} \equiv \text{Effective multiplication factor}$$

$$\rho = \frac{k_{eff} - 1}{k_{eff}} \equiv \text{Reactivity}$$

The fractional equation for NPK equation is given by [49]

$$\tau^{\kappa} \frac{d^{\kappa+1} n}{dt^{\kappa+1}} + \tau^{\kappa} \left(\frac{1}{l} + \frac{(1-\beta)}{\Lambda} \right) \frac{d^{\kappa} n}{dt^{\kappa}} + \frac{dn}{dt} = \left(\frac{\rho - \beta}{\Lambda} \right) n + \sum_{i=1}^m C_i \lambda_i + \tau^{\kappa} \sum_{i=1}^m \left(\lambda_i \frac{d^{\kappa} C_i}{dt^{\kappa}} \right) \quad (3.20)$$

where τ is the relaxation time, κ is the anomalous diffusion order (for sub-diffusion process : $0 < \kappa < 1$; while for super diffusion process : $1 < \kappa < 2$), n is the neutron density, C_i is the concentration of the i^{th} neutron delayed precursor, l is the prompt- neutron lifetime for infinite media , β is the fraction of delayed neutrons.

when $\tau^{\kappa} \rightarrow 0$, the classical NPK equation can be obtained as

$$\frac{dn}{dt} = \left(\frac{\rho - \beta}{\Lambda} \right) n + \sum_{i=1}^m C_i \lambda_i \quad (3.21)$$

The net rate of formation of the precursor of delayed neutrons corresponding to the i^{th} group is given by

$$\frac{dC_i}{dt} = \left(\frac{\beta_i}{\Lambda} \right) n - \lambda_i C_i \quad (3.22)$$

Eq. (3.20) and eq. (3.22) describe the neutron dynamics process in nuclear reactor and the delayed neutrons precursor of the i -th group respectively.

The numerical approximation of the solution of the fractional neutron point kinetic model is obtained applying the numerical method like Explicit Finite Difference Method [13, 52].

Considering one-group of delayed neutrons, the fractional NPK equation and initial conditions are given by

$$\tau^\kappa \frac{d^{\kappa+1}n}{dt^{\kappa+1}} + \tau^\kappa \left(\frac{1}{l} + \frac{(1-\beta)}{\Lambda} \right) \frac{d^\kappa n}{dt^\kappa} + \frac{dn}{dt} = \left(\frac{\rho - \beta}{\Lambda} \right) n + \lambda C + \lambda \tau^\kappa \frac{d^\kappa C}{dt^\kappa} \quad (3.23)$$

where $0 < \kappa \leq 2$

$$\text{with } n(0) = n_0 \quad (3.24)$$

The precursor concentration balance equation is

$$\frac{dC}{dt} = \frac{\beta n}{\Lambda} - \lambda C \quad (3.25)$$

$$\text{with } C(0) = C_0 = \frac{\beta}{\lambda \Lambda} n_0 \quad (3.26)$$

The initial conditions for fractional neutron model are presented by

$$n(0) = n_0 = 1$$

$$\left. \frac{d^{\kappa+1}n}{dt^{\kappa+1}} \right|_{t=0} = 0$$

$$\left. \frac{d^\kappa n}{dt^\kappa} \right|_{t=0} = 0 \quad (3.27)$$

In order to analyze the effect of anomalous diffusion order (κ) and relaxation time (τ) on the behavior of the neutron density, the numerical model was implemented for the solution of kinetic equation through the simulation in a computer program.

The nuclear parameters used were obtained from [24, 53],

$$\beta = \sum_{i=1}^6 \beta_i = 0.007$$

$$\lambda = \frac{\beta}{\sum_{i=1}^6 \frac{\beta_i}{\lambda_i}} = 0.0810958 s^{-1}$$

where β_i and λ_i are presented in Table 1, the parameter value for l was obtained from Kinard and Allen [53] $\Lambda = 0.002 s$

$$l = 0.00024 s$$

$$\tau^\kappa = 10^{-4} s^\kappa$$

where $C_0 = 43.1588$ and $n_0 = 1$.

Table-1: Neutron delayed fractions and decay constants [53]

| i^{th} Group | β_i | λ_i |
|-----------------------|-----------|-------------|
| Group 1 | 0.000266 | 0.0127 |
| Group 2 | 0.001491 | 0.0317 |
| Group 3 | 0.001316 | 0.1550 |
| Group 4 | 0.002849 | 0.3110 |
| Group 5 | 0.0008960 | 1.4000 |
| Group 6 | 0.000182 | 3.8700 |

A series of numerical computations are carried out by using Explicit Finite Difference in order to obtain a best approximation for nuclear dynamics of fractional NPK model. We considered four cases of anomalous diffusion order (κ), viz. $\kappa = 0.99$, $\kappa = 0.98$, $\kappa = 0.97$ and $\kappa = 0.96$ for relaxation time $\tau^\kappa = 10^{-4} s^\kappa$ ($s \equiv 1 \text{ second}$).

3.4 Application of Explicit Finite Difference Scheme for Fractional Neutron Point Kinetic Equation

For the fractional model (3.23)-(3.26), let us take the time step size h . Using the definition of GL fractional derivative, the numerical approximation of the eq. (3.23)-(3.26), in view of the research work [13, 52], is

$$\begin{aligned} & \tau^\kappa h^{-(\kappa+1)} \sum_{j=0}^m \omega_j^{\kappa+1} n_{m-j} + \tau^\kappa \left[\frac{1}{l} + \frac{(1-\beta)}{\Lambda} \right] h^{-\kappa} \sum_{j=0}^m \omega_j^\kappa n_{m-j} + h^{-1} [n_m - n_{m-1}] \\ & = \left(\frac{\rho - \beta}{\Lambda} \right) n_m + \lambda C_m + \lambda \tau^\kappa h^{-\kappa} \sum_{j=0}^m \omega_j^\kappa C_{m-j} \end{aligned} \quad (3.28a)$$

For the precursor concentration balance equation the scheme is

$$h^{-1} [C_m - C_{m-1}] = \frac{\beta n_m}{\Lambda} - \lambda C_m \quad (3.28b)$$

where $n_m = n(t_m) \equiv m$ -th approximation for neutron density at time t_m , $C_m = C(t_m) \equiv m$ -th approximation for precursor concentration at time t_m . Here, $n(0) = n_0 = 1$, $C_0 = \frac{\beta n_0}{\lambda \Lambda}$,

$$t_m = mh, \quad m = 0, 1, 2, \dots \quad \text{and} \quad \omega_j^\kappa = (-1)^j \binom{\kappa}{j}, \quad j = 0, 1, 2, 3, \dots$$

Now, eq. (3.28a) and eq. (3.28b) can be written respectively as

$$\begin{aligned}
n_m - n_{m-1} = & h \left(\frac{\rho - \beta}{\Lambda} \right) n_m + \lambda h C_m + \lambda \tau^\kappa h^{1-\kappa} \sum_{j=0}^m \omega_j^\kappa C_{m-j} \\
& - \tau^\kappa h^{-\kappa} \sum_{j=0}^m \omega_j^{\kappa+1} n_{m-j} - \tau^\kappa \left[\frac{1}{l} + \frac{(1-\beta)}{\Lambda} \right] h^{1-\kappa} \sum_{j=0}^m \omega_j^\kappa n_{m-j} \\
C_m - C_{m-1} = & \frac{h\beta n_m}{\Lambda} - \lambda h C_m
\end{aligned} \tag{3.29}$$

The above eq. (3.29) leads to implicit numerical iteration scheme. However, in this present work, we propose an explicit numerical scheme which leads from the time layer t_{m-1} to t_m as follows

$$\begin{aligned}
n_m = n_{m-1} + & h \left(\frac{\rho - \beta}{\Lambda} \right) n_{m-1} + \lambda h C_{m-1} + \lambda \tau^\kappa h^{1-\kappa} C_{m-1} + \lambda \tau^\kappa h^{1-\kappa} \sum_{j=1}^m \omega_j^\kappa C_{m-j} - \tau^\kappa h^{-\kappa} n_{m-1} \\
& - \tau^\kappa h^{-\kappa} - \tau^\kappa \left[\frac{1}{l} + \frac{(1-\beta)}{\Lambda} \right] h^{1-\kappa} n_{m-1} - \tau^\kappa \left[\frac{1}{l} + \frac{(1-\beta)}{\Lambda} \right] h^{1-\kappa} \sum_{j=1}^m \omega_j^\kappa n_{m-j}
\end{aligned} \tag{3.30}$$

where $m = 1, 2, 3, \dots$.

Precursor concentration balance equation is

$$C_m = C_{m-1} + \frac{h\beta n_{m-1}}{\Lambda} - \lambda h C_{m-1}, \quad m = 1, 2, 3, \dots \tag{3.31}$$

3.5 Analysis for stability of Numerical Computation

The stability of the numerical computation is calculated by taking the different time-step size h with different values of the anomalous diffusion order κ and the relaxation time τ . In order to obtain a stable result, a set of time-step sizes are considered by trial-and-error for different values of κ and τ^κ .

Many numerical experiments have been done for getting a better solution for fractional NPK. In the present numerical study, we consider $\kappa=0.99$, $\kappa=0.98$, $\kappa=0.97$ and $\kappa=0.96$ for relaxation time $\tau^\kappa = 10^{-4} s^\kappa$. The values of time-step size h are taken between $0.01 \leq h \leq 0.05$. The simulation time was considered as 1s. The stability criterion in this analysis is related with 1% of the relative error to $n_0 = 1$ at 1s for simulation time.

$$1\% \geq \left| \frac{n_f - n_0}{n_f} \right| \times 100$$

where n_f is the neutron density which is calculated from fractional model.

To exhibit the behavior of neutron density with $\tau^\kappa = 10^{-4} s^\kappa$ and $\kappa=0.99$, we consider h in the interval $[0.01s, 0.05s]$. By stability criteria, the relative error is 0.40% at $h=0.01s$, 0.402% at $h=0.025s$ and 0.405% at $h=0.05s$. To examine the behavior of neutron density with $\tau^\kappa = 10^{-4} s^\kappa$ and $\kappa=0.98$, we consider h in the interval $[0.01s, 0.05s]$ where the curves are very similar with $\kappa=0.99$. In this case, the relative error is 0.39% at $h=0.01s$, 0.399 % at $h=0.025s$ and 0.401% at $h=0.05s$. Thus, for numerical computation, we can increase the time-step size higher with respect to $\kappa=0.99$. It can be shown the neutron density behavior with $\tau^\kappa = 10^{-4} s^\kappa$ and $\kappa=0.97$, considering h in the interval $[0.01s, 0.05s]$, the curves are very similar to $\kappa=0.99$, $\kappa=0.98$ respectively. For the case $\kappa=0.97$, the numerical scheme is also stable for time-step size $h= 0.01s$ whose corresponding relative error is 0.39%. For the case when $\kappa=0.96$ and h in the interval $[0.01s, 0.05s]$, the relative error is 0.399% at $h=0.01s$, 0.392 % at $h=0.025s$ and 0.395% at $h=0.05s$. Therefore, the above numerical experiment confirms the stability of our proposed numerical scheme for the solution of fractional NPK equation.

3.6 Numerical Experiments with Change of Reactivity

The behavior of the fractional model with reactivity changes [49] is cited graphically in this section. The neutron density is analyzed by taking different values for anomalous diffusion order [49]. In the present analysis, we have taken the time step size $h = 0.01$, $h = 0.025$ and $h = 0.05$. The numerical experiments involve the insertion of three reactivity steps:

- Case-I: $\rho = 0.003$ (Positive Reactivity for Supercritical Reactor)
- Case-II: $\rho = 0$ (Reactivity for Critical Reactor)
- Case-III: $\rho = -0.003$ (Negative Reactivity for Subcritical Reactor)

The fractional model was compared with a classical solution obtained by [22-24, 32]

$$n(t) = n_0 \left[\frac{\beta}{\beta - \rho} e^{\lambda \rho t / (\beta - \rho)} - \frac{\rho}{\beta - \rho} e^{-(\beta - \rho)t / \Lambda} \right]$$

The anomalous diffusion order considered for this numerical scheme are $\kappa = 0.99$, $\kappa = 0.98$, $\kappa = 0.97$ and $\kappa = 0.96$ for relaxation time $\tau^\kappa = 10^{-4} s^\kappa$. The relaxation time increases when κ increases.

Case I: Results of Positive Reactivity for Super-Critical Reactor

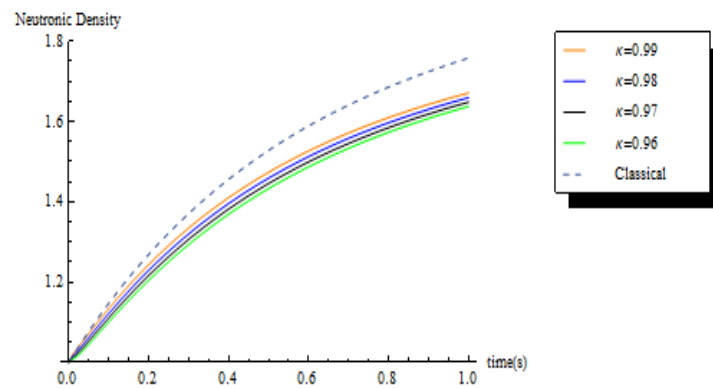


Fig.3.6.1. Comparison of Neutron Density behavior for Fractional and Classical NPK

for $\rho = 0.003$ $h = 0.01$, $\tau^\kappa = 10^{-4} s^\kappa$ with $\kappa = 0.99$, $\kappa = 0.98$, $\kappa = 0.97$ and $\kappa = 0.96$.

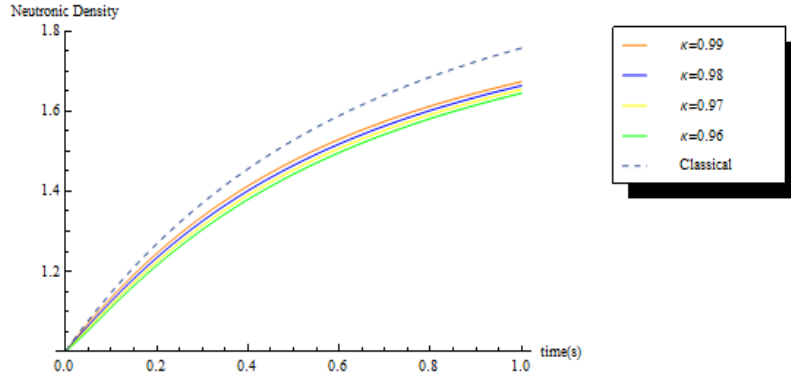


Fig.3.6.2. Comparison of Neutron Density behavior for Fractional and Classical NPK

for $\rho = 0.003$, $h = 0.025$, $\tau^\kappa = 10^{-4} s^\kappa$ with $\kappa = 0.99$, $\kappa = 0.98$, $\kappa = 0.97$ and $\kappa = 0.96$.

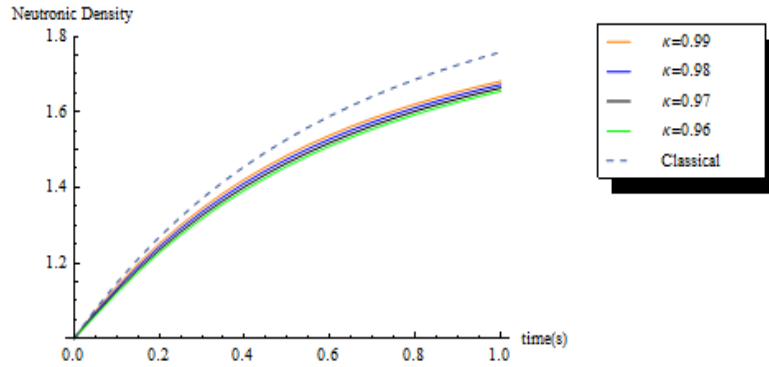


Fig.3.6.3. Comparison of Neutron Density behavior for Fractional and Classical NPK

for $\rho = 0.003$, $h = 0.05$, $\tau^\kappa = 10^{-4} s^\kappa$ with $\kappa = 0.99$, $\kappa = 0.98$, $\kappa = 0.97$ and $\kappa = 0.96$.

Case II: Results of Reactivity for Critical Reactor

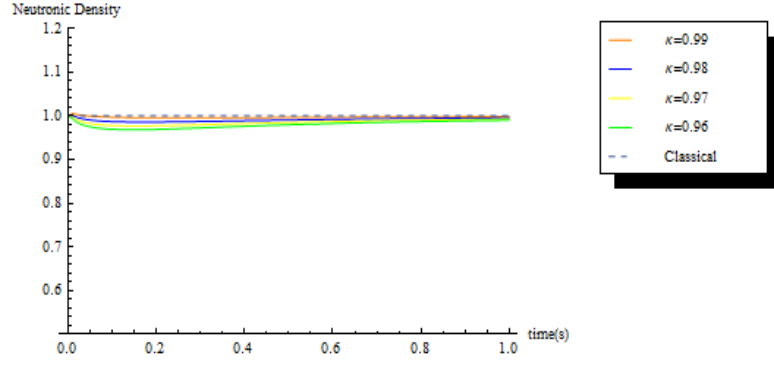


Fig.3.6.4. Comparison of Neutron Density behavior for Fractional and Classical NPK for $\rho = 0, h = 0.01, \tau^\kappa = 10^{-4} s^\kappa$ with $\kappa = 0.99, \kappa = 0.98, \kappa = 0.97$ and $\kappa = 0.96$.

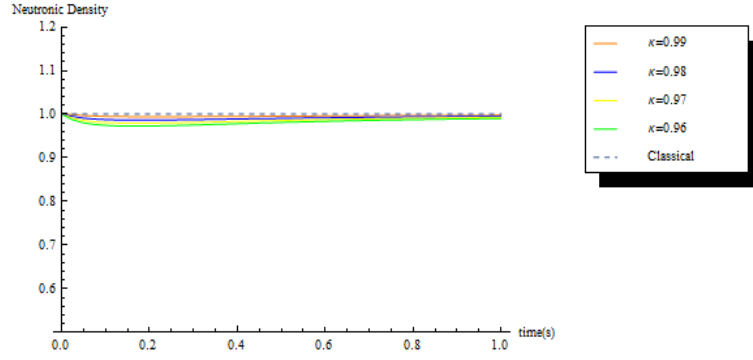


Fig.3.6.5. Comparison of Neutron Density behavior for Fractional and Classical NPK for $\rho = 0, h = 0.025, \tau^\kappa = 10^{-4} s^\kappa$ with $\kappa = 0.99, \kappa = 0.98, \kappa = 0.97$ and $\kappa = 0.96$.

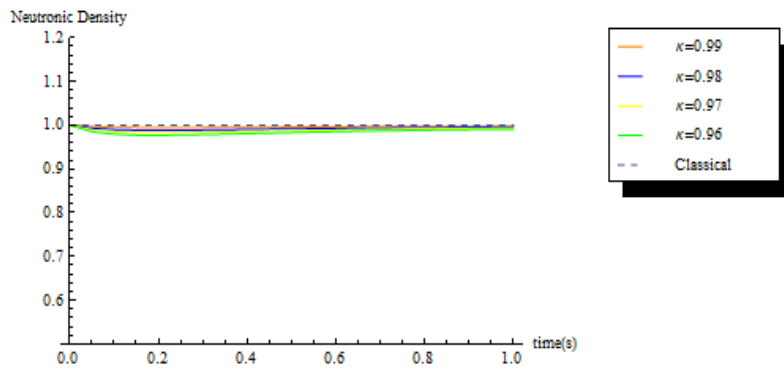


Fig.3.6.6. Comparison of Neutron Density behavior for Fractional and Classical NPK for $\rho = 0, h = 0.05, \tau^\kappa = 10^{-4} s^\kappa$ with $\kappa = 0.99, \kappa = 0.98, \kappa = 0.97$ and $\kappa = 0.96$.

Case III: Results of Negative Reactivity for Sub-Critical Reactor

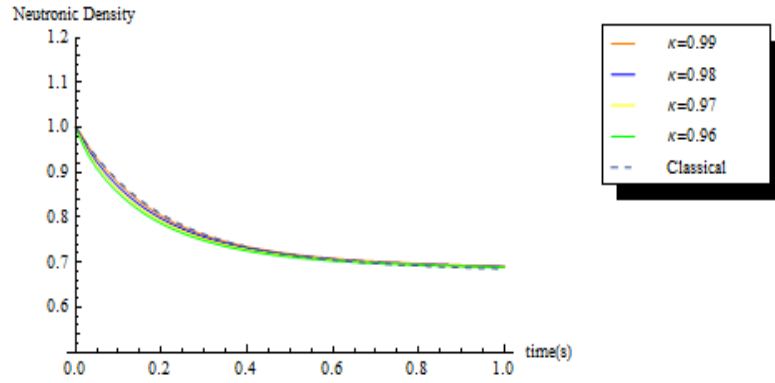


Fig.3.6.7. Comparison of Neutron Density behavior for Fractional and Classical NPK for

$\rho = -0.003$, $h = 0.01$, $\tau^\kappa = 10^{-4} s^\kappa$ with $\kappa = 0.99$, $\kappa = 0.98$, $\kappa = 0.97$ and $\kappa = 0.96$.

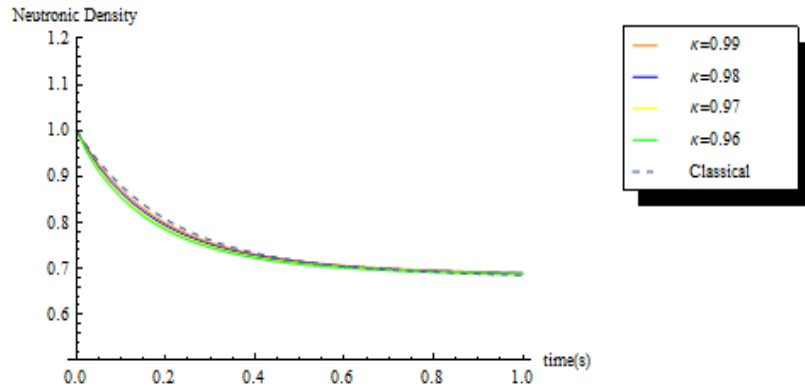


Fig.3.6.8. Comparison of Neutron Density behavior for Fractional and Classical NPK for

$\rho = -0.003$, $h = 0.025$, $\tau^\kappa = 10^{-4} s^\kappa$ with $\kappa = 0.99$, $\kappa = 0.98$, $\kappa = 0.97$ and $\kappa = 0.96$.

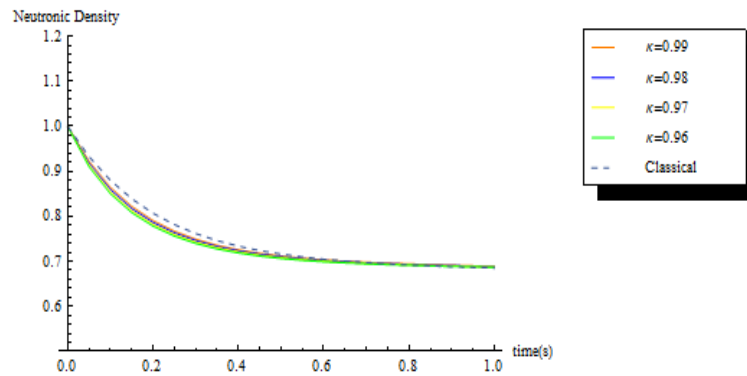


Fig.3.6.9. Comparison of Neutron Density behavior for Fractional and Classical NPK for $\rho = -0.003, h = 0.05, \tau^\kappa = 10^{-4} s^\kappa$ with $\kappa = 0.99, \kappa = 0.98, \kappa = 0.97$ and $\kappa = 0.96$.

These results exhibit the neutron dynamic behavior for positive reactivity for supercritical reactor as shown in fig. 3.6.1-3.6.3, critical reactor in fig. 3.6.4-3.6.6 and subcritical reactor in fig. 3.6.7-3.6.9 at negative reactivity for different values of time length steps and relaxation time. For critical reactor at $\rho = 0$, solution for the fractional neutron point kinetic equation coincides with classical solution. It is also compared with the classical NPK model. It can be observed from above figures (Figs. 3.6.1- Figs. 3.6.3) for positive reactivity and negative reactivity (Figs 3.6.7- Figs. 3.6.9) that the obtained results in the present numerical scheme are in good agreement with fig. 8.18 (for positive reactivity $\rho = 0.003$) and fig. 8.21 (for negative reactivity $\rho = -0.003$) obtained in [49]. In comparison to Detrended Fluctuation Analysis (DFA) method proposed by Espinosa-Paredes et al. [49], this Explicit Finite difference scheme is more convenient to use and efficient to calculate the numerical solution for fractional NPK Model. It is easily computed by using any mathematical software package having fewer rounds off errors.

In [49], Espinosa- Paredes et al. have proposed a solution procedure which has been inherited from Edwards et al. [54]. In order to apply numerical approximation method for the solution of fractional point kinetic equation, they discretized fractional derivative using Diethelm's method [55, 56]. In order to solve fractional neutron point kinetic equation, they used the numerical algorithm given by Edwards et al. [54]. In that numerical scheme, they represented the fractional kinetic model as a multi-term high order linear fractional differential equation. Then, it has been converted into a system of ordinary and fractional differential equation. In contrast to their method, in the present numerical scheme fractional derivative has been discretized by Grunwald- Letnikov derivative and the

fractional point kinetic equation has been converted directly into finite difference equation. Then it has been adjusted in the form of Explicit Finite Difference scheme. It is very much clear that, the present numerical scheme require less number of computational effort in compared to Espinosa-Paredes et al. [49].

3.7 Conclusion

In the present chapter, the dynamics of neutron fractional point kinetic equation were studied. In this article, the numerical solution for one-group delayed neutron fractional point kinetic equation was determined by Explicit Finite Difference Method. The three cases for change of reactivity have been discussed with respect to nuclear reactors in this point kinetic model. The numerical experiments including comparison with classical NPK model were carried out for both positive and negative reactivity for different values of fractional order κ . The fractional model retains the main characteristics of neutron motion where relaxation time associated with rapid variation in neutron flux contains a fractional exponent to obtain the best approximation for nuclear reactor dynamics. The procedure of the numerical approximations to the solution of fractional NPK model is represented graphically using mathematical software. The numerical solutions obtained from Explicit Finite Difference exhibit close behaviour with Classical NPK model. It has been also observed that the obtained results in the present method are in good agreement with those obtained in [49]. This numerical method is very efficient and convenient technique for solving fractional NPK model.

CHAPTER 4

4.1. *Introduction*

In the dynamical system of a nuclear reactor, the neutron point-kinetic equations are the coupled linear differential equations that are used to determine neutron density and delayed neutron precursor concentrations. These kinetic equations are the most vital model in nuclear engineering. The modelling of these equations involves the use of time dependent parameters [32]. The reactivity function and neutron source term are the parametric quantities of this essential system. The neutron density and delayed neutron precursor concentrations differ randomly with respect to time. At high power levels, the random behaviour is imperceptible. But at low power levels, such as at the beginning, random fluctuations in the neutron density and neutron precursor concentrations can be crucial. The proposed technique MDTM (Multi-step differential transform method) that we have used in this research work is based on a Taylor series expansion, which provides a solution in terms of convergent series with easily computable components. Here both classical and fractional order neutron point-kinetic equations have been analysed over step, ramp and sinusoidal reactivity functions. Fractional calculus generates the derivative and anti-derivative operations of differential and integral calculus [57-59] from non-integer orders to the entire complex plane. The semi-analytical numerical technique that we applied in this research work, is the most transparent method available for the solution of classical as well as fractional neutron point kinetic equations.

4.2. *Application of MDTM to classical Neutron Point Kinetic Equation*

In this section we consider the classical integer order neutron point kinetic equations for m delayed groups as follows [24, 53]

$$\frac{dn(t)}{dt} = \left[\frac{\rho(t) - \beta}{l} \right] n(t) + \sum_{i=1}^m \lambda_i c_i + S(t) \quad (4.1)$$

$$\frac{dc_i(t)}{dt} = \frac{\beta_i}{l} n(t) - \lambda_i c_i(t), \quad i = 1, 2, \dots, m \quad (4.2)$$

where

$n(t) \equiv$ Time-dependent neutron density, $c_i(t) \equiv i^{th}$ precursor density, $\rho(t) \equiv$ time-dependent reactivity function, $\beta_i \equiv i^{th}$ delayed fraction and $\beta = \sum_{i=1}^m \beta_i \equiv$ Total delayed fraction, $l \equiv$ Neutron generation time, $\lambda_i \equiv i^{th}$ group decay constant and $S(t) \equiv$ neutron source function.

The classical neutron point kinetic equation is considered in matrix form as follows [60]

$$\frac{d\vec{x}(t)}{dt} = A\vec{x}(t) + B(t)\vec{x}(t) + \vec{S}(t), \quad \text{where } \vec{x}(t) = \begin{bmatrix} n(t) \\ c_1(t) \\ c_2(t) \\ \vdots \\ c_m(t) \end{bmatrix} \quad (4.3)$$

with initial condition $\vec{x}(0) = \vec{x}_0$.

Here, we define A as:

$$A = \begin{bmatrix} \frac{-\beta}{l} & \lambda_1 & \lambda_2 & \cdots & \lambda_m \\ \frac{\beta_1}{l} & -\lambda_1 & 0 & \cdots & 0 \\ \frac{\beta_2}{l} & 0 & -\lambda_2 & \ddots & \vdots \\ \vdots & \vdots & \ddots & \ddots & 0 \\ \frac{\beta_m}{l} & 0 & \cdots & 0 & -\lambda_m \end{bmatrix}_{(m+1) \times (m+1)}$$

$B(t)$ can be expressed as:

$$B(t) = \begin{bmatrix} \frac{\rho(t)}{l} & 0 & 0 & \cdots & 0 \\ 0 & 0 & 0 & \cdots & 0 \\ 0 & 0 & 0 & \ddots & \vdots \\ \vdots & \vdots & \ddots & \ddots & 0 \\ 0 & 0 & \cdots & 0 & 0 \end{bmatrix}_{(m+1) \times (m+1)}$$

and $\vec{S}(t)$ is defined as:

$$\vec{S}(t) = \begin{bmatrix} q(t) \\ 0 \\ 0 \\ \vdots \\ 0 \end{bmatrix}, \text{ where } q(t) \text{ is the time-dependent neutron source term.}$$

In this section, we will apply MDTM to obtain the solution for classical neutron point kinetic equation⁴ (4.3).

Multi-step differential transform method can be described as follows:

Let us consider the following nonlinear initial value problem

$$f(t, u, u', \dots, u^{(p)}) = 0, \quad u^{(p)} \text{ is } p^{\text{th}} \text{ derivative of } u \quad (4.4)$$

subject to the initial conditions $u^{(k)}(0) = c_k$, for $k = 0, 1, \dots, p-1$

We find the solution over the interval $[0, T]$. The approximate solution of the initial value problem can be expressed by the finite series,

$$u(t) = \sum_{m=0}^M a_m t^m, \quad t \in [0, T] \quad (4.5)$$

Assume that the interval $[0, T]$ is divided into N subintervals $[t_{n-1}, t_n]$, $n = 1, 2, \dots, N$ of equal step size $h = T/N$ by using the node point $t_n = nh$. The main idea of multi-step DTM is to

⁴ **A. Patra** and S. Saha Ray, 2013, "Multi-step Differential Transform method for Numerical Solution of Classical Neutron Point Kinetic Equation", **Computational Mathematics and Modeling** (Springer), Vol. 24, No. 4, 604-615.

apply first DTM to eq. (4.3) over the interval $[0, t_1]$, we obtain the following approximate solutions

$$u_1(t) = \sum_{m=0}^{M_1} a_{1m} t^m, \quad t \in [0, t_1] \quad (4.6)$$

using the initial conditions $u_1^{(k)}(0) = c_k$. For $n \geq 2$ and at each subinterval $[t_{n-1}, t_n]$ we use the initial conditions $u_n^{(k)}(t_{n-1}) = u_{n-1}^{(k)}(t_{n-1})$ and apply the DTM to eq. (4.3) over the interval $[t_{n-1}, t_n]$, where t_0 is replaced by t_{n-1} . This process is repeated and generates a series of approximate solutions $u_n(t)$, $n = 1, 2, \dots, N$. Now

$$u_n(t) = \sum_{m=0}^{M_1} a_{nm} (t - t_{n-1})^m, \quad t \in [t_n, t_{n+1}] \quad (4.7)$$

where $M = M_1 \cdot N$. Hence, the multi-step DTM assumes the following solution

$$u(t) = \begin{cases} u_1(t), & t \in [0, t_1] \\ u_2(t), & t \in [t_1, t_2] \\ \vdots \\ u_N(t), & t \in [t_{N-1}, t_N] \end{cases} \quad (4.8)$$

The multi-step DTM is a simple for computational techniques for all values of h . It can be easily shown that if the step size $h = T$, then multi-step DTM reduces to classical DTM. The main advantage of this new algorithm is that the obtained series solution converges for wide time regions.

Here the time domain is divided into sub-domains for $i = 0, 1, 2, \dots, N$ and the approximate functions in each sub-domains are $\bar{x}_i(t)$, $i = 1, 2, \dots, N$.

By taking the differential transform method [15, 61, 62] of the eq. (4.3), we obtain

- For step reactivity, the differential transform scheme is

$$X_i(k+1) = \frac{1}{(k+1)} ((A+B)X_i(k) + F(k)) \quad (4.9)$$

- For ramp reactivity and sinusoidal reactivity, the differential transform scheme is

$$X_i(k+1) = \frac{1}{(k+1)} \left(\left(AX_i(k) + \sum_{l=0}^k B(l)X_i(k-l) \right) + F(k) \right) \quad (4.10)$$

$$\text{where } X_i(k) = \frac{1}{k!} \left(\frac{d^k (\bar{x}(t))}{dt^k} \right) \Bigg|_{t=t_i} \text{ and } F(k) = \frac{1}{k!} \left(\frac{d^k (\bar{F}(t))}{dt^k} \right) \Bigg|_{t=t_i}$$

From the initial condition, we can obtain that $X_0(0) = \bar{x}(0) = \bar{x}_0$, accordingly from eq.

$$(1.40), \text{ we have } \bar{x}_0(t) = \sum_{r=0}^p (t-t_0)^r X_0(r)$$

Here,

$$\bar{x}(t_1) \cong \bar{x}_0(t_1) = \sum_{r=0}^p (t_1-t_0)^r X_0(r) = \sum_{r=0}^p h^r X_0(r), \quad h = t_1 - t_0. \quad (4.11)$$

The final value $\bar{x}_0(t_1)$ of the first sub-domain is the initial value of second sub-domain, i.e;

$$\bar{x}_1(t_1) = X_1(0) = \bar{x}_0(t_1). \text{ In this manner } \bar{x}(t_2) \text{ can be represented as}$$

$$\bar{x}(t_2) \cong \bar{x}_1(t_2) = \sum_{r=0}^p h^r X_1(r), \quad h = t_2 - t_1. \quad (4.12)$$

Hence, the solution on the grid points t_{i+1} can be found as

$$\bar{x}(t_{i+1}) \cong \bar{x}_i(t_{i+1}) = \sum_{r=0}^p h^r X_i(r), \quad h = t_{i+1} - t_i. \quad (4.13)$$

By using eqs. (4.9) and (4.10), we can obtain the solution for constant reactivity function and time- dependent reactivity function respectively.

4.3 Numerical Results and Discussions for Classical neutron point kinetic model using different reactivity functions

In the present analysis, we consider the three cases of reactivity function such as step reactivity, ramp reactivity and sinusoidal reactivity.

4.3.1 Results obtained for Step-Reactivity

Let us consider the first example of nuclear reactor problem [53] with $m=6$ and neutron source free ($q=0$) delayed group of system with the following parameters:

$$\lambda_i = [0.0127, 0.0317, 0.115, 0.311, 1.4, 3.87], \quad l = 0.00002, \quad \beta = 0.007,$$

$$\beta_i = [0.000266, 0.001491, 0.001316, 0.002849, 0.000896, 0.000182]$$

We consider, the problem for $t \geq 0$ with three step reactivity insertions $\rho = 0.003$, $\rho = 0.007$ and $\rho = 0.008$. Here, we assume the initial condition $\vec{x}(0)$ is

$$\vec{x}(0) = \begin{bmatrix} 1 \\ \beta_1 \\ \lambda_1 l \\ \beta_2 \\ \lambda_2 l \\ \vdots \\ \beta_m \\ \lambda_m l \end{bmatrix} \quad (4.14)$$

The results of classical neutron point kinetic equations for different time step-reactivity are presented in Table 1-3. The present method is compared with those for PCA method [53], CORE method [63], Taylor Method [64] and with the exact values [65]. Also these numerical results are cited by Figs. 1-3 for three step reactivities $\rho = 0.003$, $\rho = 0.007$ and $\rho = 0.008$.

Table-1: Comparison Results at step-reactivity $\rho = 0.003$ for neutron density

| Time (s) | PCA [53] | Taylor [64] | CORE [63] | MDTM | Exact [65] |
|----------|----------|-------------|-----------|------|------------|
|----------|----------|-------------|-----------|------|------------|

| | | | | | |
|--------|----------------------|----------------------|----------------------|-----------------------|-----------------------|
| $t=1$ | 2.2098 | 2.2098 | 2.2098 | 2.20984 | 2.2098 |
| $t=10$ | 8.0192 | 8.0192 | 8.0192 | 8.0192 | 8.0192 |
| $t=20$ | 2.8297×10^1 | 2.8297×10^1 | 2.8297×10^1 | 2.82974×10^1 | 2.82974×10^1 |

Table-2: Comparison Results at step-reactivity $\rho = 0.007$ for neutron density

| Time (s) | PCA [53] | Taylor [64] | CORE [63] | MDTM | Exact [65] |
|----------|-------------------------|-------------------------|-------------------------|--------------------------|-------------------------|
| $t=0.01$ | 4.5088 | 4.5086 | 4.5088 | 4.50886 | 4.5088 |
| $t=0.5$ | 5.3459×10^3 | 5.3447×10^3 | 5.3458×10^3 | 5.34589×10^3 | 5.3459×10^3 |
| $t=2$ | 2.0591×10^{11} | 2.0566×10^{11} | 2.0600×10^{11} | 2.05916×10^{11} | 2.0591×10^{11} |

Table-3: Comparison Results at step-reactivity, $\rho = 0.008$ for neutron density

| Time (s) | PCA [53] | Taylor [64] | CORE [63] | MDTM | Exact [65] |
|----------|-------------------------|-------------------------|-------------------------|--------------------------|-------------------------|
| $t=0.01$ | 6.0229 | 6.2080 | 6.2029 | 6.20285 | 6.0229 |
| $t=0.5$ | 1.4104×10^3 | 2.1398×10^{12} | 2.1071×10^{12} | 2.10706×10^{12} | 1.4104×10^3 |
| $t=2$ | 6.1634×10^{23} | 5.6255×10^{46} | 5.2735×10^{46} | 5.27345×10^{46} | 6.1634×10^{23} |

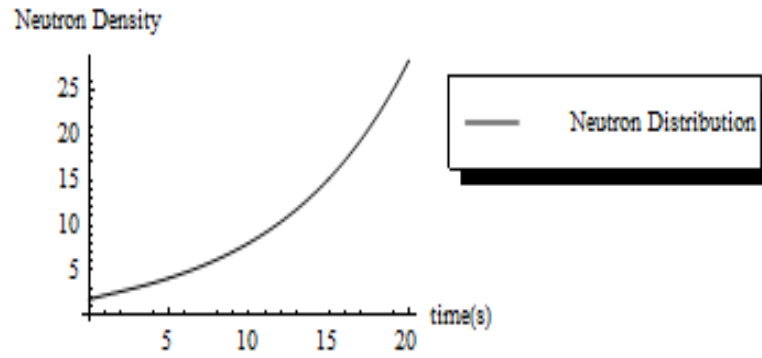


Fig.1 Neutron density at step-reactivity $\rho = 0.003$

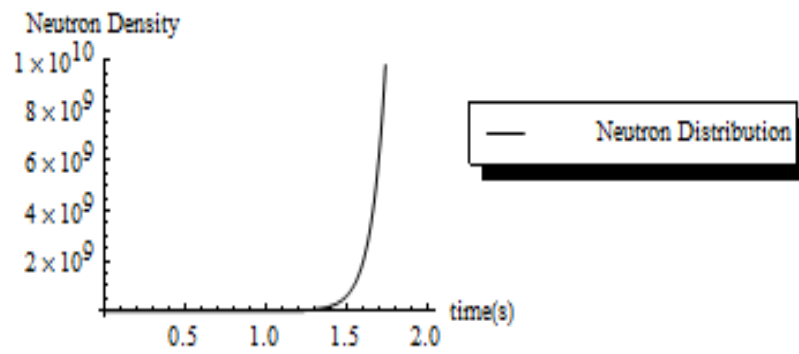


Fig.2 Neutron density at step-reactivity $\rho = 0.007$

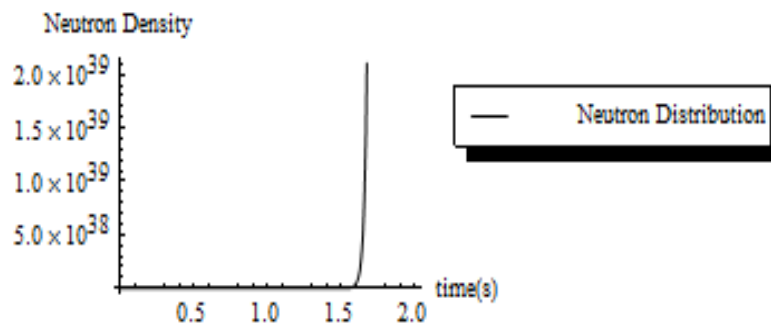


Fig. 3 Neutron density at step-reactivity $\rho = 0.008$

4.3.2. Results obtained for Ramp-Reactivity

Now we consider a ramp reactivity of 0.01\$/sec and neutron source free ($q=0$) equilibrium system where the following parameters are used:

$$\lambda_i = [0.0127, 0.0317, 0.115, 0.311, 1.4, 3.87]$$

$$\beta_i = [0.000266, 0.001491, 0.001316, 0.002849, 0.000896, 0.000182]$$

$$l = 0.00002, \beta = 0.007$$

with the same initial condition as given in eq.(4.14).

The ramp reactivity function is $\rho(t) = 0.1\beta t$. The results of classical neutron point kinetic equations for ramp reactivity (time-dependent function) are presented in Table-4 in order to exhibit the comparison results of present method with PCA method [53], Taylor method [64], and with the exact values [65]. Also the numerical result for neutron density with ramp reactivity is cited in Fig. 4.

Table-4: Comparison Results obtained with ramp reactivity for neutron density

| Time (s) | PCA [53] | Taylor [64] | MDTM | Exact [65] |
|----------|----------|-------------|--------|------------|
| $t = 2$ | 1.3382 | 1.3382 | 1.3384 | 1.3382 |
| $t = 4$ | 2.2285 | 2.2285 | 2.2287 | 2.2284 |
| $t = 6$ | 5.5822 | 5.5823 | 5.5806 | 5.5821 |
| $t = 8$ | 42.790 | 42.789 | 42.545 | 42.786 |
| $t = 9$ | 487.61 | 487.52 | 471.78 | 487.52 |

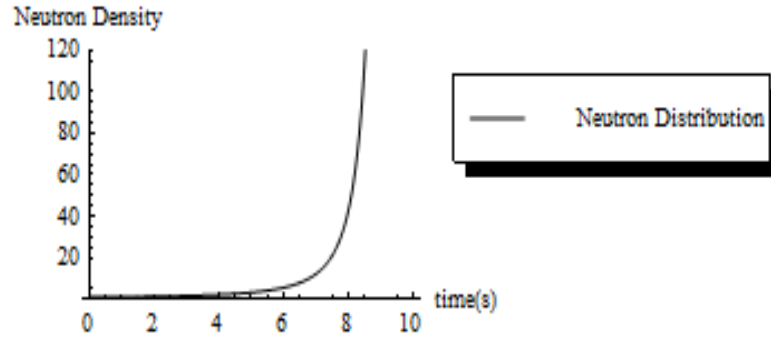


Fig.4. Neutron Density for ramp reactivity calculated with MDTM

4.3.3. *Results obtained for Sinusoidal-Reactivity*

Next we consider the last case of sinusoidal reactivity. In this case, we consider the following kinetic parameters:

$$\lambda_i = [0.0124, 0.0305, 0.111, 0.301, 1.14, 3.01]$$

$$\beta_i = [0.000215, 0.001424, 0.001274, 0.002568, 0.000748, 0.000273]$$

$$l = 0.0005, \quad \beta = 0.006502$$

The system is neutron source free ($q=0$) with the same initial condition as given in eq. (4.14). The sinusoidal reactivity (time-dependent) function is $\rho(t) = \beta \sin\left(\frac{\pi t}{T}\right)$ where T is the half-life period ($T=5\text{sec.}$)

The comparison results between the present method (MDTM) with CORE method [63], Taylor method [64] are shown in Table 5. Also the numerical results for neutron density with sinusoidal reactivity are cited in Fig. 5.

Table-5: Results obtained with sinusoidal reactivity for neutron density

| Time (s) | CORE [63] | Taylor [64] | MDTM |
|----------|-----------|-------------|------|
|----------|-----------|-------------|------|

| | | | |
|----------|---------|---------|---------|
| $t = 2$ | 10.1475 | 11.3820 | 11.3325 |
| $t = 4$ | 96.7084 | 92.2761 | 90.044 |
| $t = 6$ | 16.9149 | 16.0317 | 15.5705 |
| $t = 8$ | 8.8964 | 8.6362 | 8.4531 |
| $t = 10$ | 13.1985 | 13.1987 | 12.9915 |

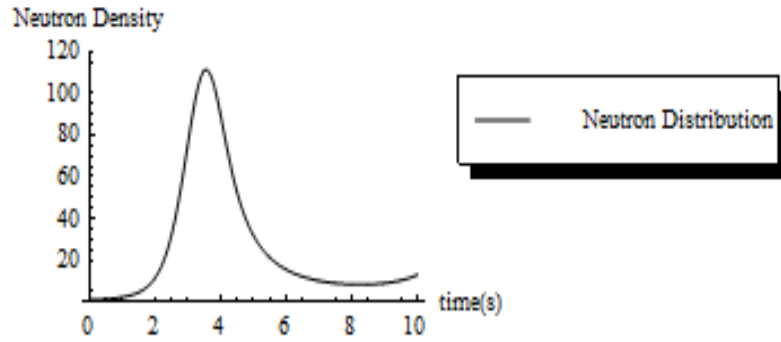


Fig. 5. Neutron Density for sinusoidal reactivity calculated by MDTM

4.4. Mathematical Model for Fractional Neutron Point Kinetic Equation

Here we consider the fractional neutron point kinetic equations⁵ for m delayed groups with Caputo derivative of order α ($\alpha > 0$ and $\alpha \in \mathfrak{R}$) in the field of nuclear reactor dynamics as follows

$$\frac{d^\alpha \vec{x}}{dt^\alpha} = A\vec{x} + B(t)\vec{x} + \vec{S}(t) \quad (4.15)$$

⁵ Saha Ray, S. and **Patra, A.**, 2014, “Numerical Simulation for Solving Fractional Neutron Point Kinetic Equations using the Multi-step Differential Transform Method”, **Physica Scripta** (IOP), 89, 015204 (8pp).

where $\vec{x}(t) = \begin{bmatrix} n(t) \\ c_1(t) \\ c_2(t) \\ \vdots \\ c_m(t) \end{bmatrix}.$

Here we define A as

$$A = \begin{bmatrix} \frac{-\beta}{l} & \lambda_1 & \lambda_2 & \cdots & \lambda_m \\ \frac{\beta_1}{l} & -\lambda_1 & 0 & \cdots & 0 \\ \frac{\beta_2}{l} & 0 & -\lambda_2 & \ddots & \vdots \\ \vdots & \vdots & \ddots & \ddots & 0 \\ \frac{\beta_m}{l} & 0 & \cdots & 0 & -\lambda_m \end{bmatrix}_{(m+1) \times (m+1)} ; \quad (4.16)$$

$B(t)$ can be expressed as

$$B(t) = \begin{bmatrix} \frac{\rho(t)}{l} & 0 & 0 & \cdots & 0 \\ 0 & 0 & 0 & \cdots & 0 \\ 0 & 0 & 0 & \ddots & \vdots \\ \vdots & \vdots & \ddots & \ddots & 0 \\ 0 & 0 & \cdots & 0 & 0 \end{bmatrix}_{(m+1) \times (m+1)} ; \quad (4.17)$$

and $\vec{S}(t)$ is defined as

$$\vec{S}(t) = \begin{bmatrix} q(t) \\ 0 \\ 0 \\ \vdots \\ 0 \end{bmatrix} \quad (4.18)$$

4.5 Fractional Differential Transform Method

At the beginning, we expand the analytical function $f(t)$ in terms of a fractional power series as follows

$$f(t) = \sum_{k=0}^{\infty} F_{\alpha}(k)(t-t_0)^{k\alpha} \quad (4.19)$$

where $0 < \alpha \leq 2$ is the order of the fractional derivative and $F_{\alpha}(k)$ is the fractional differential transform of $f(t)$ given by

$$F_{\alpha}(k) = \frac{1}{\Gamma(\alpha k + 1)} [(D_{t_0}^{\alpha})^k (f(t))]_{t=t_0} \quad (4.20)$$

where $(D_{t_0}^{\alpha})^k = D_{t_0}^{\alpha} \cdot D_{t_0}^{\alpha} \cdot D_{t_0}^{\alpha} \dots D_{t_0}^{\alpha}$, the k -times-differentiable Caputo fractional derivative.

Then, we can approximate the function $f(t)$ by the finite series

$$f(t) = \sum_{k=0}^N F_{\alpha}(k)(t-t_0)^{k\alpha} \quad (4.21)$$

Here N is the finite number of terms in the truncated series solution. The basic properties of the fractional differential transform are given in Table-6.

Table 6: The fundamental operations of fractional differential transform

| Properties | Time function | Fractional Transformed Function |
|------------|--|--|
| 1 | $f(t) = g(t) \pm h(t)$ | $F_{\alpha}(k) = G_{\alpha}(k) \pm H_{\alpha}(k)$ |
| 2 | $f(t) = g(t)h(t)$ | $F_{\alpha}(k) = \sum_{l=0}^k G_{\alpha}(l)H_{\alpha}(k-l)$ |
| 3 | $f(t) = t^{p\alpha}$ ($p \in \mathbb{Z}^+$) | $F_{\alpha}(k) = \frac{1}{\Gamma(\alpha k + 1)} [(D_{t_0}^{\alpha})^k (f(t))]_{t=t_0} = \begin{cases} 1 & , p = k \\ 0 & , p > k \\ 0 & , p < k \end{cases}$ or $F_{\alpha}(k) = \delta(k - p)$, where $\delta(k - p) = \begin{cases} 1, & k = p \\ 0, & k \neq p \end{cases}$ |
| 4 | $f(t) = D_{t_0}^{\alpha}[g(t)]$ | $F_{\alpha}(k) = \frac{\Gamma(\alpha(k+1)+1)}{\Gamma(\alpha k + 1)} G_{\alpha}(k+1)$ |

| | | |
|---|---------------------------------|--|
| 5 | $f(t) = \sin(\omega t + \beta)$ | $F_\alpha(k) = \frac{1}{k!} \frac{d^k \left(D_{t_0}^\alpha f(t) \right)}{dt^k} \Big _{t=0} = \frac{\omega^k}{k!} \sin\left(\frac{\alpha k \pi}{2} + \beta\right)$ $F_\alpha(k) = \frac{1}{k!} \frac{d^k \left(D_{t_0}^\alpha f(t) \right)}{dt^k} \Big _{t=t_i} = \frac{\omega^k}{k!} \sin\left(\frac{\alpha k \pi}{2} + \omega t_i + \beta\right)$ |
|---|---------------------------------|--|

4.6 Application of MDTM to Fractional Neutron Point Kinetic Equation

In this section we will apply the DTM to obtain the solution for fractional neutron point kinetic eq. (4.15). To illustrate the basic idea of the DTM for solving system of fractional differential equation, we consider the form

$$D^\alpha x_i(t) = N_i[x(t)] \quad , \quad i = 1, 2, \dots, n \quad (4.22)$$

where $N_i[x(t)]$ are the linear or nonlinear terms of fractional differential equation and $D^\alpha x_i(t)$ is α - order Caputo fractional derivative of unknown function $x_i(t)$.

$$x_i(t) = \sum_{k=0}^{\infty} F_i(k) (t - t_0)^{k\alpha} \quad (4.23)$$

Taking the differential transform of eq. (4.23), we obtain

$$F_i(k+1) = \frac{\Gamma(\alpha k + 1)}{\Gamma(\alpha(k+1) + 1)} DTM[N_i(x(t))], \quad i = 1, 2, \dots, n \quad (4.24)$$

$$\text{where } DTM[N_i(x(t))] = \frac{1}{\Gamma(\alpha k + 1)} \left[(D^\alpha)^k \{N_i(x(t))\} \right]_{t=t_0}.$$

Here eq. (4.24) is a recursive formula with $F_i(0)$ as the value of initial condition.

We divide the interval $[0, T]$ into subintervals with time step Δt . For getting the solution in each sub interval and to satisfy the initial condition on each subinterval, the initial value $x_i(0)$ will be changed for each subinterval, i.e. $x_i(t_j) = c_i^* = F_i(0)$, where $j = 0, 1, 2, \dots, n-1$. To obtain the solution on every subinterval of equal length Δt , we assume

that the new initial condition is the solution in the previous interval. Thus to obtain the solution in interval $[t_j, t_{j+1}]$, the initial conditions of this interval are

$$c_i = x_i(t_j) = \sum_{m=0}^N F_i(m)(t_j - t_{j-1})^{m\alpha}, \quad j=1,2,\dots,n. \quad (4.25)$$

where c_i is the initial condition in the interval $[t_{j-1}, t_j]$. After applying the Differential transformation [15, 61, 62] to eq. (4.15), we obtain the numerical scheme as

- For step reactivity, the differential transform scheme is

$$X_i(k+1) = \frac{\Gamma(\alpha k + 1)}{\Gamma(\alpha(k+1) + 1)} ((A+B)X_i(k) + S(k)) \quad (4.26)$$

- For ramp reactivity and sinusoidal reactivity, the differential transform scheme is

$$X_i(k+1) = \frac{\Gamma(\alpha k + 1)}{\Gamma(\alpha(k+1) + 1)} \left(\left(AX_i(k) + \sum_{l=0}^k B(l)X_i(k-l) \right) + S(k) \right) \quad (4.27)$$

$$\text{where } X_i(k) = \frac{1}{k!} \left(\frac{d^k (D^\alpha(\bar{x}(t)))}{dt^k} \right) \bigg|_{t=t_i}, \quad S(k) = \frac{1}{k!} \left(\frac{d^k (D^\alpha(\bar{S}(t)))}{dt^k} \right) \bigg|_{t=t_i}$$

where $i=0,1,2,\dots,N-1$ and $k=0,1,2,\dots$

For $f(t) = t^p$, we obtain

$$F_\alpha(k) = \frac{1}{\Gamma(\alpha k + 1)} [(D_{t_0}^\alpha)^k (f(t))]_{t=t_0} = \begin{cases} 1, & p = k\alpha \\ 0, & p > k\alpha \\ 0, & p < k\alpha \end{cases}$$

or we can write, $F_\alpha(k) = \delta(p - k\alpha)$ where

$$\delta(p - k\alpha) = \begin{cases} 1, & p = k\alpha \\ 0, & p \neq k\alpha \end{cases}$$

From the initial condition, we can obtain that $X_0(0) = \bar{x}(0) = \bar{x}_0$

where $\bar{x}_0(t) = \sum_{r=0}^p (t-t_0)^{r\alpha} X_0(r)$

Here,

$$c_0 \cong \bar{x}_0(t_1) = \sum_{r=0}^p (t_1-t_0)^{r\alpha} X_0(r) = \sum_{r=0}^p h^{r\alpha} X_0(r), \quad h = t_1 - t_0. \quad (4.28)$$

The final value $x_0(t_1)$ of the first sub-domain is the initial value of second sub-domain, i.e.

$\bar{x}_1(t_1) = c_1 = \bar{x}_0(t_1)$. In this manner $\bar{x}(t_2)$ can be represented as

$$\bar{x}(t_2) \cong \bar{x}_1(t_2) = \sum_{r=0}^p h^{r\alpha} X_1(r), \quad h = t_2 - t_1. \quad (4.29)$$

Hence, the solution with the grid points t_{j+1} can be found as

$$\bar{x}(t_{j+1}) \cong \bar{x}_i(t_{j+1}) = \sum_{r=0}^p h^{r\alpha} X_i(r), \quad h = t_{j+1} - t_j. \quad (4.30)$$

Using eq. (4.26) and (4.27), we can obtain the solution for the constant reactivity function and time-dependent reactivity function, respectively.

4.7 Numerical Results and Discussions for Fractional Neutron Point Kinetic Equation

In the present analysis, we consider the three cases of reactivity function such as step reactivity, ramp reactivity, and sinusoidal reactivity respectively.

4.7.1. Results obtained for Step-Reactivity

Let us consider the first example of a nuclear reactor problem [53, 64] with $m=6$ and a neutron source free $q(t) = 0$ delayed group of a system with the following parameters:

$$\lambda_i = [0.0127, 0.0317, 0.115, 0.311, 1.4, 3.87] \text{ (s}^{-1}\text{)}, \quad l = 0.00002\text{s}, \quad \beta = 0.007,$$

$$\beta_i = [0.000266 \ 0.001491 \ 0.001316 \ 0.002849 \ 0.000896 \ 0.000182]$$

We consider the problem for $t \geq 0$ with three step reactivity insertions $\rho = 0.003\%$, $\rho = 0.007\%$, and $\rho = 0.008\%$. Here, we assume that the initial $\bar{x}(0)$ equals

$$\bar{x}(0) = \begin{bmatrix} \frac{1}{\beta_1} \\ \frac{\lambda_1 l}{\beta_1} \\ \frac{\beta_2}{\lambda_2 l} \\ \vdots \\ \frac{\beta_m}{\lambda_m l} \end{bmatrix} \quad \text{and} \quad \bar{x}'(0) = 0 \quad (4.31)$$

The results of fractional neutron point kinetic equations are presented in Tables 7-9 for different time with various step reactivities. We compute the numerical solution for taking step-size $h = 0.0001$ second at time $t = 0.01$ second, $t = 0.05$ second and $t = 1$ second with steps = 20000 which are also cited by Figs. 6-8.

Table 7: Results at subcritical-reactivity $\rho = 0.003\%$ for neutron density $n(t)$ by using MDTM

| t | $\alpha = 1.5$ | $\alpha = 1.25$ | $\alpha = 1$ | $\alpha = 0.75$ | McMohan and Pierson, 2010 (classical integer order) [64] |
|------|----------------|-----------------|--------------|----------------------|--|
| 0.01 | 1.01131 | 1.1225 | 1.65208 | 1.80478 | N.A. |
| 0.5 | 1.39672 | 1.76907 | 1.99336 | 4.37265 | N.A. |
| 1 | 1.58424 | 1.79325 | 2.20988 | 8.9838 | 2.2099 |
| 10 | 1.78621 | 2.16011 | 8.0192 | 1.6548×10^6 | 8.0192 |

Table 8: Results at critical reactivity $\rho = 0.007\%$ for neutron density $n(t)$ by using MDTM

| t | $\alpha = 1.5$ | $\alpha = 1.25$ | $\alpha = 1$ | $\alpha = 0.75$ | McMohan and Pierson, 2010 (classical integer order) [64] |
|------|----------------|-----------------|--------------------------|---------------------------|--|
| 0.01 | 1.02659 | 1.31201 | 4.54413 | 51.9663 | 4.5086 |
| 0.5 | 2.31718 | 17.2111 | 5352.12 | 5.81118×10^{28} | 5.3447×10^3 |
| 1 | 3.63692 | 38.1606 | 1.80784×10^6 | 2.10571×10^{56} | N.A. |
| 2 | 6.29591 | 120.46 | 2.05916×10^{11} | 2.72997×10^{111} | 2.0566×10^{11} |

Table 9: Results at critical reactivity $\rho = 0.008\%$ for neutron density $n(t)$ by using MDTM

| t | $\alpha = 1.5$ | $\alpha = 1.25$ | $\alpha = 1$ | $\alpha = 0.75$ | McMohan and Pierson, 2010 (classical integer order) [64] |
|------|----------------|-----------------|--------------------------|---------------------------|--|
| 0.01 | 1.03045 | 1.36463 | 6.2694 | 2491.81 | 6.2415 |
| 0.5 | 2.65622 | 68.6659 | 2.11821×10^{12} | 4.1051×10^{126} | 6.9422×10^{11} |
| 1 | 4.65868 | 756.72 | 6.19596×10^{23} | 2.20782×10^{252} | 6.1215×10^{22} |

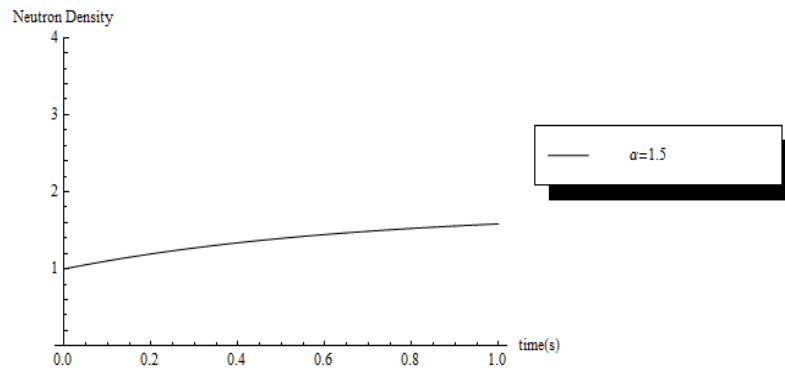


Fig. 6 (a). Neutron density for step reactivity $\rho = 0.003$ with $\alpha = 1.5$

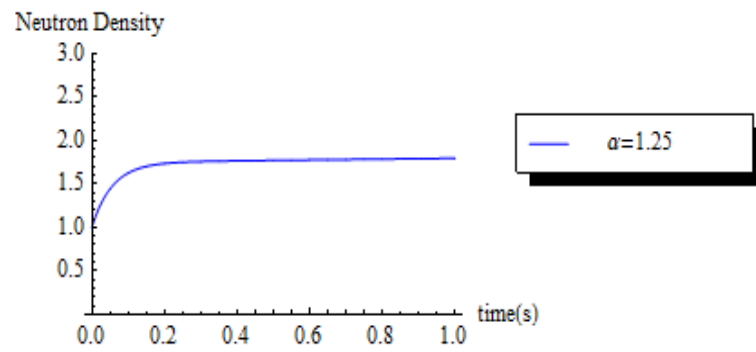


Fig. 6 (b). Neutron density for step reactivity $\rho = 0.003$ with $\alpha = 1.25$

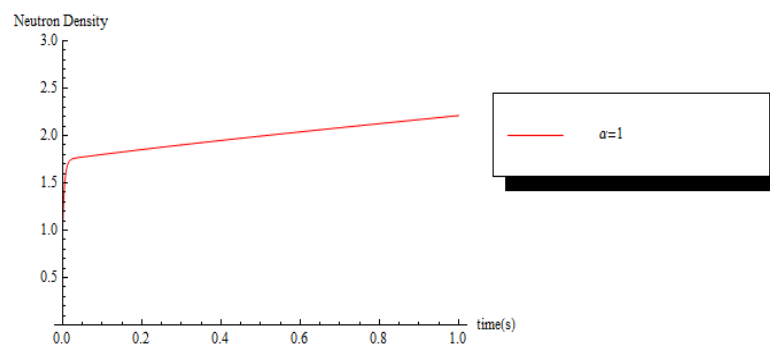


Fig. 6 (c). Neutron density for step reactivity $\rho = 0.003$ with $\alpha = 1$

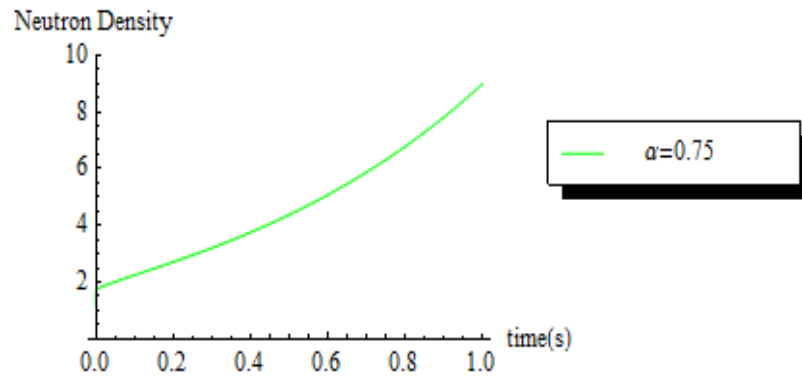


Fig. 6 (d). Neutron density for step reactivity $\rho = 0.003\%$ with $\alpha = 0.75$

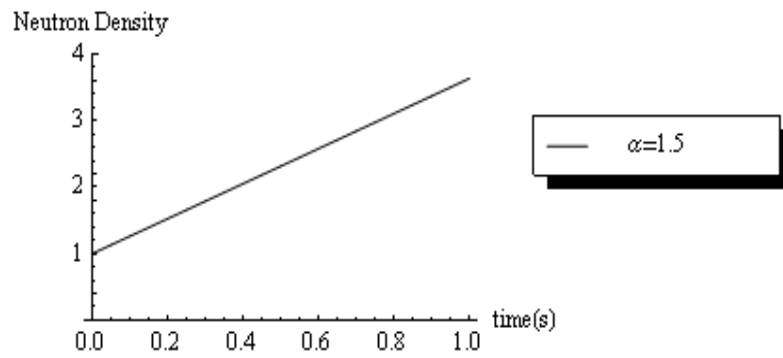


Fig. 7 (a). Neutron density for step reactivity $\rho = 0.007\%$ with $\alpha = 1.5$

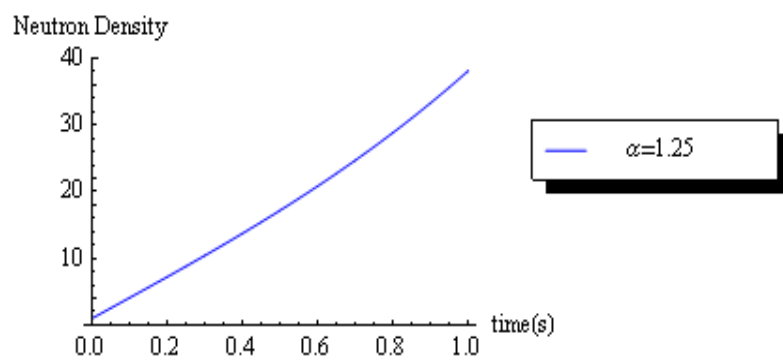


Fig. 7 (b). Neutron density for step reactivity $\rho = 0.007\%$ with $\alpha = 1.25$

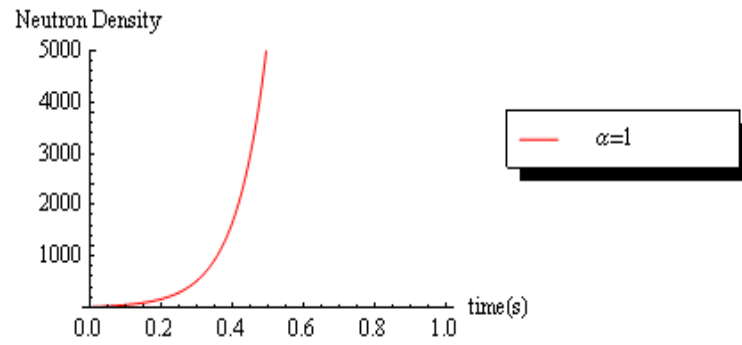


Fig. 7 (c). Neutron density for step reactivity $\rho = 0.007\%$ with $\alpha = 1$

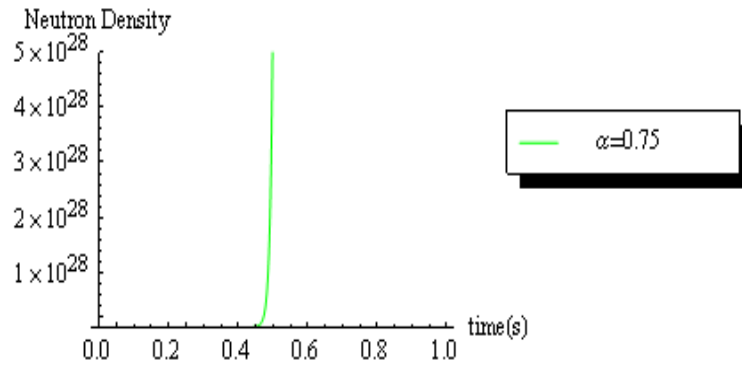


Fig. 7 (d). Neutron density for step reactivity $\rho = 0.007\%$ with $\alpha = 0.75$

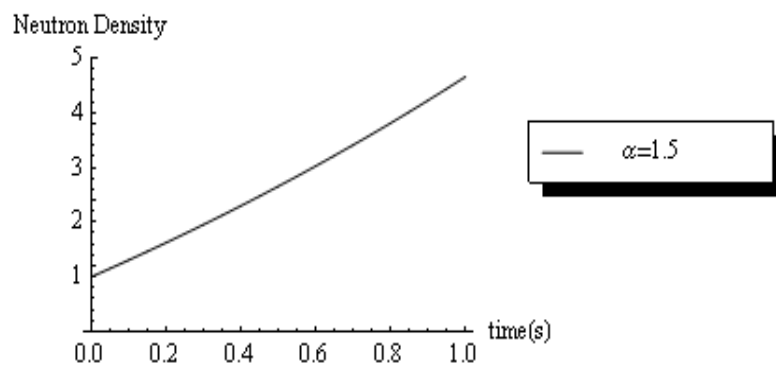


Fig. 8 (a). Neutron density for step reactivity $\rho = 0.008\%$ with $\alpha = 1.5$

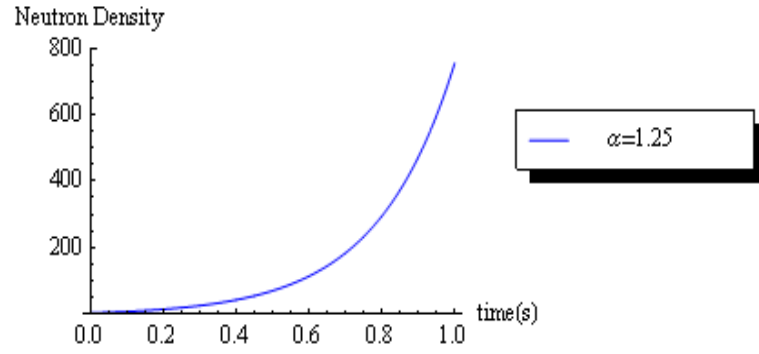


Fig. 8 (b). Neutron density for step reactivity $\rho=0.008$ with $\alpha=1.25$

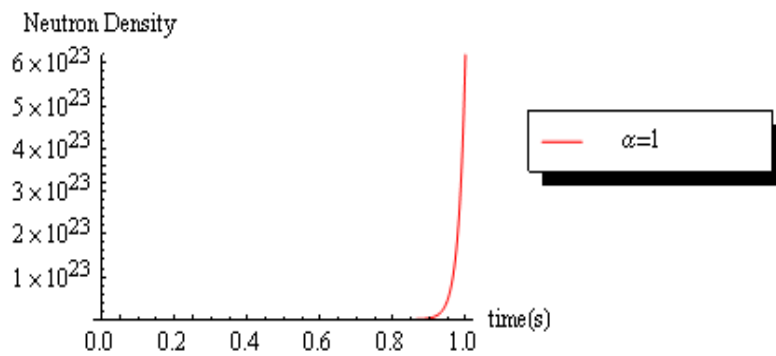


Fig. 8 (c). Neutron density for step reactivity $\rho=0.008$ with $\alpha=1$

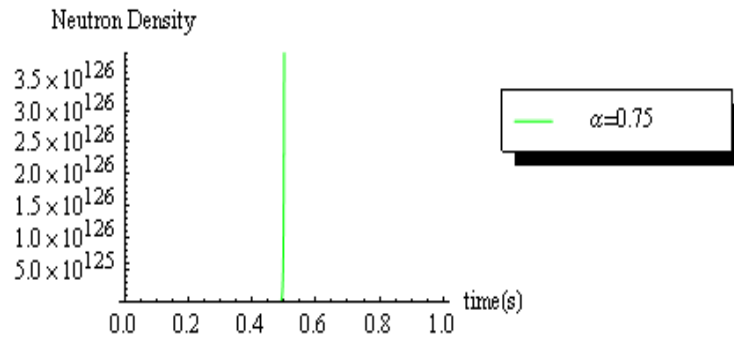


Fig. 8 (d). Neutron density for step reactivity $\rho=0.008$ with $\alpha=0.75$

Hence, from Tables 7-9, it can be observed that by taking three reactivities $\rho=0.003$, $\rho=0.007$ and $\rho=0.008$, the numerical approximation results for neutron density obtained from multi-step differential transform method are good agreement with the

results obtained by Mc Mohan and Pierson [64] using Taylor series solution for classical order $\alpha = 1$. But using these three reactivities, there are no previous results exist in open literature for fractional order point kinetic equation.

4.7.2 Results obtained for Ramp Reactivity

Now we consider a ramp reactivity of 0.01\$/sec and a neutron source free $q(t) = 0$ equilibrium system where the following parameters are used [53, 64]

$$\lambda_i = [0.0127, 0.0317, 0.115, 0.311, 1.4, 3.87] \text{ (sec.}^{-1}\text{)}$$

$$\beta_i = [0.000266, 0.001491, 0.001316, 0.002849, 0.000896, 0.000182]$$

$$l = 0.00002 \text{ sec.}, \beta = 0.007$$

with the same initial condition as given in eq.(4.31).

The ramp reactivity function is $\rho(t) = 0.1\beta t$.

The numerical results for fractional neutron point kinetic equations with ramp reactivity (time-dependent function) are cited by Figs. 9-11 by using different α . The comparison results between different α are shown in Table 10.

Table 10: Results obtained for ramp reactivity for neutron density using MDTM

| | Neutron Density $n(t)$ | | | |
|----------|------------------------|--------------|-----------------|--|
| Time (s) | $\alpha = 1.5$ | $\alpha = 1$ | $\alpha = 0.75$ | McMohan, and Pierson, 2010 (classical integer order) [64] |
| | | | | |

| | | | | |
|---------|---------|--------|---------|--------|
| $t = 2$ | 1.25661 | 1.3384 | 1.47755 | 1.3382 |
| $t = 4$ | 1.72456 | 2.2287 | 3.40974 | 2.2285 |
| $t = 6$ | 2.75227 | 5.5806 | 19.4696 | 5.5823 |
| $t = 8$ | 6.15687 | 42.545 | 1336 | 42.789 |
| $t = 9$ | 12.617 | 471.78 | 118901 | 487.52 |

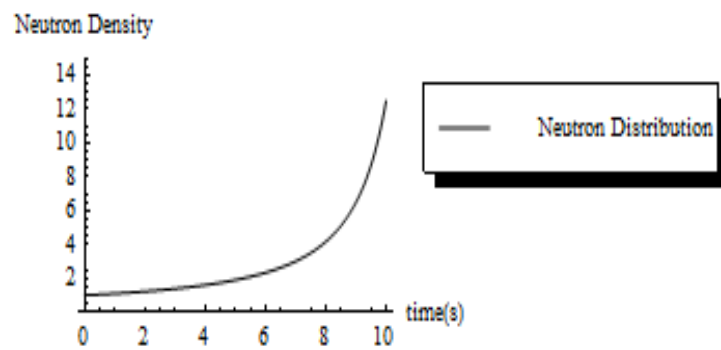


Fig. 9. Neutron Density with ramp reactivity with $\alpha = 1.5$ calculated using MDTM

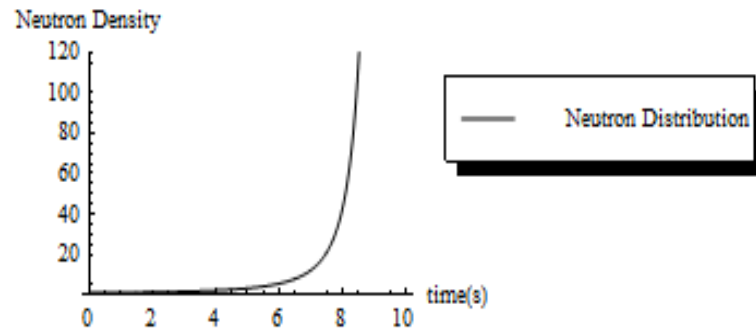


Fig. 10. Neutron Density with ramp reactivity with $\alpha = 1$ calculated using MDTM

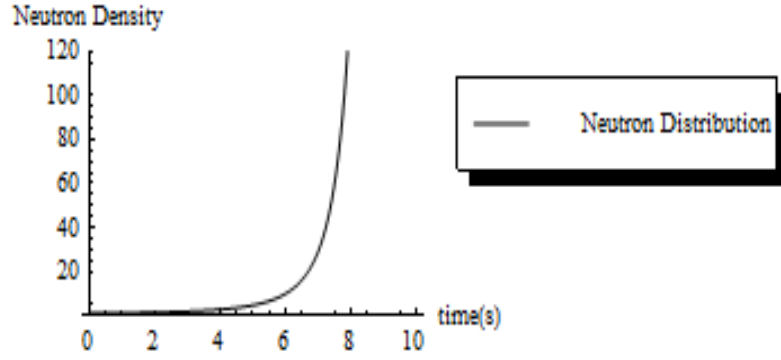


Fig. 11. Neutron Density with ramp reactivity with $\alpha = 0.75$ calculated using MDTM

Hence, the numerical approximation results for neutron density obtained from multi-step differential transform method for ramp reactivity are in good agreement with the results obtained by McMohan and Pierson [64] with the help of Taylor series solution at classical order $\alpha = 1$. But using ramp reactivity there are no previous results exist in open literature for fractional order point kinetic equation.

4.7.3 Results obtained for Sinusoidal-Reactivity

Next we consider the last case involving sinusoidal reactivity [53, 64]. In this case, we consider the following kinetic parameters:

$$\lambda_i = [0.0124, 0.0305, 0.111, 0.301, 1.14, 3.01] (\text{sec.}^{-1})$$

$$\beta_i = [0.000215, 0.001424, 0.001274, 0.002568, 0.000748, 0.000273]$$

$$l = 0.0005 \text{sec.}, \beta = 0.006502$$

The system is neutron source free $q(t) = 0$ with the same initial condition as given in eq.

(4.31). The sinusoidal reactivity (time-dependent) function is $\rho(t) = \beta \sin\left(\frac{\pi t}{T}\right)$, where T is

the half-life period ($T=5\text{sec.}$). The numerical results for fractional neutron point kinetic

equations with sinusoidal reactivity (time-dependent function) are shown in Table-11 and also cited by Figs. 12 -14.

Table 11: Results obtained for neutron density with sinusoidal reactivity using MDTM

| | Neutron Density $n(t)$ | | | |
|----------|------------------------|--------------|-----------------|---|
| Time (s) | $\alpha = 1.5$ | $\alpha = 1$ | $\alpha = 0.75$ | McMohan, and Pierson, 2010 (classical integer order) [64] |
| $t = 2$ | 8.42634 | 11.3325 | 12.9717 | 11.3820 |
| $t = 4$ | 39.1603 | 90.044 | 124.065 | 92.2761 |
| $t = 6$ | 6.69124 | 15.5705 | 21.5457 | 16.0317 |
| $t = 8$ | 3.81628 | 8.4531 | 11.5648 | 8.6362 |
| $t = 10$ | 5.97965 | 12.9915 | 17.7996 | 13.1987 |

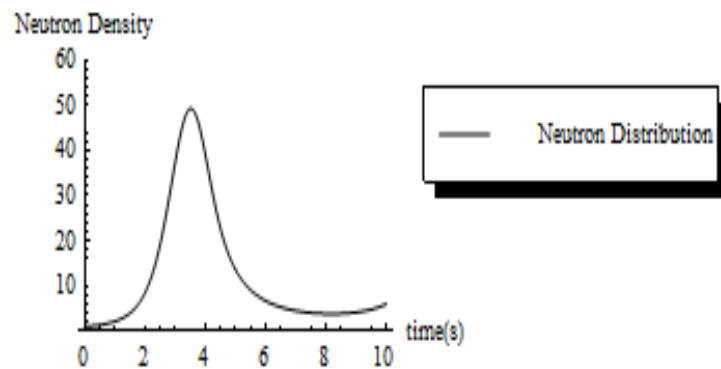


Fig. 12. Neutron Density with sinusoidal reactivity with $\alpha = 1.5$ obtained by MDTM

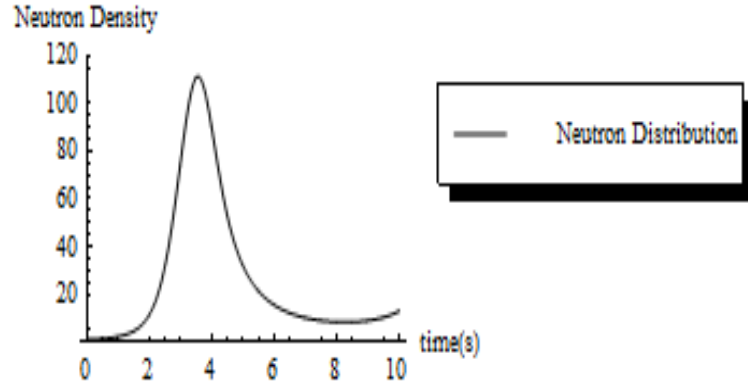


Fig. 13. Neutron Density with sinusoidal reactivity with $\alpha = 1$ obtained by MDTM

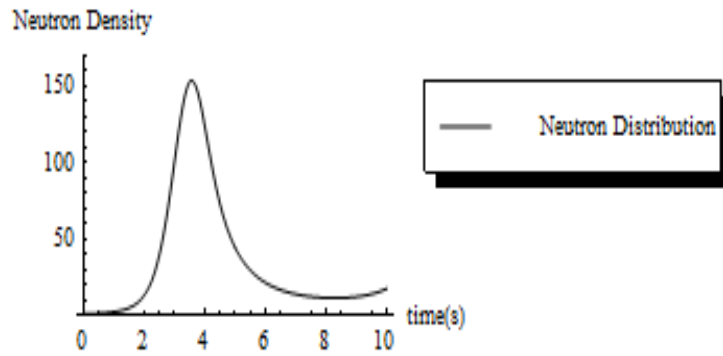


Fig. 14. Neutron Density with sinusoidal reactivity with $\alpha = 0.75$ obtained by MDTM

Thus the numerical approximation results for neutron density obtained from multi-step differential transform method for sinusoidal reactivity are in good agreement with the results obtained by Mc Mohan and Pierson [64] with the help of Taylor series solution at classical order $\alpha = 1$. But using ramp reactivity, there are no previous results exist in open literature for fractional order point kinetic equation.

In the present chapter, both classical and fractional order neutron point kinetic equations with arbitrary order α have been solved using the multi-step differential transform method [66, 67]. The present method is easier and more efficient to provide the numerical solution for classical as well as fractional neutron point kinetic equations. This method is

a powerful solver for classical and fractional neutron point kinetic equation. The present method is quite easy to apply for obtaining approximate numerical solutions for time-varying reactivities. Moreover, the accuracy can be further improved when the step size of each subinterval becomes smaller.

4.8 Conclusion

In this chapter, the classical and fractional order neutron point kinetic equations have been successfully solved by using multi-step differential transform method. From the obtained numerical results, it can be concluded that MDTM is conveniently applicable to neutron point kinetic equation. Moreover, it also shows that the present method is reliable and promising when compared with other existing methods. The multi-step differential transform method (MDTM) is clearly an effective and simple method for solving the classical and fractional order neutron point kinetic equation. It is extremely easy to apply the method. The method is more accurate to solve the problems with various types of reactivities. However, in this present method the more accurate results can be obtained by taking more terms in the series and smaller time step-size. Hence, the computational error is less.

CHAPTER 5

5.1. *Introduction*

The point-kinetic equations are most essential model in the field of nuclear science and engineering. The modelling of these equations intimates the time-dependent behaviour of a nuclear reactor [24, 32, 53, 60]. Noise in reactors can be described by conventional Point Reactor Kinetic Equations (PRKE) with fluctuation introduced in some of the parameters. Such equations may be referred to as Stochastic Point Reactor Kinetic Equations. Power reactor noise analysis may be viewed as study of a reactor's response to a stochastic reactivity or source input. The difficulty of solving Stochastic Point Reactor Kinetic Equations arises from the fact that they are nonlinear. The stochastic behaviour of a point reactor is modelled with a system of Ito stochastic differential equations.

It is well known that the reactions in a nuclear system are not fully describable by deterministic laws. This fact, at the most fundamental level, is due to the laws of quantum mechanics, which only give probabilities of various interactions for a neutron, which are manifest in the interaction cross sections of atoms with neutrons. There are various situations which this probabilistic behaviour could be readily observed for a nuclear system, e.g. in the startup of the reactors, in zero power reactors, in most laboratory source-detector configurations, etc. There has been an extensive research effort to model this stochastic behaviour. Measuring higher order moments requires more data from the system for a given accuracy. Actually, most of the times in practice, one only measures the first and second order moments in a system, i.e. the mean and variance.

The standard deterministic point-kinetic model has been the subject of countless studies and applications to understand the neutron dynamics and its effects, such as developed of different methods for their solution [49, 50, 68-71]. The reactivity function and neutron source term are the parametric quantities of this vital system. The dynamical process explained by the point-kinetic equations is stochastic in nature. The neutron density and delayed neutron precursor concentrations differ randomly with respect to time. At the levels of high power, the random behaviour is imperceptible. But at low-power levels, such as at the beginning, random fluctuation in the neutron density and neutron precursor concentrations can be crucial.

The numerical solutions for neutron population density and sum of precursors concentration population density have been solved with stochastic Piecewise Constant Approximation (PCA) method and Monte Carlo computations by using different step reactivity functions [60]. The derivation and the solution for stochastic neutron point-kinetics equation have elaborately described in the work of [71] by considering the same parameters and different step reactivity with Euler–Maruyama method and strong order 1.5 Taylor method. It can be observed that the numerical methods like Euler-Maruyama method and strong order 1.5 Taylor method are likely reliable with stochastic PCA method and Monte Carlo computations. Here, Euler–Maruyama method and Taylor 1.5 strong order approximations method have been applied efficiently and conveniently for the solution of stochastic point-kinetic equation with sinusoidal reactivity. The resulting systems of Stochastic Differential Equations (SDE) are solved over each time-step size in the partition. In the present investigation, the main attractive advantage, of these computational numerical methods, is their simplicity, efficiency and applicability.

In this research work, the numerical solution of Fractional Stochastic Neutron Point Kinetic Equation has been obtained very efficiently and elegantly. In the present research work, for the first time ever, the random behavior of neutron density and neutron precursor concentrations have been analyzed in fractional order. Here, a numerical procedure has been used for efficiently calculating the solution for fractional stochastic neutron point kinetic equation (FSNPK) in the dynamical system of nuclear reactor. The explicit finite difference method has been applied to solve the fractional stochastic neutron point kinetic equation with the Grunwald- Letnikov (GL) definition [44, 72]. Fractional Stochastic Neutron Point Kinetic Model has been analyzed for the dynamic behavior of the neutron.

5.2. *Classical order Stochastic Neutron Point Kinetic Model*⁶

A point reactor is a reactor in which the spatial effects have been eliminated. This is obviously possible if the reactors length is infinite in all spatial dimensions. Study of a point reactor, i.e. studying the properties of Eq. (5.2.1), is desirable in the sense that it captures some of the most essential features of the reactor dynamics without involving into the complexities of integro-differential equations, i.e. the transport equation, or partial differential equations, i.e. the diffusion equation.

In order to separate the birth and death process of neutron population, Hetrick [24] and Hayes and Allen [60] derived the deterministic point-kinetic equation as

$$\frac{dn}{dt} = -\left[\frac{-\rho + 1 - \alpha}{l}\right]n + \left[\frac{1 - \alpha - \beta}{l}\right]n + \sum_{i=1}^m \lambda_i c_i + q \quad (5.2.1)$$

⁶ S. Saha Ray and **A. Patra**, 2012, “Numerical Solution for Stochastic Point Kinetics Equations with Sinusoidal Reactivity in Dynamical System of Nuclear Reactor”, **Int. Journal of Nuclear Energy Science and Technology** (InderScience), Vol. 7, No. 3, 231-242.

$$\frac{dc_i}{dt} = \frac{\beta_i}{l} n - \lambda_i c_i, \quad i = 1, 2, \dots, m$$

Here, $n(t)$ is the population size of neutrons and $c_i(t)$ is the population size of the i th neutron precursor. The rate of transformations from neutron precursors to the neutron population is

$\sum_{i=1}^m \lambda_i c_i$ where the delayed constant is λ_i and $c_i(r, t)$ is the density of the i th type of precursor

for $i = 1, 2, \dots, m$. A source of neutrons extraneous to the fission process is represented by $q(t)$

and $\rho(t)$ is reactivity function, neutron generation time $l = \frac{1}{k_\infty v \Sigma_a}$, α is defined as

$\alpha = \frac{\Sigma_f}{\Sigma_a k_\infty} \approx \frac{1}{\nu}$ and ν is the average number of neutrons emitted per fission. $\beta = \sum_{i=1}^m \beta_i$ is the

delayed-neutron fraction and $(1 - \beta)$ is the prompt-neutron fraction. The neutron reactions can be separated into three terms as follows

$$\frac{dn}{dt} = - \underbrace{\left[\frac{-\rho + 1 - \alpha}{l} \right]}_{\text{deaths}} n + \underbrace{\left[\frac{1 - \alpha - \beta}{l} \right]}_{\text{births}} n + \underbrace{\sum_{i=1}^m \lambda_i c_i}_{\text{transformations}} + q$$

$$\frac{dc_i}{dt} = \frac{\beta_i}{l} n - \lambda_i c_i, \quad i = 1, 2, \dots, m \quad (5.2.2)$$

The neutron birth rate due to fission is $b = \frac{1 - \alpha - \beta}{l(-1 + (1 - \beta)\nu)}$, where the denominator has the

term $(-1 + (1 - \beta)\nu)$ represents the number of neutrons (new born) produced in each fission

process. The neutron death rate due to captures or leakage is $d = \frac{-\rho + 1 - \alpha}{l}$. The

transformation rate $\lambda_i c_i$ represents the rate that the i th precursor is transformed into neutrons.

For deriving the stochastic dynamical system, we consider for simplicity only one precursor

i.e. $\beta = \beta_1$, where β is the total delayed neutron fraction for one precursor.

The point kinetic equations for one precursor is

$$\left. \begin{aligned} \frac{dn}{dt} &= -\left[\frac{-\rho+1-\alpha}{l}\right]n + \left[\frac{1-\alpha-\beta}{l}\right]n + \lambda_1 c_1 + q \\ \frac{dc_1}{dt} &= \frac{\beta_1}{l}n - \lambda_1 c_1 \end{aligned} \right\} \quad (5.2.3)$$

Now, we consider for the small duration of time-interval Δt where probability of more than one occurred event is small. Let $[\Delta n, \Delta c_1]^T$ be the change of n and c_1 in time Δt where the changes are assumed approximately normally distributed. For $\Delta t \rightarrow 0$, the following system has been derived by the learned researcher Saha Ray [71]

$$\frac{d}{dt} \begin{bmatrix} n \\ c_1 \end{bmatrix} = \hat{A} \begin{bmatrix} n \\ c_1 \end{bmatrix} + \begin{bmatrix} q \\ 0 \end{bmatrix} + \hat{B}^{1/2} \frac{d\vec{W}}{dt} \quad (5.2.4)$$

where

$$\vec{W}(t) = \begin{bmatrix} W_1(t) \\ W_2(t) \end{bmatrix} = \lim_{\Delta t \rightarrow 0} \frac{1}{\sqrt{\Delta t}} \begin{bmatrix} \eta_1 \\ \eta_2 \end{bmatrix}, \quad \text{for } \eta_1, \eta_2 \sim N(0, 1)$$

$$\text{and } \hat{A} = \begin{bmatrix} \frac{\rho-\beta}{l} & \lambda_1 \\ \frac{\beta_1}{l} & -\lambda_1 \end{bmatrix}$$

Here, $W_1(t)$ and $W_2(t)$ are two Wiener process and $\hat{B}^{1/2}$ is the square root of the matrix

$$\hat{B} = \begin{bmatrix} m + \lambda_1 c_1 + q & \frac{\beta_1}{l}(-1 + (1-\beta)\nu)n - \lambda_1 c_1 \\ \frac{\beta_1}{l}(-1 + (1-\beta)\nu)n - \lambda_1 c_1 & \frac{\beta_1^2 \nu}{l}n + \lambda_1 c_1 \end{bmatrix}$$

$$\text{where } \gamma = \frac{-1 - \rho + 2\beta + (1-\beta)^2 \nu}{l}$$

The eq. (5.2.4) represents the stochastic point kinetic equation for one precursor.

Now generalizing the above arguments to m precursors, we can obtain the following Itô stochastic differential equation system for m precursors

$$\frac{d}{dt} \begin{bmatrix} n \\ c_1 \\ c_2 \\ \vdots \\ c_m \end{bmatrix} = \hat{A} \begin{bmatrix} n \\ c_1 \\ c_2 \\ \vdots \\ c_m \end{bmatrix} + \begin{bmatrix} q \\ 0 \\ 0 \\ \vdots \\ 0 \end{bmatrix} + \hat{B}^{1/2} \frac{d\vec{W}}{dt} \quad (5.2.5)$$

In the above eq. (5.2.5), \hat{A} and \hat{B} are as follows

$$\hat{A} = \begin{bmatrix} \frac{\rho - \beta}{l} & \lambda_1 & \lambda_2 & \cdots & \lambda_m \\ \frac{\beta_1}{l} & -\lambda_1 & 0 & \cdots & 0 \\ \frac{\beta_2}{l} & 0 & -\lambda_2 & \ddots & \vdots \\ \vdots & \vdots & \ddots & \ddots & 0 \\ \frac{\beta_m}{l} & 0 & \cdots & 0 & -\lambda_m \end{bmatrix}$$

and

$$\hat{B} = \begin{bmatrix} \zeta & a_1 & a_2 & \cdots & a_m \\ a_1 & r_1 & b_{2,3} & \cdots & b_{2,m+1} \\ a_2 & b_{3,2} & r_2 & \ddots & \vdots \\ \vdots & \vdots & \ddots & \ddots & b_{m-1,m} \\ a_m & b_{m,2} & \cdots & b_{m,m-1} & r_m \end{bmatrix} \quad (5.2.6)$$

where

$$\zeta = \mathcal{M} + \sum_{j=1}^m \lambda_j c_j + q$$

$$\gamma = \frac{-1 - \rho + 2\beta + (1 - \beta)^2 \nu}{l}$$

$$a_j = \frac{\beta_j}{l} (-1 + (1 - \beta)v)n - \lambda_j c_j$$

$$b_{i,j} = \frac{\beta_{i-1}\beta_{j-1}v}{l} n$$

and

$$r_i = \frac{\beta_i^2 v}{l} n + \lambda_i c_i$$

If $\hat{B} = 0$, then eq. (5.2.5) reduces to standard deterministic point-kinetic model.

Hence, the stochastic point-kinetic equations for m delayed groups is defined as

$$\frac{d\vec{x}}{dt} = A\vec{x} + B(t)\vec{x} + \vec{F}(t) + \hat{B}^{1/2} \frac{d\vec{W}}{dt} \quad (5.2.7)$$

with initial condition $\vec{x}(0) = \vec{x}_0$

$$\text{Here } \vec{x} = \begin{bmatrix} n \\ c_1 \\ c_2 \\ \vdots \\ c_m \end{bmatrix} \text{ and } \hat{B} \text{ is given in eq. (5.2.6).} \quad (5.2.8)$$

A is $(m+1) \times (m+1)$ matrix given by

$$A = \begin{bmatrix} \frac{-\beta}{l} & \lambda_1 & \lambda_2 & \cdots & \lambda_m \\ \frac{\beta_1}{l} & -\lambda_1 & 0 & \cdots & 0 \\ \frac{\beta_2}{l} & 0 & -\lambda_2 & \ddots & \vdots \\ \vdots & \vdots & \ddots & \ddots & 0 \\ \frac{\beta_m}{l} & 0 & \cdots & 0 & -\lambda_m \end{bmatrix} \quad (5.2.9)$$

B is the $(m+1) \times (m+1)$ matrix

$$B = \begin{bmatrix} \frac{\rho(t)}{l} & 0 & 0 & \cdots & 0 \\ 0 & 0 & 0 & \cdots & 0 \\ 0 & 0 & 0 & \ddots & \vdots \\ \vdots & \vdots & \ddots & \ddots & 0 \\ 0 & 0 & \cdots & 0 & 0 \end{bmatrix} \quad (5.2.10)$$

and $\vec{F}(t)$ is given as

$$\vec{F}(t) = \begin{bmatrix} q(t) \\ 0 \\ 0 \\ \vdots \\ 0 \end{bmatrix} \quad (5.2.11)$$

It can be noticed that $\hat{A} = A + B(t)$ where A is a constant matrix.

5.3. Numerical solution of classical Stochastic Neutron Point Kinetic Equation

5.3.1 Euler–Maruyama method for the solution of stochastic point-kinetic model

The Euler-Maruyama approximation is the simplest time discrete approximations of an Itô process. Let $\{Y_\tau\}$ be an Itô process on $\tau \in [t_0, T]$ satisfying the stochastic differential equation (SDE)

$$\begin{cases} dY_\tau = a(\tau, Y_\tau)d\tau + b(\tau, Y_\tau)dW_\tau \\ Y_{t_0} = Y_0 \end{cases} \quad (5.3.1.1)$$

For a given time-discretization $t_0 = \tau_0 < \tau_1 < \cdots < \tau_n = T$, (5.3.1.2)

an Euler approximation is a continuous time stochastic process $\{X(\tau), t_0 \leq \tau \leq T\}$ satisfying the iterative scheme (5.3.1.3)

for $n = 0, 1, 2, \dots, N-1$

with initial value $X_0 = X(\tau_0)$

where $X_n = X(\tau_n)$, $\Delta\tau_{n+1} = \tau_{n+1} - \tau_n$ and $\Delta W_{n+1} = W(\tau_{n+1}) - W(\tau_n)$. Here, each random number ΔW_n is computed as $\Delta W_n = \eta_n \sqrt{\Delta\tau_n}$ where η_n is chosen from standard normal distribution $N(0,1)$.

We have considered the equidistant discretized times

$$\tau_n = \tau_0 + n\Delta \text{ with } \Delta = \Delta_n = \frac{(T - \tau_0)}{N} \text{ for some integer } N \text{ large enough so that } \Delta \in (0,1).$$

The Euler-Maruyama method is also known as order 0.5 strong Itô - Taylor approximation. By applying Euler Maruyama method to eq. (5.2.7) in view of eq. (5.3.1.1), we obtain the scheme as

$$\vec{x}_{i+1} = \vec{x}_i + (A + B_i)\vec{x}_i h + \vec{F}(t_i)h + \hat{B}^{1/2} \sqrt{h} \vec{\eta}_i \quad (5.3.1.4)$$

where $d\vec{W}_i = \vec{W}_i - \vec{W}_{i-1} = \sqrt{h} \vec{\eta}_i$ and $h = t_{i+1} - t_i$

where $\vec{\eta}_i$ is a vector whose components are random numbers chosen from $N(0,1)$.

5.3.2. Strong order 1.5 Taylor Method for the Solution of Stochastic Point-Kinetic Model

Here we consider Taylor approximation having strong order $\alpha = 1.5$. The order 1.5 strong Taylor scheme can be obtained by adding more terms from Itô -Taylor expansion to the Milstein scheme [19, 21]. The order 1.5 strong Itô -Taylor scheme is

$$\begin{aligned} Y_{n+1} = & Y_n + a\Delta_n + b\Delta W_n + \frac{1}{2}bb_x(\Delta W_n^2 - \Delta_n) + a_x b\Delta Z_n + \frac{1}{2}(aa_x + \frac{1}{2}b^2a_{xx})\Delta_n^2 \\ & + (ab_x + \frac{1}{2}b^2b_{xx})(\Delta W_n\Delta_n - \Delta Z_n) + \frac{1}{2}b(bb_{xx} + b_x^2)(\frac{1}{3}\Delta W_n^2 - \Delta_n)\Delta W_n \end{aligned} \quad (5.3.2.1)$$

for $n = 0, 1, 2, \dots, N - 1$

with initial value

$$Y_0 = Y(\tau_0) \text{ and } \Delta_n = \Delta\tau_n$$

Here, partial derivatives are denoted by subscripts and the random variable ΔZ_n is normally distributed with mean $E(\Delta Z_n) = 0$ and variance $E(\Delta Z_n^2) = \frac{1}{3} \Delta\tau_n^3$ and correlated with ΔW_n by covariance $E(\Delta Z_n \Delta W_n) = \frac{1}{2} \Delta\tau_n^2$.

We can generate ΔZ_n as

$$\Delta Z_n = \frac{1}{2} \Delta\tau_n (\Delta W_n + \Delta V_n / \sqrt{3}) \quad (5.3.2.2)$$

where ΔV_n is chosen independently from $\sqrt{\Delta\tau_n} N(0,1)$. Here the approximation, $Y_n = Y(\tau_n)$ is the continuous time stochastic process $\{Y(\tau), t_0 \leq \tau \leq T\}$, the time step-size $\Delta\tau_n = \tau_n - \tau_{n-1}$ and $\Delta W_n = W(\tau_n) - W(\tau_{n-1})$.

By applying Strong order 1.5 Taylor Approximation methods to eq. (5.2.7) in view of eq. (5.3.2.1) yielding

$$\bar{x}_{i+1} = \bar{x}_i + \left((A + B_i) \bar{x}_i + \bar{F}_i \right) h + \hat{B}^{1/2} \sqrt{h} \bar{\eta}_i + (A + B_i) \hat{B}^{1/2} \Delta Z_i + \frac{1}{2} \left((A + B_i) \bar{x}_i + \bar{F}_i \right) (A + B_i) h^2 \quad (5.3.2.3)$$

where $\Delta Z_i = \frac{1}{2} h (\Delta W_i + \Delta V_i / \sqrt{3})$ and $\Delta V_i = \sqrt{h} N(0,1)$.

5.4 Numerical Results and Discussions for the Solution of Stochastic Point-Kinetic Model

At first, the one group delayed neutron point kinetics model of a reactor has been considered. In the present analysis, reactivity has been considered as sinusoidal reactivity function $\rho(t) = \rho_0 \sin \frac{\pi t}{T}$ in nuclear reactor [24, 53] with $m=1$ delayed group and the parameters are as follows $\rho_0 = 0.005333(68 \text{ cents})$, $\lambda_1 = 0.077 \text{ sec}^{-1}$, $\beta_1 = 0.0079 = \beta$, neutron source $q(t) = 0$, $l = 10^{-3} \text{ sec}$, a half-life period $T = 50 \text{ sec}$ and $t \geq 0$. The initial condition is $\bar{x}(0) = \begin{bmatrix} 1 & \beta_1 / \lambda_1 l \end{bmatrix}^T$. We observe through a period of 800 sec., there is a good agreement available between two present methods Euler Maruyama method and Strong 1.5 Taylor method. The computational results are shown by the following graphs in Fig.1-Fig.2 for neutron population density with respect to time with different time-step size at different trials. The neutron population density obtained by Euler-Maruyama Method and Strong 1.5 Order Taylor Method using a sinusoidal reactivity for $t=800 \text{ sec.}$ with step-size $h=0.001$ at 100 trials are cited by Figs. 1(a) and (b). Then we reduce the number of trials to 30 and the neutron population density obtained by Euler-Maruyama Method and Strong 1.5 Order Taylor Method using a sinusoidal reactivity for $t=800 \text{ sec.}$ with step-size $h=0.001$ are cited by Figs. 1(c) and (d). Similarly in Figs. 2 (a) and (b) the numerical computation of the neutron population density obtained by Euler-Maruyama Method and Strong 1.5 Order Taylor Method for $t=800 \text{ Sec.}$ with step-size $h=0.01$ at 100 trials are plotted. We have considered two random samples of neutrons at 25th trial and 30th trial of the total sample of 5000 trial for the solution. In comparison to the deterministic point kinetic model with sinusoidal reactivity given in the work of Kinard and Allen [53], the present numerical methods are more efficient and accurate to give the solution of stochastic neutron point kinetic equation with sinusoidal reactivity for one precursor.

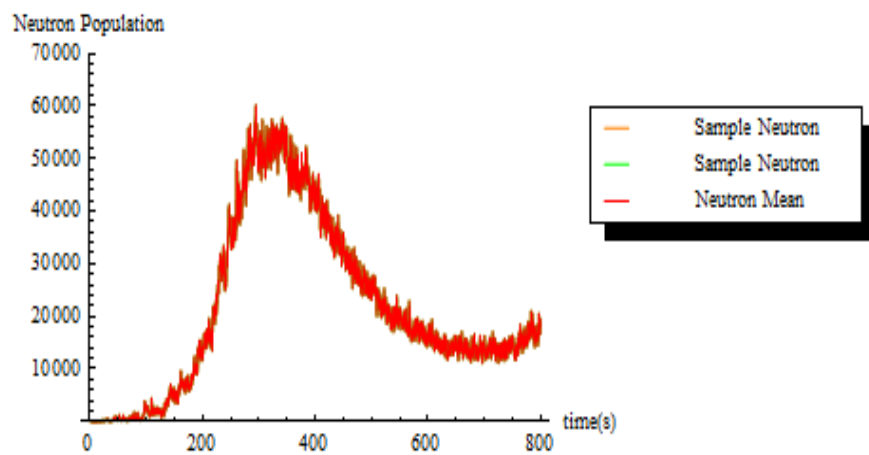


Fig.1. (a)

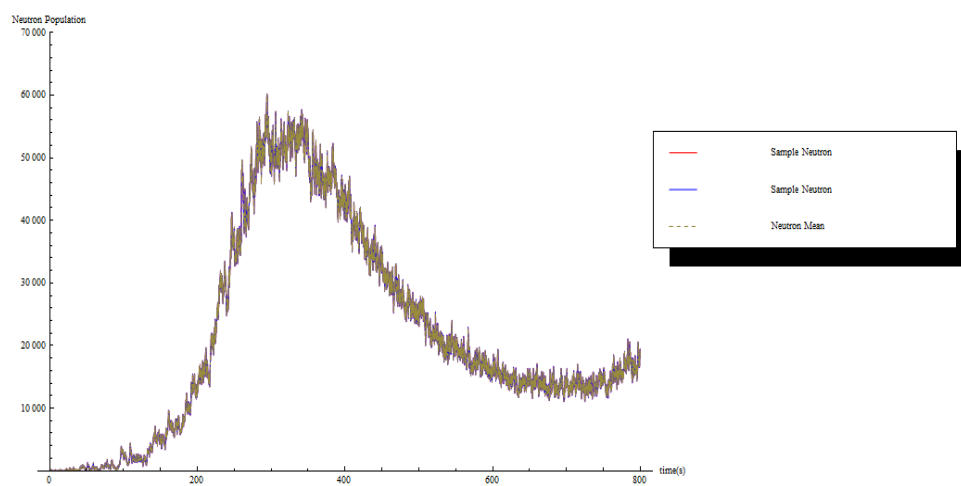


Fig.1.(b)

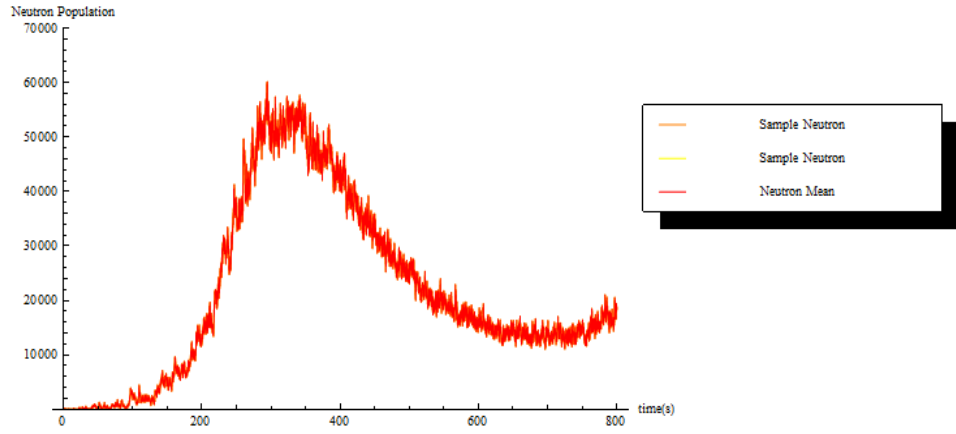


Fig.1. (c)

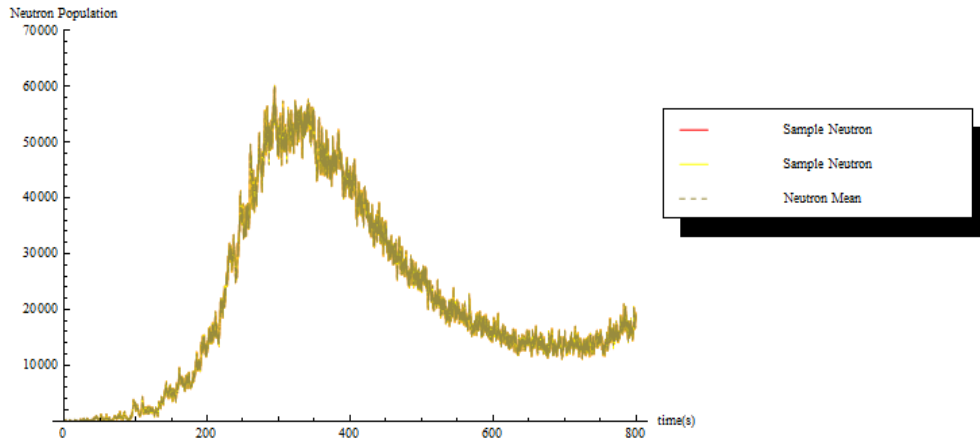


Fig.1. (d)

Fig.1. (a) Neutron Population density obtained by Euler-Maruyama Method with step-size $h=0.001$ at 100 trials, (b) Neutron density obtained by Strong 1.5 Order Taylor Method with step-size $h=0.001$ at 100 trials, (c) Neutron Population density obtained by Euler-Maruyama Method with step-size $h=0.001$ at 30 trials, (d) Neutron density obtained by Strong 1.5 Order Taylor Method with step-size $h=0.001$ at 30 trials.

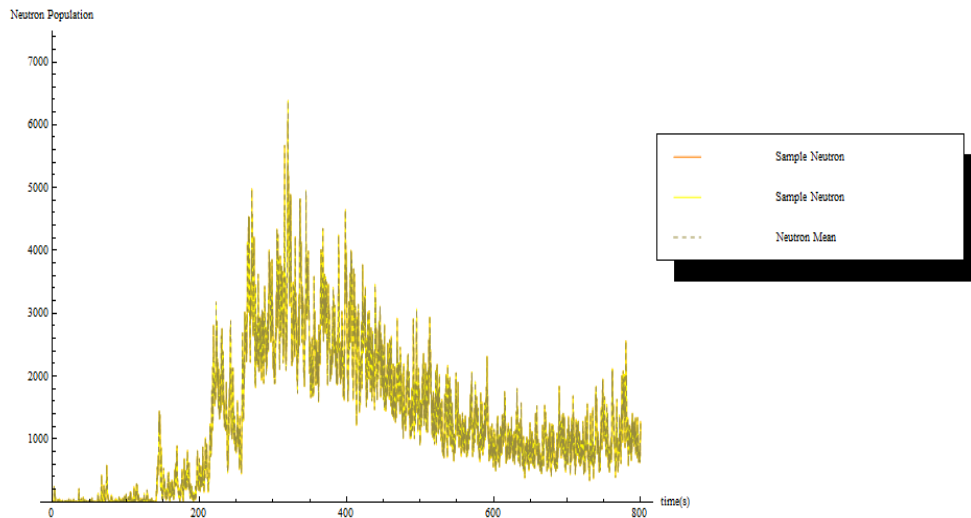


Fig.2. (a)

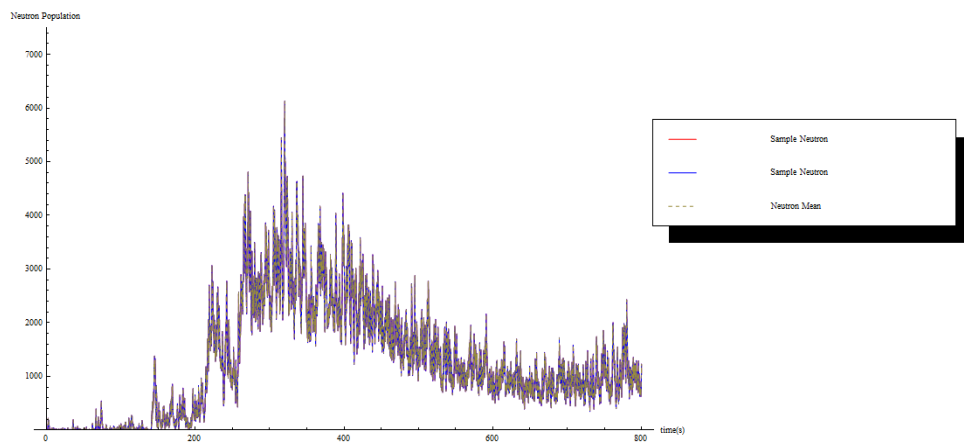


Fig.2. (b)

Fig. 2. (a) Neutron population density obtained by Euler-Maruyama Method with step-size $h=0.01$ at 100 trials, (b) Neutron population density obtained by Strong 1.5 Order Taylor Method with step-size $h=0.01$ at 100 trials.

Next, it has been considered the effect of pulse reactivity function⁷ [24, 32, 64]

$$\rho(t) = \begin{cases} 4\beta(e^{-2t^2}), & t < 1 \\ 0, & \text{otherwise} \end{cases} \quad \text{in nuclear reactor with } m=1 \text{ neutron precursor and the parameters}$$

used are as follows: $\lambda_1 = 0.077 \text{ sec}^{-1}$, $\beta_1 = 0.006502 = \beta$, neutron source $q = 0$, $l = 10^{-3} \text{ sec}$. [64].

Mathematically, we can define neutron mean $E(n(t)) = \frac{1}{N} \sum_{j=1}^N n_j(t)$ and similarly mean of m -

group precursor $E(c(t)) = \frac{1}{N} \sum_{j=1}^N \left(\sum_{k=1}^m c_{jk}(t) \right)$, where N is total number of trials. The initial

condition is $\bar{x}(0) = \begin{bmatrix} 1 & \beta_1 / \lambda_1 l \end{bmatrix}^T$. We observe the behavior through a period of 1sec. The

obtained numerical approximation results for mean neutron population $E(n(t))$ and mean of m -group precursor population $E(c(t))$ is given by Table-1 for time 0.001 sec., 0.1 sec. and 1 sec.

with step size $h=0.0001$ at single trial. The mean of neutron population density and the mean of sum of precursor density obtained by Euler-Maruyama Method and Strong 1.5 Order Taylor Method using a pulse reactivity for $t=1\text{sec}$. with step-size $h=0.01$ at 100 trials are cited by Figs. 3-6.

Table-1 Comparison between Numerical Computational methods for one precursor

| | Euler-Maruyama Approximation | Strong Order 1.5 Taylor Approximation |
|-----------------|---|--|
| $E(n(0.001))$ | 1.98979 | 1.99135 |
| $E(c_1(0.001))$ | 84.528 | 84.5285 |

⁷ **A. Patra** and S. Saha Ray, 2014, "The Effect of Pulse Reactivity for Stochastic Neutron Point Kinetics Equation in Nuclear Reactor Dynamics", **Int. Journal of Nuclear Energy Science and Technology** (Inderscience), Vol. 8, No. 2, pp. 117-130.

| | | |
|---------------|-----------------------|-----------------------|
| $E(n(0.1))$ | 522.98 | 525.137 |
| $E(c_1(0.1))$ | 212.141 | 212.78 |
| $E(n(1))$ | 1.42861×10^6 | 1.43966×10^6 |
| $E(c_1(1))$ | 4.40479×10^6 | 4.4397×10^6 |

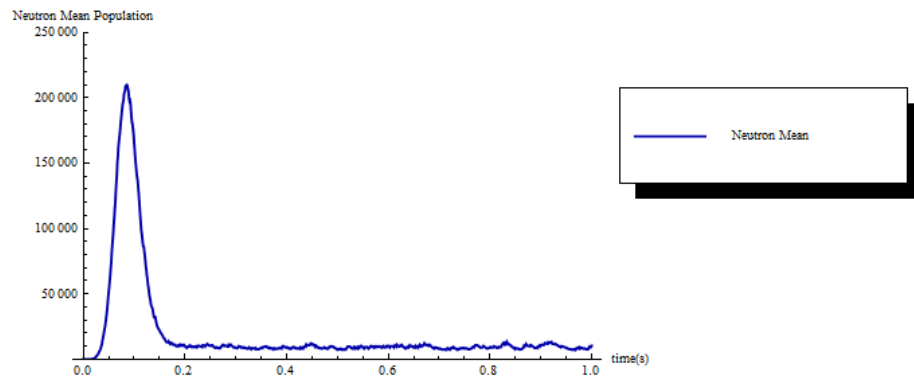


Fig. 3. Neutron Mean Population density obtained by using Euler-Maruyama Method

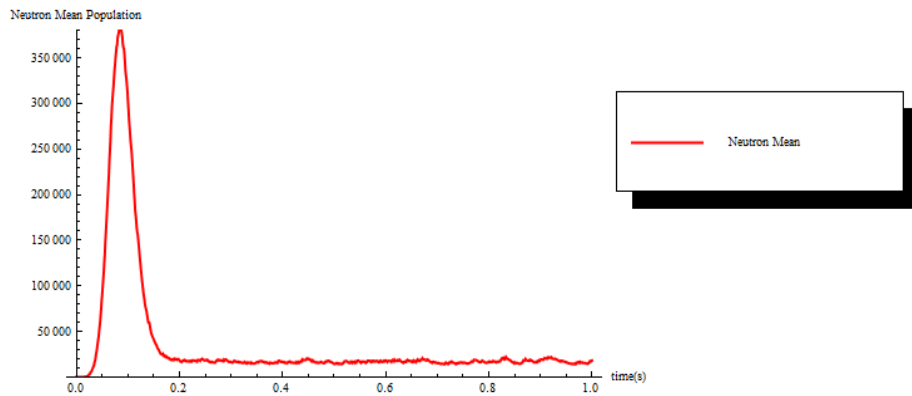


Fig. 4. Neutron Mean Population density obtained by using Strong Order 1.5 Taylor Method

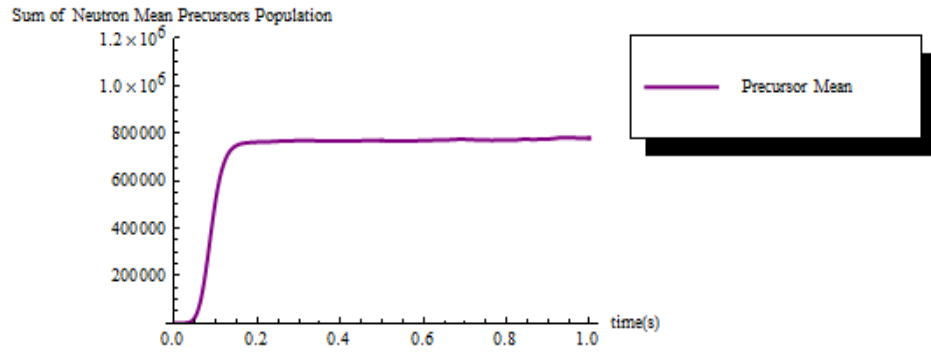


Fig. 5. Sum of Neutron Mean Precursor density obtained by using Euler-Maruyama Method

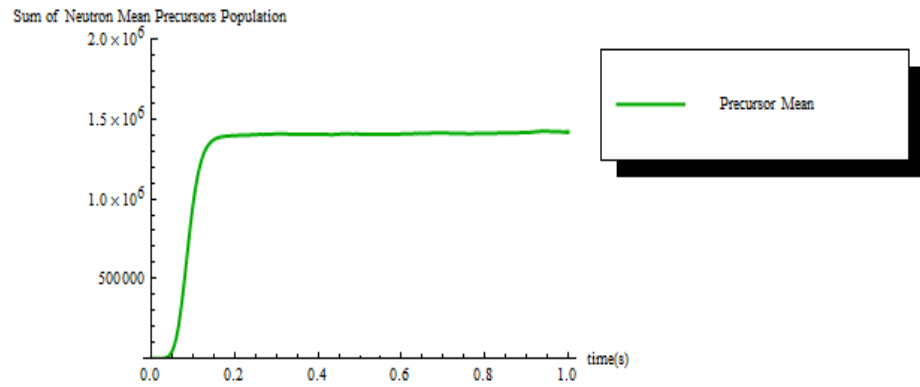


Fig. 6. Sum of Neutron Mean Precursor density obtained by using Strong Order 1.5 Taylor Method

The main advantages of Euler-Maruyama method and strong order 1.5 Taylor method are firstly Piecewise Constant Approximation (PCA) [53, 60] over a partition is not required for reactivity function and source function. There is no need to obtain the eigenvalues and eigen vectors of point-kinetics matrices for getting the solution of stochastic point-kinetics equation. By use of inhour equation to calculate eigen values by finding roots of polynomial function

was presented in the work of Hetrick [24]. But it is very cumbersome and complicated procedure. In present methods, such types of unwieldy computations are not required.

The limitation of the Euler–Maruyama method is that its order of convergence is $\alpha = 1/2$, which is slower in comparison to strong order 1.5 Taylor method where order of convergence is $\alpha = 3/2$.

5.5 Application of Explicit Finite Difference method for solving *Fractional order Stochastic Neutron Point Kinetic Model*⁸

We consider the neutron point kinetic equations with Grunwald-Letnikov fractional time derivative [49, 50, 68-70] and having behavior of Itô type stochastic system [60, 71] for m group delayed neutron precursors, in the field of nuclear reactor dynamics, as follows

$$\frac{d^\alpha \vec{x}}{dt^\alpha} = A\vec{x} + B(t)\vec{x} + \vec{F}(t) + \hat{B}^{1/2} \frac{d\vec{W}}{dt}, \quad 0 < \alpha \leq 1 \quad (5.5.1)$$

subject to initial condition $\vec{x}(0) = \vec{x}_0$.

In nuclear reactor, at the lower power levels during the start-up of nuclear reactor operation, the random fluctuation in the neutron population density and neutron precursor concentrations have been observed and it is significant. Random behavior of neutron population and precursors concentrations played a vital role in the process of diffusion occurred inside the

⁸ S. Saha Ray and A. Patra, 2013, “Numerical Solution of Fractional Stochastic Neutron Point Kinetic Equation for Nuclear Reactor Dynamics”, **Annals of Nuclear Energy** (Elsevier), Vol. 54, pp. 154-161.

reactor [60]. If $\alpha=1$, the process is normal diffusion and when $0<\alpha<1$, then the diffusion process is anomalous diffusion.

To examine the behavior of anomalous diffusion, we have considered the stochastic neutron point kinetic equation in fractional order. The study of random nature and anomalous diffusion has not been investigated by any researchers for fractional stochastic point kinetic equations (FSNPK).

$$\text{Here, } \bar{x}(t) = \begin{bmatrix} n(t) \\ c_1(t) \\ c_2(t) \\ \vdots \\ c_m(t) \end{bmatrix}$$

$$A = \begin{bmatrix} \frac{-\beta}{l} & \lambda_1 & \lambda_2 & \cdots & \lambda_m \\ \frac{\beta_1}{l} & -\lambda_1 & 0 & \cdots & 0 \\ \frac{\beta_2}{l} & 0 & -\lambda_2 & \ddots & \vdots \\ \vdots & \vdots & \ddots & \ddots & 0 \\ \frac{\beta_m}{l} & 0 & \cdots & 0 & -\lambda_m \end{bmatrix}_{(m+1) \times (m+1)} \quad (5.5.2)$$

$$B = \begin{bmatrix} \frac{\rho(t)}{l} & 0 & 0 & \cdots & 0 \\ 0 & 0 & 0 & \cdots & 0 \\ 0 & 0 & 0 & \ddots & \vdots \\ \vdots & \vdots & \ddots & \ddots & 0 \\ 0 & 0 & \cdots & 0 & 0 \end{bmatrix}_{(m+1) \times (m+1)} \quad (5.5.3)$$

and $\bar{F}(t)$ is given as

$$\vec{F}(t) = \begin{bmatrix} q(t) \\ 0 \\ 0 \\ \vdots \\ 0 \end{bmatrix} \quad (5.5.4)$$

Let us take the time step size h . Using the definition of GL fractional derivative, the numerical approximation of the eq. (5.5.1), in view of the research work, [13, 50, 52], is

$$h^{-\alpha} \sum_{j=0}^m \omega_j^{(\alpha)} \vec{x}_{(m-j)} = A\vec{x}_{(m)} + B\vec{x}_{(m)} + \vec{F}_{(m)} + \hat{B}^{1/2} h^{-1/2} \vec{\eta}_{(m)} \quad (5.5.5)$$

The above eq. (5.5.5) leads to Implicit numerical iteration scheme. However, in this present work, we propose an explicit numerical scheme which leads from the time layer t_{m-1} to t_m as follows:

$$\vec{x}_{(m)} = -\sum_{j=1}^m \omega_j^{(\alpha)} \vec{x}_{(m-j)} + h^{\alpha} \left(A\vec{x}_{(m-1)} + B\vec{x}_{(m-1)} + \vec{F}_{(m)} + \hat{B}^{1/2} h^{-1/2} \vec{\eta}_{(m)} \right) \quad (5.5.6)$$

where $m=1,2,3,\dots$.

where $\vec{x}_m = \vec{x}(t_m) \equiv m$ -th approximation at time t_m , $t_m = mh$, $m=0,1,2,\dots$ and $\omega_j^{\alpha} = (-1)^j \binom{\alpha}{j}$,

$j=0,1,2,3,\dots$. Here $d\vec{W} = \vec{W}_{m+1} - \vec{W}_m = \Delta W_m = \sqrt{h} \vec{\eta}_m$ where $\vec{\eta}_m$ is chosen from $N(0,1)$ and

$h = t_{m+1} - t_m$ with initial condition $\vec{x}_0 = \vec{x}(t_0)$.

5.6 Numerical Results and Discussions for Fractional Stochastic Neutron Point Kinetic Equation

In this section, we consider the first example of nuclear reactor problems [60], $\lambda_1 = 0.1 \text{ sec}^{-1}$,

$\beta_1 = 0.05 = \beta$, $\nu = 2.5$, neutron source $q = 200$, $l = 2/3 \text{ sec.}$ and $\rho(t) = -1/3$ for $t \geq 0$. The initial

condition is $\vec{x}(0) = [400 \ 300]^T$. We applied explicit finite difference methods for 40 intervals

at time $t = 2\text{sec}$. The mean and standard deviation of $n(2)$ and $c_1(2)$ are presented in Table-2 for different values of fractional order α . The numerical results for the time period of $t = 1\text{sec}$. are cited graphically with positive and negative reactivity by Figs. 7 to 10. For negative reactivity at $\rho(t) = -1/3$, it can be observed from Figs. 7-8, the neutron population decreases with small time variation and for positive reactivity at $\rho(t) = 1/3$, the neutron population gradually increases with time in Figs. 9-10.

Moreover, for negative reactivity $\rho(t) = -1/3$, Figs. 7 and 8 exhibit the comparison of neutron population behavior in case of fractional order $1/2$ and classical integer order respectively. Similarly, for positive reactivity $\rho(t) = 1/3$, Figs. 9 and 10 exhibit the comparison of neutron population behavior in case of fractional order $1/2$ and classical integer order respectively.

Table-2 Mean and Standard deviation of Neutron and precursor for different values of α

| | $\alpha = 0.25$ | $\alpha = 0.5$ | $\alpha = 0.75$ | $\alpha = 1$ (Classical) |
|------------------|-----------------|----------------|-----------------|--------------------------|
| $E(n(2))$ | 162.236 | 201.703 | 267.868 | 412.23 |
| $\sigma(n(2))$ | 56.2242 | 34.4135 | 29.3493 | 34.3918 |
| $E(c_1(2))$ | 21.0623 | 46.2477 | 117.343 | 315.969 |
| $\sigma(c_1(2))$ | 5.13641 | 4.43681 | 5.61876 | 8.26569 |

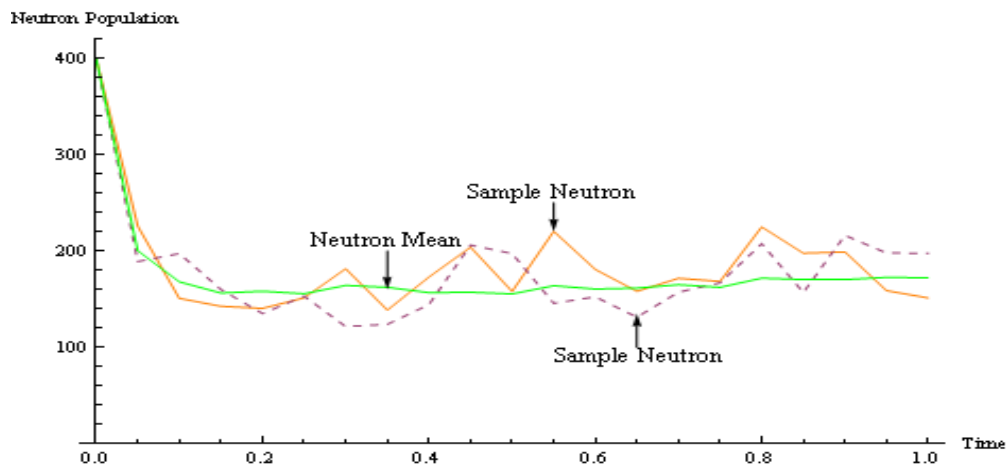


Fig.7. Neutron Population density with $\alpha = 0.5$ and $\rho = -1/3$

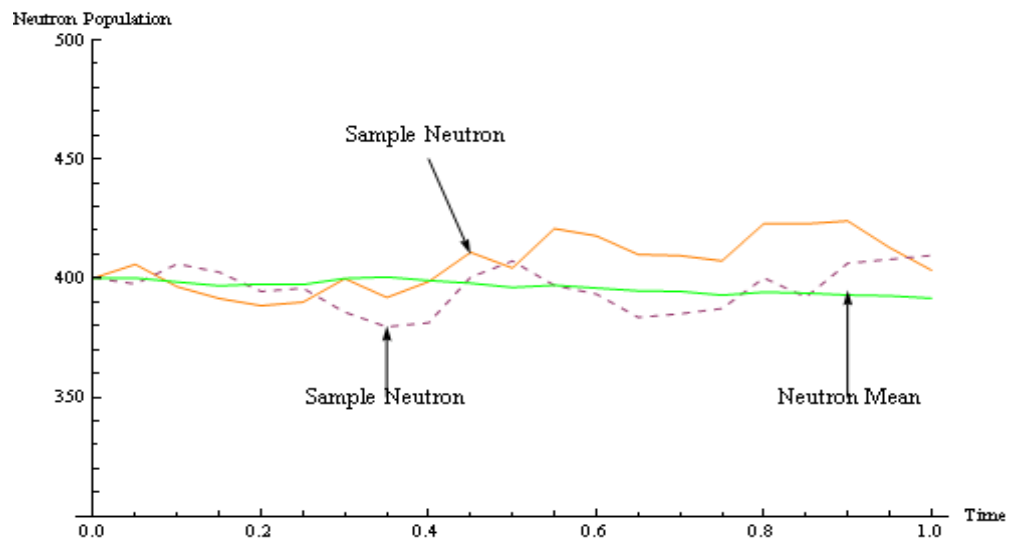


Fig.8. Neutron Population density with $\alpha = 1$ and $\rho = -1/3$

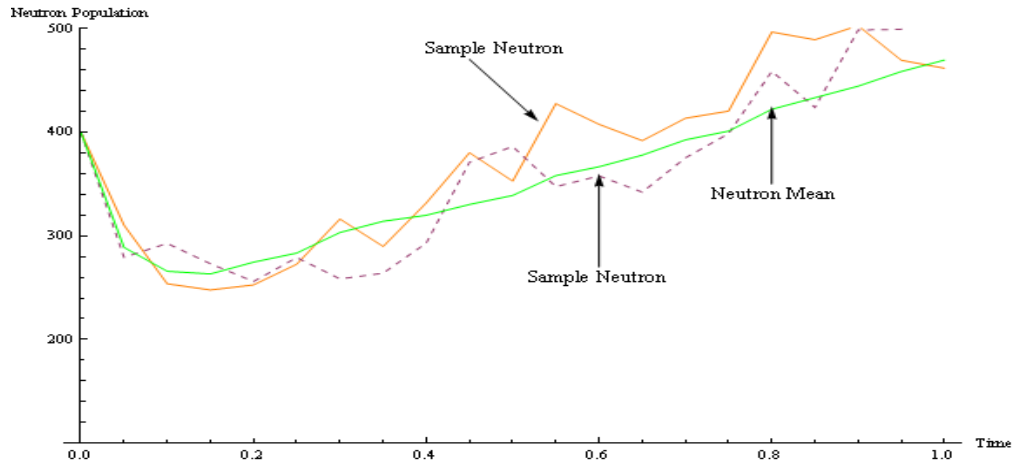


Fig.9. Neutron Population density with $\alpha = 0.5$ and $\rho = 1/3$

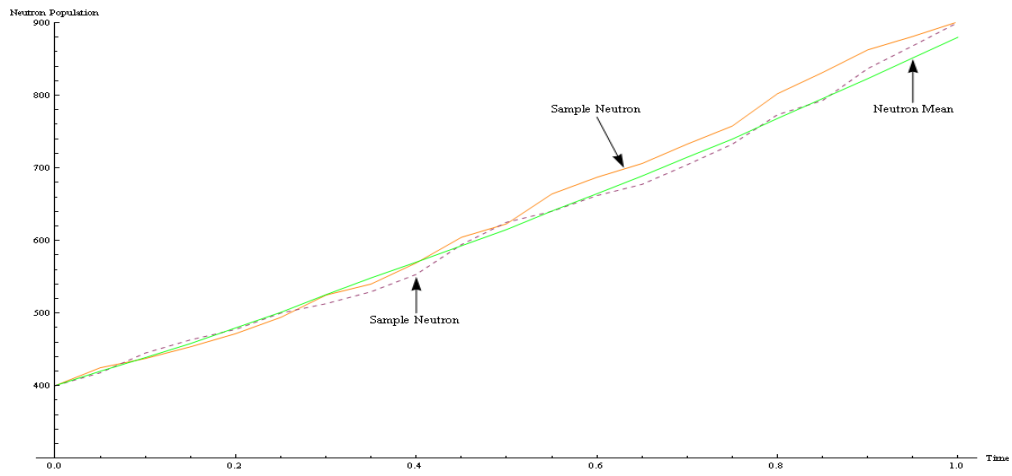


Fig.10. Neutron Population density with $\alpha = 1$ and $\rho = 1/3$

In the second example, we assume the initial condition as

$$\bar{x}(0) = 100 \begin{bmatrix} 1 \\ \frac{\beta_1}{\lambda_1 l} \\ \frac{\beta_2}{\lambda_2 l} \\ \vdots \\ \frac{\beta_m}{\lambda_m l} \end{bmatrix}$$

The following parameters used in this example [53, 60]:

$$\beta = 0.007, \quad \nu = 2.5, \quad l = 0.00002 \text{sec.}, \quad q = 0, \quad \rho = 0.003, \quad \lambda_i = [0.0127, 0.0317, 0.115, 0.311, 1.4, 3.87]$$

and $\beta_i = [0.000266, 0.001491, 0.001316, 0.002849, 0.000896, 0.000182]$ with $m = 6$ delayed groups. The computational results at $t = 0.1$ is given in Table-3 respectively and the numerical results are presented graphically by Figs. 11 to 18.

Table-3 Mean and Standard deviation of Neutron and precursor for different values of α with $\rho = 0.003$

| | $\alpha = 0.25$ | $\alpha = 0.5$ | $\alpha = 0.75$ | $\alpha = 1$ (Classical) |
|--------------------|--------------------------|----------------|-----------------|--------------------------|
| $E(n(0.1))$ | 1.12011×10^{20} | 6635.54 | 356.469 | 208.599 |
| $\sigma(n(0.1))$ | 4.45894×10^{20} | 7755.62 | 664.685 | 255.954 |
| $E(c_1(0.1))$ | 5.50437×10^{22} | 492804 | 164494 | 449815 |
| $\sigma(c_1(0.1))$ | 4.00827×10^{22} | 112512 | 4794.21 | 1233.38 |

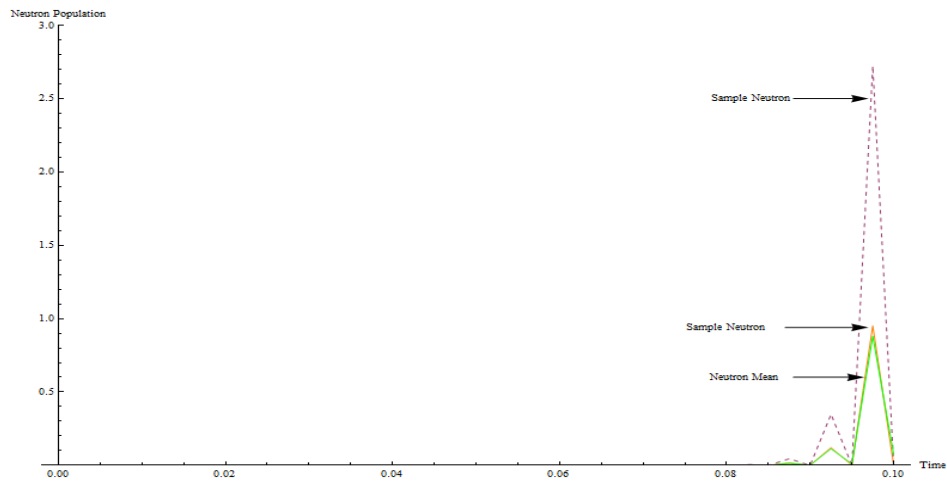


Fig.11. Neutron Population density with $\alpha = 0.25$

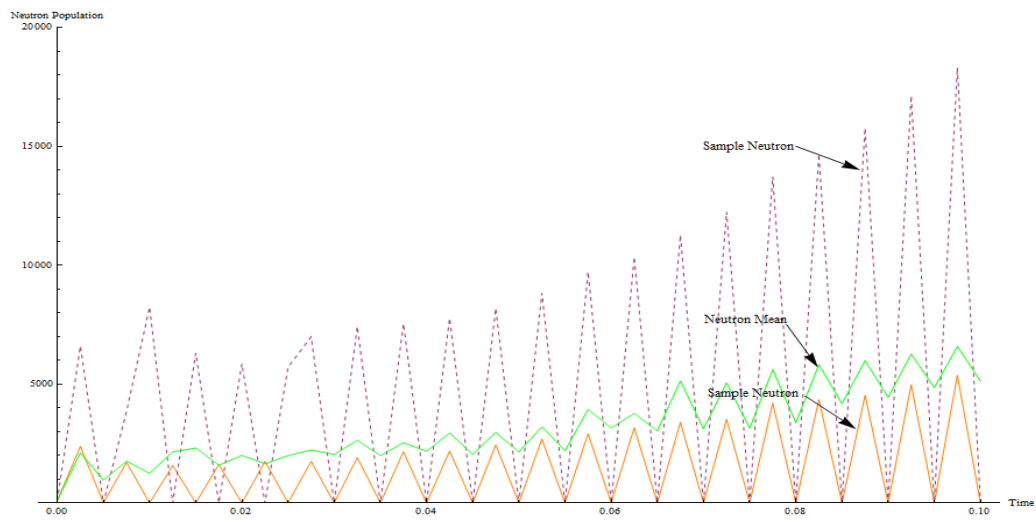


Fig.12. Neutron Population density with $\alpha = 0.5$

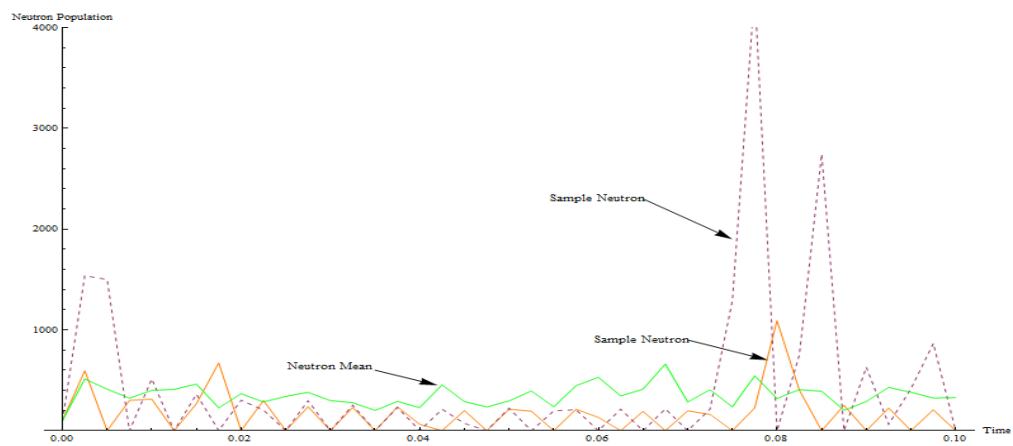


Fig.13. Neutron Population density with $\alpha = 0.75$

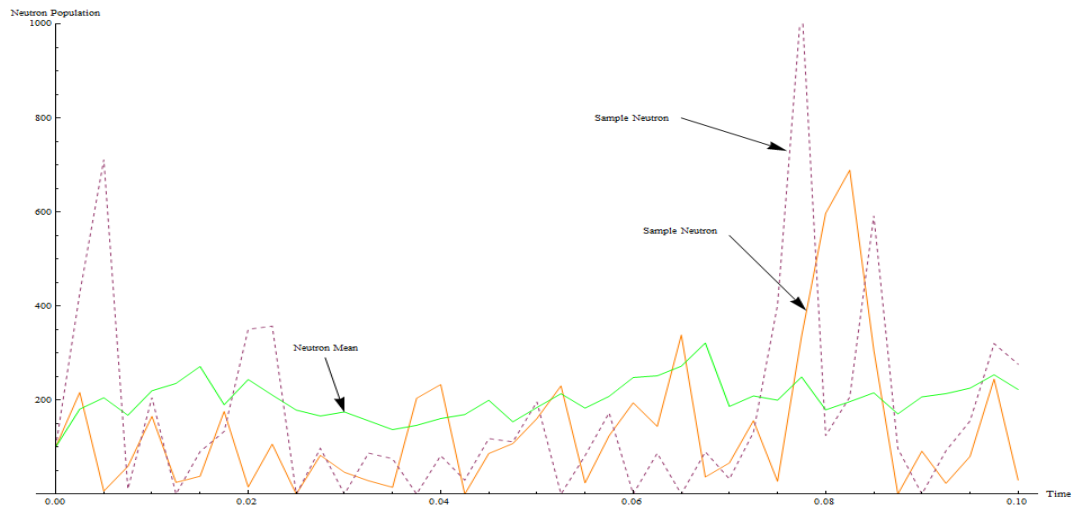


Fig.14. Neutron Population density with $\alpha = 1$

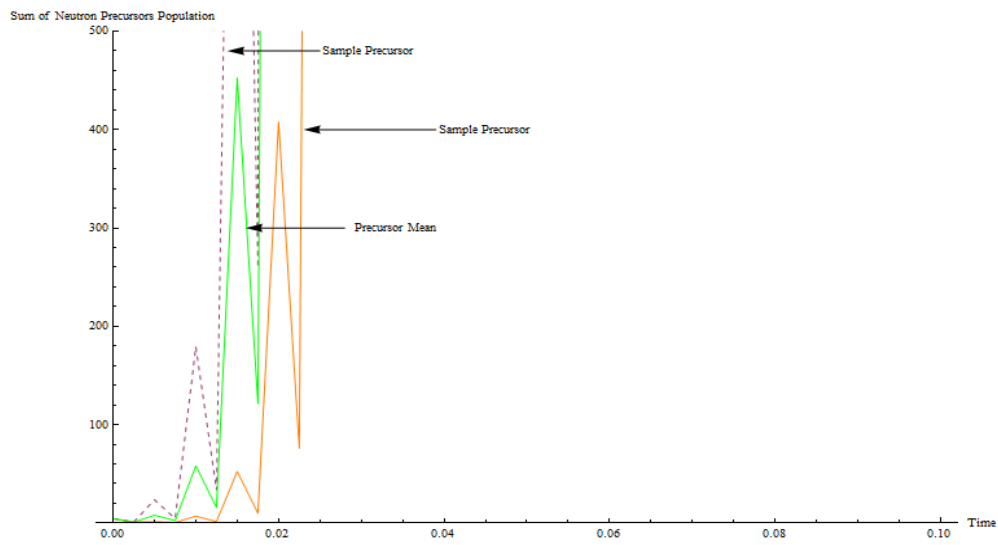


Fig.15. Sum of Neutron precursors population with $\alpha = 0.25$

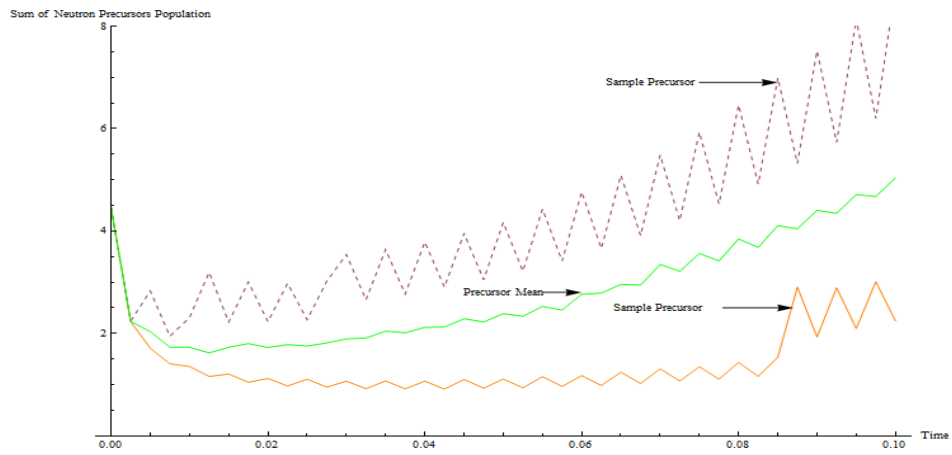


Fig.16. Sum of Neutron precursors population with $\alpha = 0.5$

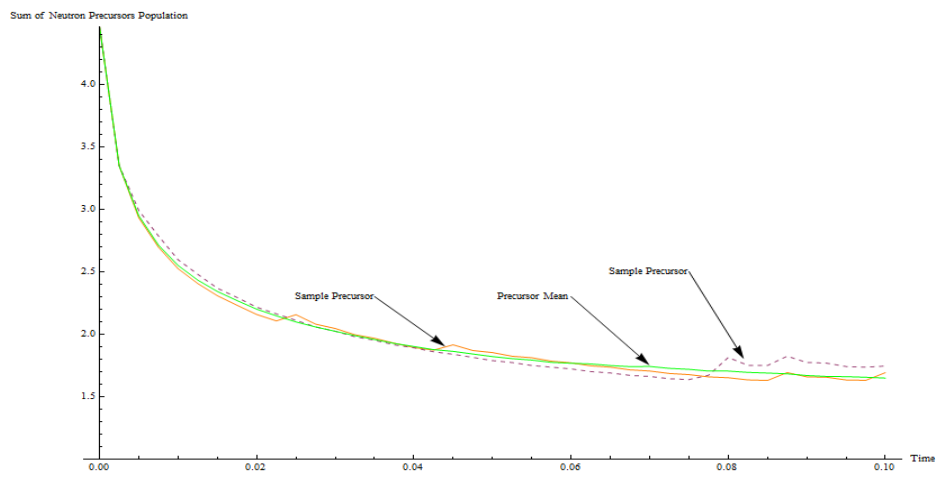


Fig.17. Sum of Neutron precursors population with $\alpha = 0.75$

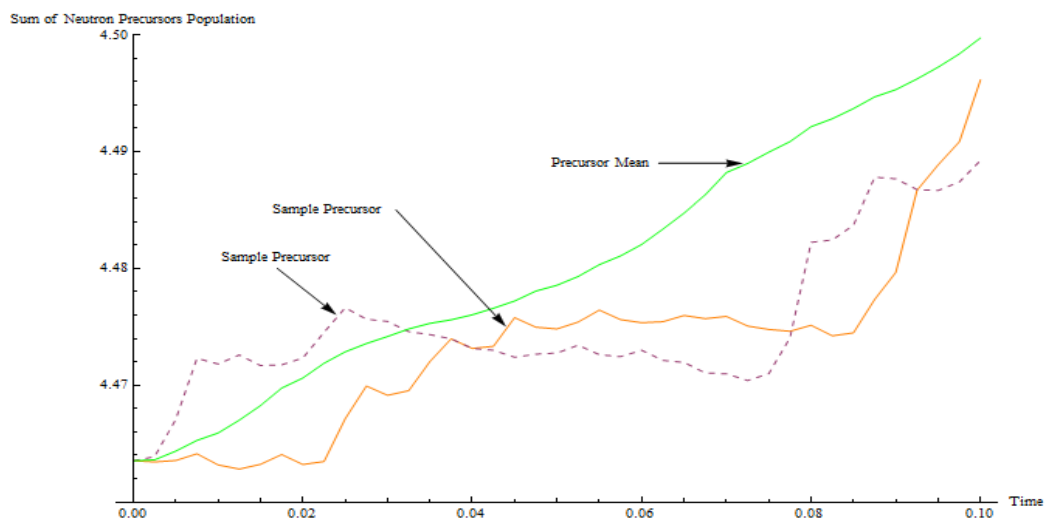


Fig.18. Sum of Neutron precursors population with $\alpha = 1$

5.7 Analysis for Stability of numerical computation for Fractional Stochastic Neutron Point Kinetic Equation

The stability of the numerical computation is calculated by taking the different time-step size h with different values of the anomalous diffusion order α . In order to obtain a stable result, a set of time-step sizes are considered by trial-and-error for different values of α .

A series of numerical experiments have been done for getting a better solution for FSNPK. In the present numerical study, we consider $\alpha = 0.25$, $\alpha = 0.5$, $\alpha = 0.75$, and $\alpha = 1$. The values of time-step size h are taken between $0.005 \leq h \leq 0.025$. The simulation time was considered as 0.1sec. The stability criterion in this analysis is related with 0.01% of the relative error to $n_0 = 100$ at time 0.1sec. for simulation.

$$0.01\% \geq \left| \frac{n_f - n_0}{n_f} \right| \times 100$$

where n_f is the neutron density which is calculated from fractional stochastic model.

To exhibit the behavior of neutron density with $\alpha = 0.25$, we consider h in the interval [0.005sec., 0.025sec.]. In order to check stability criteria, the relative error is 0.009403% at $h=0.005$ sec., 0.009928% at $h=0.01$ sec. and 0.0099998% at $h=0.025$ sec. To examine the behavior of neutron density with $\alpha = 0.5$, we consider h in the interval [0.005sec., 0.025sec.] where the numerical solutions are similar with $\alpha = 0.25$. In this case, the relative error is 0.0088019% at $h=0.005$ sec., 0.008984 % at $h=0.01$ sec. and 0.009141% at $h=0.025$ sec. It can be shown the neutron density behavior with $\alpha = 0.75$ by considering h in the interval [0.005sec., 0.025sec.]. For this case, the numerical scheme is also stable for time-step size $h=0.005$ sec. whose corresponding relative error is 0.006554% whereas the relative error is 0.006393% at $h=0.01$ sec. and 0.006204% at $h=0.025$ sec. For the case when $\alpha = 1$ and h in the interval [0.005sec., 0.025sec.], the relative error is 0.004932% at $h=0.005$ sec., 0.005230 % at $h=0.01$ sec. and 0.002776% at $h=0.025$ sec. Therefore, the above numerical experiment

confirms the stability of our numerical scheme for the solution of fractional stochastic neutron point kinetics equation (FSNPK).

5.8 Conclusion

The numerical methods like Euler Maruyama and Strong order 1.5 Taylor are clearly efficient and convenient for solving classical order stochastic neutron point kinetic equations [73, 74]. The methods are easily applicable to obtain the solution of stochastic neutron point kinetic equations with sinusoidal reactivity and pulse reactivity function. The obtained results exhibit its justification. This chapter shows the applicability of the two numerical stochastic methods like Euler Maruyama and Strong order 1.5 Taylor methods for the numerical solution of stochastic neutron point kinetic equation with sinusoidal reactivity and pulse reactivity for one precursor. The two present methods are quite easy to apply for obtaining accurate numerical solutions for time-varying reactivities like sinusoidal, and pulse reactivity. Moreover, the accuracy can be further improved when the smaller step size of each subinterval.

In this present research work, the fractional stochastic neutron point kinetics equation also has been solved by using Explicit Finite Difference method [75]. The method in this investigation clearly explores an effective numerical method for solving the fractional stochastic point kinetics equation. The method is simple, efficient to calculate and accurate with fewer round off error. This method can be used as a powerful solver for fractional stochastic neutron point kinetic equation. The random behaviors of neutron density and neutron precursor concentrations have not been analyzed in fractional order before of this research work. The results of the numerical approximations for the solution of neutron population density and sum of precursors population are also cited graphically for different arbitrary values of α .

CHAPTER 6

6.1 *Introduction*

The multi-group delayed neutron point kinetic equations in the presence of temperature feedback reactivity are a system of stiff nonlinear ordinary differential equations. The neutron flux and the delayed neutron precursor concentration are important parameters for the study in safety and transient behavior of the reactor power. The point kinetic equations of multi-group delayed neutrons with temperature feedback reactivity describe the neutron density representing the reactor power level, time-dependent reactivity, the precursors concentrations of multi-group of delayed neutrons and thermodynamic variables that enter into the reactivity equation. The solution of this system of equation is useful for providing an estimation for transient behavior of reactor power and other systems of variables of the reactor cores which are fairly tightly coupled.

The fission neutrons are usually of different energies and move in different directions than the incident neutrons. Furthermore, there will generally be a change in the position, energy and direction of motion of the neutron. The interactions of neutrons with nuclei in a medium thus results in transfer of the neutrons from one location to another, from one energy to another and from one direction to another. Then neutron population distribution in nuclear reactor is described by transport equations. One of the simplest approximations to neutron transport that has been widely used in research and practice is the approximation given by diffusion theory.

Reactivity is the most important parameter in nuclear reactor operation. When it is positive the reactor is supercritical, zero at criticality, and negative the reactor is subcritical. Reactivity can

be controlled in various ways: by adding or removing fuel; by changing the fraction of neutrons that leaks from the system; or by changing the amount of an absorber that competes with the fuel for neutrons. The amount of reactivity in a reactor core determines the change of neutron population and the reactor power. Hence reactivity plays a vital role in reactor control.

In this present research work, explicit finite difference method [13, 50, 75] has been applied for solving the classical order and fractional order point kinetics equations of multi-group delayed neutrons with temperature feedback reactivity. Fractional neutron point kinetic equation is useful in the context of anomalous diffusion phenomena due to highly heterogeneous configuration in nuclear reactors. Espinosa et al. [49] proposed a fractional diffusion model as a constitutive equation of the neutron current density. This fractional diffusion model can be applied where large variations of neutron cross sections normally prevent the use of classical diffusion equation, specifically the presence of strong neutron absorbers in the fuel, control rods, and the coolant when injected boron forces the reactor to shutdown. Espinosa et al. [49] proposed a solution procedure which has been inherited from Edwards et al. [54]. In contrast to their method, in the present numerical scheme fractional derivative has been discretized by Grunwald–Letnikov derivative and the fractional point kinetic equation has been converted directly into finite difference equation. Then it has been adjusted in the form of explicit finite difference scheme. The present numerical scheme is simple and efficient in compared to Espinosa-Paredes et al. [49]. Although Caputo derivative has been chosen by Espinosa et al. [49] but in numerical computation for discretizing the fractional derivative we have to apply Grunwald-Letnikov fractional derivative rather than Caputo derivative. It is very much clear that, the present numerical scheme requires less computational effort in compared to Generalization of the analytical exponential model (GAEM) [76] and Padé approximation method [77] for classical order $\alpha = 1$.

Due to the use of this finite difference numerical technique for solving coupled reactor kinetic equations, we apply Grunwald-Letnikov fractional derivative which is useful for discretizing the fractional derivative. The obtained results are presented graphically and also compared to the other methods exist in open literature for classical order at $\alpha = 1$ [76, 77].

6.2 Classical order Nonlinear Neutron Point Kinetic Model⁹

The multi-group delayed neutron point kinetics equations [22, 23, 32] and the Newtonian temperature feedback reactivity are the stiff nonlinear ordinary differential equations which presented as

$$\frac{dn(t)}{dt} = \left(\frac{\rho(t) - \beta}{l} \right) n(t) + \sum_{i=1}^m \lambda_i c_i(t) \quad (6.2.1)$$

$$\frac{dc_i(t)}{dt} = \left(\frac{\beta_i}{l} \right) n(t) - \lambda_i c_i(t), \quad i = 1, 2, 3, \dots, m \quad (6.2.2)$$

and

$$\rho(t) = at - b \int_0^t n(t') dt' \quad (6.2.3)$$

where $n(t) \equiv$ the neutron density

$\rho(t) \equiv$ the reactivity as a function of time,

$\beta = \sum_{i=1}^m \beta_i \equiv$ the total fraction of delayed neutrons,

$\beta_i \equiv$ the fraction of i - group of delayed neutrons,

$\lambda_i \equiv$ the decay constant of i -group of delayed neutrons,

$l \equiv$ the prompt neutron generation time,

$c_i(t) \equiv$ the precursor concentrations of i^{th} -group of delayed neutron,

⁹ **A. Patra** and S. Saha Ray, "Solution for Nonlinear Neutron Point Kinetics Equation with Newtonian Temperature feedback reactivity in Nuclear Reactor dynamics", **Int. Journal of Nuclear Energy Science and Technology** (Inderscience), Communicated.

m = the total number of delayed neutrons group,

$\rho(t)$ = the impressed reactivity variation,

β = the shutdown coefficient of the reactor system.

These equations have been the subject of extensive study using all kinds of approximations.

We are interested here in the general problem, a time dependent reactivity function $\rho(t)$. It is well-known that these sets of ordinary differential equations are quite stiff.

One of the important properties in a nuclear reactor is the reactivity, due to the fact that it is directly related to the control of the reactor. For safety analysis and transient behaviour of the reactor, the neutron population and the delayed neutron precursor concentration are important parameters to be studied. The start-up process of a nuclear reactor requires that reactivity is varied in the system by lifting the control rods discontinuously. In practice, the control rods are withdrawn at time intervals such that reactivity is introduced in the reactor core linearly, to allow criticality to be reached in a slow and safe manner.

6.3 Numerical solution of Nonlinear Neutron Point Kinetic Equation in presence of reactivity function

Let us take the time step size h . Using the finite difference for time derivative, the numerical approximations of the eqs. (6.2.1) to (6.2.3), in view of the research work [13, 50, 75], have been obtained as

$$n_{k+1} = n_k + h \left(\frac{\rho_k - \beta}{l} \right) n_k + h \left(\sum_{i=1}^m \lambda_i c_{i,k} \right) \quad (6.3.1)$$

$$c_{i,k+1} = c_{i,k} + h \left(\left(\frac{\beta_i}{l} \right) n_k - \lambda_i c_{i,k} \right) \quad (6.3.2)$$

$$\rho_{k+1} = \rho_k + h(a - b n_k) \quad (6.3.3)$$

The above eqs. (6.3.1) to (6.3.3) represent the explicit finite difference scheme which leads from the time layer t_k to t_{k+1} where $k=0,1,2,\dots$.

Here $n_k = n(t_k) \equiv$ neutron density at time t_k ,

$c_{i,k} = c_i(t_k) \equiv$ the precursor concentrations of i^{th} -group of delayed neutron at time t_k ,

$\bar{x}_k = \bar{x}(t_k) \equiv k$ -th approximation at time t_k , $t_k = kh$, $k=0,1,2,\dots$. Here $h = t_{k+1} - t_k$ with initial condition $\bar{x}_0 = \bar{x}(t_0)$.

The main advantage of explicit finite difference method is that the method is relatively simple and easily computable.

6.4 Numerical Results and Discussions for classical order Nonlinear Neutron Point Kinetic Equation

In the present analysis, we discussed three cases of reactivity function [76, 78, 79] of step, ramp (positive and negative) and feedback reactivity. All results started from equilibrium conditions with neutron density $n(0)=1.0$ and k^{th} of delayed neutron precursors density $c_k(0) = (n(0)\beta_k / \lambda_k l)$. In the following, each case will be discussed separately. The numerical results are presented in the Tables 1-4 and cited by graphically.

6.4.1 Step-reactivity insertions

In this case, for checking the efficiency of the numerical scheme, it is applied to the thermal reactor with the following parameters [78, 79]:

$\lambda_1 = 0.0127 \text{sec}^{-1}$, $\lambda_2 = 0.0317 \text{sec}^{-1}$, $\lambda_3 = 0.115 \text{sec}^{-1}$, $\lambda_4 = 0.311 \text{sec}^{-1}$, $\lambda_5 = 1.40 \text{sec}^{-1}$, $\lambda_6 = 3.87 \text{sec}^{-1}$, $\beta_1 = 0.000285$, $\beta_2 = 0.0015975$, $\beta_3 = 0.00141$, $\beta_4 = 0.0030525$, $\beta_5 = 0.00096$, $\beta_6 = 0.000195$, $\beta = 0.0075$, $l = 0.0005 \text{sec}$. The relative errors of neutron density with four cases of step reactivity -1.0\$, -0.5\$, +0.5\$ and +1.0\$ are presented in Table-1. The present scheme is an efficient numerical technique to obtain the solution for point kinetic equations with the step reactivity insertions.

6.4.2 *Ramp reactivity insertions*

In this example, the numerical scheme is applied to the thermal reactor with the following parameters [78, 79]:

$\lambda_1 = 0.0127 \text{sec}^{-1}$, $\lambda_2 = 0.0317 \text{sec}^{-1}$, $\lambda_3 = 0.115 \text{sec}^{-1}$, $\lambda_4 = 0.311 \text{sec}^{-1}$, $\lambda_5 = 1.40 \text{sec}^{-1}$, $\lambda_6 = 3.87 \text{sec}^{-1}$, $\beta_1 = 0.000266$, $\beta_2 = 0.001491$, $\beta_3 = 0.001316$, $\beta_4 = 0.002849$, $\beta_5 = 0.000896$, $\beta_6 = 0.000182$, $\beta = 0.007$, $l = 0.00002 \text{sec}$. The neutron density of the thermal reactor with positive ramp reactivity is $\rho(t) = +0.1t$ and the negative ramp reactivity is $\rho(t) = -0.1t$ whence the numerical results are cited in Table-2 and Table-3 respectively.

6.4.3 *Temperature Feedback Reactivity*

In this case, the numerical scheme is applied to solve the point kinetic equations of delayed neutrons with the presence of Newtonian temperature feedback reactivity for U^{235} -graphite reactor. The following parameters of U^{235} -graphite reactor are used [76]:

$\lambda_1 = 0.0127 \text{sec}^{-1}$, $\lambda_2 = 0.0317 \text{sec}^{-1}$, $\lambda_3 = 0.115 \text{sec}^{-1}$, $\lambda_4 = 0.311 \text{sec}^{-1}$, $\lambda_5 = 1.40 \text{sec}^{-1}$, $\lambda_6 = 3.87 \text{sec}^{-1}$, $\beta_1 = 0.00246$, $\beta_2 = 0.001363$, $\beta_3 = 0.001203$, $\beta_4 = 0.002605$, $\beta_5 = 0.00819$, $\beta_6 = 0.00167$, $\beta = 0.0064$. The value of generation time is 0.00005sec , a takes the values 0.1, 0.01, 0.003

and b takes the values 10^{-11} and 10^{-13} . The numerical results obtained for feedback reactivity are presented in Table-4 and cited by Figs. 1-6.

Table-1: The relative errors and the exact neutron density $n(t)$ (*neutrons/cm³*) of the thermal reactor with step reactivity for step-size $h=0.0001$ s

| Reactivity (\$) | Time (s) | Exact Solution [79] | Present numerical scheme Explicit Finite Difference Method | Relative Errors |
|--------------------|----------|------------------------|--|-----------------------|
| -1.0 | 0.1 | 0.5205643 | 0.520454 | 2.11×10^{-4} |
| | 1.0 | 0.4333335 | 0.433332 | 0 |
| | 10 | 0.2361107 | 0.23611 | 0 |
| -0.5 | 0.1 | 0.6989252 | 0.698838 | 1.24×10^{-4} |
| | 1.0 | 0.6070536 | 0.607053 | 0 |
| | 10 | 0.3960777 | 0.396077 | 0 |
| +0.5 | 0.1 | 1.533113 | 1.53323 | 0 |
| | 1.0 | 2.511494 | 2.5115 | 0 |
| | 10 | 14.21503 | 14.2148 | 1.61×10^{-5} |
| +1.0 | 0.1 | 2.515766 | 2.51572 | 0 |
| | 0.5 | 10.36253 | 10.3614 | 0 |
| | 1.0 | 32.18354 | 32.176 | 2.34×10^{-4} |

Table-2: The neutron density $n(t)$ (*neutrons/cm³*) of the thermal reactors with a positive ramp reactivity (+0.1\$/s) for step-size $h=0.0001s$

| Time (s) | TSM [79] | BBF [80] | SCM [81] | Explicit Finite Difference Method |
|-------------|----------------------|----------------------|----------------------|--------------------------------------|
| 2.0 | 1.3382 | 1.3382 | 1.3382 | 1.3382 |
| 4.0 | 2.2284 | 2.2284 | 2.2284 | 2.22842 |
| 6.0 | 5.5822 | 5.5820 | 5.5819 | 5.58192 |
| 8.0 | 42.789 | 42.786 | 42.788 | 42.7817 |
| 10.0 | 4.5143×10^5 | 4.5041×10^5 | 4.5391×10^5 | 4.49850×10^5 |

Table-3: The neutron density $n(t)$ (*neutrons/cm³*) of the thermal reactors with a negative ramp reactivity (-0.1\$/s) for step-size $h=0.0001s$

| Time (s) | TSM [79] | GAEM [76] | Padé [77] | Explicit Finite Difference Method |
|-------------|----------|-----------|-----------|--------------------------------------|
| 2.0 | 0.791955 | 0.792007 | 0.792007 | 0.792006 |
| 4.0 | 0.612976 | 0.613020 | 0.613018 | 0.613017 |
| 6.0 | 0.474027 | 0.474065 | 0.474058 | 0.474058 |
| 8.0 | 0.369145 | 0.369172 | 0.369169 | 0.369168 |
| 10.0 | 0.290636 | 0.290653 | 0.290654 | 0.290654 |

Table-4: The neutron density $n(t)$ (*neutrons/cm³*) at the first peak of U^{235} - reactor with feedback reactivity for step-size $h=0.0001s$

| <i>a</i> | <i>b</i> | Delayed Neutrons at the first peak | | | Time of the first peak | | |
|----------|------------|------------------------------------|-------------------------|--|------------------------|--------------|--|
| | | GAEM [76] | Padé [77] | Explicit Finite Difference Method | GAEM [76] | Padé [77] | Explicit Finite Difference Method |
| 0.1 | 10^{-11} | 2.4202×10^{11} | 2.4197×10^{11} | 2.42275×10^{11} | 0.224 | 0.224 | 0.2245 |
| | 10^{-13} | 2.9057×10^{13} | 2.9055×10^{13} | 2.9037×10^{13} | 0.238 | 0.238 | 0.2385 |
| 0.01 | 10^{-11} | 2.0103×10^{10} | 2.0107×10^{10} | 2.02264×10^{10} | 1.100 | 1.100 | 1.1014 |
| | 10^{-13} | 2.4882×10^{12} | 2.4890×10^{12} | 2.5043×10^{12} | 1.149 | 1.149 | 1.150 |
| 0.003 | 10^{-11} | Not available | Not available | 5.24943×10^9 | Not | Not | 2.897 |
| | 10^{-13} | | | 6.73756×10^{11} | available | available | 2.996 |

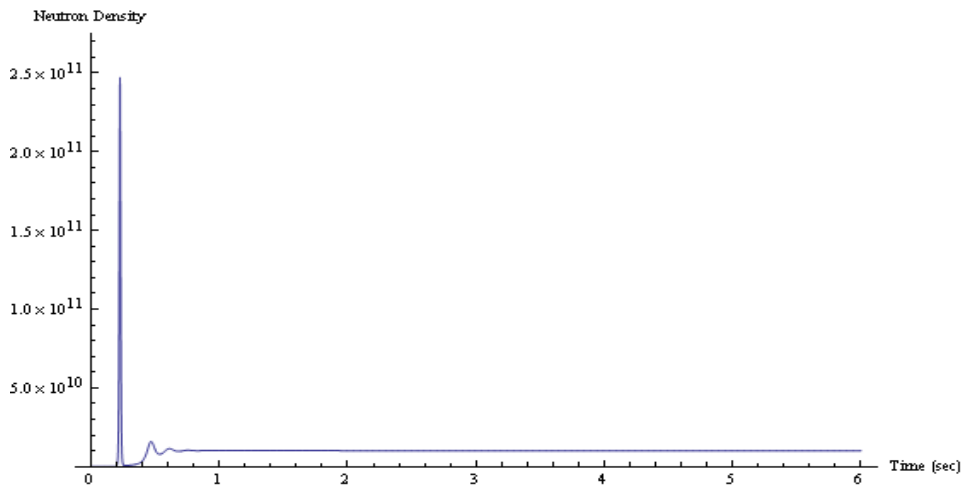


Fig. 1. Neutron density $n(t)$ (neutrons/cm³) for $a=0.1$ and $b=10^{-11}$

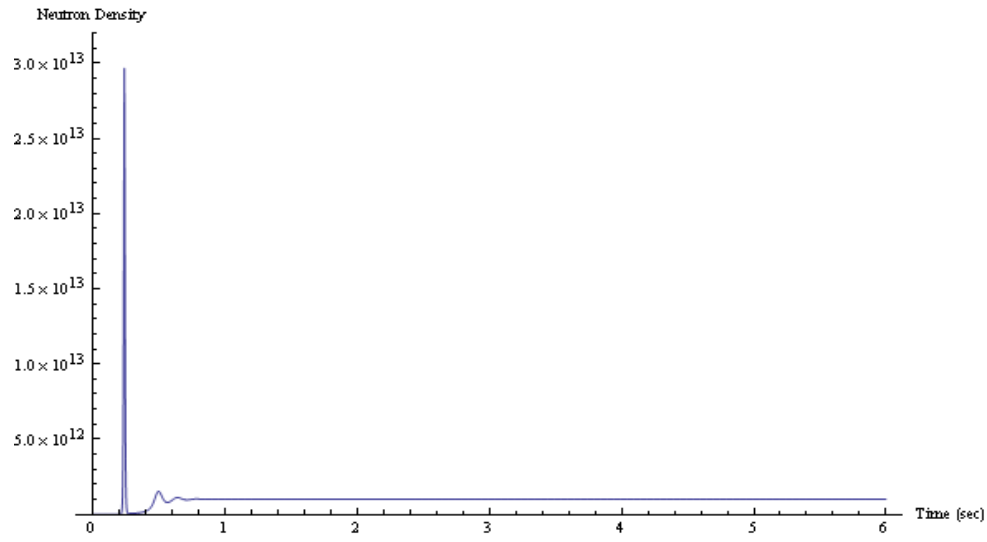


Fig. 2. Neutron density $n(t)$ (neutrons/cm³) for $a=0.1$ and $b=10^{-13}$

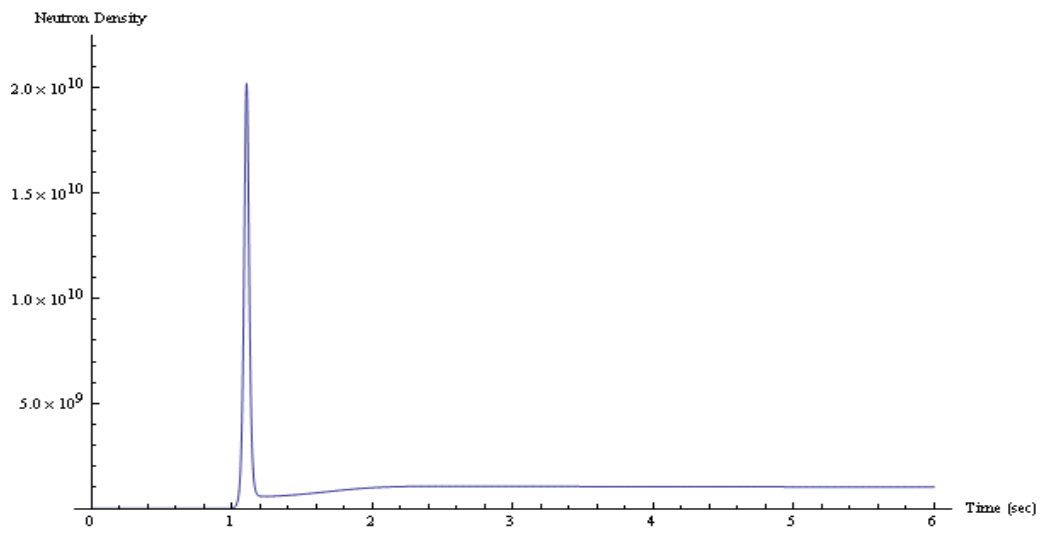


Fig. 3. Neutron density $n(t)$ (neutrons/cm³) for $a=0.01$ and $b=10^{-11}$

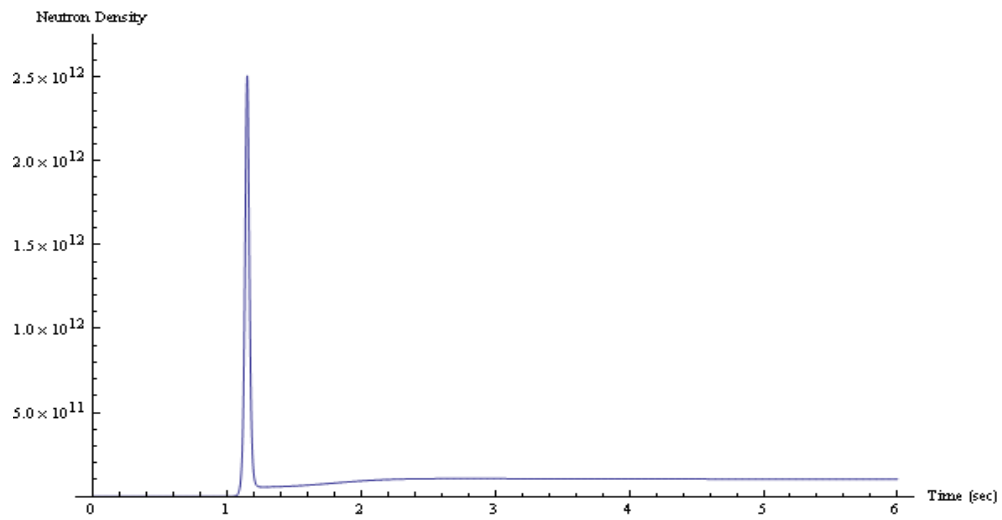


Fig.4. Neutron density $n(t)$ (neutrons/cm³) for $a=0.01$ and $b=10^{-13}$

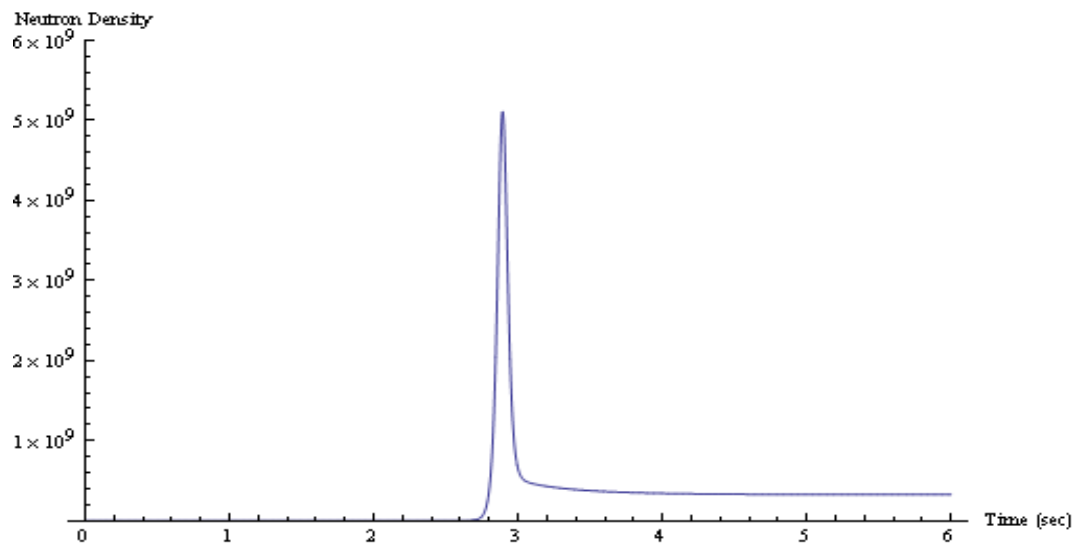


Fig.5. Neutron density $n(t)$ (neutrons/cm³) for $a=0.003$ and $b=10^{-11}$

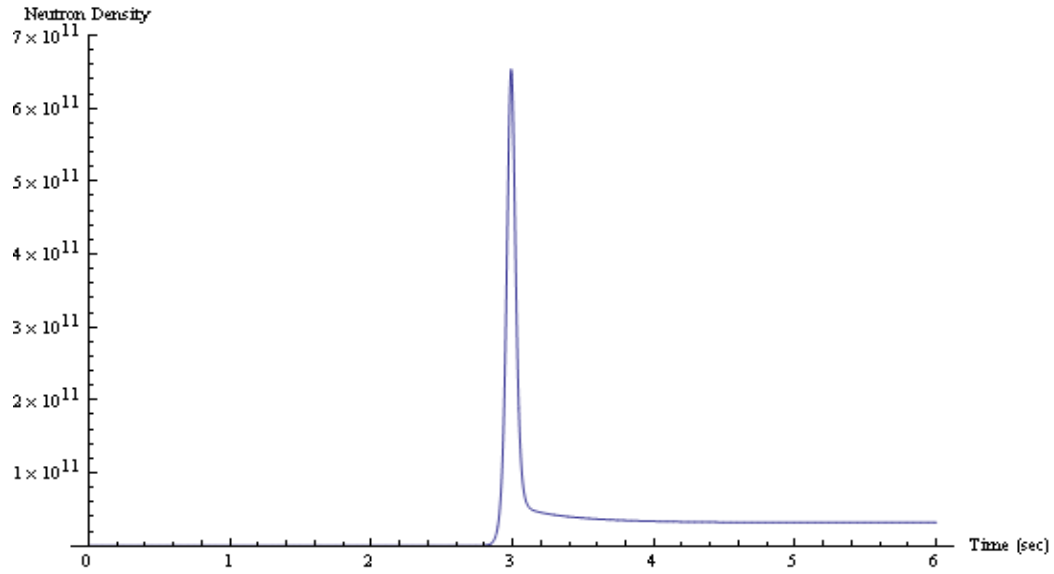


Fig.6. Neutron density $n(t)$ (neutrons/cm³) for $a=0.003$ and $b=10^{-13}$

The objective of this study was to develop an accurate and computationally efficient method (Explicit finite difference scheme) for solving time-dependent reactor dynamics equations with Newtonian temperature feedback. To test the developed solution and to prove the validity of the method for application purposes, a comparison with the other conventional methods indicates the superiority of the proposed explicit finite difference method (EFDM).

6.5 *Mathematical Model for Nonlinear Fractional Neutron Point Kinetics Equation*¹⁰

The fractional calculus was first anticipated by Leibnitz, one of the founders of standard calculus, in a letter written in 1695. Now-a-days real physical problems are best modeled by Fractional Calculus. This calculus involves different definitions of the fractional operators viz. the Riemann- Liouville fractional derivative, Caputo derivative, Riesz derivative and

¹⁰ **A. Patra** and S. Saha Ray, “On the Solution of Nonlinear Fractional Neutron Point Kinetics Equation with Newtonian Temperature feedback reactivity”, **Nuclear Technology** (American Nuclear Society), Accepted.

Grünwald- Letnikov fractional derivative [44, 82]. The non-integer order of calculus has gained considerable importance during the past decades mainly due to its applications in diverse fields of science and engineering.

Here, we consider Grunwald- Letnikov definition of fractional derivative which is defined as

$${}_a D_t^p f(t) = \lim_{\substack{h \rightarrow 0 \\ nh=t-a}} h^{-p} \sum_{r=0}^n \omega_r^p f(t-rh) \quad (6.5.1)$$

where $\omega_r^p = (-1)^r \binom{p}{r}$

$$\omega_0^p = 1 \quad \text{and} \quad \omega_r^p = \left(1 - \frac{p+1}{r}\right) \omega_{r-1}^p, \quad r=1,2,\dots$$

Fractional neutron point kinetic equation is useful in the context of anomalous diffusion phenomena due to highly heterogeneous configuration in nuclear reactors. The multi-group delayed fractional order ($\alpha > 0$) neutron point kinetics equations [83] with Newtonian temperature feedback reactivity are the stiff nonlinear ordinary differential equations [22-24, 32] which is presented as

$$\frac{d^\alpha n(t)}{dt^\alpha} = \left(\frac{\rho(t) - \beta}{l} \right) n(t) + \sum_{i=1}^m \lambda_i c_i(t) \quad (6.5.2)$$

$$\frac{dc_i(t)}{dt} = \left(\frac{\beta_i}{l} \right) n(t) - \lambda_i c_i(t), \quad i=1,2,3,\dots,m \quad (6.5.3)$$

$$\text{and } \rho(t) = at - b \int_0^t n(s) ds \quad (6.5.4)$$

where $n(t) \equiv$ the neutron density

$\rho(t) \equiv$ the reactivity as a function of time,

$\beta = \sum_{i=1}^m \beta_i \equiv$ the total fraction of delayed neutrons,

$\beta_i \equiv$ the fraction of i^{th} - group of delayed neutrons,

$\lambda_i \equiv$ the decay constant of i^{th} -group of delayed neutrons,

$l \equiv$ the prompt neutron generation time,

$c_i(t) \equiv$ the precursor concentrations of i^{th} -group of delayed neutron,

$m =$ the total number of delayed neutrons group,

$a \equiv$ the impressed reactivity variation,

$b \equiv$ the shutdown coefficient of the reactor system.

6.6 Application of Explicit Finite Difference Method (EFDM) for solving Fractional order Nonlinear Neutron Point Kinetic Model

Let us take the time step size h . Using the finite difference for time derivative, the numerical approximations of the eqs. (6.5.2) to (6.5.4), in view of the research work [13, 50, 75], have been obtained as

$$h^{-\alpha} \sum_{j=0}^r \omega_j^{(\alpha)} n_{(r-j)} = \left(\frac{\rho_{(r)} - \beta}{l} \right) n_{(r)} + \sum_{i=1}^m \lambda_i c_{i,r} \quad (6.6.1)$$

$$\left(\frac{c_{(r)} - c_{(r-1)}}{h} \right) = \left(\frac{\beta_i}{l} \right) n_{(r)} - \lambda_i c_{i,r}, \quad i = 1, 2, 3, \dots, m \quad (6.6.2)$$

$$\left(\frac{\rho_{(r)} - \rho_{(r-1)}}{h} \right) = a - b n_{(r)} \quad (6.6.3)$$

The above eqs. (6.6.1) - (6.6.3) leads to implicit numerical iteration scheme owing to the fact that explicit finite difference method is relatively simple and computationally fast. In this present work, we propose an explicit numerical scheme which leads from the time layer t_{r-1} to t_r as follows

$$n_{(r)} = -\sum_{j=1}^r \omega_j^{(\alpha)} n_{(r-j)} + h^\alpha \left[\left(\frac{\rho_{(r-1)} - \beta}{l} \right) n_{r-1} + \sum_{i=1}^m \lambda_i c_{i,r-1} \right] \quad (6.6.4)$$

where $n_{(r)} = n(t_r) \equiv r$ -th approximation of neutron density at time t_r ,

with initial condition $n_0 = n(t_0)$.

$c_{i,r} = c_i(t_r) \equiv$ the precursor concentrations of i^{th} -group of delayed neutron at time t_r ,

$\rho_{(r)} \equiv r$ -th approximation of feedback reactivity function,

$$t_r = rh, \quad r = 0, 1, 2, \dots \text{ and } \omega_j^\alpha = (-1)^j \binom{\alpha}{j}, \quad j = 0, 1, 2, 3, \dots \text{ and } h = t_{r+1} - t_r.$$

The main advantage of explicit finite difference method is that the method is relatively simple and easily computable.

6.7 Numerical Results and Discussions for Fractional Nonlinear Neutron Point Kinetic Equation with temperature feedback reactivity function

In this case, the numerical scheme explicit finite difference is applied to solve the fractional order ($\alpha > 0$ and $\alpha \in R^+$) point kinetic equations with delayed neutrons in presence of Newtonian temperature feedback reactivity for U^{235} -graphite reactor. The Newtonian temperature feedback reactivity which is dependent on time and neutron density is given by

$$\rho(t) = at - b \int_0^t n(s) ds, \text{ where the first term represents the impressed reactivity variation and } b$$

presents the shutdown coefficient of the reactor system. The point kinetics equation with temperature feedback corresponds to a stiff system of nonlinear differential equations for the neutron density and delayed precursor concentrations. The computed solutions of the present point kinetics equations provide information on the dynamics of nuclear reactor operation in

presence of Newtonian temperature feedback reactivity. The following parameters of U^{235} -graphite reactor are used [76, 84]

$\lambda_1 = 0.0127\text{sec}^{-1}$, $\lambda_2 = 0.0317\text{sec}^{-1}$, $\lambda_3 = 0.115\text{sec}^{-1}$, $\lambda_4 = 0.311\text{sec}^{-1}$, $\lambda_5 = 1.40\text{sec}^{-1}$, $\lambda_6 = 3.87\text{sec}^{-1}$, $\beta_1 = 0.00246$, $\beta_2 = 0.001363$, $\beta_3 = 0.001203$, $\beta_4 = 0.002605$, $\beta_5 = 0.00819$, $\beta_6 = 0.00167$, $\beta = 0.0064$. The value of generation time is $l = 5 \times 10^{-5}\text{sec.}$, a takes the values 0.1, 0.01 and b takes the values 10^{-11} and 10^{-13} . We have considered the values for fractional order $\alpha = 0.5$, 0.75, 1.25 and 1.5 respectively. If $\alpha = 1$, the process is normal diffusion and when $0 < \alpha < 1$, then the diffusion process is anomalous diffusion. The fractional neutron point kinetics equation considering temperature feedback to reactivity with Newtonian temperature approximation is analyzed in this present paper. The numerical results obtained for neutron density of delayed neutrons in fractional order neutron point kinetics equation with feedback reactivity are introduced in Table-5 and with classical order $\alpha = 1$ in Table 6. The maximum peak for the neutron density can be observed from Figs. 7-14 in four cases of fractional order $\alpha = 0.5, 0.75, 1.25$ and 1.75 using $a = 0.01$ in presence of $b = 10^{-11}$ and $b = 10^{-13}$.

The behavior of the neutron density after the peak in cited Figs. 7-14 indicates that the system asymptotically leads to equilibrium state. In Fig. 13, the second peak tries to get the equilibrium state and in Fig. 12 after 1.6 second the system follows equilibrium state. From Figs 8-14, it can be observed that the neutron density of delayed neutron tries to follow equilibrium behavior after a high density in first peak. The obtained results from explicit finite difference scheme for neutron density using temperature feedback reactivity have been compared with Generalization of the analytical exponential method (GAEM) [76] and Padé approximation method [77] for classical order $\alpha = 1$. Moreover, the absolute errors of the proposed scheme with respect to Generalization of the analytical exponential method

(GAEM) [76] and Padé approximation method [77] have been presented in Table 7. In our present research work, for the first time ever, we have been analysed the behaviour of the first peak of the neutron density in fractional order using temperature feedback reactivity.

Table-5: The neutron density $n(t)$ at the first peak of U^{235} - reactor with feedback reactivity for fractional order point kinetic equation when step-size $h=0.0001$ sec.

| a | b | Delayed Neutron at the first peak by Explicit Finite Difference Method | | | | Time of the first peak by Explicit Finite Difference Method | | | |
|------|------------|---|------------------------|-------------------------|-------------------------|--|-----------------|-----------------|----------------|
| | | $\alpha = 0.5$ | $\alpha = 0.75$ | $\alpha = 1.25$ | $\alpha = 1.5$ | $\alpha = 0.5$ | $\alpha = 0.75$ | $\alpha = 1.25$ | $\alpha = 1.5$ |
| 0.1 | 10^{-11} | 2.042×10^{11} | 2.138×10^{11} | 2.862×10^{11} | 3.113×10^{11} | 0.0919 | 0.1391 | 0.3549 | 0.5144 |
| | 10^{-13} | 2.548×10^{13} | 2.592×10^{13} | 3.420×10^{13} | 3.7511×10^{13} | 0.0939 | 0.1451 | 0.3833 | 0.5641 |
| 0.01 | 10^{-11} | 1.401×10^{10} | 1.690×10^{10} | 2.4605×10^{10} | 2.8465×10^{10} | 0.754 | 0.8938 | 1.377 | 1.702 |
| | 10^{-13} | 1.7847×10^{12} | 2.113×10^{12} | 3.039×10^{12} | 3.4975×10^{12} | 0.763 | 0.917 | 1.4 | 1.832 |

Table-6: The neutron density $n(t)$ (neutrons/cm³) at the first peak of U^{235} - reactor with feedback reactivity taking step-size $h=0.0001$ s for classical order $\alpha = 1$

| a | b | Delayed Neutrons at the first peak | | | Time of the first peak | | |
|-----|-----|------------------------------------|--------------|----------------------------------|------------------------|--------------|----------------------------------|
| | | GAEM [76] | Padé [77] | Explicit Finite Difference | GAEM [76] | Padé [77] | Explicit Finite Difference |

| | | | | Method | | | Method |
|------|------------|-------------------------|-------------------------|--------------------------|-------|-------|--------|
| 0.1 | 10^{-11} | 2.4202×10^{11} | 2.4197×10^{11} | 2.42275×10^{11} | 0.224 | 0.224 | 0.2245 |
| | 10^{-13} | 2.9057×10^{13} | 2.9055×10^{13} | 2.9037×10^{13} | 0.238 | 0.238 | 0.2385 |
| 0.01 | 10^{-11} | 2.0103×10^{10} | 2.0107×10^{10} | 2.02264×10^{10} | 1.100 | 1.100 | 1.1014 |
| | 10^{-13} | 2.4882×10^{12} | 2.4890×10^{12} | 2.5043×10^{12} | 1.149 | 1.149 | 1.150 |

Table-7: Absolute Errors for neutron density $n(t)$ (*neutrons/cm³*) at the first peak of U^{235} -reactor in presence of feedback reactivity taking step-size $h=0.0001$ s for classical order $\alpha = 1$

| a | b | Delayed Neutrons at the first peak | | Time of the first peak | |
|------|------------|--|--|--|--|
| | | Absolute Error of Present method (EFDM) with regard to GAEM [76] | Absolute Error of Present method (EFDM) with regard to Padé [77] | Absolute Error of Present method (EFDM) with regard to GAEM [76] | Absolute Error of Present method (EFDM) with regard to Padé [77] |
| 0.1 | 10^{-11} | 0.00255×10^{11} | 0.00305×10^{11} | 0.0005 | 0.0005 |
| | 10^{-13} | 0.002×10^{13} | 0.0018×10^{13} | 0.0005 | 0.0005 |
| 0.01 | 10^{-11} | 0.01234×10^{10} | 0.0119×10^{10} | 0.0014 | 0.0014 |

| | | | | | |
|--|------------|-------------------------|-------------------------|-------|-------|
| | 10^{-13} | 0.0161×10^{12} | 0.0153×10^{12} | 0.001 | 0.001 |
|--|------------|-------------------------|-------------------------|-------|-------|

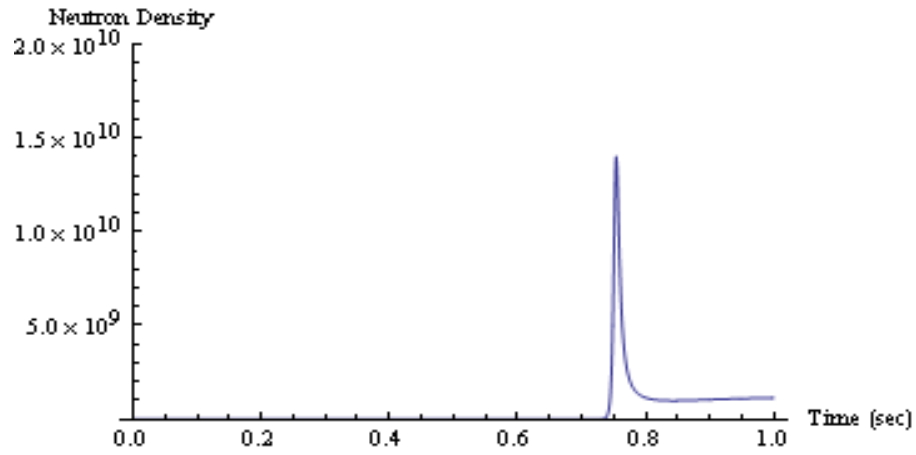


Fig. 7. Neutron Density of delayed neutron for $\alpha = 0.5$ with $a = 0.01$ and $b = 10^{-11}$

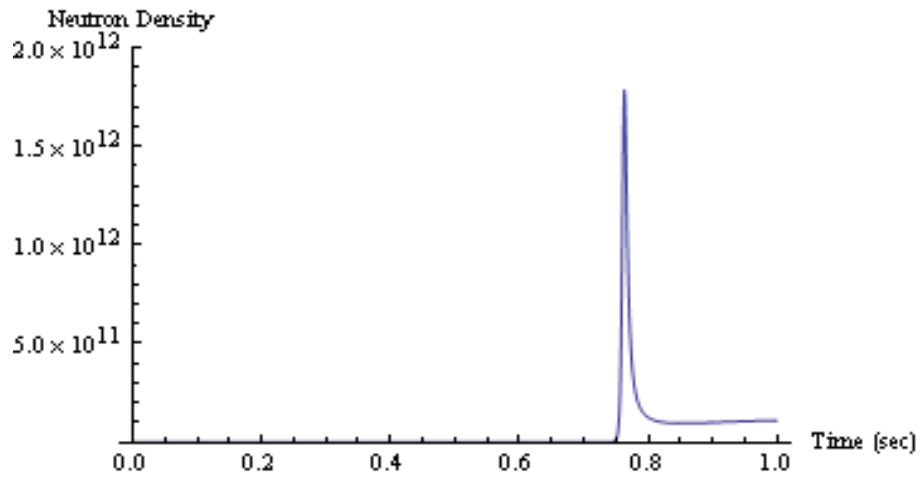


Fig. 8. Neutron Density of delayed neutron for $\alpha = 0.5$ with $a = 0.01$ and $b = 10^{-13}$

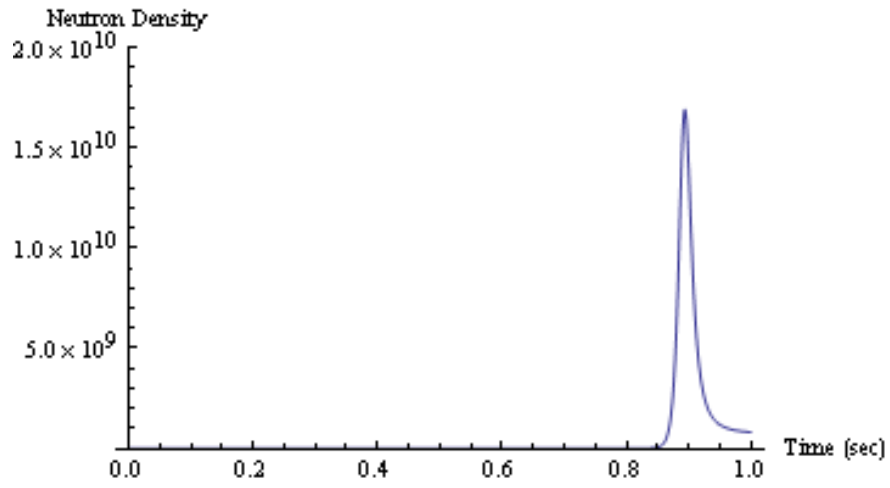


Fig. 9. Neutron Density of delayed neutron for $\alpha = 0.75$ with $a = 0.01$ and $b = 10^{-11}$

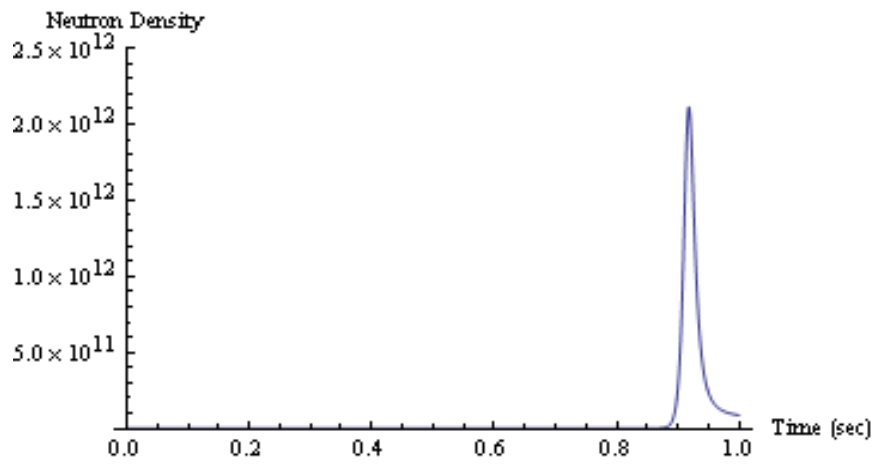


Fig. 10. Neutron Density of delayed neutron for $\alpha = 0.75$ with $a = 0.01$ and $b = 10^{-13}$

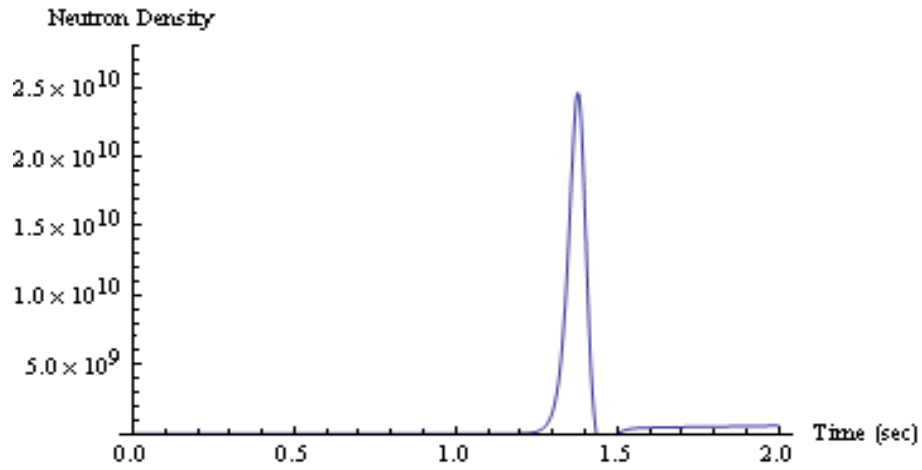


Fig. 11. Neutron Density of delayed neutron for $\alpha=1.25$ with $a=0.01$ and $b=10^{-11}$

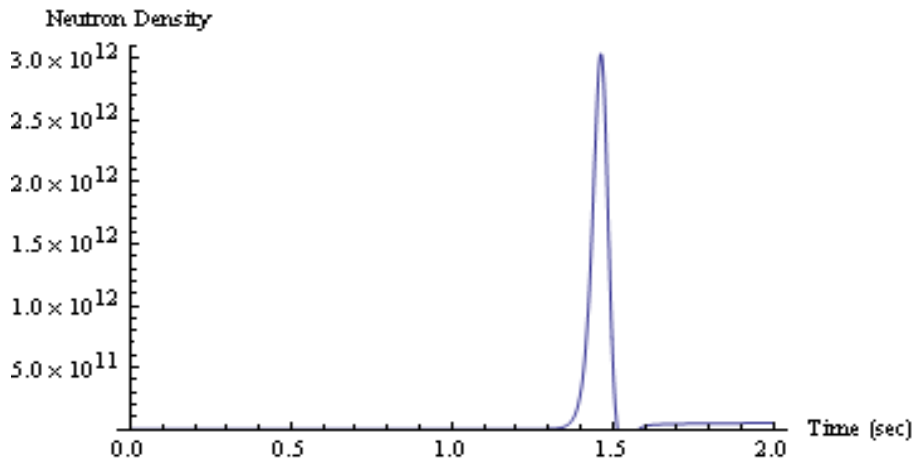


Fig. 12. Neutron Density of delayed neutron for $\alpha=1.25$ with $a=0.01$ and $b=10^{-13}$

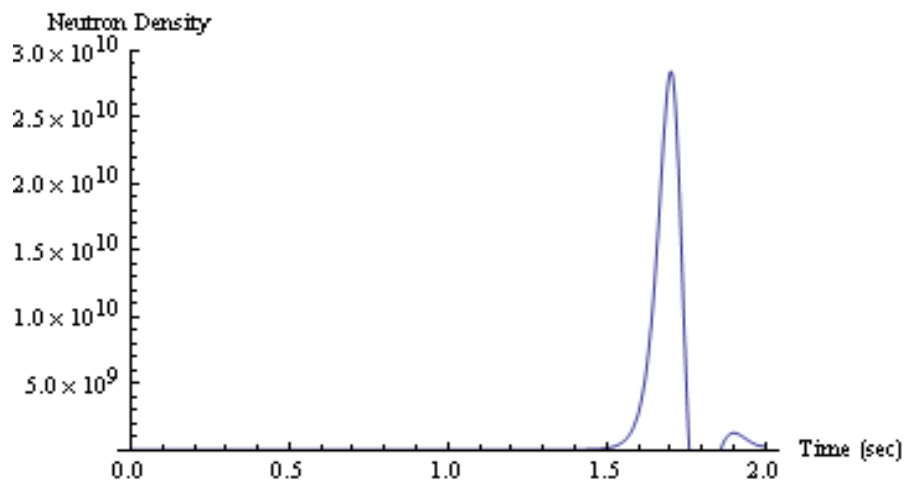


Fig.13. Neutron Density of delayed neutron for $\alpha=1.5$ with $a=0.01$ and $b=10^{-11}$

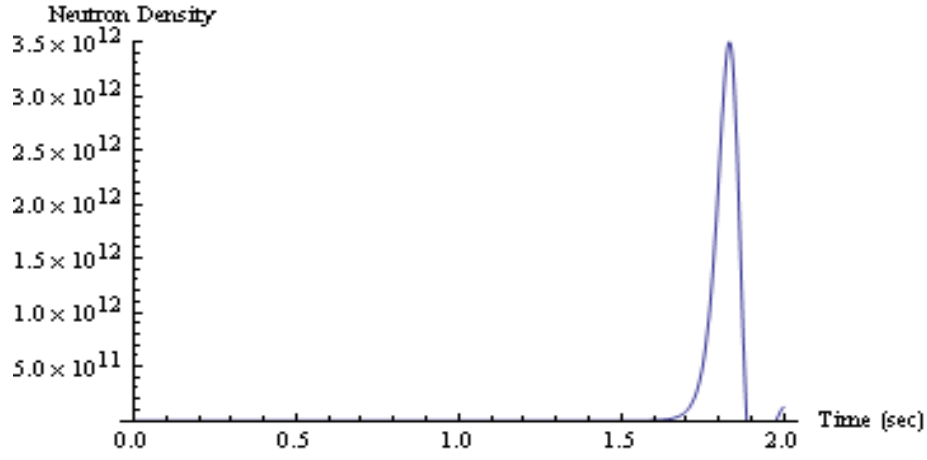


Fig. 14. Neutron Density of delayed neutron for $\alpha = 1.5$ with $a = 0.01$ and $b = 10^{-13}$

6.8 Computational Error Analysis for Fractional order Nonlinear Neutron Point Kinetic Equation

Grunwald-Letnikov fractional derivative presented in eq. (6.5.1) is important for discretizing fractional derivative $\frac{d^\alpha n(t)}{dt^\alpha}$ numerically in a simple and efficient way:

$$\frac{d^\alpha n(t)}{dt^\alpha} = \frac{1}{h^\alpha} \sum_{j=0}^r \omega_j^{(\alpha)} n_{(r-j)} + O(h^p), \text{ where } p \text{ is the order of approximation.}$$

The truncation error in eq. (6.6.1) is

$$\frac{1}{h^\alpha} \sum_{j=0}^r \omega_j^{(\alpha)} n_{(r-j)} - \left(\frac{\rho_{(r)} - \beta}{l} \right) n_{(r)} - \sum_{i=1}^m \lambda_i c_{i,r} = O(h^p)$$

Again, the truncating error in eq. (6.6.2) is

$$\left(\frac{c_{(r)} - c_{(r-1)}}{h} \right) - \left(\frac{\beta_i}{l} \right) n_{(r)} + \lambda_i c_{i,r} = O(h)$$

And finally the truncating error in eq. (6.6.3) is

$$\left(\frac{\rho_{(r)} - \rho_{(r-1)}}{h} \right) - a + bn_{(r)} = O(h) .$$

Therefore, we finally get the total truncation error for eqns. (6.6.1)-(6.6.3) as follows

$$= O(h^p) + O(h) + O(h) \cong O(h^p)$$

Hence, we obtain the computational error as $O(h^p)$ and eventually it tends to zero as $h \rightarrow 0$.

Moreover, it shows that the computational overhead is less for the proposed explicit finite difference scheme.

6.9 Conclusion

The objective of this study is to develop an accurate and computationally efficient method for solving time-dependent reactor dynamics equations. The numerical solutions of integer and fractional order nonlinear point kinetic equations with multi-group of delayed neutrons are presented. The explicit finite difference method constitutes an easy algorithm that provides the results with sufficient accuracy for most applications and is being both conceptually and structurally simple. The method is simple, efficient to calculate and accurate with fewer computational error. Results of this method are compared with other available methods from which it can be concluded that the method is simple and computationally fast. To assess utility of the developed technique, different cases of reactivity were studied.

The numerical solutions for both classical and fractional order point kinetic equations [83] with multi-group of delayed neutrons are presented in presence of Newtonian Temperature feedback reactivity. To predict the dynamical behavior for U^{235} reactors with time-dependent reactivity function and to obtain the solution of multi-group delayed neutron point kinetic

equation [67, 71], this numerical scheme (EFDM) is simple and efficient method. This numerical technique gives a good result for the nonlinear neutron point kinetic equations with time-dependent reactivity function. The method is simple, efficient to calculate and accurate with fewer computational error. The obtained results exhibit its justification. In Table 6, the solutions of classical order ($\alpha=1$) point kinetic equations using Newtonian temperature feedback reactivity have been compared with the results available in [76, 77]. From Table 6, it can be observed that there is a very good agreement of results between the present method and the methods viz. Generalized analytical exponential method and also Padé approximation method applied in [76, 77]. The authors have cited the computed absolute errors for their proposed numerical scheme with regard to the other reference results exist in open literature in Table 7 for classical integer order (i.e. $\alpha=1$). In this aspect, it can be concluded that the present method is very simple and efficient technique. The present analysis exhibits that the featured method is applicable equally well to nonlinear problem in which the reactivity depends on the neutron density through temperature feedback. This research work shows the applicability of the explicit finite difference method for the numerical solution of nonlinear classical and fractional order neutron point kinetic equation. The results representing the numerical approximate solutions of neutron density involving feedback reactivity have been cited graphically.

CHAPTER 7

7.1 *Introduction*

The numerical solution of point kinetics equation with a group of delayed neutrons is useful in predicting neutron density variation during the operation of a nuclear reactor. The continuous indication of the neutron density and its rate of change are important for the safe startup and operation of reactors. The Haar wavelet operational method (HWOM) has been proposed to obtain the numerical approximate solution of neutron point kinetic equation appeared in nuclear reactor with time-dependent and independent reactivity function. The present method has been applied to solve stiff point kinetics equations elegantly with step, ramp, zig-zag, sinusoidal and pulse reactivity insertions. This numerical method has turned out as an accurate computational technique for many applications. In dynamical system of nuclear reactor, the point-kinetic equations are the coupled linear differential equations for neutron density and delayed neutron precursor concentrations. These equations which expresses the time dependence of the neutron population and the decay of the delayed neutron precursors within a reactor are first order and linear, and essentially describe the change in neutron population within the reactor due to a change in reactivity. As reactivity is directly related to the control of the reactor, so it is the important property in a nuclear reactor. For purpose of safety analysis and transient behavior of the reactor, the neutron population and the delayed neutron precursor concentration are important parameters to be studied. An important property of the kinetics equations is the stiffness of the system. The stiffness is a severe problem in numerical solutions of the point kinetics equations and it necessarily requires the need for small time steps in a computational scheme.

Aboanber and Nahla [77] presented an analytical Padé approximate solution for group of six delayed neutrons with constant, ramp and temperature feedback reactivity insertions. Again Aboanber and Nahla [85, 86] presented the solution of a point kinetic equation with exponential mode analysis and generalization of analytical inversion method. Kinard and Allen [53] described the numerical solution based on PCA (Piecewise Constant Approximation) for the point kinetic equations in nuclear reactor dynamics. Nahla [76-79] presented the analytical methods to solve nonlinear point kinetic equations and generalized power series solution for neutron point kinetic equation has been proposed by Hamada [87]. A numerical integral method that efficiently provides the solution of the point kinetics equations by using the better basis function (BBF) for the approximation of the neutron density in one time step integrations has been described and investigated by Li et al [80]. Chao and Attard [81] proposed the stiffness confinement method (SCM) for solving the kinetic equations to overcome the stiffness problem in reactor kinetics.

Quintero-Leyva [63] has also solved the neutron point kinetic equation by a numerical algorithm CORE for a lumped and temperature feedback. Using very simple technique like backward Euler finite difference method (BEFD), Ganapol [88] has also solved neutron point kinetic equation. Mc. Mohan and Pierson [64] has also solved neutron point kinetic equation using Taylor series method (TSM) involving reactivity functions. Again Picca et al. [89] has solved neutron point kinetic equation by applying enhanced piecewise constant approximation (EPCA) involving both linear and non-linear reactivity insertion.

Wavelet analysis is a newly developed mathematical tool for applied analysis, image manipulation and numerical analysis. Wavelets have been applied in numerous disciplines

such as image compression, data compression, and many more [90, 91]. Among the different wavelet families mathematically most simple are the Haar wavelets [92].

Haar functions have been used from 1910 when they were introduced by the Hungarian mathematician Alfred Haar [93]. The Haar transform is one of the earliest examples of what is known now as a compact, dyadic, orthonormal wavelet transform. The Haar function, being an odd rectangular pulse pair, is the simplest and oldest orthonormal wavelet with compact support. In the meantime, several definitions of the Haar functions and various generalizations have been published and used. They were intended to adapt this concept to some practical applications, as well as to extend its application to different classes of signals. Thanks to their useful features and possibility to provide a local analysis of signals, the Haar functions appear very attractive in many applications as for example, image coding, edge extraction, and binary logic design.

Haar wavelets are made up of pairs of piecewise constant functions and mathematically the simplest orthonormal wavelets with a compact support. Due to the mathematical simplicity the Haar wavelets method has turned out to be an effective tool for solving differential and integral equations. The Haar wavelets have the following features: (1) Orthogonal and normalization, (2) having closed support and (3) the simple expression [94, 95]. Due to its simplicity, the Haar wavelets are very effective for solving differential and integral equations. It is worthwhile attempt to develop the numerical scheme for the solution of the point reactor kinetic equations. The importance of this scheme is that it can usually be applied to more realistic mathematical or physical models. Therefore, the main focus of the present paper is the application of Haar wavelet technique for solving the problem of coupled point kinetic equations with reactivity function in nuclear reactor dynamics.

In this present work, Haar wavelet operational method for solving the point kinetics equation with a group of six-delayed neutrons has been applied. The obtained numerical approximation results of this method are then compared with the referenced methods for different reactivities. In the present investigation, the main attractive advantage of this computational numerical method is its simplicity, efficiency and applicability.

7.2 Haar Wavelets

Haar wavelets are the simplest wavelets among various types of wavelets. They are step functions on the real line that can take only three values -1, 0 and 1. The method has been used for being its simpler, fast and computationally attractive feature. The Haar functions are the family of switched rectangular waveforms where amplitudes can differ from one function to another function. Usually the Haar wavelets are defined for the interval $t \in [0, 1]$ but in general case $t \in [A, B]$, we divide the interval $[A, B]$ into m equal subintervals; each of width $\Delta t = (B - A)/m$. In this case, the orthogonal set of Haar functions are defined in the interval $[A, B]$ by [95]

$$h_0(t) = \begin{cases} 1 & t \in [A, B], \\ 0 & \text{elsewhere} \end{cases},$$

and

$$h_i(t) = \begin{cases} 1, & \zeta_1(i) \leq t < \zeta_2(i) \\ -1, & \zeta_2(i) \leq t < \zeta_3(i) \\ 0, & \text{otherwise} \end{cases} \quad (7.2.1)$$

where

$$\zeta_1(i) = A + \left(\frac{k-1}{2^j} \right) (B-A) = A + \left(\frac{k-1}{2^j} \right) m\Delta t,$$

$$\zeta_2(i) = A + \left(\frac{k-(1/2)}{2^j} \right) (B-A) = A + \left(\frac{k-(1/2)}{2^j} \right) m\Delta t,$$

$$\zeta_3(i) = A + \left(\frac{k}{2^j}\right)(B - A) = A + \left(\frac{k}{2^j}\right)m\Delta t,$$

$i = 1, 2, \dots, m$, $m = 2^J$ and J is a positive integer, called the maximum level of resolution. Here, j and k represent the integer decomposition of the index i . i.e. $i = k + 2^j - 1$, $0 \leq j < i$ and $1 \leq k < 2^j + 1$.

7.3 Function Approximation and Operational Matrix of the general order Integration

Any function $y(t) \in L^2([0, 1])$ can be expanded in Haar series as

$$y(t) = c_0 h_0(t) + c_1 h_1(t) + c_2 h_2(t) + \dots, \quad \text{where } c_j = \int_0^1 y(t) h_j(t) dt. \quad (7.3.1)$$

If $y(t)$ is approximated as piecewise constant in each subinterval, the sum in eq. (7.3.1) may be terminated after m terms and consequently we can write discrete version in the matrix form as

$$Y \approx \sum_{i=0}^{m-1} c_i h_i(t_l) = C_m^T H_m, \quad (7.3.2)$$

$$\text{for collocation points } t_l = A + (l - 0.5)\Delta t, \quad l = 1, 2, \dots, m \quad (7.3.3)$$

where Y and C_m^T are the m -dimensional row vectors.

Here H is the Haar wavelet matrix of order m defined by $H = [h_0, h_1, \dots, h_{m-1}]^T$, i.e.

$$H = \begin{bmatrix} h_0 \\ h_1 \\ \dots \\ h_{m-1} \end{bmatrix} = \begin{bmatrix} h_{0,0} & h_{0,1} & \dots & h_{0,m-1} \\ h_{1,0} & h_{1,1} & \dots & h_{1,m-1} \\ \dots & & & \\ h_{m-1,0} & h_{m-1,1} & \dots & h_{m-1,m-1} \end{bmatrix}, \quad (7.3.4)$$

where h_0, h_1, \dots, h_{m-1} are the discrete form of the Haar wavelet bases.

Operational matrix of the general order integration

The integration of the $H_m(t) = [h_0(t), h_1(t), \dots, h_{m-1}(t)]^T$ can be approximated by Chen and Hsiao [96]

$$\int_0^t H_m(\tau) d\tau \cong QH_m(t), \quad (7.3.5)$$

where Q called as Haar wavelet operational matrix of integration which is a square matrix of m -dimension. To derive the Haar wavelet operational matrix of the general order of integration, we recall the fractional integral of order $\alpha(>0)$ which is defined by Podlubny [44]

$$J^\alpha f(t) = \frac{1}{\Gamma(\alpha)} \int_0^t (t-\tau)^{\alpha-1} f(\tau) d\tau, \quad t > 0, \alpha \in R^+, \quad (7.3.6)$$

where R^+ is the set of positive real numbers.

The Haar wavelet operational matrix Q^α for integration of the general order α is given by

$$\begin{aligned} Q^\alpha H_m(t) &= J^\alpha H_m(t) = [J^\alpha h_0(t), J^\alpha h_1(t), \dots, J^\alpha h_{m-1}(t)]^T \\ &= [Qh_0(t), Qh_1(t), \dots, Qh_{m-1}(t)]^T \end{aligned} \quad (7.3.7)$$

where

$$Qh_0(t) = \begin{cases} \frac{t^\alpha}{\Gamma(1+\alpha)}, & t \in [A, B], \\ 0, & elsewhere, \end{cases} \quad (7.3.8)$$

and

$$Qh_i(t) = \begin{cases} 0, & A \leq t < \zeta_1(i), \\ \phi_1, & \zeta_1(i) \leq t < \zeta_2(i), \\ \phi_2, & \zeta_2(i) \leq t < \zeta_3(i), \\ \phi_3, & \zeta_3(i) \leq t < B, \end{cases} \quad (7.3.9)$$

where

$$\phi_1 = \frac{(t - \zeta_1(i))^\alpha}{\Gamma(\alpha + 1)},$$

$$\phi_2 = \frac{(t - \zeta_1(i))^\alpha}{\Gamma(\alpha + 1)} - 2 \frac{(t - \zeta_2(i))^\alpha}{\Gamma(\alpha + 1)},$$

$$\phi_3 = \frac{(t - \zeta_1(i))^\alpha}{\Gamma(\alpha + 1)} - 2 \frac{(t - \zeta_2(i))^\alpha}{\Gamma(\alpha + 1)} + \frac{(t - \zeta_3(i))^\alpha}{\Gamma(\alpha + 1)},$$

for $i = 1, 2, \dots, m$, $m = 2^J$ and J is, a positive integer, called the maximum level of resolution.

Here, j and k represent the integer decomposition of the index i . i.e. $i = k + 2^j - 1$, $0 \leq j < i$ and

$$1 \leq k < 2^j + 1.$$

7.4 Application of Haar wavelet Operational Method for solving Neutron Point Kinetics Equation¹¹

The point reactor kinetic equations without effect of the extraneous neutron source are given by [24, 32]

$$\frac{dn(t)}{dt} = \left[\frac{\rho(t) - \beta}{l} \right] n(t) + \sum_{i=1}^M \lambda_i c_i \quad (7.4.1)$$

$$\frac{dc_i(t)}{dt} = \frac{\beta_i}{l} n(t) - \lambda_i c_i(t), \quad i = 1, 2, \dots, M \quad (7.4.2)$$

¹¹ **A. Patra** and S. Saha Ray, 2014, “A Numerical Approach based on Haar wavelet operational method to solve Neutron Point Kinetics Equation involving Imposed Reactivity Insertions”, **Annals of Nuclear Energy** (Elsevier), Vol. 68, pp. 112-117.

with the initial condition $n(0) = n_0$ and $c_k(0) = (n(0)\beta_k / \lambda_k l)$, for $k = 1, 2, \dots, M$

where $n(t)$ is the time-dependent neutron density, $c_i(t)$ is the i^{th} precursor density, $\rho(t)$ is the time-dependent reactivity function, β_i is the i^{th} delayed fraction and $\beta = \sum_{i=1}^M \beta_i$ is the total delayed fraction, l is the neutron generation time, and λ_i is the i^{th} group decay constant.

Let us divide the interval $[A, B]$ into m equal subintervals; each of width $\Delta t = (B - A) / m$. We assume,

$$\frac{dn(t)}{dt} = Dn(t) = \sum_{i=1}^m c_i h_i(t) \quad (7.4.3)$$

Integrating eq. (7.4.3) from 0 to t , we can derive that

$$n(t) = n(0) + \sum_{i=1}^m c_i Q h_i(t) \quad (7.4.4)$$

where $Q h_i(t)$ is given by in eq. (7.3.9) for $\alpha = 1$.

Next, we consider

$$\frac{dc_k(t)}{dt} = Dc_k(t) = \sum_{i=1}^m d_{k,i} h_i(t) \quad (7.4.5)$$

From eq. (7.4.5), we can again derive that $c_k(t) = c_k(0) + \sum_{i=1}^m d_{k,i} Q h_i(t)$. (7.4.6)

Here also $Q h_i(t)$ is given by in eq. (7.3.9) for $\alpha = 1$.

Now, we substitute all these eqs. (7.4.3)-(7.4.6) together in eq. (7.4.1) and (7.4.2), we obtained the following numerical scheme as [97]

$$\sum_{i=1}^m c_i h_i(t) = \frac{(\rho - \beta)}{l} \left(n(0) + \sum_{i=1}^m c_i Q h_i(t) \right) + \sum_{r=1}^M \lambda_r \left(c_r(0) + \sum_{i=1}^m d_{r,i} Q h_i(t) \right) \quad (7.4.7)$$

and

$$\sum_{i=1}^m d_{k,i} h_i(t) = \left(\frac{\beta_k}{l} \right) \left(n(0) + \sum_{i=1}^m c_i Q h_i(t) \right) - \lambda_k \left(c_k(0) + \sum_{i=1}^m d_{k,i} Q h_i(t) \right) \quad (7.4.8)$$

By considering all the wavelet collocation points $t_l = A + (l - 0.5)\Delta t$, $l = 1, 2, \dots, m$, we may obtain the system of m -number of algebraic equations. By solving these system of equations using any mathematical software, we can obtained the Haar coefficients c_i and $d_{k,i}$. Then we can find the approximate solution for neutron density $n(t)$. The main advantage of the Haar wavelet operational method is that it always converts the system of equations into set of algebraic equations which can be easily solvable by any mathematical software. The limitation of this wavelet method is only that it requires high level of resolution for large time duration.

7.5 Numerical Results and Discussions

In this chapter, the Haar wavelet operational method has been used for numerical solution of the point reactor kinetic Eq. (7.4.1) and (7.4.2). In the present analysis, the above numerical method has been applied to solve the point kinetics equations with group six delayed neutrons. The four types of cases involving step, ramp, zig-zag and sinusoidal reactivates have been presented. The values for λ_k and β_k and neutron generation time l for the reactor have been taken from Ganapol [88]. All results started from equilibrium conditions with neutron density $n(0) = 1.0$ and k^{th} of delayed neutron precursors density $c_k(0) = (n(0)\beta_k / \lambda_k l)$. In the following, each case will be discussed separately.

7.5.1 Step Reactivity Insertions

To check the accuracy of Haar wavelet method, it has been applied to the thermal reactor with the following parameters obtained from Ganapol [88]: $\lambda_1 = 0.0127\text{sec.}^{-1}$, $\lambda_2 = 0.0317\text{sec.}^{-1}$, $\lambda_3 = 0.115\text{sec.}^{-1}$, $\lambda_4 = 0.311\text{sec.}^{-1}$, $\lambda_5 = 1.40\text{sec.}^{-1}$, $\lambda_6 = 3.87\text{sec.}^{-1}$, $\beta = 0.0075$, $\beta_1 = 0.000285$, $\beta_2 = 0.0015975$, $\beta_3 = 0.00141$, $\beta_4 = 0.0030525$, $\beta_5 = 0.00096$, $\beta_6 = 0.000195$ and $l = 0.0005\text{sec.}$. The obtained results justify that Haar wavelet operational method is an accurate and efficient computational technique for solving point kinetic equation using step reactivity insertions.

Table 1 represents the solution for neutron density involving step reactivity -1.0\$, -0.5\$, +0.5\$ and +1.0\$ using Haar wavelet operational method (HWOM) and consequently the obtained results have been compared with backward Euler finite difference method (BEFD) [88] taking level of resolution $J = 8$.

Table-1: Neutron density $n(t)$ of the thermal reactor with step reactivity insertions

| ρ (\$) | t (s) | HWOM with $m = 2^8$ | BEFD [88] |
|-------------|---------|---------------------|-----------------|
| -1.0 | 0.1 | 5.20563444767E-01 | 5.205642866E-01 |
| | 1.0 | 4.33333406022E-01 | 4.333334453E-01 |
| | 10 | 2.36110396447E-01 | 2.361106508E-01 |
| | 100 | 2.86673059802E-02 | 2.866764245E-02 |
| -0.5 | 0.1 | 6.989247254605E-01 | 6.989252256E-01 |
| | 1.0 | 6.070535313626E-01 | 6.070535656E-01 |
| | 10 | 3.960774713631E-01 | 3.960776907E-01 |
| | 100 | 7.158236238460E-02 | 7.158285444E-02 |

| | | | |
|------|-----|--------------------|-----------------|
| | 0.1 | 1.53311290367E+00 | 1.53311264E+00 |
| +0.5 | 1.0 | 2.51149468921E+00 | 2.511494291E+00 |
| | 10 | 1.42151199462E+01 | 1.421502524E+01 |
| | 100 | 8.05861718287E+07 | 8.006143562E+07 |
| | | | |
| | 0.1 | 2.51576625250E+00 | 2.515766141E+00 |
| +1.0 | 0.5 | 1.036255172721E+01 | 1.036253381E+01 |
| | 1.0 | 3.218390468938E+01 | 3.218354095E+01 |
| | 10 | 3.282476942940E+09 | 3.246978898E+09 |
| | | | |

7.5.2 Ramp Reactivity Insertions

In this case, Haar wavelet method has applied to the thermal reactor with the following parameters obtained from Nahla [78, 79] and Ganapol [88]: $\lambda_1 = 0.0127\text{sec.}^{-1}$, $\lambda_2 = 0.0317\text{sec.}^{-1}$, $\lambda_3 = 0.115\text{sec.}^{-1}$, $\lambda_4 = 0.311\text{sec.}^{-1}$, $\lambda_5 = 1.40\text{sec.}^{-1}$, $\lambda_6 = 3.87\text{sec.}^{-1}$, $\beta = 0.007$, $l = 0.00002\text{sec.}$, $\beta_1 = 0.000266$, $\beta_2 = 0.001491$, $\beta_3 = 0.001316$, $\beta_4 = 0.002849$, $\beta_5 = 0.000896$, $\beta_6 = 0.000182$. Two cases of ramp reactivity, one is positive and another is negative ramp, are introduced.

7.5.2.1 Positive ramp reactivity

Here, the neutron density of the thermal reactor with positive ramp reactivity $\rho(t) = 0.1t$ is introduced. The numerical solution of neutron density with positive ramp reactivity obtained from HWOM with $m=1024$ number of collocation points cited in Table 2. Also Table 2 represents the comparison results with Taylor series method (TSM) [64], Better Basis function (BBF) [80], stiffness confinement method (SCM) [81] and with backward Euler finite difference method (BEFD) [88]. It can be observed that there is a good agreement between the

obtained results and the other available results. More accurate results for large time can be obtained with increase of collocation points.

Table-2: The neutron density $n(t)$ of the thermal reactor with positive ramp reactivity (+0.1\$/s)

| Time (s) | TSM[64] | BBF[80] | SCM[81] | HWOM with $m = 1024$ | BEFD[88] |
|----------|------------|------------|------------|----------------------|-----------------|
| 2.0 | 1.3382E+00 | 1.3382E+00 | 1.3382E+00 | 1.338200011E+00 | 1.338200050E+00 |
| 4.0 | 2.2284E+00 | 2.2284E+00 | 2.2284E+00 | 2.228441300E+00 | 2.228441897E+00 |
| 6.0 | 5.5822E+00 | 5.5820E+00 | 5.5819E+00 | 5.582043255E+00 | 5.582052449E+00 |
| 8.0 | 4.2789E+01 | 4.2786E+01 | 4.2788E+01 | 4.278584501E+01 | 4.278629573E+01 |
| 10.0 | 4.5143E+05 | 4.5041E+05 | 4.5391E+05 | 4.522953180E+05 | 4.511636239E+05 |
| 11.0 | N.A. | N.A. | N.A. | 1.828233653E+16 | 1.792213607E+16 |

7.5.2.2 *Negative ramp reactivity*

The neutron density of the thermal reactor with a negative ramp reactivity, $\rho(t) = -0.1t$, has been exhibited in Table 3. Table 3 cites the solution for neutron density with negative ramp reactivity obtained from HWOM and the comparison with Taylor series method (TSM) [64], generalized analytical exponential method [76] and Padé approximation method [77] taking $m=1024$ number of collocation points. Thus, it can be also observed that there is a good agreement between the obtained results and the other available results.

Table-3: The neutron density $n(t)$ of the thermal reactor with negative ramp reactivity (-0.1\$/s)

| Time (s) | TSM[64] | GAEM[76] | Padé [77] | HWOM with $m = 1024$ |
|----------|-------------|-------------|-------------|-----------------------|
| 2.0 | 7.91955E-01 | 7.92007E-01 | 7.92007E-01 | 7.920047444289586E-01 |
| 4.0 | 6.12976E-01 | 6.13020E-01 | 6.13018E-01 | 6.13015745981558E-01 |
| 6.0 | 4.74027E-01 | 4.74065E-01 | 4.74058E-01 | 4.74056567958244E-01 |
| 8.0 | 3.69145E-01 | 3.69172E-01 | 3.69169E-01 | 3.69167718232784E-01 |
| 10.0 | 2.90636E-01 | 2.90653E-01 | 2.90654E-01 | 2.90653117814878E-01 |
| 11.0 | N.A. | N.A. | N.A. | 2.59129648117922E-01 |

7.5.3 Zig-zag Reactivity

In this case, a zig-zag reactivity function for the thermal reactor has been considered as follows

$$\rho(t) = \begin{cases} 0.0075 & 0 \leq t \leq 0.5 \\ -0.0075(t - 0.5) + 0.00375 & 0.5 \leq t \leq 1 \\ 0.0075(t - 1) & 1 \leq t \leq 1.5 \\ 0.00375 & 1.5 \leq t \end{cases}$$

where the kinetic parameters are taken from Picca et al [89]

$$\lambda_1 = 0.0127 \text{sec.}^{-1}, \quad \lambda_2 = 0.0317 \text{sec.}^{-1}, \quad \lambda_3 = 0.115 \text{sec.}^{-1}, \quad \lambda_4 = 0.311 \text{sec.}^{-1}, \quad \lambda_5 = 1.40 \text{sec.}^{-1},$$

$$\lambda_6 = 3.87 \text{sec.}^{-1}, l = 0.0005 \text{sec.}, \beta_1 = 0.000285 \quad \beta_2 = 0.0015975 \quad \beta_3 = 0.001410 \quad \beta_4 = 0.0030525$$

$$\beta_5 = 0.00096 \quad \beta_6 = 0.000195 \quad \beta = 0.0075.$$

Table 4 represents the numerical solution for neutron density involving zig-zag reactivity obtained from Haar wavelet operational method (HWOM) by considering level of resolution $J = 8$. Simultaneously the obtained results have been also compared with enhanced piecewise constant approximation (EPCA) [89].

Table-4: The neutron density $n(t)$ of the thermal reactors with zig-zag ramp reactivity

| Time (s) | EPCA[89] | HWOM with $m=256$ |
|----------|-----------------|--------------------|
| 0.5 | 1.721422424E+00 | 1.721419616600E+00 |
| 1 | 1.211127414E+00 | 1.211121251790E+00 |
| 1.5 | 1.892226142E+00 | 1.892197202560E+00 |
| 2 | 2.521600530E+00 | 2.521593863891E+00 |
| 10 | 1.204710536E+01 | 1.204676703380E+01 |
| 100 | 6.815556889E+07 | 6.792200468046E+07 |

7.5.4 Sinusoidal Reactivity Insertion¹²

7.5.4.1 For group of one delayed neutron

¹² **A. Patra** and S. Saha Ray, "Numerical Simulation based on Haar Wavelet Operational Matrix method for solving Point Kinetics Equations involving Sinusoidal and Pulse reactivity", **Annals of Nuclear Energy** (Elsevier), Communicated.

To check the accuracy of Haar wavelet method with nonlinear reactivity insertion, it is applied to the fast reactor with the following parameters obtained from Ganapol [88]: $\lambda_1 = 0.077 \text{sec.}^{-1}$, $\beta = \beta_1 = 0.0079$, $l = 10^{-7} \text{sec.}$, $\rho_0 = 0.0053333$. The reactivity is a time-dependent function of the form $\rho(t) = \rho_0 \sin\left(\frac{\pi t}{50}\right)$. The numerical results obtained for neutron density using sinusoidal reactivity have been presented in Table-5. The obtained results justify that Haar wavelet operational method is an accurate and efficient computational technique for solving point kinetic equation in presence of nonlinear sinusoidal reactivity insertion. It can be observed that there is a good agreement between the obtained results and the other available method results [88]. More accurate results for large time can be obtained with increase of collocation points viz. high level of resolution. Fig. 1 cites the neutron density for sinusoidal reactivity obtained by Haar wavelet method.

Table-5: The neutron density $n(t)$ of the fast reactor with sinusoidal reactivity

| Time (s) | BEFD [88] | HWOM with $m=256$ |
|----------|-----------------|---------------------|
| 10 | 2.065383519E+00 | 2.065379972801E+00 |
| 20 | 8.854133921E+00 | 8.854133966731E+00 |
| 30 | 4.064354222E+01 | 4.064695450288E+01 |
| 40 | 6.135607517E+01 | 6.1364077105064E+01 |
| 50 | 4.610628770E+01 | 4.6114226208650E+01 |
| 60 | 2.912634840E+01 | 2.9133486699766E+01 |

| | | |
|-----|-----------------|---------------------|
| 70 | 1.895177042E+01 | 1.8958245424550E+01 |
| 80 | 1.393829211E+01 | 1.3944612597243E+01 |
| 90 | 1.253353406E+01 | 1.2540632819535E+01 |
| 100 | 1.544816514E+01 | 1.5480673682222E+01 |

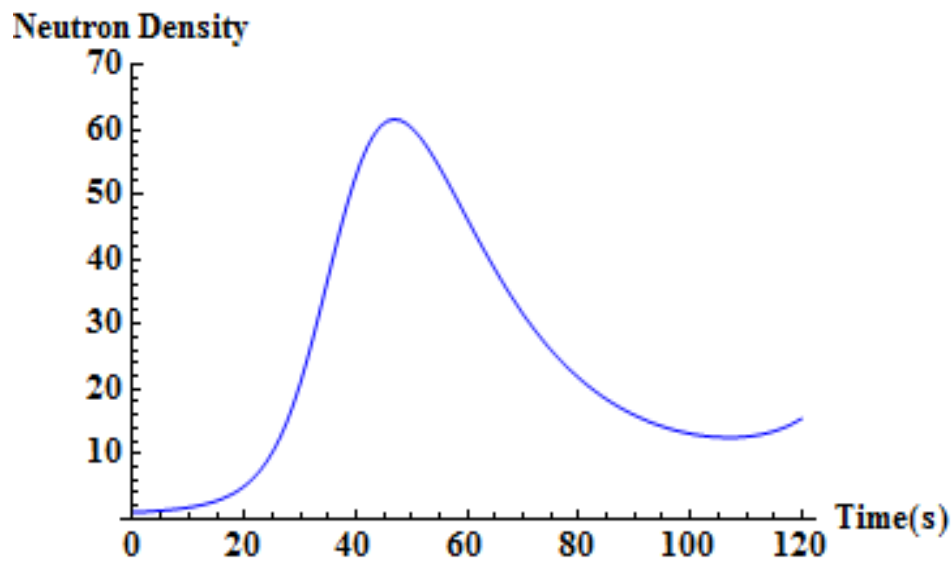


Fig. 1. Neutron density for sinusoidal reactivity

7.5.4.2 For group of six delayed neutron

To check the accuracy of Haar wavelet method, it is applied to the thermal reactor with the following parametres from McMohan and Pierson [64] and Patra and Saha Ray [66]:

$\lambda_1 = 0.0124 \text{sec}^{-1}$, $\lambda_2 = 0.0305 \text{sec}^{-1}$, $\lambda_3 = 0.111 \text{sec}^{-1}$, $\lambda_4 = 0.301 \text{sec}^{-1}$, $\lambda_5 = 1.14 \text{sec}^{-1}$, $\lambda_6 = 3.01 \text{sec}^{-1}$, $\beta_1 = 0.000215$, $\beta_2 = 0.001424$, $\beta_3 = 0.001274$, $\beta_4 = 0.002568$, $\beta_5 = 0.000748$, $\beta_6 = 0.000273$, $\beta = 0.006502$, $l = 0.0005 \text{sec}.$. The reactivity is a time-dependent function of the form

$\rho(t) = \beta \sin\left(\frac{\pi t}{5}\right)$. The numerical results obtained for neutron density using sinusoidal reactivity have been presented in Table-6. The obtained results justify that Haar wavelet method is an efficient computational technique for solving point kinetic equation using sinusoidal reactivity insertions. It can be observed that there is a good agreement between the obtained results and the other available method results [63, 64]. More accurate results for large time can be obtained with increase of collocation points. Fig. 2 cites the neutron density for sinusoidal reactivity obtained by Haar wavelet method.

Table-6: Results obtained for neutron density $n(t)$ with sinusoidal reactivity function

| Time (s) | Taylor [64] | CORE [63] | Haar wavelet operational method with collocation points $m=32$ |
|-----------------|------------------------|----------------------|--|
| 2.0 | 11.3820 | 10.1475 | 11.3131 |
| 4.0 | 92.2761 | 96.7084 | 90.3934 |
| 6.0 | 16.9149 | 16.9149 | 15.6511 |
| 8.0 | 8.8964 | 8.8964 | 8.52265 |
| 10.0 | 13.1985 | 13.1985 | 13.1255 |

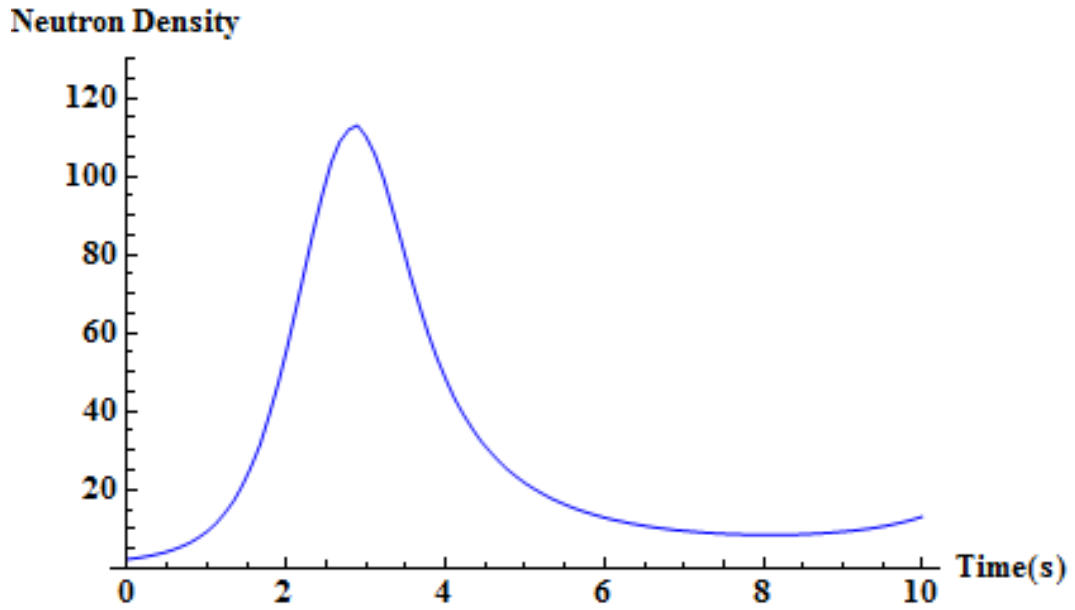


Fig.2. Neutron Density for sinusoidal reactivity calculated with the Haar Wavelet Method

7.5.5 Pulse Reactivity Insertion

In the present case, we consider the effect of pulse reactivity function [89]

$$\rho(t) = \begin{cases} 4\beta(e^{-2t^2}), & t < 1 \\ 0, & t > 1 \end{cases} \quad \text{in nuclear reactor for one group delayed neutron i.e. } M=1 \text{ and the}$$

parameters are used as follows from [89] : $\lambda_1 = 0.077 \text{sec.}^{-1}$, $\beta_1 = 0.006502 = \beta$, neutron source $q = 0$, $l = 5 \times 10^{-4} \text{sec.}$ The results for neutron density using pulse reactivity is cited in Table 7 and illustrated in Fig. 3. It can be observed that there is a good agreement between the obtained results and the other available method results [89, 98]. This curve has the expected shape for pulse reactivity. Here, we consider the number of collocation points $m=32$.

Table-7: Results obtained for neutron density $n(t)$ with pulse reactivity function

| Time (s) | EPCA | CATS | Present | Haar |
|----------|------|------|----------------|------|
| | [89] | [98] | wavelet method | |

| | | | |
|-----|-----------------|-----------------|-------------------|
| 0.5 | 9.38004427E+06 | 9.380044272E+06 | 9.383312098E+06 |
| 0.8 | 1.69477616E+08 | 1.694776161E+08 | 1.6963295571E+08 |
| 1 | 1.075131704E+08 | 1.075131704E+08 | 1.07551610768E+08 |
| 2 | 4.834117624E+06 | 4.834106369E+06 | 4.8410195087E+06 |
| 3 | 4.833903589E+06 | 4.833892339E+06 | 4.8516408749E+06 |

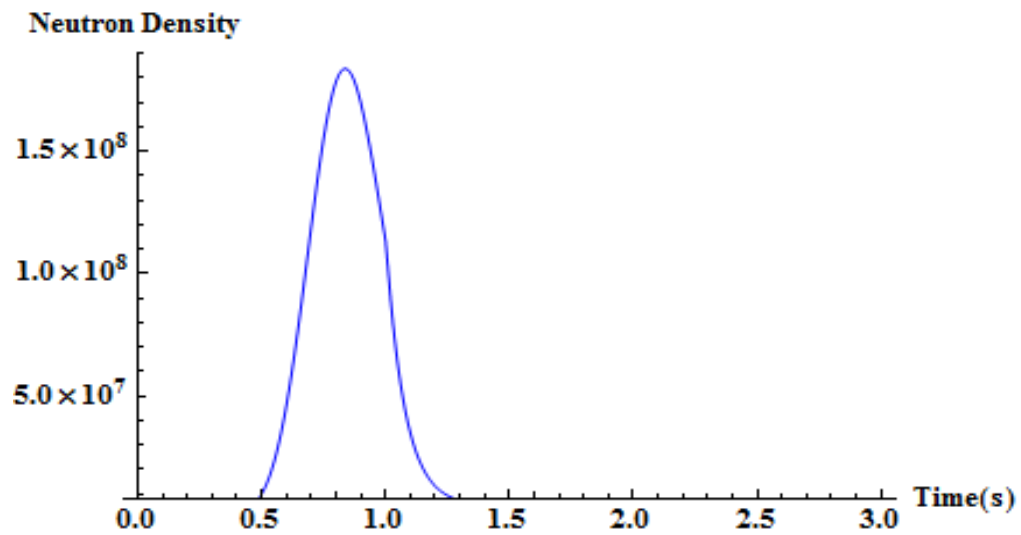


Fig. 3. Neutron density calculated using the Haar Wavelet Method in response to pulse reactivity.

7.6 Convergence Analysis and Error estimation

In this section, we have introduced the error analysis for the Haar wavelet method.

Lemma:

Let, $f(x) \in L^2(R)$ be a continuous function defined in $(0,1]$. Then the error norm at J^{th} level resolution satisfies the following inequalities

$$\|E_J\| \leq \frac{\eta^2}{12} 2^{-2J},$$

where $|f'(x)| \leq \eta$, $\forall x \in [0,1)$ and $\eta > 0$. Here M is a positive number related to the J^{th} level resolution of the wavelet given by $M = 2^J$.

Proof:

$$|E_J| = |f(x) - f_J(x)| = \left| \sum_{i=2M}^{\infty} a_i h_i(x) \right|,$$

$$\text{where } f_J(x) = \sum_{i=0}^{2M-1} a_i h_i(x), \quad \text{for } M = 2^j$$

$$\begin{aligned} \|E_J\|^2 &= \int_{-\infty}^{\infty} \left(\sum_{i=2M}^{\infty} a_i h_i(x), \sum_{r=2M}^{\infty} a_r h_r(x) \right) dx \\ &= \sum_{i=2M}^{\infty} \sum_{r=2M}^{\infty} a_i a_r \int_{-\infty}^{\infty} h_i(x) h_r(x) dx \\ &\leq \sum_{i=2M}^{\infty} |a_i|^2 \end{aligned}$$

$$\text{Now, we consider } a_i = \int_0^1 2^{j/2} f(x) \phi(2^j x - k) dx$$

$$\text{where } h_i(x) = 2^{j/2} h(2^j x - k), \quad k = 0, 1, 2, \dots, 2^j - 1 \text{ and } j = 0, 1, \dots, J.$$

$$h(2^j x - k) = \begin{cases} 1, & k 2^{-j} \leq x < (k + \frac{1}{2}) 2^{-j}, \\ -1, & (k + \frac{1}{2}) 2^{-j} \leq x < (k + 1) 2^{-j}, \\ 0, & \text{elsewhere} \end{cases}$$

Therefore, applying Mean Value Theorem

$$a_i = 2^{j/2} \left[\int_{k2^{-j}}^{(k+\frac{1}{2})2^{-j}} f(x)dx - \int_{(k+\frac{1}{2})2^{-j}}^{(k+1)2^{-j}} f(x)dx \right]$$

$$= 2^{j/2} \left[\left(\left(k + \frac{1}{2} \right) 2^{-j} - k 2^{-j} \right) f(\psi_1) - \left((k+1) 2^{-j} - \left(k + \frac{1}{2} \right) 2^{-j} \right) f(\psi_2) \right].$$

$$\text{where } \psi_1 \in \left(k 2^{-j}, \left(k + \frac{1}{2} \right) 2^{-j} \right) \text{ and } \psi_2 \in \left(\left(k + \frac{1}{2} \right) 2^{-j}, (k+1) 2^{-j} \right)$$

Consequently, $a_i = 2^{-j/2-1}(\psi_1 - \psi_2)(f'(\psi))$,

applying Lagrange's Mean Value Theorem, where $\psi \in (\psi_1, \psi_2)$.

This implies,

$$a_i^2 = 2^{-j-2}(\psi_2 - \psi_1)^2 f'(\psi)^2$$

$$\leq 2^{-j-2} 2^{-2j} \eta^2, \text{ since } |f'(x)| \leq \eta$$

$$= 2^{-3j-2} \eta^2$$

Therefore $\|E_J\|^2 \leq \sum_{i=2M}^{\infty} a_i^2 \leq \sum_{i=2M}^{\infty} 2^{-3j-2} \eta^2 \leq \eta^2 \sum_{j=J+1}^{\infty} \sum_{i=2}^{2^{j+1}-1} 2^{-3j-2}$

$$= \eta^2 \sum_{j=J+1}^{\infty} 2^{-3j-2} (2^{j+1} - 1 - 2^j + 1) = \frac{\eta^2}{4} \sum_{j=J+1}^{\infty} 2^{-2j} = \frac{\eta^2}{4} \frac{2^{-2(J+1)}}{\left(1 - \frac{1}{4}\right)} = \frac{\eta^2}{12} 2^{-2J} \quad (7.6.1)$$

From eq. (7.6.1), it can be observed that the error bound is inversely proportional to the level of resolution J . So, more accurate result can be obtained by increasing the level of resolution.

7.7 Conclusion

A numerical approximate solution has been presented in this chapter to explore the behavior of neutron density using reactivity functions. It can be seen that the proposed numerical method Haar Wavelet Operational Method certainly perform quite well. To predict the dynamical behavior for thermal and fast reactors with constant and time-dependent reactivity function and to obtain the solution of neutron point kinetic equation, the numerical method viz. Haar wavelet operational method is undoubtedly very simple and efficient. This numerical technique provides a good result for the point reactor kinetic equations with a constant and time-dependent reactivity function. Results of this method have been compared with other available methods exist in open literature in order to show justification of the present method. The cited comparisons revealed that the obtained numerical solutions agree well with the other solutions in open literature.

The accuracy of the obtained solutions are quite high even if the number of collocation points is small. By increasing the number of collocation points, the error of the approximation solution rapidly decreases. In a systematic comparison with other existing methods, it may be concluded that the present method is simple and efficient. This method is applied to different types of reactivity in order to check the validity of the proposed method. Moreover, the obtained approximate results have been also compared with other available numerical results exist in open literature. It manifests that the results obtained by the Haar Wavelet Operational Method are in good agreement with other available results even for large time range and it is certainly simpler than other methods in open literature. Haar wavelets are preferred due to their useful properties such as simple applicability, orthogonality and compact support. Haar Wavelet Operational Method needs less computational effort as the major blocks of Haar Wavelet Operational Method are calculated only once and used in the subsequent

computations repeatedly. Simply availability and fast convergence of the Haar wavelets provide a solid foundation for highly linear as well as nonlinear problems of differential equations. This proposed method with far less degrees of freedom and small computational overhead provides better solution. It can be concluded that this method is quite suitable, accurate, and efficient in comparison to other classical methods. The pertinent feature of the method is that the errors for solutions may be reduced for large value of m viz. $m=1024$ or more number of collocation points. The main advantage of this method is that it transfers the whole scheme into a system of algebraic equations by virtue of it the computation is very easy and simple in compared to other methods. This paper shows the applicability of the Haar wavelet method for the numerical solution of neutron point kinetic equation in nuclear reactor dynamics. The obtained results manifest plausibility of the Haar wavelet method for neutron point kinetic equations.

CHAPTER 8

8.1 *Introduction*

The neutron transport denotes the study of the motions and interactions of neutrons with atom nuclei of the medium. The fractional neutron transport equation represents a linear case of the Boltzmann equation and it has many applications in physics as well as in engineering. The neutron transport model in a nuclear reactor is anomalous diffusion process. Anomalous diffusion is different from the normal diffusion and is characterized by features like, slower or faster movement of diffusing particles. A useful characterization of the diffusion process is again through the scaling of the mean square displacement with time, which can be defined as $\langle x^2(t) \rangle \sim t^\gamma, \gamma \neq 1$. Diffusion is then classified through the scaling index γ . The case $\gamma = 1$ is normal diffusion, all other cases are termed anomalous. The cases $\gamma > 1$ form the family of super-diffusive processes, including the particular case $\gamma = 2$, which is called ballistic diffusion, and the cases $\gamma < 1$ are the sub-diffusive processes. Hence, the solution of the fractional order transport model characterizes the dynamics of an anomalous process [99-101].

The motivation of this research work is to solve a typical problem of the mathematical-physics: the solving a neutral particle transport equation that has numerous applications in physics [102, 103]. In nuclear reactor, neutrons are generated by fission of the nucleus and they are named as fast neutrons with an average speed equal to 2×10^7 m/s. In the thermal nuclear reactor, fast neutrons are subjected to a slowness process, decreasing their energy until they are in a state of equilibrium with the other atoms in the environment. The main goal in reactor theory is to find neutron profile within the nuclear reactor core, and hence the power

distribution. The flux profile can be mathematically identified by the solution of an integro-differential equation known as neutron transport equation.

Integro-differential equations (IDEs) have many applications in different fields of mechanical [104], nuclear engineering, chemistry, astronomy, biology, economics, potential theory and electrostatics. An exact solution of this integro-differential equation was found only in the particular cases. In many cases analytical solutions of IDEs is unwieldy task; therefore our aim is focused on exploring accurate and efficient numerical method [105].

In this study, we consider a linear form of Boltzmann equation with a source function of the form $f(x, \eta) = A(\eta) \cos \pi \eta + B(\eta) \sin \pi \eta$. To obtain the solution of this stationary transport equation, we have applied two-dimensional Haar wavelet transform method. Some numerical examples illustrate the advantage of this method applied to stationary transport equation.

Analysis of wavelet theory is a new branch of mathematics and widely applied in signal analysis, image processing and numerical analysis etc. [106, 107]. Among the different wavelet families, mathematically most simple are the Haar wavelets [108]. In 1910, Alfred Haar introduced the notion of wavelets. Haar wavelets have the properties of orthogonality and normalization having close support and the simple expression [94, 95, 97]. Due to its simplicity, the Haar wavelets are very efficient and effective tool for solving both differential and integral equations.

8.2 *Formulation of Neutron Transport Equation model*

$$\eta \frac{\partial \phi(x, \eta)}{\partial x} + \sigma_t \phi(x, \eta) = \int_{-1}^1 \sigma_s(\eta, \eta') \phi(x, \eta') d\eta' + \frac{q(x)}{2} \quad (8.2.1)$$

with

$$\sigma_s(\eta, \eta') = \sum_{k=0}^{\infty} \frac{2k+1}{2} \sigma_{sk} P_k(\eta) P_k(\eta')$$

where $\sigma_t \equiv$ total cross-section; σ_{sl} with $l = 0, 1, \dots, L$ are the components of differential scattering cross section, $P_k(\eta)$ are the Legendre polynomial of degree k and $q(x) \equiv$ source function.

Here, we consider the integro-differential equation for stationary case of transport theory [102] by considering $\sigma_t \equiv 1$, $\sigma_s(\eta, \eta') \equiv \frac{1}{2}$ and $q(x) \equiv 2f(x, \eta)$ in eq. (8.2.1), which yields the integral-differential equation for the stationary case of transport theory [103]

$$\eta \frac{\partial \phi(x, \eta)}{\partial x} + \phi(x, \eta) = \frac{1}{2} \int_{-1}^1 \phi(x, \eta') d\eta' + f(x, \eta), \quad (8.2.2)$$

$$\forall (x, \eta) \in D_1 \times D_2 = [0, 1] \times [-1, 1], \quad D_2 = D'_2 \cup D''_2 = [-1, 0] \cup [0, 1]$$

with the following boundary conditions:

$$\phi(0, \eta) = 0 \text{ if } \eta > 0 \quad \text{and} \quad \phi(1, \eta) = 0 \text{ if } \eta < 0 \quad (8.2.3)$$

where $\phi(x, \eta)$ is the neutron density which migrate in a direction which makes an angle μ with the x -axis and $\eta = \cos \mu$; $f(x, \eta)$ is a given source function.

Now, we split the eq. (8.2.2) into two equations using the following notations

$$\phi^+ = \phi(x, \eta) \text{ if } \eta > 0 \quad \text{and} \quad \phi^- = \phi(x, -\eta) \text{ if } \eta < 0 \quad (8.2.4)$$

By denoting, $\eta' = -\eta$, we can obtain

$$\int_{-1}^0 \phi(x, \eta') d\eta' = \int_0^1 \phi(x, -\eta) d\eta = \int_0^1 \phi^- d\eta$$

In view of eq. (8.2.4), the eq. (8.2.2) can be written as

$$\eta \frac{\partial \phi^+}{\partial x} + \phi^+ = \frac{1}{2} \int_0^1 (\phi^+ + \phi^-) d\eta' + f^+ \text{ for } \eta > 0 \quad (8.2.5)$$

$$-\eta \frac{\partial \phi^-}{\partial x} + \phi^- = \frac{1}{2} \int_0^1 (\phi^+ + \phi^-) d\eta' + f^- \text{ for } \eta < 0 \quad (8.2.6)$$

with the boundary conditions $\phi^+(0, \eta) = 0$, $\phi^-(1, \eta) = 0$.

Adding and subtracting the eqs. (8.2.5) and (8.2.6) and then introducing the following notations, we obtain

$$u = \frac{1}{2}(\phi^+ + \phi^-), \quad v = \frac{1}{2}(\phi^+ - \phi^-), \quad g = \frac{1}{2}(f^+ + f^-) \text{ and } r = \frac{1}{2}(f^+ - f^-) \quad (8.2.7)$$

We also obtain the following system

$$\eta \frac{\partial v}{\partial x} + u = \int_0^1 u d\eta + g, \quad (8.2.8)$$

$$\eta \frac{\partial u}{\partial x} + v = r \quad (8.2.9)$$

along with the following boundary conditions

$$\left. \begin{aligned} u + v &= 0 \text{ for } x = 0 \\ u - v &= 0 \text{ for } x = 1 \end{aligned} \right\} \quad (8.2.10)$$

Eliminating the value of v from eqs. (8.2.8) and (8.2.9), we rewrite the problem (8.2.8)-(8.2.10) in the following form

$$-\eta^2 \frac{\partial^2 u}{\partial x^2} + u = \int_0^1 u d\eta + g - \eta \frac{\partial r}{\partial x} \quad (8.2.11)$$

$$\left(u - \eta \frac{\partial u}{\partial x} \right) \Big|_{x=0} = -r(0, \eta), \quad (8.2.12)$$

$$\left(u + \eta \frac{\partial u}{\partial x} \right) \Big|_{x=1} = r(1, \eta) , \quad (8.2.13)$$

where $\eta \in [0, 1]$.

8.3 Mathematical model of the stationary neutron transport equation in a homogeneous isotropic medium

Let us consider the stationary transport equation

$$\eta \frac{\partial \phi(x, \eta)}{\partial x} + \phi(x, \eta) = \frac{1}{2} \int_{-1}^1 \phi(x, \eta') d\eta' + f(x, \eta) \quad (8.3.1)$$

$$\text{where } f(x, \eta) = P(\eta) \cos \pi x + Q(\eta) \sin \pi x \quad (8.3.2)$$

with $P(\eta)$ be an odd function and $Q(\eta)$ be an even function.

The equation is accompanied by boundary conditions:

$$\phi(0, \eta) = 0 \text{ if } \eta > 0 \text{ and } \phi(1, \eta) = 0 \text{ if } \eta < 0.$$

According to the notations introduced in eq. (8.2.7), the functions g and r can be obtained as

$$g(x, \eta) = Q(\eta) \sin \pi x \text{ and } r(x, \eta) = P(\eta) \cos \pi x \quad (8.3.3)$$

and u satisfies the equation

$$\eta^2 \frac{\partial^2 u}{\partial x^2} - u + \int_0^1 u(x, \eta') d\eta' + (Q(\eta) + \pi \eta P(\eta)) \sin \pi x = 0 \quad (8.3.4)$$

with the boundary conditions

$$u(0, \eta) - \eta \frac{du(0, \eta)}{dx} = -r(0, \eta) = -P(\eta) , \quad (8.3.5)$$

$$u(1, \eta) + \eta \frac{du(1, \eta)}{dx} = r(1, \eta) = -P(\eta) . \quad (8.3.6)$$

In particular case, we consider the source function

$$f(x, \eta) = \pi \eta^3 \cos \pi x + \left(\eta^2 - \frac{1}{3} \right) \sin \pi x$$

where

$$P(\eta) = \pi \eta^3 \text{ and } Q(\eta) = \eta^2 - \frac{1}{3} .$$

According to eqs. (8.3.3), the functions g and r will be

$$g(x, \eta) = \left(\eta^2 - \frac{1}{3} \right) \sin \pi x \text{ and } r(x, \eta) = \pi \eta^3 \cos \pi x$$

and u satisfies the equation

$$\eta^2 \frac{\partial^2 u}{\partial x^2} - u + \int_0^1 u(x, \eta') d\eta' + \left(\eta^2 - \frac{1}{3} + \pi^2 \eta^4 \right) \sin \pi x = 0 \quad (8.3.7)$$

The boundary conditions become now

$$\left. \begin{aligned} u(0, \eta) - \eta \frac{du(0, \eta)}{dx} &= -r(0, \eta) = -\pi \eta^3 \\ u(1, \eta) + \eta \frac{du(1, \eta)}{dx} &= r(1, \eta) = -\pi \eta^3 \end{aligned} \right\} , \quad (8.3.8)$$

Here, in this case the exact solution is $u_{exact} = \phi_{exact}(x, \eta) = \eta^2 \sin \pi x$ and $v_{exact} = 0$.

8.4 Application of two-dimensional Haar wavelet collocation method to solve stationary neutron transport equation¹³

Let us divide the intervals D_1 and D_2'' into m equal subintervals each of width $\Delta_1 = \frac{1}{m}$ and $\Delta_2 = \frac{1}{m}$ respectively. We assume,

$$\frac{\partial^2 u(x, \eta)}{\partial x^2} \equiv D^2 u(x, \eta) = \sum_{i=1}^m \sum_{j=1}^m c_{ij} h_i(x) h_j(\eta) \quad (8.4.1)$$

Integrating eq. (8.4.1) two times from 0 to x , we can obtain

$$u(x, \eta) = \sum_{i=1}^m \sum_{j=1}^m c_{ij} Q h_i(x) h_j(\eta) + C_1 + x C_2 \quad (8.4.2)$$

where $Q h_i(x)$ is given by in eq. (7.3.7) for $\alpha = 2$.

Substitute $x=0$ in eq. (8.4.2), we can obtain

$$u(0, \eta) = C_1. \quad (8.4.3)$$

Similarly at the boundary $x=1$, we have

$$u(1, \eta) = \sum_{i=1}^m \sum_{j=1}^m c_{ij} Q h_i(x) \Big|_{x=1} h_j(\eta) + C_1 + C_2 \quad (8.4.4)$$

Next, together with eq. (8.4.3) and (8.4.4), we have

$$C_2 = u(1, \eta) - u(0, \eta) - \sum_{i=1}^m \sum_{j=1}^m c_{ij} Q h_i(x) \Big|_{x=1} h_j(\eta) \quad (8.4.5)$$

¹³ **A. Patra** and S. Saha Ray, 2014. "Two-dimensional Haar wavelet Collocation method for the solution of Stationary Neutron Transport Equation in a Homogeneous Isotropic medium", **Annals of Nuclear Energy** (Elsevier), 70, pp. 30-35.

Now, by using eqs. (8.4.3) and (8.4.5) in eq. (8.4.2), we can obtain the approximate solution

$$u(x, \eta) = \sum_{i=1}^m \sum_{j=1}^m c_{ij} Qh_i(x) h_j(\eta) + u(0, \eta) + x \left(u(1, \eta) - u(0, \eta) - \sum_{i=1}^m \sum_{j=1}^m c_{ij} Qh_i(x) \Big|_{x=1} h_j(\eta) \right) \quad (8.4.6)$$

In view of conditions (8.2.2) and (8.3.8), we assume the boundary conditions

$$u(0, \eta) = 0 \quad \text{and} \quad u(1, \eta) = 0 \quad (8.4.7)$$

Now by putting eqs. (8.4.7) into eq. (8.4.6), we have

$$u(x, \eta) = \sum_{i=1}^m \sum_{j=1}^m c_{ij} Qh_i(x) h_j(\eta) - x \left(\sum_{i=1}^m \sum_{j=1}^m c_{ij} Qh_i(x) \Big|_{x=1} h_j(\eta) \right) \quad (8.4.8)$$

Then by using eq. (8.4.1) and (8.4.8) into eq. (8.3.7), we obtain the numerical scheme as

$$\begin{aligned} & \sum_{i=1}^m \sum_{j=1}^m c_{ij} h_i(x) h_j(\eta) - \left(\frac{1}{\eta^2} \right) \left(\sum_{i=1}^m \sum_{j=1}^m c_{ij} Qh_i(x) h_j(\eta) - x \left(\sum_{i=1}^m \sum_{j=1}^m c_{ij} Qh_i(x) \Big|_{x=1} h_j(\eta) \right) \right) \\ & + \left(\frac{1}{\eta^2} \right) \left(\sum_{i=1}^m \sum_{j=1}^m c_{ij} Qh_i(x) \int_0^1 h_j(\eta') d\eta' - x \left(\sum_{i=1}^m \sum_{j=1}^m c_{ij} Qh_i(x) \Big|_{x=1} \int_0^1 h_j(\eta') d\eta' \right) \right) \\ & + \left(\frac{1}{\eta^2} \right) \left(\eta^2 - \frac{1}{3} + \pi^2 \eta^4 \right) \sin \pi x = 0 \end{aligned} \quad (8.4.9)$$

or we can write

$$\begin{aligned} & \sum_{i=1}^m \sum_{j=1}^m c_{ij} h_i(x) h_j(\eta) - \left(\frac{1}{\eta^2} \right) \left(\sum_{i=1}^m \sum_{j=1}^m c_{ij} Qh_i(x) h_j(\eta) - x \left(\sum_{i=1}^m \sum_{j=1}^m c_{ij} Qh_i(x) \Big|_{x=1} h_j(\eta) \right) \right) \\ & + \left(\frac{1}{\eta^2} \right) \left(\sum_{i=1}^m \sum_{j=1}^m c_{ij} Qh_i(x) \tilde{P}_j(\eta) - x \left(\sum_{i=1}^m \sum_{j=1}^m c_{ij} Qh_i(x) \Big|_{x=1} \tilde{P}_j(\eta) \right) \right) \\ & + \left(\frac{1}{\eta^2} \right) \left(\eta^2 - \frac{1}{3} + \pi^2 \eta^4 \right) \sin \pi x = 0 \end{aligned} \quad (8.4.10)$$

where
$$\tilde{P}_j(\eta) = \int_0^1 h_j(\eta') d\eta' = \begin{cases} 1, & j=1 \\ 0, & j \neq 1 \end{cases}$$

By considering all the wavelet collocation points $\eta_l = A + (l - 0.5)\Delta_2$ for $l = 1, 2, \dots, m$ and $x_k = A + (k - 0.5)\Delta_1$ for $k = 1, 2, \dots, m$, we may obtain the system of m^2 -number of algebraic equations involving m^2 unknown coefficients c_{ij} . By solving these system of equations using any mathematical software, we can obtained the Haar coefficients c_{ij} . Hence we can obtain the approximate solution for neutron density $u(x, \eta)$ or $\phi(x, \eta)$ for stationary neutron transport equation.

8.5 Numerical results and discussions for stationary integer-order neutron transport equation

Let us consider the numerical example for stationary neutron transport equation [103]

$$\eta^2 \frac{\partial^2 u}{\partial x^2} - u + \int_0^1 u(x, \eta') d\eta' + (Q(\eta) + \pi\eta P(\eta)) \sin \pi x = 0$$

where $P(\eta) = \pi\eta^3$ and $Q(\eta) = \eta^2 - \frac{1}{3}$ with boundary conditions

$$\left. \begin{aligned} u(0, \eta) - \eta \frac{du(0, \eta)}{dx} &= -r(0, \eta) = -\pi\eta^3 \\ u(1, \eta) + \eta \frac{du(1, \eta)}{dx} &= r(1, \eta) = -\pi\eta^3 \end{aligned} \right\}.$$

We obtain the numerical approximate solutions for neutron density for $x \in [0, 1]$ and with $\eta = 0.2, 0.4, 0.6$ and 0.8 . Here, we compare the numerical results with the exact solutions and the absolute errors thus obtained are shown in Tables 1-4. Figures 1-7 cite the graphical comparison between the exact and numerical solutions for different values of x and η . Here, we have considered $m=16$ and $m=32$.

Table 1: Numerical solution for neutron density at $\eta = 0.2$

| | $\eta = 0.2$ | | | | |
|-----|---|---|---------------------------|-----------------------------------|-----------------------------------|
| x | $u_{\text{approximate}}$ at $m = 16$ | $u_{\text{approximate}}$ at $m = 32$ | u_{exact} | Absolute Error for $m = 16$ | Absolute Error for $m = 32$ |
| 0 | 0 | 0 | 0 | 0 | 0 |
| 0.1 | 0.0145110 | 0.0126787 | 0.0123607 | 0.00215028 | 0.000318068 |
| 0.2 | 0.0276062 | 0.0241160 | 0.0235114 | 0.00409481 | 0.000604573 |
| 0.3 | 0.0379918 | 0.0331925 | 0.0323607 | 0.00563116 | 0.000831859 |
| 0.4 | 0.0446648 | 0.0390202 | 0.0380423 | 0.00662251 | 0.000977905 |
| 0.5 | 0.0469623 | 0.0410283 | 0.04 | 0.00696235 | 0.001028320 |
| 0.6 | 0.0446648 | 0.0390202 | 0.0380423 | 0.00662251 | 0.000977905 |
| 0.7 | 0.0379918 | 0.0331925 | 0.0323607 | 0.00563116 | 0.000831859 |
| 0.8 | 0.0276062 | 0.0241160 | 0.0235114 | 0.00409481 | 0.000604573 |
| 0.9 | 0.0145110 | 0.0126787 | 0.0123607 | 0.00215028 | 0.000318068 |
| 1 | -5.55112×10^{-16} | 0 | 2.26622×10^{-17} | 7.81733×10^{-17} | 2.26622×10^{-17} |

Table 2: Numerical solution for neutron density at $\eta = 0.4$

| | $\eta = 0.4$ | | | | |
|-----|---|---|--------------------|-----------------------------------|-----------------------------------|
| x | $u_{\text{approximate}}$ at $m = 16$ | $u_{\text{approximate}}$ at $m = 32$ | u_{exact} | Absolute Error for $m = 16$ | Absolute Error for $m = 32$ |

| | | | | | |
|-----|---------------------------|---------------------------|---------------------------|---------------------------|---------------------------|
| 0 | 0 | 0 | 0 | 0 | 0 |
| 0.1 | 0.050795 | 0.047102 | 0.0494427 | 0.00135228 | 0.00234008 |
| 0.2 | 0.096634 | 0.089593 | 0.0940456 | 0.00258878 | 0.00445269 |
| 0.3 | 0.132989 | 0.123313 | 0.1294430 | 0.00354611 | 0.00612958 |
| 0.4 | 0.156347 | 0.144963 | 0.1521690 | 0.00417811 | 0.00720577 |
| 0.5 | 0.164390 | 0.152424 | 0.16 | 0.00438973 | 0.00757626 |
| 0.6 | 0.156347 | 0.144963 | 0.1521690 | 0.00417811 | 0.00720577 |
| 0.7 | 0.132989 | 0.123313 | 0.1294430 | 0.00354611 | 0.00612958 |
| 0.8 | 0.096634 | 0.089593 | 0.0940456 | 0.00258878 | 0.00445269 |
| 0.9 | 0.050795 | 0.047102 | 0.0494427 | 0.00135228 | 0.00234008 |
| 1 | -1.1103×10^{-16} | 1.11022×10^{-16} | 9.06486×10^{-17} | 2.01671×10^{-17} | 2.03737×10^{-17} |

Table 3: Numerical solution for neutron density at $\eta = 0.6$

| | $\eta = 0.6$ | | | | |
|-----|------------------------------------|------------------------------------|--------------------|-----------------------------------|-----------------------------------|
| x | $u_{\text{approx at}}$ $m = 16$ | $u_{\text{approx at}}$ $m = 32$ | u_{exact} | Absolute Error for $m = 16$ | Absolute Error for $m = 32$ |
| 0 | 0 | 0 | 0 | 0 | 0 |
| 0.1 | 0.108707 | 0.114695 | 0.111246 | 0.00253901 | 0.00344893 |
| 0.2 | 0.206809 | 0.218159 | 0.211603 | 0.00479398 | 0.00655639 |
| 0.3 | 0.284611 | 0.300268 | 0.291246 | 0.00663480 | 0.00902171 |
| 0.4 | 0.334601 | 0.352986 | 0.34238 | 0.00777956 | 0.01060560 |
| 0.5 | 0.351813 | 0.371152 | 0.36 | 0.00818717 | 0.01115220 |
| 0.6 | 0.334601 | 0.352986 | 0.34238 | 0.00777956 | 0.01060560 |
| 0.7 | 0.284611 | 0.300268 | 0.291246 | 0.00663480 | 0.00902171 |

| | | | | | |
|-----|---------------------------|----------|---------------------------|--------------------------|---------------------------|
| 0.8 | 0.206809 | 0.218159 | 0.211603 | 0.00479398 | 0.00655639 |
| 0.9 | 0.108707 | 0.114695 | 0.111246 | 0.00253901 | 0.00344893 |
| 1 | 4.44089×10^{-16} | 0 | 2.03959×10^{-16} | 2.4013×10^{-16} | 2.03959×10^{-16} |

Table 4: Numerical solution for neutron density at $\eta = 0.8$

| | $\eta = 0.8$ | | |
|-----|--|---------------------------|--------------------------------|
| x | $u_{\text{approx}} \text{ at } m = 32$ | u_{exact} | Absolute Error for $m = 32$ |
| 0 | 0 | 0 | 0 |
| 0.1 | 0.188276 | 0.197771 | 0.0094945 |
| 0.2 | 0.358184 | 0.376183 | 0.0179982 |
| 0.3 | 0.492935 | 0.517771 | 0.0248355 |
| 0.4 | 0.579515 | 0.608676 | 0.0291610 |
| 0.5 | 0.609326 | 0.64 | 0.0306743 |
| 0.6 | 0.579515 | 0.608676 | 0.0291610 |
| 0.7 | 0.492935 | 0.517771 | 0.0248355 |
| 0.8 | 0.358184 | 0.376183 | 0.0179982 |
| 0.9 | 0.188276 | 0.197771 | 0.0094953 |
| 1 | 4.44089×10^{-16} | 3.62594×10^{-16} | 8.14947×10^{-17} |

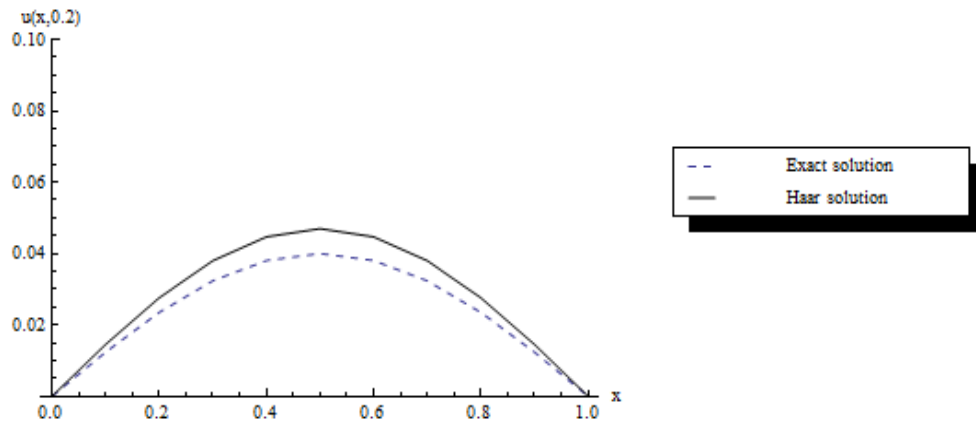


Fig. 1. Comparison between exact and numerical approximate solutions for neutron density at $\eta = 0.2$ and $m = 16$.

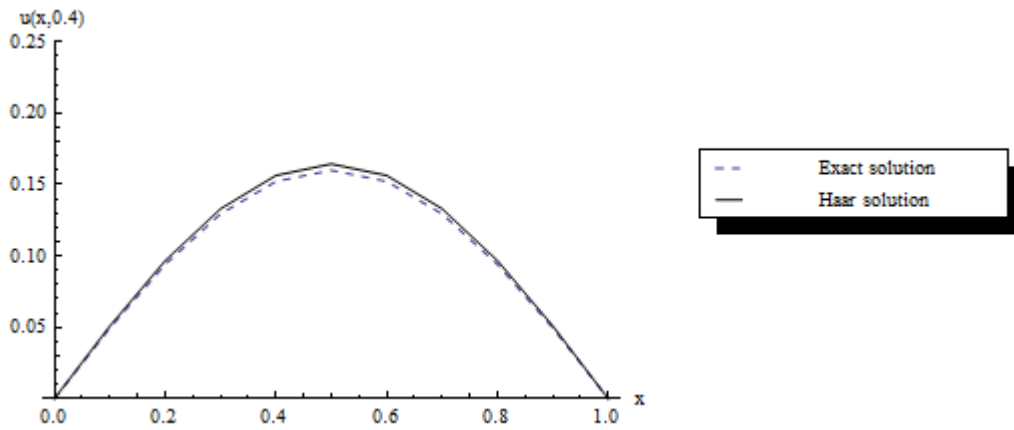


Fig. 2. Comparison between exact and numerical approximate solutions for neutron density at $\eta = 0.4$ and $m = 16$.

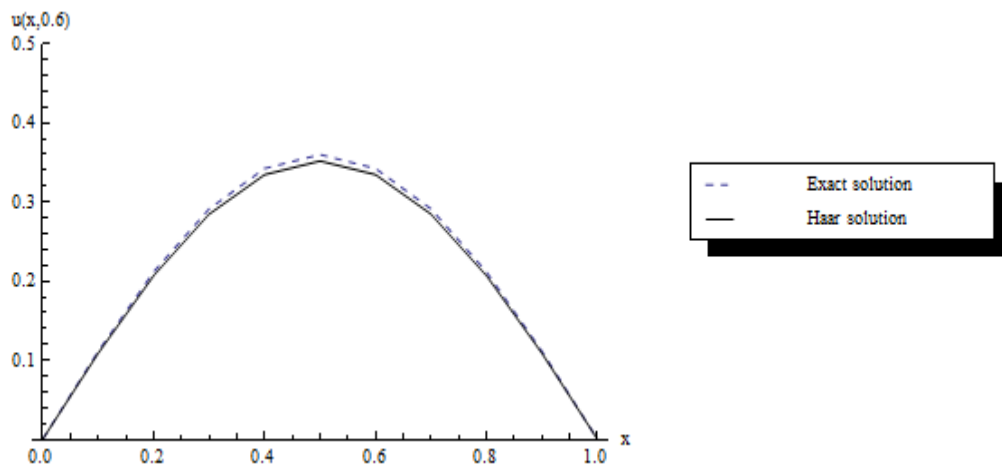


Fig. 3. Comparison between exact and numerical approximate solutions for neutron density at $\eta=0.6$ and $m=16$.

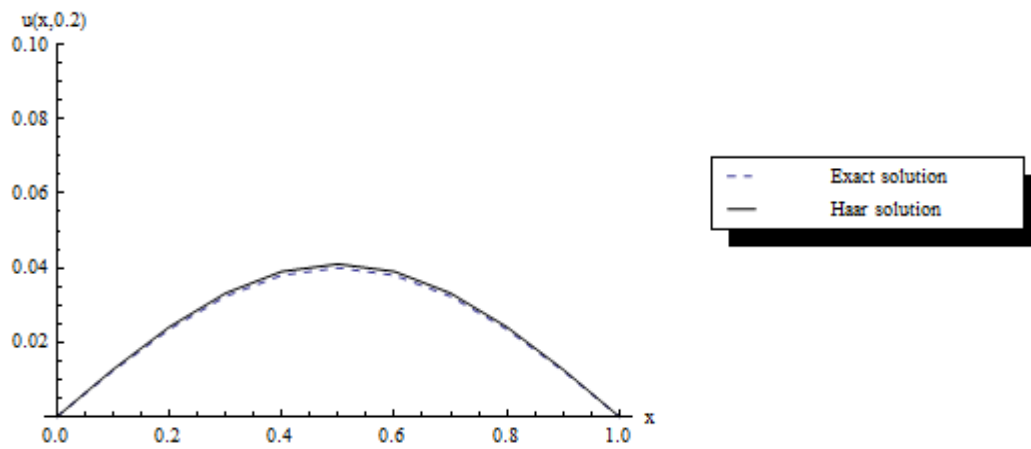


Fig. 4. Comparison between exact and numerical approximate solutions for neutron density at $\eta = 0.2$ and $m=32$.

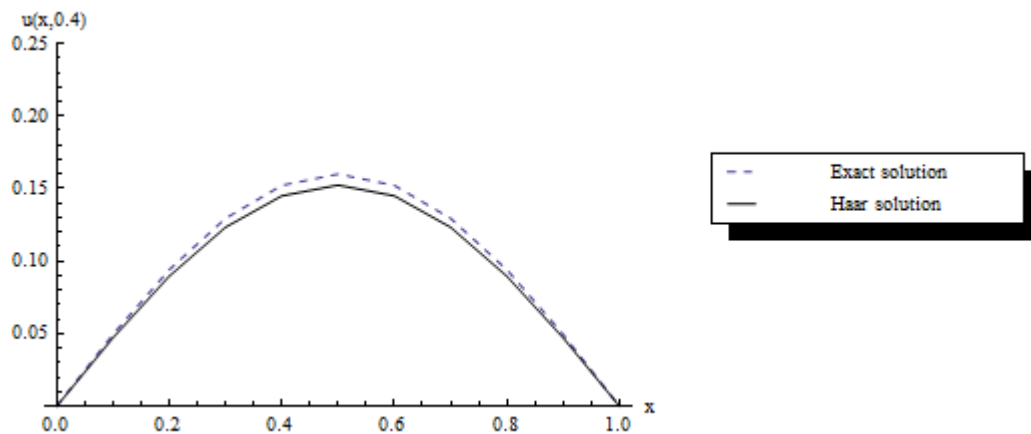


Fig. 5. Comparison between exact and numerical approximate solutions for neutron density at $\eta = 0.4$ and $m=32$

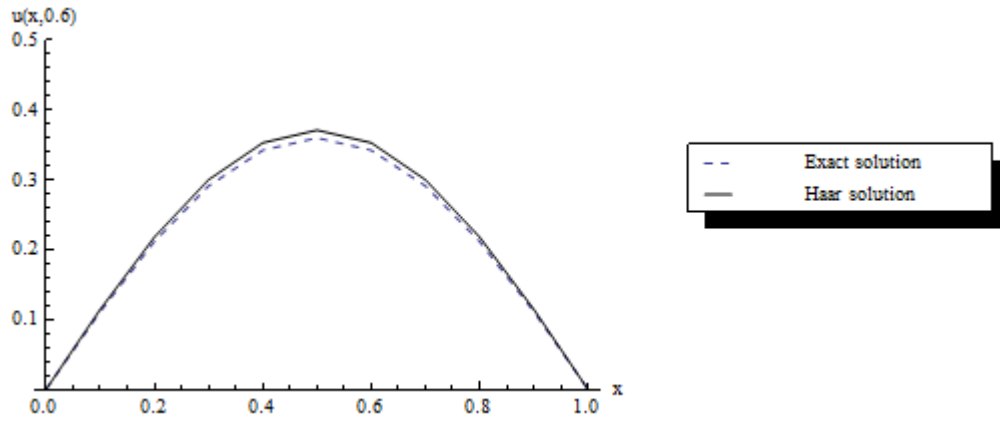


Fig. 6. Comparison between exact and numerical approximate solutions for neutron density at $\eta = 0.6$ and $m=32$.

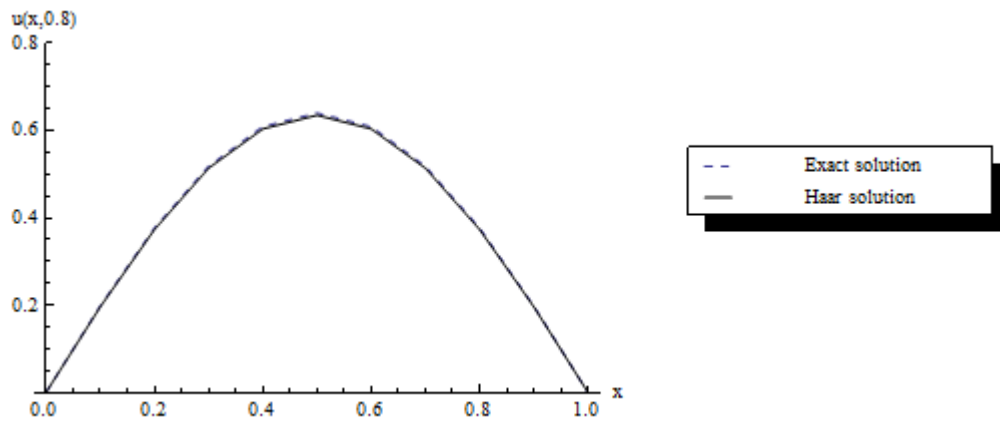


Fig. 7. Comparison between exact and numerical approximate solutions for neutron density at $\eta = 0.8$ and $m=32$.

8.6 Mathematical Model for fractional order Stationary Neutron Transport Equation

The fractional order neutron transport is the process of anomalous diffusion. This model removes the lacunae of the conventional integer-order model of neutron movements. This research analysis based on Haar wavelet is probably being performed for the first time for the fractional order model of steady state neutron transport. The analysis carried out in this paper thus forms a crucial step in the process of development of fractional-order transport model for a nuclear reactor.

In view of eq. (8.2.11), let us consider the fractional order ($\beta > 0$) stationary neutron transport equation

$$\eta^2 \frac{\partial^\beta u}{\partial x^\beta} - u + \int_0^1 u(x, \eta') d\eta' + g - \eta \frac{\partial r}{\partial x} = 0 \quad , \quad 1 < \beta \leq 2 \quad (8.6.1)$$

with the boundary conditions

$$\left(u - \eta \frac{\partial u}{\partial x} \right) \Big|_{x=0} = -r(0, \eta) , \quad (8.6.2)$$

$$\left(u + \eta \frac{\partial u}{\partial x} \right) \Big|_{x=1} = r(1, \eta) , \quad (8.6.3)$$

where $\eta \in [0, 1]$.

❖ Case-I

In this case, we consider the source function

$$f(x, \eta) = \pi \eta^3 \cos \pi x + \left(\eta^2 - \frac{1}{3} \right) \sin \pi x \quad (8.6.4)$$

According to eqs. (8.2.7), the functions g and r can be defined as

$$g(x, \eta) = \left(\eta^2 - \frac{1}{3} \right) \sin \pi x \quad \text{and} \quad r(x, \eta) = \pi \eta^3 \cos \pi x .$$

Therefore, u satisfies the equation

$$\eta^2 \frac{\partial^\beta u}{\partial x^\beta} - u + \int_0^1 u(x, \eta') d\eta' + \left(\eta^2 - \frac{1}{3} + \pi^2 \eta^4 \right) \sin \pi x = 0 \quad (8.6.5)$$

The boundary conditions become now

$$\left. \begin{aligned} u(0, \eta) - \eta \frac{du(0, \eta)}{dx} &= -r(0, \eta) = -\pi \eta^3 \\ u(1, \eta) + \eta \frac{du(1, \eta)}{dx} &= r(1, \eta) = -\pi \eta^3 \end{aligned} \right\}, \quad (8.6.6)$$

Here, the integer order i.e. classical solution [103] is

$$u_{classical} = \phi_{classical}(x, \eta) = \eta^2 \sin \pi x \quad (8.6.7)$$

❖ Case-II

In this case, we consider the source function as

$$f(x, \eta) = -2\pi^2 \eta^4 \cos(2\pi x) + \left(\eta^2 - \frac{2}{3} \right) \sin^2 \pi x \quad (8.6.8)$$

Therefore, according to eqs. (8.2.7), the functions g and r will be

$$g(x, \eta) = f(x, \eta) = -2\pi^2 \eta^4 \cos(2\pi x) + \left(\eta^2 - \frac{2}{3} \right) \sin^2 \pi x \quad \text{and} \quad r(x, \eta) = 0.$$

Therefore, u satisfies the equation

$$\eta^2 \frac{\partial^\beta u}{\partial x^\beta} - u + \int_0^1 u(x, \eta') d\eta' + \left(-2\pi^2 \eta^4 \cos(2\pi x) + \left(\eta^2 - \frac{2}{3} \right) \sin^2 \pi x \right) = 0 \quad (8.6.9)$$

The boundary conditions become now

$$\left. \begin{aligned} u(0, \eta) - \eta \frac{du(0, \eta)}{dx} &= 0 \\ u(1, \eta) + \eta \frac{du(1, \eta)}{dx} &= 0 \end{aligned} \right\}, \quad (8.6.10)$$

In this case, the integer order, i.e. classical solution is [109]

$$u_{classical} = \phi_{classical}(x, \eta) = \eta^2 \sin^2 \pi x. \quad (8.6.11)$$

8.7 Application of Two-dimensional Haar Wavelet Collocation Method to fractional order Stationary Neutron transport equation¹⁴

Let us divide the intervals D_1 and D_2'' into m equal subintervals each of width $\Delta_1 = \frac{1}{m}$ and $\Delta_2 = \frac{1}{m}$ respectively. We assume,

$$\frac{\partial^\beta u(x, \eta)}{\partial x^\beta} \equiv D^\beta u(x, \eta) = \sum_{i=1}^m \sum_{j=1}^m c_{ij} h_i(x) h_j(\eta) \quad (8.7.1)$$

Operating Riemann-Liouville fractional integral operator J^β both sides of eq. (8.7.1), we obtain

$$u(x, \eta) = \sum_{i=1}^m \sum_{j=1}^m c_{ij} Q^\beta h_i(x) h_j(\eta) + C_1 + xC_2 \quad (8.7.2)$$

where $Q^\beta h_i(x)$ is given by in eq. (7.3.7) for $\alpha = \beta$.

Substituting $x = 0$ into eq. (8.7.2), we can obtain

$$u(0, \eta) = C_1. \quad (8.7.3)$$

Similarly at the boundary $x = 1$, we have

$$u(1, \eta) = \sum_{i=1}^m \sum_{j=1}^m c_{ij} Q^\beta h_i(x) \Big|_{x=1} h_j(\eta) + C_1 + C_2 \quad (8.7.4)$$

Next, together with eqs. eq. (8.7.3) and (8.7.4), we have

$$C_2 = u(1, \eta) - u(0, \eta) - \sum_{i=1}^m \sum_{j=1}^m c_{ij} Q^\beta h_i(x) \Big|_{x=1} h_j(\eta) \quad (8.7.5)$$

¹⁴ S. Saha Ray and **A. Patra.**, 2014. "Numerical Simulation for Fractional order Stationary Neutron Transport Equation using Two-dimensional Haar wavelet Collocation method", **Nuclear Engineering and Design** (Elsevier), Communicated.

Now, by using eqs. (8.7.3) and (8.7.5) in eq. (8.7.2), we can obtain the approximate solution

$$u(x, \eta) = \sum_{i=1}^m \sum_{j=1}^m c_{ij} Q^\beta h_i(x) h_j(\eta) + u(0, \eta) + x \left(u(1, \eta) - u(0, \eta) - \sum_{i=1}^m \sum_{j=1}^m c_{ij} Q^\beta h_i(x) \Big|_{x=1} h_j(\eta) \right) \quad (8.7.6)$$

In view of conditions (8.2.2) and (8.6.10), we assume the boundary conditions

$$u(0, \eta) = u(1, \eta) = 0 \quad (8.7.7)$$

Now by putting eqs. (8.7.7) into eq. (8.7.6), we have

$$u(x, \eta) = \sum_{i=1}^m \sum_{j=1}^m c_{ij} Q^\beta h_i(x) h_j(\eta) - x \left(\sum_{i=1}^m \sum_{j=1}^m c_{ij} Q^\beta h_i(x) \Big|_{x=1} h_j(\eta) \right) \quad (8.7.8)$$

Then by using eq. (8.7.1) and (8.7.8) into eqs. (8.6.5) and (8.6.9), we obtain the numerical scheme for Case-I as

$$\begin{aligned} & \sum_{i=1}^m \sum_{j=1}^m c_{ij} h_i(x) h_j(\eta) - \left(\frac{1}{\eta^2} \right) \left(\sum_{i=1}^m \sum_{j=1}^m c_{ij} Q^\beta h_i(x) h_j(\eta) - x \left(\sum_{i=1}^m \sum_{j=1}^m c_{ij} Q^\beta h_i(x) \Big|_{x=1} h_j(\eta) \right) \right) \\ & + \left(\frac{1}{\eta^2} \right) \left(\sum_{i=1}^m \sum_{j=1}^m c_{ij} Q^\beta h_i(x) \Big|_0^1 h_j(\eta') d\eta' - x \left(\sum_{i=1}^m \sum_{j=1}^m c_{ij} Q^\beta h_i(x) \Big|_{x=1} \Big|_0^1 h_j(\eta') d\eta' \right) \right) \\ & + \left(\frac{1}{\eta^2} \right) \left(\eta^2 - \frac{1}{3} + \pi^2 \eta^4 \right) \sin \pi x = 0 \end{aligned} \quad (8.7.9)$$

and we also obtain the numerical scheme for Case-II as ,

$$\begin{aligned} & \sum_{i=1}^m \sum_{j=1}^m c_{ij} h_i(x) h_j(\eta) - \left(\frac{1}{\eta^2} \right) \left(\sum_{i=1}^m \sum_{j=1}^m c_{ij} Q^\beta h_i(x) h_j(\eta) - x \left(\sum_{i=1}^m \sum_{j=1}^m c_{ij} Q^\beta h_i(x) \Big|_{x=1} h_j(\eta) \right) \right) \\ & + \left(\frac{1}{\eta^2} \right) \left(\sum_{i=1}^m \sum_{j=1}^m c_{ij} Q^\beta h_i(x) \tilde{P}_j(\eta) - x \left(\sum_{i=1}^m \sum_{j=1}^m c_{ij} Q^\beta h_i(x) \Big|_{x=1} \tilde{P}_j(\eta) \right) \right) \end{aligned}$$

$$+\left(\frac{1}{\eta^2}\right)\left(-2\pi^2\eta^4\cos(2\pi x)+\left(\eta^2-\frac{2}{3}\right)\sin^2\pi x\right)=0 \quad (8.7.10)$$

where
$$\tilde{P}_j(\eta)=\int_0^1 h_j(\eta')d\eta'=\begin{cases} 1, & j=1 \\ 0, & j\neq 1 \end{cases}$$

By considering all the wavelet collocation points $\eta_l = A + (l - 0.5)\Delta_2$ for $l = 1, 2, \dots, m$ and $x_k = A + (k - 0.5)\Delta_1$ for $k = 1, 2, \dots, m$, we may obtain the system of m^2 -number of algebraic equations involving m^2 unknown coefficients c_{ij} . By solving this system of equations, we obtain the Haar coefficients c_{ij} . Hence we can obtain an approximate solution for neutron density $u(x, \eta)$ or $\phi(x, \eta)$ for fractional order stationary neutron transport equation.

8.8 Numerical Results and Discussions for fractional order neutron transport equation

In the present section, we have considered two test problems for the solution of fractional order stationary neutron transport equation [103, 109]. In Case-I and Case-II, we obtain approximate numerical solutions for neutron density for $x \in [0, 1]$ with $\eta = 0.2, 0.4, 0.6, 0.8$ and $\eta = 0.3, 0.5, 0.7$ and 0.9 respectively. Here, we compare the numerical results with the exact or integer order classical solutions by considering fractional order $\beta = 1.94, 1.96, 1.98$ and 2 . For Case-I, the numerical solution obtained by Haar wavelet collocation method have been displayed in Tables 5-8 and for Case-II, the numerical solution obtained by Haar wavelet collocation method has been displayed in Tables 9-12. Here, in both cases we have taken $m = 16$. Figs. 8(a)-(d) and Figs. 9(a)-(d) show the graphical comparison between the classical and numerical approximate solutions for the two test problems respectively. In both the test problems, from Tables 5-12 it can be shown that the value of angular flux of neutrons ϕ increases with increase value of η . In practical applications it should be concluded that the value of the density is equal to zero when the direction of the movement of particles makes an

angle of 90 degrees to the x -axis. Figs. 8(a)-(d) and Figs. 9(a)-(d) have shown that the solution has vanished at the physical domain. Fig. 10(a)-(b) and Fig. 11(a)-(b) display the convergence plot of absolute error for increasing collocation points $m=16$ and 32 in Case-I and Case-II respectively.

Table 5: Numerical solution of neutron density when $\eta = 0.2$ for Case-I

| x | $\eta = 0.2$ and $m = 16$ | | | | $\phi_{classical} = u_{classical}$ given in eq. (8.6.7) |
|-----|--|----------------|----------------|-------------|---|
| | Approximate solution of u for fractional order | | | | |
| | $\beta = 1.94$ | $\beta = 1.96$ | $\beta = 1.98$ | $\beta = 2$ | |
| 0 | 0 | 0 | 0 | 0 | 0 |
| 0.1 | 0.018967 | 0.017470 | 0.015984 | 0.014511 | 0.012360 |
| 0.2 | 0.035522 | 0.032889 | 0.030248 | 0.027606 | 0.023511 |
| 0.3 | 0.047793 | 0.044580 | 0.041309 | 0.037991 | 0.032360 |
| 0.4 | 0.054643 | 0.051439 | 0.048108 | 0.044664 | 0.038042 |
| 0.5 | 0.055636 | 0.052936 | 0.050039 | 0.046962 | 0.041031 |
| 0.6 | 0.051071 | 0.049175 | 0.047033 | 0.044664 | 0.038042 |
| 0.7 | 0.041835 | 0.040804 | 0.039517 | 0.037991 | 0.032360 |
| 0.8 | 0.029273 | 0.028927 | 0.028367 | 0.027606 | 0.023511 |
| 0.9 | 0.014864 | 0.014867 | 0.014748 | 0.014511 | 0.012360 |
| 1 | 1.665E-16 | 5.551E-17 | 2.775E-17 | 2.775E-17 | 2.266E-17 |

Table 6: Numerical solution of neutron density when $\eta = 0.4$ for Case-I

| x | $\eta = 0.4$ and $m = 16$ | | | | $\phi_{classical} = u_{classical}$ |
|-----|--|----------------|----------------|-------------|------------------------------------|
| | Approximate solution of u for fractional order | | | | given in |
| | $\beta = 1.94$ | $\beta = 1.96$ | $\beta = 1.98$ | $\beta = 2$ | eq. (8.6.7) |
| 0 | 0 | 0 | 0 | 0 | 0 |
| 0.1 | 0.055022 | 0.053607 | 0.052197 | 0.050795 | 0.049442 |
| 0.2 | 0.104035 | 0.101578 | 0.099108 | 0.096634 | 0.094045 |
| 0.3 | 0.141999 | 0.139043 | 0.136036 | 0.132989 | 0.129443 |
| 0.4 | 0.165340 | 0.162439 | 0.159437 | 0.156347 | 0.152169 |
| 0.5 | 0.171963 | 0.169584 | 0.167054 | 0.064390 | 0.161100 |
| 0.6 | 0.161591 | 0.160023 | 0.158270 | 0.156347 | 0.152169 |
| 0.7 | 0.135634 | 0.134940 | 0.134054 | 0.132989 | 0.129443 |
| 0.8 | 0.097132 | 0.097127 | 0.096957 | 0.096634 | 0.094045 |
| 0.9 | 0.050239 | 0.050521 | 0.050704 | 0.050795 | 0.049442 |
| 1 | 9.064E-17 | 3.330E-16 | 0 | 0 | 9.0648E-17 |

Table 7: Numerical solution of neutron density when $\eta = 0.6$ for Case-I

| x | $\eta = 0.6$ and $m = 16$ | | | | $\phi_{classical} = u_{classical}$ |
|-----|--|----------------|----------------|-------------|------------------------------------|
| | Approximate solution of u for fractional order | | | | given in |
| | $\beta = 1.94$ | $\beta = 1.96$ | $\beta = 1.98$ | $\beta = 2$ | eq. (8.6.7) |
| 0 | 0 | 0 | 0 | 0 | 0 |
| 0.1 | 0.115270 | 0.113072 | 0.110883 | 0.108707 | 0.111246 |
| 0.2 | 0.218149 | 0.214376 | 0.210594 | 0.206809 | 0.211603 |
| 0.3 | 0.298169 | 0.293702 | 0.289180 | 0.284611 | 0.291246 |

| | | | | | |
|-----|-----------|----------|----------|-----------|-----------|
| 0.4 | 0.347777 | 0.343499 | 0.339103 | 0.334601 | 0.342380 |
| 0.5 | 0.362414 | 0.359056 | 0.355517 | 0.351813 | 0.360102 |
| 0.6 | 0.341260 | 0.339261 | 0.337036 | 0.334601 | 0.342380 |
| 0.7 | 0.287031 | 0.286459 | 0.285648 | 0.284611 | 0.291246 |
| 0.8 | 0.205932 | 0.206430 | 0.206718 | 0.206809 | 0.211603 |
| 0.9 | 0.106660 | 0.107470 | 0.108151 | 0.108707 | 0.111246 |
| 1 | 2.224E-16 | 0 | 0 | 4.440E-16 | 2.266E-17 |

Table 8: Numerical solution of neutron density when $\eta = 0.8$ for Case-I

| x | $\eta = 0.8$ and $m = 16$ | | | | $\phi_{classical} = u_{classical}$ |
|-----|--|----------------|----------------|-------------|------------------------------------|
| | Approximate solution of u for fractional order | | | | given in |
| | $\beta = 1.94$ | $\beta = 1.96$ | $\beta = 1.98$ | $\beta = 2$ | eq. (8.6.7) |
| 0 | 0 | 0 | 0 | 0 | 0 |
| 0.1 | 0.198969 | 0.195385 | 0.191820 | 0.188276 | 0.197771 |
| 0.2 | 0.376595 | 0.370464 | 0.364325 | 0.358184 | 0.376183 |
| 0.3 | 0.514830 | 0.507608 | 0.500306 | 0.492935 | 0.517771 |
| 0.4 | 0.600624 | 0.593758 | 0.586716 | 0.579515 | 0.608676 |
| 0.5 | 0.626066 | 0.620751 | 0.615164 | 0.609326 | 0.640001 |
| 0.6 | 0.589683 | 0.586629 | 0.588323 | 0.579515 | 0.608676 |
| 0.7 | 0.496110 | 0.495410 | 0.494346 | 0.492935 | 0.517771 |
| 0.8 | 0.356021 | 0.357059 | 0.357776 | 0.358184 | 0.376183 |
| 0.9 | 0.184429 | 0.185910 | 0.187190 | 0.188276 | 0.197771 |
| 1 | 0 | 2.220E-16 | 2.220E-16 | 0 | 3.623E-16 |

Table 9: Numerical solution of neutron density when $\eta = 0.3$ for Case-II

| x | $\eta = 0.3$ and $m = 16$ | | | | $\phi_{classical} = u_{classical}$ given in eq. (8.6.11) |
|-----|--|----------------|----------------|-------------|--|
| | Approximate solution of u for fractional order | | | | |
| | $\beta = 1.94$ | $\beta = 1.96$ | $\beta = 1.98$ | $\beta = 2$ | |
| 0 | 0 | 0 | 0 | 0 | 0 |
| 0.1 | 0.015777 | 0.012747 | 0.009854 | 0.007094 | 0.008594 |
| 0.2 | 0.044167 | 0.038002 | 0.032073 | 0.026378 | 0.031094 |
| 0.3 | 0.074620 | 0.066278 | 0.058163 | 0.050283 | 0.058905 |
| 0.4 | 0.096080 | 0.087184 | 0.078388 | 0.069717 | 0.081405 |
| 0.5 | 0.100511 | 0.092802 | 0.084993 | 0.077123 | 0.090012 |
| 0.6 | 0.086444 | 0.081151 | 0.075559 | 0.069717 | 0.081405 |
| 0.7 | 0.059151 | 0.056593 | 0.053621 | 0.050283 | 0.058905 |
| 0.8 | 0.028955 | 0.028475 | 0.027605 | 0.026378 | 0.031094 |
| 0.9 | 0.006682 | 0.007048 | 0.007180 | 0.007094 | 0.008594 |
| 1 | 9.714E-17 | 6.938E-18 | 6.938E-18 | 3.035E-17 | 2.888E-19 |

Table 10: Numerical solution of neutron density when $\eta = 0.5$ for Case-II

| x | $\eta = 0.5$ and $m = 16$ | | | | $\phi_{classical} = u_{classical}$ |
|-----|--|----------------|----------------|-------------|------------------------------------|
| | Approximate solution of u for fractional order | | | | given in |
| | $\beta = 1.94$ | $\beta = 1.96$ | $\beta = 1.98$ | $\beta = 2$ | eq. (8.6.11) |

| | | | | | |
|-----|-----------|-----------|-----------|-----------|----------|
| 0 | 0 | 0 | 0 | 0 | 0 |
| 0.1 | 0.035669 | 0.032509 | 0.029496 | 0.026624 | 0.023872 |
| 0.2 | 0.118640 | 0.111055 | 0.103752 | 0.096716 | 0.086372 |
| 0.3 | 0.215028 | 0.204108 | 0.193483 | 0.183154 | 0.163627 |
| 0.4 | 0.288103 | 0.276323 | 0.264715 | 0.253296 | 0.226127 |
| 0.5 | 0.309460 | 0.299676 | 0.289851 | 0.280010 | 0.250420 |
| 0.6 | 0.271311 | 0.265558 | 0.259541 | 0.253296 | 0.226127 |
| 0.7 | 0.188134 | 0.186868 | 0.185196 | 0.183154 | 0.163627 |
| 0.8 | 0.092364 | 0.094211 | 0.095653 | 0.096716 | 0.086372 |
| 0.9 | 0.020262 | 0.022630 | 0.024746 | 0.026624 | 0.023872 |
| 1 | 1.942E-16 | 1.179E-16 | 9.194E-17 | 5.052E-17 | 0 |

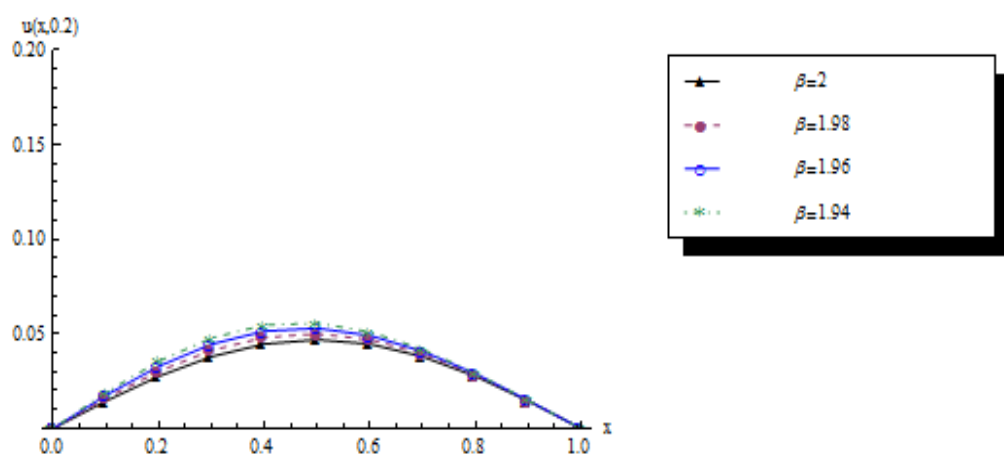
Table 11: Numerical solution of neutron density when $\eta = 0.7$ for Case-II

| x | $\eta = 0.7$ and $m = 16$ | | | | $\phi_{classical} = u_{classical}$ given in eq. (8.6.11) |
|-----|--|----------------|----------------|-------------|--|
| | Approximate solution of u for fractional order | | | | |
| | $\beta = 1.94$ | $\beta = 1.96$ | $\beta = 1.98$ | $\beta = 2$ | |
| 0 | 0 | 0 | 0 | 0 | 0 |
| 0.1 | 0.062774 | 0.057931 | 0.053321 | 0.048928 | 0.046790 |
| 0.2 | 0.212450 | 0.200322 | 0.188649 | 0.177420 | 0.169291 |
| 0.3 | 0.387385 | 0.369697 | 0.352498 | 0.335786 | 0.320709 |
| 0.4 | 0.520599 | 0.501516 | 0.482740 | 0.464282 | 0.443209 |
| 0.5 | 0.560127 | 0.544511 | 0.528864 | 0.513218 | 0.492200 |
| 0.6 | 0.491478 | 0.482783 | 0.473703 | 0.464282 | 0.443209 |
| 0.7 | 0.340763 | 0.339704 | 0.338031 | 0.335786 | 0.320709 |
| 0.8 | 0.166944 | 0.171045 | 0.174526 | 0.177420 | 0.169291 |

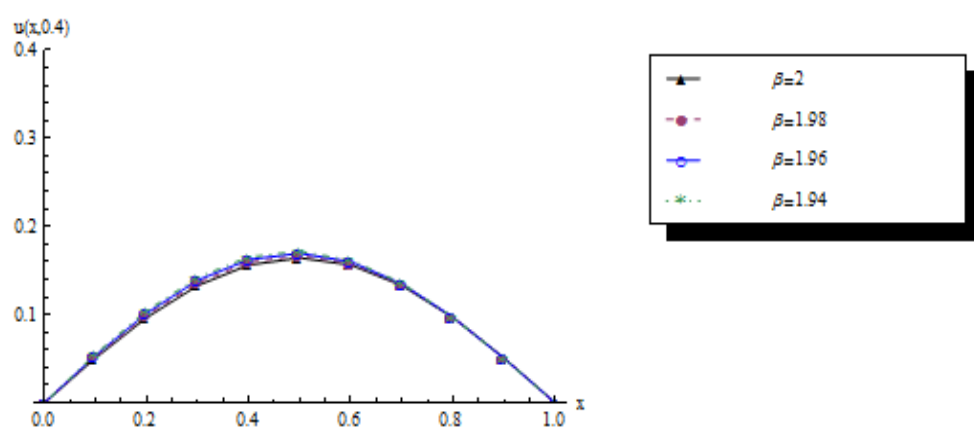
| | | | | | |
|-----|-----------|-----------|-----------|-----------|----------|
| 0.9 | 0.036162 | 0.040802 | 0.045052 | 0.048928 | 0.046790 |
| 1 | 2.567E-16 | 2.046E-16 | 1.249E-16 | 1.110E-16 | 0 |

Table 12: Numerical solution of neutron density when $\eta = 0.9$ for Case-II

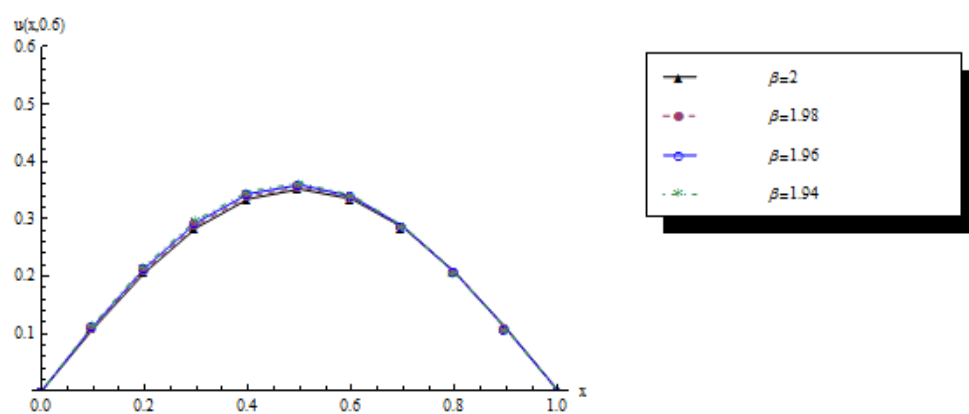
| x | $\eta = 0.9$ and $m = 16$ | | | | $\phi_{classical} = u_{classical}$ |
|-----|--|----------------|----------------|-------------|------------------------------------|
| | Approximate solution of u for fractional order | | | | given in |
| | $\beta = 1.94$ | $\beta = 1.96$ | $\beta = 1.98$ | $\beta = 2$ | eq. (8.6.11) |
| 0 | 0 | 0 | 0 | 0 | 0 |
| 0.1 | 0.099190 | 0.091723 | 0.084614 | 0.077846 | 0.077348 |
| 0.2 | 0.336621 | 0.317767 | 0.299627 | 0.282178 | 0.279848 |
| 0.3 | 0.614366 | 0.586809 | 0.560021 | 0.533993 | 0.530152 |
| 0.4 | 0.825999 | 0.796276 | 0.767040 | 0.738306 | 0.732652 |
| 0.5 | 0.888904 | 0.864663 | 0.840385 | 0.816115 | 0.810001 |
| 0.6 | 0.780004 | 0.766671 | 0.752752 | 0.738306 | 0.732652 |
| 0.7 | 0.540735 | 0.539414 | 0.537147 | 0.533993 | 0.530152 |
| 0.8 | 0.264761 | 0.271508 | 0.277298 | 0.282178 | 0.279848 |
| 0.9 | 0.057183 | 0.064668 | 0.071547 | 0.077846 | 0.077348 |
| 1 | 3.198E-16 | 2.081E-16 | 2.775E-17 | 3.156E-16 | 0 |



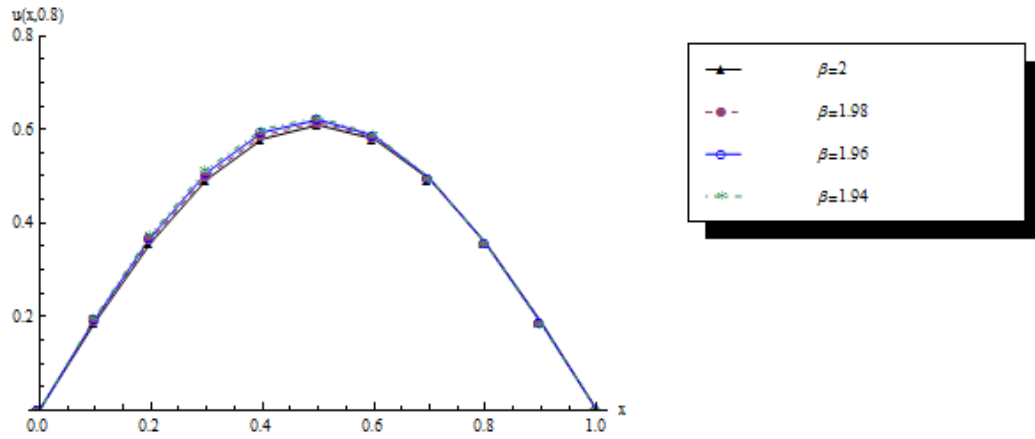
(a)



(b)

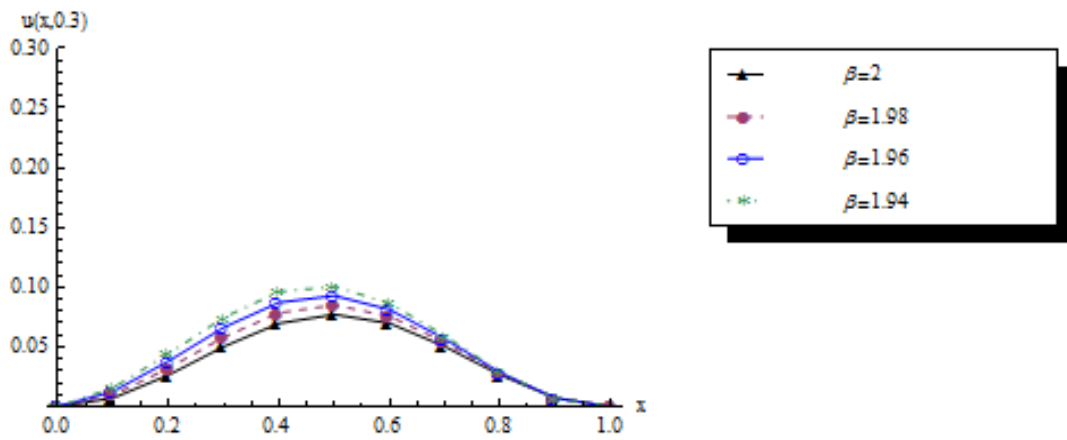


(c)

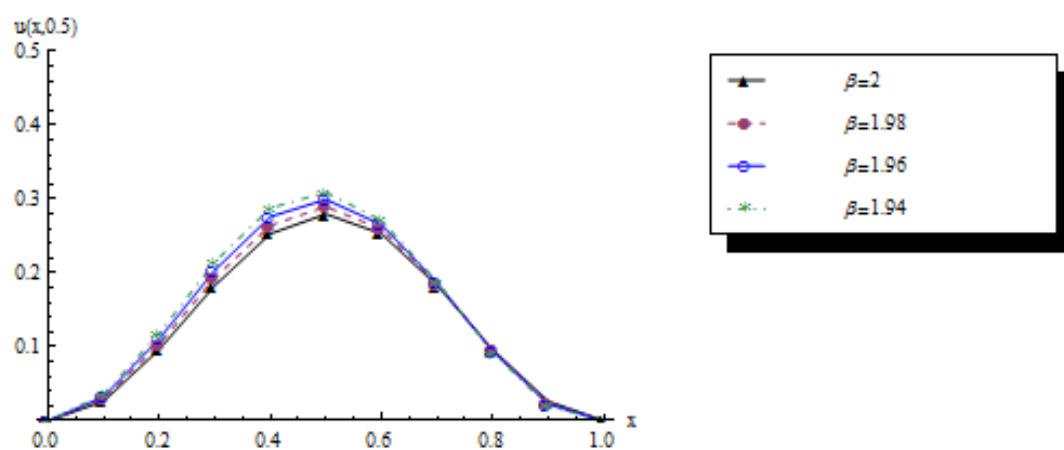


(d)

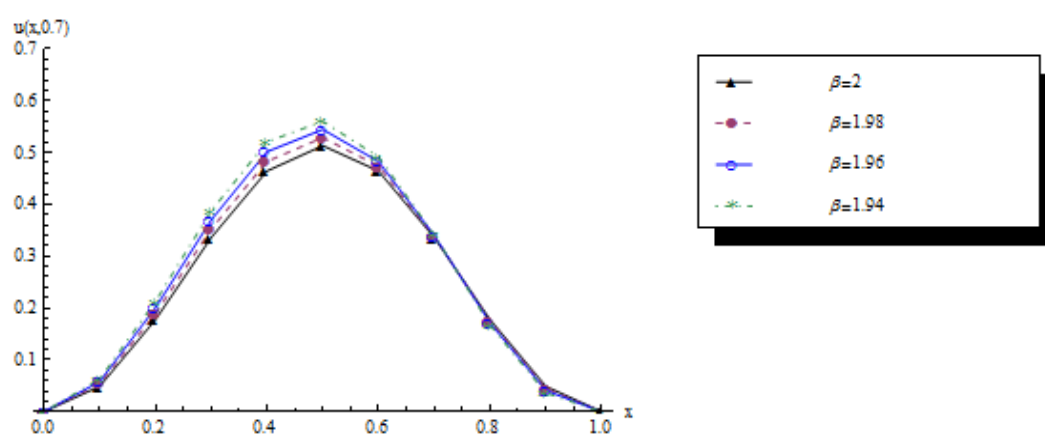
Fig. 8. Comparison between classical and fractional-order numerical Haar solutions with $m = 16$ for neutron density in **Case-I** (a) $\eta = 0.2$ (b) $\eta = 0.4$ (c) $\eta = 0.6$ (d) $\eta = 0.8$.



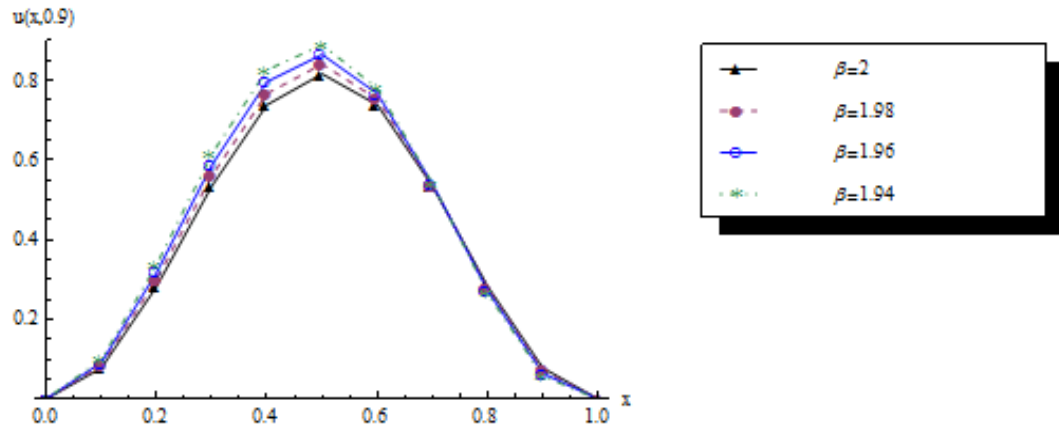
(a)



(b)

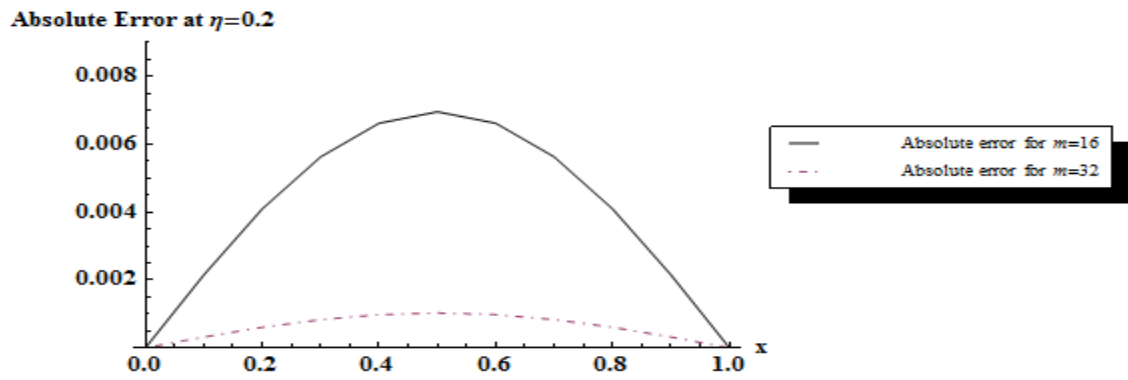


(c)

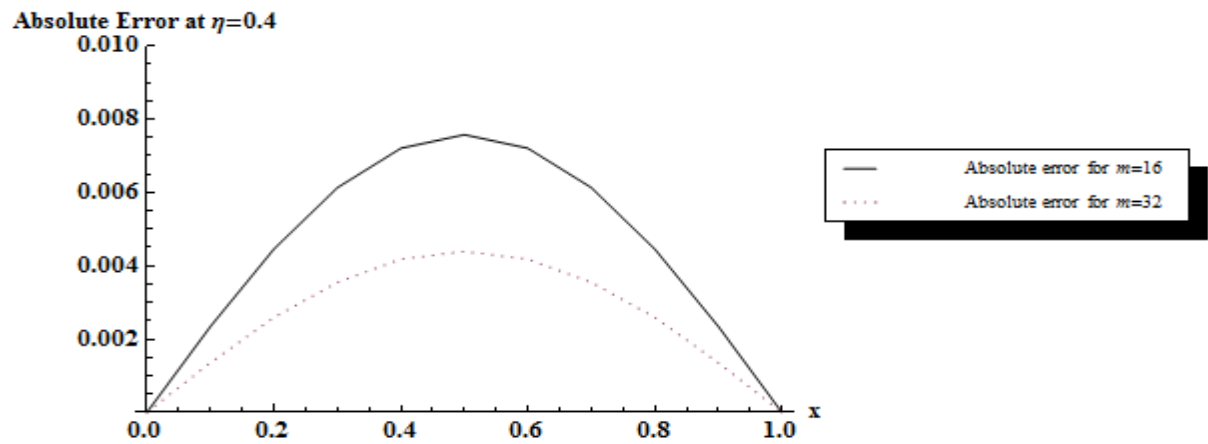


(d)

Fig. 9. Comparison between classical and fractional-order numerical Haar solutions with $m = 16$ for neutron density in **Case-II** (a) $\eta = 0.3$ (b) $\eta = 0.5$ (c) $\eta = 0.7$ (d) $\eta = 0.9$.

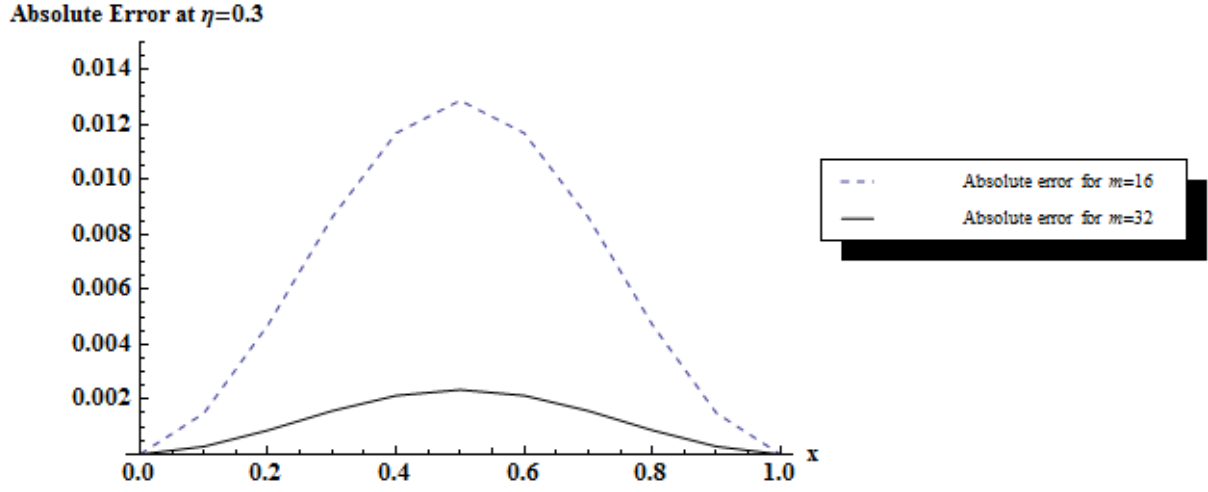


(a)

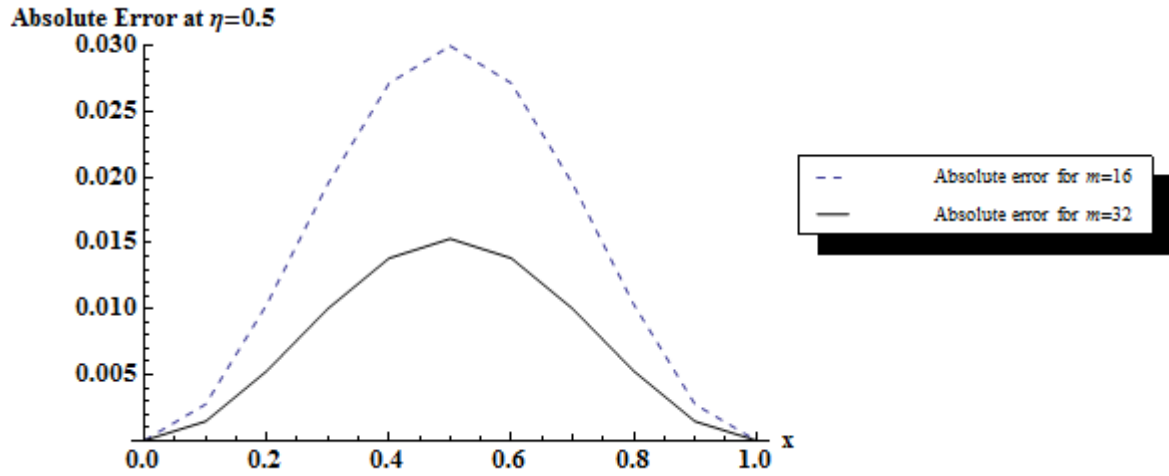


(b)

Fig. 10. Absolute Error for neutron density in **Case-I** at (a) $\eta = 0.2$ (b) $\eta = 0.4$.



(a)



(b)

Figure 4. Absolute Error for neutron density in **Case-II** at (a) $\eta = 0.3$ (b) $\eta = 0.5$.

8.9 Convergence Analysis of Two-dimensional Haar Wavelet Method

In this section, we have introduced the error analysis for the two-dimensional Haar wavelet method.

We assume that, $f(x, y) \in C^2([a, b] \times [a, b])$ and there exist $M > 0$; for which

$$\left| \frac{\partial^2 f(x, y)}{\partial x \partial y} \right| \leq M, \quad \forall x, y \in [a, b] \times [a, b].$$

Next, we may proceed as follows, suppose $f_{nm}(x, y) = \sum_{i=0}^{n-1} \sum_{j=0}^{m-1} c_{ij} h_i(x) h_j(y)$,

where, $n = 2^{\alpha+1}$, $\alpha = 0, 1, 2, \dots$ and $m = 2^{\beta+1}$, $\beta = 0, 1, 2, \dots$.

Then,

$$f(x, y) - f_{nm}(x, y) = \sum_{i=n}^{\infty} \sum_{j=m}^{\infty} c_{ij} h_i(x) h_j(y) + \sum_{i=n}^{\infty} \sum_{j=0}^{m-1} c_{ij} h_i(x) h_j(y) + \sum_{i=0}^{n-1} \sum_{j=m}^{\infty} c_{ij} h_i(x) h_j(y).$$

From Parseval's formula, we have

$$\begin{aligned} \|f(x, y) - f_{nm}(x, y)\|^2 &= \int_a^b \int_a^b (f(x, y) - f_{nm}(x, y))^2 dx dy \\ &= \sum_{p=n}^{\infty} \sum_{s=m}^{\infty} \sum_{i=n}^{\infty} \sum_{j=m}^{\infty} c'_{ij} c'_{ps} \int_a^b h_i(x) h_p(x) dx \int_a^b h_j(y) h_s(y) dy \\ &+ \sum_{p=n}^{\infty} \sum_{s=0}^{m-1} \sum_{i=n}^{\infty} \sum_{j=0}^{m-1} c'_{ij} c'_{ps} \int_a^b h_i(x) h_p(x) dx \int_a^b h_j(y) h_s(y) dy \\ &+ \sum_{p=0}^{n-1} \sum_{s=m}^{\infty} \sum_{i=0}^{n-1} \sum_{j=m}^{\infty} c'_{ij} c'_{ps} \int_a^b h_i(x) h_p(x) dx \int_a^b h_j(y) h_s(y) dy \\ &= \sum_{i=n}^{\infty} \sum_{j=m}^{\infty} c'^2_{ij} + \sum_{i=n}^{\infty} \sum_{j=0}^{m-1} c'^2_{ij} + \sum_{i=0}^{n-1} \sum_{j=m}^{\infty} c'^2_{ij}, \end{aligned}$$

where, $c'^2_{ij} = \frac{c_{ij}^2 (b-a)^2}{2^{i+j}}$ and

$$c_{ij} = \int_a^b \left(\int_a^b f(x, y) h_i(y) dy \right) h_j(x) dx.$$

$$= \int_a^b \left(\int_{a+k\left(\frac{b-a}{2^i}\right)}^{a+\left(k+\frac{1}{2}\right)\left(\frac{b-a}{2^i}\right)} f(x, y) dy - \int_{a+\left(k+\frac{1}{2}\right)\left(\frac{b-a}{2^i}\right)}^{a+(k+1)\left(\frac{b-a}{2^i}\right)} f(x, y) dy \right) h_j(x) dx$$

Using the mean value theorem of integral calculus we have,

$$a + k \frac{(b-a)}{2^i} \leq y_1 \leq a + \left(k + \frac{1}{2}\right) \frac{(b-a)}{2^i}, \quad a + \left(k + \frac{1}{2}\right) \frac{(b-a)}{2^i} \leq y_2 \leq a + (k+1) \frac{(b-a)}{2^i}.$$

Hence, we obtain

$$c_{ij} = (b-a) \int_a^b (f(x, y_1) 2^{-i-1} - f(x, y_2) 2^{-k-1}) h_j(x) dx.$$

Again by using the mean value theorem,

$$c_{ij} = 2^{-i-1} (b-a) \int_a^b (f(x, y_1) - f(x, y_2)) h_j(x) dx.$$

Using Lagrange's mean value theorem,

$$\begin{aligned} &= 2^{-i-1} (b-a) \int_a^b \left((y_1 - y_2) \frac{\partial f(x, y^*)}{\partial y} \right) h_j(x) dx \quad \text{where } y_1 \leq y^* \leq y_2 \\ &= 2^{-i-1} (b-a) (y_1 - y_2) \left(\int_{a+k\left(\frac{b-a}{2^j}\right)}^{a+\left(k+\frac{1}{2}\right)\left(\frac{b-a}{2^j}\right)} \frac{\partial f(x, y^*)}{\partial y} dx - \int_{a+\left(k+\frac{1}{2}\right)\left(\frac{b-a}{2^j}\right)}^{a+(k+1)\left(\frac{b-a}{2^j}\right)} \frac{\partial f(x, y^*)}{\partial y} dx \right) \\ &= 2^{-i-1} (b-a) (y_1 - y_2) \left(2^{-j-1} (b-a) \frac{\partial f}{\partial y}(x_1, y^*) - 2^{-j-1} (b-a) \frac{\partial f}{\partial y}(x_2, y^*) \right) \end{aligned}$$

Now, we use the mean value theorem of integral calculus

$$a + k \frac{(b-a)}{2^j} \leq x_1 \leq a + \left(k + \frac{1}{2}\right) \frac{(b-a)}{2^j}, \quad a + \left(k + \frac{1}{2}\right) \frac{(b-a)}{2^j} \leq x_2 \leq a + (k+1) \frac{(b-a)}{2^j}$$

$$\leq 2^{-i-j-2} (b-a)^2 (y_1 - y_2) (x_1 - x_2) \frac{\partial^2 f(x^*, y^*)}{\partial x \partial y}.$$

But for $x_1 \leq x^* \leq x_2$, $(y_1 - y_2) \leq (b-a)$ and $(x_1 - x_2) \leq (b-a)$,

We obtain,

$$c_{ij} \leq \frac{(b-a)^4}{2^{i+j+2}} M \quad \text{if} \quad \left| \frac{\partial^2 f(x^*, y^*)}{\partial x \partial y} \right| \leq M$$

Therefore,

$$c'_{ij}{}^2 = c_{ij}{}^2 \frac{(b-a)^2}{2^{i+j}} \leq \frac{(b-a)^{10}}{2^{3i+3j+4}} M^2$$

$$\sum_{n=k}^{\infty} \sum_{m=l}^{\infty} c'_{nm}{}^2 \leq \sum_{n=2^{\alpha+1}}^{\infty} \sum_{m=2^{\beta+1}}^{\infty} \frac{(b-a)^{10}}{2^{3i+3j+4}} M^2, \quad \alpha, \beta = 0, 1, 2, \dots$$

$$\leq (b-a)^{10} M^2 \sum_{n=2^{\alpha+1}}^{\infty} \sum_{i=\beta+1}^{\infty} \sum_{m=2^i}^{2^{i+1}-1} 2^{-3i-3j-4}$$

$$\leq (b-a)^{10} M^2 \sum_{n=2^{\alpha+1}}^{\infty} 2^{-3j-4} \sum_{i=\beta+1}^{\infty} (2^{i+1} - 1 - 2^i + 1) 2^{-3i}$$

$$\leq (b-a)^{10} M^2 \sum_{n=2^{\alpha+1}}^{\infty} 2^{-3j-4} \sum_{i=\beta+1}^{\infty} 2^{-2i}$$

$$\leq (b-a)^{10} M^2 \sum_{n=2^{\alpha+1}}^{\infty} 2^{-3j-4} 2^{-2(\beta+1)} \frac{1}{\left(1 - \frac{1}{2^2}\right)}$$

$$\leq \frac{4(b-a)^{10}}{3l^2} M^2 2^{-4} \sum_{j=\alpha+1}^{\infty} \sum_{n=2^j}^{2^{j+1}-1} 2^{-3j}$$

$$\leq \frac{4(b-a)^{10}}{3l^2} M^2 2^{-4} \sum_{j=\alpha+1}^{\infty} 2^{-2j}$$

$$\leq \frac{4(b-a)^{10}}{3l^2} M^2 2^{-4} \left(\frac{4}{3}\right) 2^{-2(\alpha+1)}$$

$$\leq \left(\frac{16}{9}\right) \frac{(b-a)^{10}}{l^2 k^2} M^2 2^{-4}$$

$$= \left(\frac{16}{144}\right) \frac{(b-a)^{10}}{l^2 k^2} M^2$$

Next,
$$\sum_{n=k}^{\infty} \sum_{m=0}^{l-1} c'_{nm} 2 \leq \sum_{n=k}^{\infty} \sum_{m=0}^{l-1} \frac{(b-a)^{10} M^2}{2^{3i+3j+4}} \leq \sum_{n=2^{\alpha+1}}^{\infty} \frac{(b-a)^{10} M^2}{2^{3j+4}} \sum_{i=0}^{\beta} \sum_{m=2^i-1}^{2^{i+1}-1} 2^{-3i}$$

$$\leq \sum_{n=2^{\alpha+1}}^{\infty} \frac{(b-a)^{10} M^2}{2^{3j+4}} \sum_{i=0}^{\beta} (2^{-2i} + 2^{-3i})$$

$$\leq \left(\frac{52}{21}\right) 2^{-4} (b-a)^{10} M^2 \sum_{j=\alpha+1}^{\infty} \sum_{n=2^j}^{2^{j+1}-1} 2^{-3j}$$

$$\leq \left(\frac{52}{336}\right) (b-a)^{10} M^2 \sum_{j=\alpha+1}^{\infty} 2^{-2j}$$

$$\leq \left(\frac{52}{336}\right) (b-a)^{10} M^2 \left(\frac{2^{-2(\alpha+1)}}{(1 - \frac{1}{2^2})} \right)$$

$$= \frac{52(b-a)^{10} M^2}{252k^2}.$$

Similarly, we have

$$\sum_{n=0}^{k-1} \sum_{m=l}^{\infty} c_{nm}'^2 \leq \frac{52(b-a)^{10} M^2}{252l^2}.$$

Then

$$\sum_{n=k}^{\infty} \sum_{m=l}^{\infty} c_{nm}'^2 + \sum_{n=k}^{\infty} \sum_{m=0}^{l-1} c_{nm}'^2 + \sum_{n=0}^{k-1} \sum_{m=l}^{\infty} c_{nm}'^2 \leq \left(\frac{16}{144} \right) \frac{(b-a)^{10}}{l^2 k^2} M^2 + \frac{52(b-a)^{10} M^2}{252k^2} + \frac{52(b-a)^{10} M^2}{252l^2}.$$

Hence, we obtain $\|f(x, y) - f_{kl}(x, y)\| \leq \frac{(b-a)^{10} M^2}{3} \left(\frac{1}{3l^2 k^2} + \frac{13}{2lk^2} + \frac{13}{2l^2} \right)$

As $l \rightarrow \infty$ and $k \rightarrow \infty$ we can get $\|f(x, y) - f_{kl}(x, y)\| \rightarrow 0$.

8.10 Conclusion

In the present research work, we have successfully applied Haar Wavelet Collocation Method (HWCM) to obtain the numerical approximation solution for classical order [110] and fractional order stationary neutron transport equation in a homogeneous isotropic medium. The cited numerical examples well establish that there is a good agreement of results in comparison to the classical solutions. By analyzing the Tables 1-12, it can be concluded that if we increase the number of collocation point m , we can get more accurate solution for transport problems. This research work proves the validity and the great potential applicability of Haar wavelet collocation method (HWCM) for solving both classical and fractional order stationary neutron transport equation.

BIBLIOGRAPHY

- [1] Liao, S. J., 2004. "On the homotopy analysis method for nonlinear problems", *Applied Mathematics and Computation*, **147**, 499-513.
- [2] Liao, S. J., 2005. "Comparison between the homotopy analysis method and homotopy perturbation method", *Applied Mathematics and Computation*, **169**, 1186-1194.
- [3] Adomian, G., 1994. *Solving Frontier Problems of Physics: Decomposition Method*. Kluwer Academic Publishers, Athens, USA.
- [4] Adomian, G., 1989. *Nonlinear Stochastic Systems Theory and Applications to Physics*. Kluwer Academic Publishers, Dordrecht, The Netherlands.
- [5] Wazwaz A., 1999. "A Reliable Modification of Adomian Decomposition Method", *Applied Mathematics and Computation*, **102** (1), 77-86.
- [6] Cherruault Y., 1989. "Covergence of Adomian's Method", *Kybernetes*, **18**, 31-38.
- [7] Cherruault Y., Adomian G., 1993. "Decomposition Methods: a new proof of convergence", *Mathematics and Computer Modeling*, **18**, 103-106.
- [8] He J.H., 1999. "Variational Iteration Method-a kind of non-linear analytical technique; Some examples", *International Journal of Nonlinear Mechanics*, **34**, 699-708.
- [9] He J.H., 2000. "A review on some new recently developed nonlinear analytical techniques", *International Journal of Nonlinear Sciences and Numerical Simulation*, **1**, 51-70.

- [10] Sweilam N.H., 2007. “Variational iteration method for solving cubic nonlinear Schrodinger equation”, *Journal of Computational and Applied Mathematics*, **207**, 155-163.
- [11] Mehdi, T., Mehedi, D., 2007. “On the convergence of He’s variational iteration method”, *Journal of Computational and Applied Mathematics*, **207**, 121-128.
- [12] Smith, G.D., 1985. *Numerical Solution of Partial Differential Equations: Finite Difference Methods* (Third Edition), Oxford Applied Mathematics and Computing Science Series, Oxford University Press, New York.
- [13] Yuste, S.B., Acedo, L., 2005. “On an explicit finite difference method for fractional diffusion equations”, *SIAM Journal of Numerical Analysis*, **52**, 1862–1874.
- [14] Zhou, J. K., 1986. *Differential Transformation and Its Applications for Electrical Circuits*, Huazhong University Press, Wuhan, China.
- [15] Odibat, Z. M., Bertelle, C., Aziz-Alaoui, M. A., Duchamp, G. H. E., 2010. “A multi-step differential transform method and application to non-chaotic or chaotic systems”, *Computers and Mathematics with Applications*, **59** (4), 1462-1472.
- [16] Arikoglu, A., Ozkol, I., 2005. “Solution of boundary value problems for integro-differential equations by using differential transform method”, *Applied Mathematics and Computation*, **168** (2), 1145–1158.
- [17] Arikoglu, A., Ozkol, I., 2006. “Solution of difference equations by using differential transform method”, *Applied Mathematics and Computation*, **174** (2), 1216-1228.
- [18] Liu., H., Song, Y., 2007. “Differential transform method applied to high index differential-algebraic equations”, *Applied Mathematics and Computation*, **184** (2), 748–753.
- [19] Higham, D.J., 2001. “An algorithmic introduction to numerical simulation of stochastic differential equations”, *SIAM Review*, **43**, 525-546.

- [20] Sauer, T., 2012. “Numerical Solution of Stochastic Differential Equation in Finance”, *Handbook of Computational Finance*, Springer, Part 4, 529-550.
- [21] Kloeden, P.E., Platen, E., 1992. *Numerical Solution of Stochastic Differential Equations*, Springer-Verlag, New York.
- [22] Stacey, W.M., 2001. *Nuclear Reactor Physics*, John Wiley & Sons Publication, Germany.
- [23] Glasstone, S., Sesonske, A., 1981. *Nuclear Reactor Engineering*, third ed. VNR, New York.
- [24] Hetrick, D.L., 1993. *Dynamics of Nuclear Reactors*, American Nuclear Society, Chicago, London.
- [25] He, J.H., 1997. “A new approach to nonlinear partial differential equations”, *Communication Nonlinear Science and Numerical Simulation*, **2**, 230-235.
- [26] Inokti, M., Sekin, H., Mura, T., 1978. *General use of the Lagrange multiplier in nonlinear mathematical physics*, In: Nemat-Nassed S, editor. Variational method in the mechanics of solids. Pergamon Press, 156-162.
- [27] Wazwaz, A. M., EI-Sayed, S. M., 2001. “A newmodification of the Adomian Decomposition method for linear and nonlinear operators”, *Applied Mathematics and Computation*, **122** (3), 393-405.
- [28] Saha Ray, S., 2008. “An application of the modified decomposition method for the solution of the coupled Klein–Gordon–Schrödinger equation”, *Comminication in Nonlinear Science and Numerical Simulation*, **13**, 1311-1317.
- [29] Kaya, D., Yokus, A., 2002. “A numerical comparison of partial solutions in the decomposition method for linear and nonlinear partial differential equations”, *Mathematics Computer in Simulation*, **60**(6), 507-512.

- [30] Büyük, S., Çavdar, S., Ahmetolan, S., 2010. “Solution of fixed source neutron diffusion equation via homotopy perturbation method”, ICAST 2010, May, İzmir, Turkey (in English).
- [31] Saha Ray, S., Patra, A., 2011. “Application of Modified decomposition method and Variational Iteration Method for the solution of the one group neutron diffusion equation with fixed source”, *International Journal of Nuclear Energy Science and Technology*, **6**(4), 310-320.
- [32] Duderstadt J. J., Hamilton L.J. 1976. *Nuclear Reactor Analysis*, John Wiley & Sons, Michigan, USA.
- [33] Liao, S. J., 1997. “Homotopy analysis method: A new analytical technique for nonlinear problems”, *Communications in Nonlinear Science & Numerical Simulation*, **2** (2), 95–100.
- [34] Liao, S. J., 2003. *Beyond Perturbation: Introduction to the Homotopy Analysis Method*, CRC Press, Chapman & Hall.
- [35] Saha Ray, S., Patra, A., 2011. “Application of Homotopy Analysis Method and Adomian Decomposition Method for the Solution of Neutron Diffusion Equation in the Hemisphere and Cylindrical Reactors”, *Journal of Nuclear Engineering and Technology*, **1** (1-3), 1-14.
- [36] Cassell J.S., Williams M.M.R., 2004. “A solution of the neutron diffusion equation for a hemisphere with mixed boundary conditions”, *Annals of Nuclear Energy*, **31**, 1987–2004.
- [37] Williams, M.M.R., Matthew, E., 2004. “A solution of the neutron diffusion equation for a hemisphere containing a uniform source”, *Annals of Nuclear Energy*, **31**, 2169-2184.
- [38] Adomian, G., 1991. “A review of the decomposition method and some recent results for nonlinear equations”, *Computational Mathematics and Application*, **21**, 101 – 127.

- [39] Dababneh S., Khasawneh K., Odibat Z., 2011. “An alternative solution of the neutron diffusion equation in cylindrical symmetry”, *Annals of Nuclear Energy*, **38**, 1140–1143.

- [40] Khasawneh K., Dababneh S., Odibat Z., 2009. “A solution of the neutron diffusion equation in hemispherical symmetry using the homotopy perturbation method”, *Annals of Nuclear Energy*, **36**, 1711–1717.

- [41] Kilbas, A. A., Srivastava, H. M., Trujillo, J.J., 2006. *Theory and Applications of Fractional Differential Equations*, North-Holland Mathematical Studies, 204, Elsevier (North-Holland) Sci. Publishers, Amsterdam, London.

- [42] Sabatier, J., Agrawal, O.P., Tenreiro Machado, J.A., 2007. *Advances in Fractional Calculus: Theoretical Developments and Applications in Physics and Engineering*, Springer, Dordrecht, Netherlands.

- [43] Gorenflo, R., Mainardi, F., 1997. *Fractional calculus integral and differential equations of fractional order*, in: A. Carpinteri, F. Mainardi (Eds.), *Fractals and Fractional Calculus in Continuum Mechanics*, Springer Verlag, Wein, 223–276.

- [44] Podlubny, I., 1999. *Fractional Differential Equations*, Academic Press, San Diego, California, United States of America.

- [45] Holmgren, H. J., 1865-1866. *Om differentialkalkylen med indecies of hvad natur som helst*, Kungl. Svenska Vetenskaps-Akademins Handlingar, Bd 5, No.11, 1-83, Stockholm (in Swedish).

- [46] Riemann, B., 1876. *Versuch einer allgemeinen Auffassung der Integration und Differentiation*, Gesammelte Werke und Wissenschaftlicher Nachlass. Teubner, Leipzig, (Dover, New York, 1953), 331-344.

- [47] Zhang, D.L., Qiu, S.Z., Su, G.H., Liu, C.L., Qian, L.B., 2009. “Analysis on the neutron kinetics for a molten salt reactor”, *Progress in Nuclear Energy*, **51**, 624–636.
- [48] Espinosa-Paredes, G., Morales-Sandoval, J.B., Vázquez-Rodríguez, R., EspinosaMartínez, E.-G., 2008. “Constitutive laws for the neutron density current”, *Annals of Nuclear Energy*, **35**, 1963–1967.
- [49] Espinosa-Paredes, G., Polo-Labarrios, M.-A., Espinosa-Martínez, E.-G., Valle-Gallegos, E. D., 2011. “Fractional neutron point kinetics equations for nuclear reactor dynamics”, *Annals of Nuclear Energy*, **38**, 307–330.
- [50] Saha Ray, S., Patra A., 2012. “An Explicit Finite Difference Scheme for numerical solution of fractional neutron point kinetic equation”, *Annals of Nuclear Energy*, **41**, 61-66.
- [51] Lamarsh, J.R., Baratta, A.J., 2001. *Introduction to Nuclear Engineering*, third ed. Prentice-Hall Inc, New Jersey.
- [52] Sardar, T., Saha Ray, S., Bera, R. K., Biswas, B. B., 2009. “The analytical approximate solution of the multi-term fractionally damped Vander Pol equation”, *Physica Scripta*, **80**, 025003.
- [53] Kinard, M., Allen, K. E. J., 2004. “Efficient numerical solution of the point kinetics equations in nuclear reactor dynamics”, *Annals of Nuclear Energy*, **31**, 1039–1051.
- [54] Edwards, J.T., Ford, N. J., Simpson, A.C., 2002. “The numerical solution of linear multiterm fractional differential equations”, *Journal of Computational and Applied Mathematics*, **148**, 401–418.
- [55] Diethelm, K., 1997. “An algorithm for the numerical solution of differential equations of fractional order”, *Electronic Transactions on Numerical Analysis*, **5**, 1–6.

- [56] Diethelm, K., 1997. "Numerical approximation of finite-part integrals with generalized compound quadrature formulae", *IMA Journal of Numerical Analysis*, **17**, 479–493.
- [57] Khan, Y., Faraz, N., Yildirim, A., Wu, Q., 2011. "Fractional variational iteration method for fractional initial-boundary value problems arising in the application of nonlinear science", *Computers and Mathematics with Applications*, **62** (5), 2273-2278.
- [58] Khan, Y., Wu, Q., Faraz, N., Yildirim, A., Madani, M., 2012. "A new fractional analytical approach via a modified Riemann- Liouville derivative", *Applied Mathematics Letters*, **25** (10), 1340-1346.
- [59] Khan, Y., Fardi, M., Seyevand, K., Ghasemi, M., 2014. "Solution of nonlinear fractional differential equations using an efficient approach", *Neural Computing and Applications*, **24**, 187-192.
- [60] Hayes J.G., Allen E.J., 2005. "Stochastic point-kinetics equations in nuclear reactor dynamics", *Annals of Nuclear Energy*, **32**, 572-587.
- [61] Darania, P., Ebadian, A., 2007. "A method for the numerical solution of the integro-differential equations", *Applied Mathematics and Computation*, **188**, 657-668.
- [62] Patrico, M. F., Rosa, P. M., 2007. "The Differential Transform Method for Advection-Diffusion Problems", *International Journal of Mathematical, Computational Science and Engineering*, **1**(9), 73-77.
- [63] Quintero-Leyva, B., 2008. CORE: "A numerical algorithm to solve the point kinetics equations with lumped model temperature and feedback", *Annals of Nuclear Energy*, **36**, 246-250.

- [64] McMohan, D., Pierson, A., 2010. "A Taylor series solution of the reactor point kinetic equations," available online at <http://arxiv.org/ftp/arxiv/papers/1001/1001.4100.pdf>.
- [65] Van den Eynde, G., 2006. "A Resolution of the Stiffness Problem of Reactor Kinetics", *Nuclear Science and Engineering*, **153**, 200-202.
- [66] Patra, A., Saha Ray, S., 2013. "Multi-step Differential Transform method for Numerical Solution of Classical Neutron Point Kinetic Equation", *Computational Mathematics and Modeling*, **24** (4), 604-615.
- [67] Saha Ray, S., Patra, A., 2014. "Numerical Simulation for Solving Fractional Neutron Point Kinetic Equations using the Multi-step Differential Transform Method", *Physica Scripta*, **89**, 015204.
- [68] Espinosa-Paredes, G., Polo-Labarrios, M.-A., Diaz-Gonzalez, L., Vazquez-Rodriguez, A., Espinosa-Matinez, E.-G., 2012. "Sensitivity and uncertainty analysis of the fractional neutron point kinetics equations", *Annals of Nuclear Energy*, **42**, 169-174.
- [69] Polo-Labarrios M.-A, Espinosa-Paredes, G., 2012. "Application of the Fractional neutron point kinetic equation: Start-up of a nuclear reactor", *Annals of Nuclear Energy*, **46**, 37-42.
- [70] Polo-Labarrios, M.-A., Espinosa-Paredes, G., 2012. "Numerical Analysis of Start-up PWR with Fractional Neutron Point Kinetic Equation", *Progress in Nuclear Energy*, **60**, 38-46.
- [71] Saha Ray, S., 2012. "Numerical Simulation of Stochastic point kinetic equation in the dynamical system of nuclear reactor", *Annals of Nuclear Energy*, **49**, 154-159.
- [72] Oldham, K. B., Spanier, J., 1974. *The Fractional Calculus*, Academic Press, NewYork.
- [73] Saha Ray, S., Patra, A., 2012. "Numerical Solution for Stochastic Point Kinetics Equations with Sinusoidal Reactivity in Dynamical System of Nuclear Reactor", *Int. Journal of Nuclear Energy Science and Technology*, **7** (3), 231-242.

- [74] Patra, A., Saha Ray, S., 2014. “The Effect of Pulse Reactivity for Stochastic Neutron Point Kinetics Equation in Nuclear Reactor Dynamics”, *Int. Journal of Nuclear Energy Science and Technology*, **8** (2), 117-130.
- [75] S Saha Ray, S., Patra, A., 2013. “Numerical Solution of Fractional Stochastic Neutron Point Kinetic Equation for Nuclear Reactor Dynamics”, *Annals of Nuclear Energy*, **54**, 154-161.
- [76] Nahla, A. A., 2008. “Generalization of the analytical exponential model to solve the point kinetics equations of Be- and D₂O –moderated reactors”, *Nuclear Engineering and Design*, **238**, 2648-2653.
- [77] Aboander, A. E., Nahla, A.A., 2002. “Solution of the point kinetics equations in the presence of Newtonian temperature feedback by Padé approximations via the analytical inversion method”, *Journal of Physics A: Mathematical and General*, **35**, 9609-9627.
- [78] Nahla, A. A., 2010. “Analytical solution to solve the point reactor kinetics equations”, *Nuclear Engineering and Design*, **240**, 1622-1629.
- [79] Nahla, A. A., 2011. “Taylor’s series method for solving the nonlinear point kinetics equations”, *Nuclear Engineering and Design*, **241**, 1592-1595.
- [80] Li, H., Chen, W., Luo, L., Zhu, Q., 2009. “A new integral method for solving the point reactor neutron kinetics equations”, *Annals of Nuclear Energy*, **36**, 427-432.
- [81] Chao, Y., Attard, A., 1985. “A resolution of the stiffness problem of reactor kinetics”, *Nuclear Science and Engineering*, **90**, 40-46.
- [82] Miller, K. S., Ross, B., 1993. *An Introduction to the Fractional Calculus and Fractional Differential Equations*, Wiley, New York.
- [83] Patra A., Saha Ray, S., 2014. “On the Solution of Nonlinear Fractional Neutron Point Kinetics Equation with Newtonian Temperature feedback reactivity”, *Nuclear Technology (American Nuclear Society)*, Accepted.

- [84] Nahla, A. A., 2011. "An efficient technique for the point kinetics equations with Newtonian temperature feedback effects", *Annals of Nuclear Energy*, **38**, 2810-2817.
- [85] Aboanber, A. E., Nahla, A.A., 2003. "Analytical solution of the point kinetics equations by Exponential Mode Analysis", *Progress in Nuclear Energy*, **42**, 179-197.
- [86] Aboanber, A.E., Nahla, A.A., 2002. "Generalization of the analytical inversion method for the solution of the point kinetics equations", *Journal of Physics A: Mathematical and General*, **35**, 3245-3263.
- [87] Hamada, Y.M., 2011. "Generalized power series method with step size control for neutron kinetics equations," *Nuclear Engineering and Design*, **241**, 3032-3041.
- [88] Ganapol, B.D., 2013. "A highly accurate algorithm for the solution of the point kinetics equations", *Annals of Nuclear Energy*, **62**, 564-571.
- [89] Picca, P., Furfaro, R., Ganapol, B.D., 2013. "A highly accurate technique for the non-linear point kinetics equations", *Annals of Nuclear Energy*, **58**, 43-53.
- [90] Chui, C.K., 1992. *An Introduction to Wavelets*, Academic Press, London, UK.
- [91] Mallat, S.G., 2009. *A wavelet tour of signal processing: the sparse way* (3rd Edition), Academic Press, San Diego, California, USA.
- [92] Debnath, L., 2007. *Wavelet transforms and their applications*, Birkhäuser, Boston.
- [93] Haar A., 1910. "Zur theorie der orthogonalen Funktionsysteme", *Mathematical Annals*, **69**, 331–71.
- [94] Li, Y., Zhao, W., 2010. "Haar wavelet operational matrix of fractional order integration and its applications in solving the fractional order differential equations", *Applied Mathematics and Computation*, **216**, 2276-2285.
- [95] Saha Ray, S., 2012. "On Haar wavelet operational matrix of general order and its application for the numerical solution of fractional Bagley Torvik equation", *Applied Mathematics and Computation*, **218**, 5239-5248.

- [96] Chen, C.F., Hsiao, C.H., 1997. "Haar wavelet method for solving lumped and distributed parameter-systems", *IEE Proc-Control Theory Application*, **144** (1) 87-94.
- [97] Saha Ray, S., Patra A., 2013. "Haar wavelet operational methods for the numerical solutions of Fractional order nonlinear oscillatory Van der Pol system", *Applied Mathematics and Computation*, **220**, 659-667.
- [98] Ganapol, B.D., Picca, P., Previti, A., Mostacci, D., 2012. *The solution of the point kinetics equations via Convergence Acceleration Taylor Series (CATS)*, Knoxville, Tennessee (April 15-20).
- [99] Baleanu, D., Kadem, A., 2011. *About the F_N Approximation to fractional neutron transport equation in slab geometry*, Proceedings of the ASME 2011 International Design engineering Technical Conference and Computers and Information in Engineering Conference, Washington, DC (United States of America).
- [100] Kadem, A., Kilicman, A., 2011. "Note on transport equation and fractional Sumudu transform", *Computers and Mathematics with Applications*, **62**, 2995-3003.
- [101] Kadem, A., Baleanu, D., 2011. "Solution of a fractional transport equation by using the generalized quadratic form", *Communication Nonlinear Science and Numerical Simulation*, **16**, 3011-3014.
- [102] Kulikowska, T., 2000. *An introduction to the neutron transport Phenomena*, in Proceedings of the Workshop on Nuclear Data and Nuclear Reactors: Physics, Design and Safety, Trieste, Italy.
- [103] Martin, O., 2011. "A homotopy perturbation method for solving a neutron transport equation", *Applied Mathematics and Computation*, **217**, 8567-8574.
- [104] Šmarda, Z. and Khan, Y., 2012. "Singular Initial value problem for a system of integro-differential equations", *Abstract and Applied Analysis*, **2012**, Article Id-918281.

- [105] Islam, S., Imran, A., and Muhammad, F., 2013. "A new approach for numerical solution of integro-differential equations via Haar wavelets", *International Journal of Computer Mathematics*, **90**, 1971-1989.
- [106] Chang, P., Piau, P., 2008. "Haar wavelet matrices designation in Numerical solution of ordinary differential equations", *IAENG International Journal of Applied Mathematics*, **38**, 3-11.
- [107] Chen, Y., Wu, Y., Cui, Y., Wang, Z., Jin, D., 2010. "Wavelet method for a class of fractional convection-diffusion equation with variable coefficients", *Journal of Computational Science*, **1**, 146-149.
- [108] Lepik, U., 2009. "Solving fractional integral equations by the Haar wavelet method", *Applied Mathematics and Computation*, **214**, 468-478.
- [109] Martin, O., 2006. "Numerical Algorithm for a Transport Equation with Periodic Source Function", *International Journal of Information and Systems Sciences*, **2**, 436-451.
- [110] Patra, A., Saha Ray, S., 2014. "Two-dimensional Haar wavelet Collocation method for the solution of Stationary Neutron Transport Equation in a Homogeneous Isotropic medium", *Annals of Nuclear Energy*, **70**, 30-35.

LIST OF RESEARCH PAPERS PUBLISHED/ACCEPTED/COMMUNICATED

❖ Research Publications in International Journals

1. S. Saha Ray and **A. Patra**, 2011, “Application of Modified decomposition method and Variational Iteration Method for the solution of the one group neutron diffusion equation with fixed source”, **Int. Journal of Nuclear Energy Science and Technology** (Inderscience), **6** (4), pp. 310-320.
2. S. Saha Ray and **A. Patra**, 2011, “Application of Homotopy Analysis Method and Adomian Decomposition Method for the Solution of Neutron Diffusion Equation in the Hemisphere and Cylindrical Reactors”, **Journal of Nuclear Engineering and Technology** (STM), **1** (2-3), pp. 1-12.
3. S. Saha Ray and **A. Patra**, 2012, “An Explicit Finite Difference Scheme for numerical solution of fractional neutron point kinetic equation”, **Annals of Nuclear Energy** (Elsevier), **41**, pp. 61-66.
4. S. Saha Ray and **A. Patra**, 2013, “Numerical Solution of Fractional Stochastic Neutron Point Kinetic Equation for Nuclear Reactor Dynamics”, **Annals of Nuclear Energy** (Elsevier), **54**, pp. 154-161.
5. S. Saha Ray and **A. Patra**, 2012, “Numerical Solution for Stochastic Point Kinetics Equations with Sinusoidal Reactivity in Dynamical System of Nuclear Reactor”, **Int. Journal of Nuclear Energy Science and Technology** (InderScience), **7** (3), 231-242.
6. **A. Patra** and S. Saha Ray, 2013, “Multi-step Differential Transform method for Numerical Solution of Classical Neutron Point Kinetic Equation”, **Computational Mathematics and Modeling** (Springer), **24**(4), 604-615.
7. **A. Patra** and S. Saha Ray, 2014, “The Effect of Pulse Reactivity for Stochastic Neutron Point Kinetics Equation in Nuclear Reactor Dynamics”, **Int. Journal of Nuclear Energy Science and Technology** (Inderscience), **8** (2), pp. 117-130.

8. S. Saha Ray and **A. Patra**, 2014. “Numerical Simulation Methods for Solving Fractional Neutron Point Kinetic Equations using Multi-step Differential Transform Method”, **Physica Scripta** (IOP), **89**, pp. 015204(8pp).
9. **A. Patra** and S. Saha Ray, 2014, “A Numerical Approach based on Haar wavelet operational method to solve Neutron Point Kinetics Equation involving Imposed Reactivity Insertions”, **Annals of Nuclear Energy** (Elsevier), **68**, pp. 112-117.
10. **A. Patra** and S. Saha Ray, “On the Solution of Nonlinear Fractional Neutron Point Kinetics Equation with Newtonian Temperature feedback reactivity”, **Nuclear Technology** (American Nuclear Society) (**Accepted**).
11. **A. Patra** and S. Saha Ray. “Two-dimensional Haar wavelet Collocation method for the solution of Stationary Neutron Transport Equation in a Homogeneous Isotropic medium”, **Annals of Nuclear Energy** (Elsevier), **70**, pp. 30-35.

❖ **Conference Published Paper**

12. **A. Patra**, S. Saha Ray, R. K. Bera, B.B Biswas and S. Das, 2011, “Eigen Function Expansion Method for Solving One-Group Neutron Diffusion Equation”, **Journal of International Academy of Physical Sciences**, ISSN 0974-9373: **16** (2), 163-170.

❖ **Communicated Papers**

13. **A. Patra** and S. Saha Ray, “Solution for Nonlinear Neutron Point Kinetics Equation with Newtonian Temperature feedback reactivity in Nuclear Reactor dynamics”, **Int. Journal of Nuclear Energy Science and Technology** (Inderscience).
14. **A. Patra** and S. Saha Ray, “Numerical Simulation based on Haar Wavelet Operational Matrix method for solving Point Kinetics Equations involving Sinusoidal and Pulse reactivity”, **Annals of Nuclear Energy** (Elsevier).
15. S. Saha Ray and **A. Patra**. “Numerical Simulation for Fractional order Stationary Neutron Transport Equation using Two-dimensional Haar wavelet Collocation method”, **Nuclear Engineering and design** (Elsevier).

BIO-DATA

Ashrita Patra
Senior Research Fellow (SRF)
Roll No.- 509MA602
Department of Mathematics
National Institute of Technology Rourkela
Odisha, PIN-769008
Mobile: +91-9439335550
Email: ashrita.patra@gmail.com

OBJECTIVE

“To contribute my ideas and knowledge in the field of teaching and to be a good researcher.”

PERSONAL DETAILS

- | | |
|---|---|
| <input type="checkbox"/> Date of Birth: | 23.12.1984 |
| <input type="checkbox"/> Marital Status: | Married |
| <input type="checkbox"/> Nationality: | Indian |
| <input type="checkbox"/> Gender: | Female |
| <input type="checkbox"/> Phone: | 09439335550, 09692773491 , 08895182019 |
| <input type="checkbox"/> Email: | ashrita.patra@gmail.com |
| <input type="checkbox"/> Present Address: | H/424, Sector-1, Rourkela, Odisha, India, Pin -769008 |

EDUCATIONAL QUALIFICATION

- ☐ 10th BSE, Ispat High School, Sector-2, Rourkela, Odisha. Year - 2000 with Agg. 81.2%.
12th CHSE, Ispat Vidya Mandir, Sector-19, Rourkela, Odisha. Year – 2002 with Agg. 61%.
- ☐ B.Sc., S. G. Women’s College, Sector-3, Rourkela, (Sambalpur University). Year – 2005 with Agg 63.57%.
- ☐ M.Sc. (Mathematics), National Institute of Technology, Rourkela. Year – 2007 with CGPA 9.21 out of 10.
- ☐ Presently as Senior Research Fellow (SRF) under CSIR, I am doing my Ph. D. under the supervision of Prof. S. Saha Ray bearing Roll No. 509Ma602 in the Department of Mathematics, National Institute of Technology Rourkela, India. I am going to submit my thesis on July, 2014.

AREA OF INTEREST

- ☐ Analytical and Numerical Solution for Neutron Kinetic Problems
- ☐ Numerical Analysis
- ☐ Differential Equations
- ☐ Fractional Differential Equations
- ☐ Computational Mathematics

I am awarded as Senior Research Fellow from Council of Scientific and Industrial Research (CSIR), Govt. of India in 2013.

WORK EXPERIENCE:

| Name of the organization | Position | Period | | Job Description |
|--------------------------|----------|--------------|--------------|-----------------|
| | | From | To | |
| PIET, Rourkela | Lecturer | April, 2008 | - July, 2009 | Teaching |
| REC, BBSR | Lecturer | August, 2009 | - May, 2010 | Teaching |

PERMANENT ADDRESS

Qrs. No: H/424, Sector-1, Rourkela, Odisha, India, Pin – 769008